**Drug Disposition during Pregnancy: Transport, Metabolism, and the Gut Microbiome**

Lyrialle Wei Han

A dissertation

submitted in partial fulfillment of the

requirements for the degree of

Doctor of Philosophy

University of Washington

2020

Reading Committee:

Qingcheng Mao, Chair

Kenneth E. Thummel

Edward J. Kelly

Program Authorized to Offer Degree:

Pharmaceutics

University of Washington

## Abstract

Drug Disposition during Pregnancy: Transport, Metabolism, and Effects of the Gut Microbiome

Lyrialle Wei Han

Chair of Supervisory Committee:
Qingcheng Mao, PhD. Associate Professor
Pharmaceutics

Medication use during pregnancy is increasingly prevalent and medically necessary to maintain maternal health. Yet, a quarter of medications used by pregnant women have unknown safety for the pregnant population. It is therefore imperative to better understand how drug disposition is altered by pregnancy for each drug. Bupropion (BUP) is an antidepressant and smoking cessation aid that is prescribed to pregnant women. It is extensively metabolized to three pharmacologically active metabolites erythrohydrobupropion (EB), hydroxybupropion (OHB) and threohydrobupropion (TB). However, at the time of study, the overall disposition mechanisms remained poorly understood, and most studies have focused their efforts on elucidating metabolism. Hence, we screened major hepatic uptake and efflux transporters for the transport of BUP and the three active metabolites using cell lines that overexpressed organic anion transporting polypeptide (OATP) 1B1, OATP1B3, OATP2B1, OATP4A1, organic cation transport (OCT)1, breast cancer resistance protein (BCRP), multidrug resistance-associated protein 2 (MRP2), and P-glycoprotein (P-gp). We found that although there was observably significant net active uptake by OATP overexpressing cell lines, the active uptake could not be

inhibited by prototypical inhibitors of OATPs. We also reported that none of the compounds were substrates of OCT1, BCRP, MRP2, or P-gp. Hence, the overall contribution of hepatic transporters in BUP disposition should be minor. Metabolism is another key drug processing event that can be altered during pregnancy. To extend efforts in this regard, we explored N-acetyltransferase 2 (NAT2) dependent pharmacokinetics on oral hydralazine in pregnant women. Hydralazine is used to treat hypertension during pregnancy because of its low risk to the fetus. Only the parent compound is reported to be pharmacologically active, and its major route of elimination is by metabolism via NAT2 to its major inactive metabolite 3-methyl-1,2,4-triazolo[3,4-a]phthalazine (MTP). NAT2 is highly polymorphic and hydralazine plasma concentrations in non-pregnant subjects could vary up to 15-fold, and adverse events have been reported at high doses in slow acetylators (SA). In this study, 12 pregnant women in their second or third trimester who were already receiving oral hydralazine (5-25mg QID) as a part of their antihypertension treatments were recruited. During one steady state interval, serial blood samples and buccal swabs were collected for *NAT2* genotyping. In total, we classified 6 subjects to be rapid acetylators (RA) and 6 to be SAs. We found that SAs had significantly slower weight-adjusted apparent oral hydralazine clearance (20 vs 70 L/h, $P < 0.05$), higher dose-normalized area under time-concentration curve (5.9 vs 1.5 ng*h/ml, $P < 0.05$), lower dose-normalized peak concentrations (4.04 vs 0.77 ng/mL, $P < 0.05$), and larger weight-adjusted apparent oral volume of distribution (116 vs 302, $P < 0.05$) compared to RAs. We observed no gestational age effects between subjects in their second or third trimester. And dose effects were also not observed. Taken together, this was the first study to show NAT2 dependent oral hydralazine pharmacokinetics in pregnancy. Next, we explored the effect of the gut microbiome on hepatic drug processing genes during pregnancy using C57BL/6 conventional (CV) and germ-free (GF)

mice. Four groups of female mice were used, namely CV non-pregnant (CVNP), GF non-pregnant (GFNP), CV pregnant (CVP), and GF pregnant (GFP) mice. Pregnant mice were sacrificed on gestation day 15. Hepatic mRNA was quantified by RNA-sequencing; hepatic proteomics and plasma metabolomics were performed by LC-MS/MS. We observed that pregnancy-induced effects were similar in both CV and GF mice, but the magnitudes of changes were significantly different for some hepatic enzymes. Most remarkable was the Cyp3a isoform Cyp3a11, with a 2-fold greater downregulation by pregnancy at the mRNA level in GF mice compared to CV mice, but at protein level both were elevated around 2-fold by pregnancy. Microsomal incubation revealed induction of Cyp3a activity by pregnancy in both CV and GF mice, but the induction was 5 times greater in CV mice compared to GF mice. We also analyzed the effect of the gut microbiome on overall metabolic pathways. We performed untargeted hepatic transcriptomics and untargeted plasma metabolomics on the same mice. We found that the same pathways were significantly enriched by pregnancy in CV and GF mice. However, four pathways were further modulated by germ-free in pregnancy, namely retinol metabolism, linoleic acid metabolism, arachidonic acid metabolism, and steroid hormone biosynthesis. Taken together, our studies provide clear evidence that the gut microbiome can alter host hepatic enzymes and metabolic pathways in pregnancy.

**Dedication**

To my parents,

Thank you for allowing me to pursue my dream with your love and support.

To my late grandparents,

Thank you for inspiring me to always be the best version of myself. You were always optimistic, persistent, and laughed at all the obstacles that life threw at you. Your strength motivates me to hang on even during the tough times.

To everyone that believed in me, even when I didn’t believe in myself,

Thank you. You gave me the strength and motivation I needed to continue this path. I am here today because of you.

## Acknowledgement

Over the past five and half years, I met some of the best mentors, colleagues, and friends in my life. They helped guide me along my entire graduate school journey, offered their hands to lift me up when I stumbled, laughed with me when I succeeded, and boosted me with motivation when I faltered. Without them, I wouldn't be where I am today.

Dr. Qingcheng Mao, my doctoral advisor, whom I have the utmost respect for. He teaches by example and leads by setting the same high standards for himself, yet, he guides with so much patience and flexibility. He never pushed me harder than what he knew what I was capable of, and he was always ready to guide me a step further than I thought I could do. Even during my earlier years of training, he trusted in my abilities and gave me the freedom to explore projects on my own, to make the falls and stumbles that he knew would make me a stronger scientist today. He helped me build the solid scientific background and critical thinking skills that I will continue to carry with me onwards. I'm forever grateful for the opportunity he gave me.

Dr. Kenneth Thummel, Dr. Yvonne Lin, Dr. Edward Kelly, Dr. Julia Cui, and Dr. Rheem Totah, my dissertation committee members, all of you have given me so much guidance and encouraged me to look deeper and think deeper about my projects. You helped build my scientific foundation to never accept things as they are, and to ask questions that would push the science to a new level. You never gave up on me when I struggled, and you told me that you knew what I was capable of. Thank you for taking the time to teach me, guide me, support me, and believing in me. I will always be indebted to you and will do my best in my future career to make you all proud.

Dr. Hebert, Dr. Shen, my project mentors on the oral hydralazine project, thank you. You gave me the opportunity to be a part of a project that is precious to you, and you trusted me to grow my technical and analytical skills while working on these projects. Because of these projects, I developed my clinical pharmacokinetic skills and scientific writing skills. You held me to the highest of standards and enabled me to see what I was capable of. The insights and feedback you gave me helped me see through the eyes of an expert in the field. You helped me overcome my weaknesses and to become a stronger team player, collaborator, and independent scientist.

Matt Eng, Alvin Chau, Susan Taylor, Betsy Stearman, Kate Reinking, Janeth Talty, and all faculty and staff in Pharmaceutics department, thank you for everything you helped me with behind the scenes. From troubles in payroll to health insurance to logistics in figuring out paperwork for my internship gap, you always offered help without hesitation and would go out of your way to help me find a solution. You really make the engines run and you keep it so well oiled. I will never forget that every time I go to you with a problem and you welcomed me with your smiles, every time.

My dear labmates from H259: Dr. Michael Liao, Dr. Chuying Gao, and Dr. Naveen Neradugomma, we had the best times together and you made the lab life so incredibly fun. You were my first family in the graduate school, and you welcomed me with open arms. You taught me technical skills, personal skills, and tips on how to survive graduate school. We shared professional and personal problems and always rooted for each other. I will never forget the times that we shared.

My orange lab family: Justina Calamia, Dr. Theresa Aliwarga, Nathan Alade, Chris Arian, Michelle Guignet, thank you for your companionship and support over the last year. I love

our orange bubble where we can share everything from science to personal life stories. I love that we are able to freely communicate with each other and find ways to help each other anyway we can. You would always take the time to listen to me when I needed an extra ear or sounding board. You always encouraged me and filled me with so much optimism. I will always miss being along side you in the lab and the fun times we shared. Thank you.

My dear colleagues and collaborators, Lindsay Henderson, Mackenzie Bergagnini-Kolev, Kevin Lidberg, Zhican Wang, Zufei Zhang, Yuchen Zhang, Robert Pelletier, Yuanyuan Shi, Shih Yu Chang, Yanfei Li, Alison Paquette, Joseph Dempsey, Sara Shum, Lindsay Czuba, Brian Phillips, and Laura Shireman. You have been incredible sources of knowledge and support throughout my graduate studies. Thank you for sharing your companionship and expertise.

Dr. Tracey Wei, my FDA ORISE fellowship mentor, who gave me the opportunity to work on two projects related to anti-bacterial combination drugs and apply my PKPD modeling skills. I am indebted to her incredible patience and guidance throughout my internship, and for her continued mentorship after my fellowship at the Office of Clinical Pharmacology ended.

I also want to thank my family and friends who have supported me along the entire way. My parents, grandmother, aunt, and cousin have always been understanding about my busy schedule and not able to visit them even during the holidays. My boyfriend and fur friend, who always gave me their moral support in every way they can. Thank you for always being there for me.

My dissertation research was supported in parts by the following grants: National Institute on Drug Abuse [Grant DA032507], the University of Washington Drug Metabolism, Transport and Pharmacogenomics Research Program (DMTPR), and the National Center for

Advancing Translational Sciences of the National Institutes of Health [Grant TL1TR000 422], National Center for Advancing Translational Sciences [Grant UL1TR002319], National Institute of General Medical Sciences [Grant R01GM124264], Eunice Kennedy Shriver National Institute of Child Health and Human Development [Grant U10HD047892], and the National Institute of General Medical Sciences [Grant R01GM111381].

## Table of Contents

# CHAPTER 1: INTRODUCTION

## 1.1 MEDICATION USE DURING PREGNANCY

The CDC reported in 2019 that 90% of women take at least 1 medication at some point during their pregnancy [1,2]. This translates to 6 million pregnancies being exposed to xenobiotics in the United States alone [2]. The increased prevalence of medication use in pregnancy is alarming, because researchers have shown that drug disposition characteristics can change dynamically with pregnancy, affecting the safety to the mother and her fetus, as well as the efficacy of the medication. According to a meta study in Sweden, of 587 drugs used by women in Europe during pregnancy, the current regulatory agencies worldwide still do not have data on 23% of those drugs to provide safety information specific for this vulnerable population [3]. While most medications prescribed to pregnant women are intended to treat chronic conditions that threaten their health, dosing recommendations during pregnancy are not always available. The Food and Drugs Administration (FDA) has acknowledged the need for better dosing guidance and safety information for this special population [4]. In 2014, a new regulatory guidance known as the “Pregnancy and Lactation Labeling Rule” was published, requiring that each drug be labeled to include a pregnancy risk summary and indicate whether or not there is systemic absorption, data used to support the statement, and clinical considerations for the medication in pregnancy [4].

It is imperative that more research be done to fill an important gap in knowledge that still exists between how drugs behave in the "typical" population (healthy and/or non-pregnant volunteers; the predominant study population) and that of pregnant women [5]. Furthermore, medication exposure not only affects maternal health, but can also pose a risk to the developing fetus. During early gestation, the fetus is more vulnerable to xenobiotic exposure due to the leaky placental barrier and the inability to eliminate drugs from the fetal compartment [6,7]. Additionally, because of safety concerns, it is almost impossible to clinically assess actual fetal exposure before the time of delivery. To better understand the cumulative effects of fetal exposure, it is imperative that we first understand the factors that determine the maternal disposition and elimination of drugs during pregnancy and extrapolate fetal exposures from there through the application of physiologically-based pharmacokinetic modeling. Therefore, the focus of my PhD dissertation is on understanding various aspects of drug disposition during pregnancy.

## 1.2 DRUG DISPOSITION DURING PREGNANCY

The maternal body undergoes remarkable physiological and cellular biochemical changes from conception through a term-pregnancy. The changes can be broken down by their effect on drug absorption, distribution, metabolism, and excretion (ADME) – the four key components to pharmacokinetics. There are two main routes of drug administration – intravenous and oral. Since intravenous absorption goes directly into the systemic circulation, only oral absorption is susceptible to various factors that can be altered in pregnancy. Oral drug absorption can be affected by drug formulation and dissolution, gastric pH, gastric emptying time, blood flow to intestinal tissues, and intestinal pH [8]. It has been reported that during pregnancy, gastric motility is greatly reduced and gastric emptying time is increased by up to 50% [8,9].

Furthermore, gastric pH in pregnant woman was also found to be more basic, which can affect the nonionized drug concentration in both the stomach and small intestine [8]. In terms of drug distribution, body water volume increases with the progression of pregnancy, including a rapid increase in early and mid-gestation by up to 65% of pre-pregnancy plasma volume [10]. The increase in plasma volume in turn creates an apparent decrease in plasma albumin concentration. Decreased plasma albumin concentration can lead to higher unbound drug concentrations, which can in turn alter the drug's efficacy and toxicity profile [8,11]. Furthermore, cardiac output is increased by up to 45% in a uncomplicated pregnancy [12]. This results in increased blood flow throughout the systemic circulation, which has profound impact on hepatic and renal clearance of drugs. The metabolism of drugs takes place predominately in the liver by the action of phase I and phase II enzymes. Cytochrome P450 (CYP) enzymes are responsible for majority of Phase I xenobiotic biotransformation [13] and the hepatic abundances of many have been shown to change during pregnancy. For example, probe substrate studies demonstrated an increase in CYP2D6 and CYP3A4 activity and a decrease in CYP2C19 and CYP1A2 activity during pregnancy [14–17]. In addition, the expression of some CYPs varies in a gestational age-dependent manner. Studies with phenytoin, a model substrate of CYP2C9, showed no change in CYP2C9 activity in early gestation but increased activity from mid- to late pregnancy [18,19]. Transporters are another important factor in drug disposition, modulating the uptake and efflux of drugs into and out of a cell [20]. P-glycoprotein, an efflux transporter widely expressed in the intestine, liver, brain, and placenta, has increased expression in the kidney during late gestation [17]. As mentioned previously, since cardiac output is increased over gestation, hepatic blood flow is also increased, which can affect hepatic clearance, especially of high extraction drugs [11]. In the kidneys, glomerular filtration rate (GFR) increases by up to 85% as a consequence of

a 65% increase in  renal blood flow during pregnancy [21]. Together, the ADME of any drug could be significantly changed in pregnant women compared to non-pregnant women or men. For my dissertation, I have investigated the role of transporters on bupropion disposition, the metabolism of hydralazine, and the effect of the gut microbiome on hepatic drug processing gene expressions and overall metabolic pathways during pregnancy.

## 1.3 BUPROPION USE DURING PREGNANCY

### DEPRESSION AND SMOKING IN PREGNANCY

The prevalence of depression during pregnancy has been reported to be as high as 20% [22]. The standard of care for depression during pregnancy is psychotherapy counseling and prescription of antidepressant medications [22,23]. Traditionally, selective serotonin reuptake inhibitors (SSRIs) and selective serotonin and norepinephrine reuptake inhibitors (SNRIs) are prescribed [22]. However, there have been studies showing that these drugs can cross the placenta, which is a concern for fetal exposure and toxicity [22]. For example, fluoxetine is the most commonly prescribed SSRI in non-pregnant patient population, but it has been found to be associated with premature birth, lower birth weight, and transient withdrawal symptoms when used during pregnancy [24–29].

On a separate note, smoking during pregnancy was reported by the CDC to be prevalent in 20% of pregnancies [30]. Fetal exposure to the constituents of maternal cigarette smoke in utero is associated with lower birth weight, increased morbidity and mortality, cognitive disabilities, and some adverse effects can persist throughout childhood [31–34]. Despite the risks, only 18 to 25% of women can successfully quit smoking during pregnancy [30]. Instead of forcing pregnant women to quit, medications can be used to assist in the smoking cessation

process. However, this presents a new set of potential risks to the developing fetus, with mediation exposure.

### BUPROPION

Bupropion (BUP) is a relatively new drug that can be used in pregnancy for treatment of depression and smoking cessation [35,36]. Pharmacologically, it is a dopamine-norepinephrine reuptake inhibitor and nicotinic receptor antagonist [35–37]. According to studies, only 1% of BUP is excreted unchanged in urine and a majority of the drug dose undergoes extensive metabolism [38–40]. Three major metabolites that have been identified to be pharmacologically active are hydroxybupropion (OHB), erythrohydrobupropion (EB) and threohydrobupropion (TB) [41,42]. The principal enzymes responsible for the formation of these metabolites have been identified to be CYP3A4, CYP2B6, CYP2C19, 11β-hydroxysteroid dehydrogenase-1 (11β-HSD1), and aldoketoreductases [43–45]. Despite this valuable knowledge of metabolite formation, the full disposition of bupropion is not fully understood. Based on results from a drug-drug interaction study with BUP and clopidogrel, the BUP AUC change elicited by clopidogrel could not be fully explained by the inhibition of known metabolic pathways alone [46]. This raised the question as to whether transporters could be contributing to BUP disposition. The potential impact of transporters on drug efficacy and safety is significant. There has been evidence of increased risk of drug-induced livery injury (DILI) when using BUP [47], and a common cause of DILI is intracellular accumulation of the toxic compound [48]. When a drug is dependent on a transporter for uptake from systemic circulation into hepatocytes or effluxed from hepatocytes into the bile, it is vulnerable to drug interactions that decrease or inhibit the activity of those transporters. It is also susceptible to pregnancy-induced changes in

transporter function. When efflux processes are decreased, the intracellular concentration of a drug can increase, leading to cytotoxicity.

In **Chapter 2**, we performed *in vitro* uptake and efflux assays to characterize the role of transporters in the hepatic and placental disposition of BUP and its major metabolites. We tested, using overexpressed cell lines, all major hepatic transporters important for drug disposition, including organic anion transporting polypeptide (OATP) 1B1, OATP1B3, OATP2B1, multidrug resistance-associated protein (MRP) 2, P-gp and breast cancer resistance protein (BCRP); as well as OATP4A1, an uptake transporter found on the apical membrane of placental syncytiotrophoblasts.

## 1.4 ORAL HYDRALAZINE KINETICS DURING PREGNANCY

### HYPERTENSION IN PREGNANCY

Hypertensive disorders are prevalent in 10% of pregnancies, and have been on the rise over the past decade according to the CDC [49–52]. Per the International Classification of Diseases, Ninth Revision, Clinical Modification (ICD-9-CM), hypertensive disorders in pregnancy include gestational hypertension, (pre)eclampsia, and chronic hypertension [53]. If left untreated, maternal hypertension can lead to placental abruption, organ injuries, cerebral hemorrhage, seizures, adverse fetal growth, preterm birth, and increased mortality and morbidity [54]. The standard of care is close monitoring of the mother's conditions, and intervention by pharmacotherapy whenever necessary [54–57]. There are several types of antihypertensive medications prescribed to pregnant women. Beta blockers, such as labetalol, or central agents such as methyldopa, can be effective in maintaining normal maternal blood pressure, but has also been reported to have adverse effects on the fetus due to reduced uteroplacental blood flow [58].

Calcium channel blockers such as nifedipine do not restrict placental blood flow, but can potentially cause fetal distress or hypotension [58]. Hydralazine is a vasodilator recommended by The American College of Obstetricians and Gynecologists for pregnant women and does not have significant adverse effects, as do the other drugs, and therefore is considered relatively safe for the mother and her fetus [54].

### NAT2 Polymorphism Effects in Hydralazine Kinetics

Hydralazine is active as its parent form and controls blood pressure by decreasing total peripheral resistance [59]. Previous studies in non-pregnant male subjects showed that only 10% of the drug excreted unchanged in urine [60]. Hydralazine is highly protein bound and circulates systemically in its acid labile metabolite form [61–64]. The major acid labile metabolite, hydralazine pyruvate hydrazone (HPH), is not pharmacologically active, and only a small amount could be found excreted in urine [61–63,65–68]. The major route of elimination is via metabolism by *N*-acetyltransferase 2 (NAT2) [69,70]. After metabolism by NAT2, hydralazine is biotransformed to 3-methyl-1,2,4-triazolo[3,4-a]phthalazine (MTP) [60]. Subsequent glucuronide metabolites of MTP are recovered in urine and, based on the fraction recovered, acetylation was identified as the predominant route of hydralazine elimination.

NAT2 is a highly polymorphic enzyme that is abundantly expressed in the intestine and liver [71–73]. Those with high NAT2 activity are identified as rapid acetylators (*4 genotype), and those with low activity (*5, *6, or *7 genotypes) are classified as slow acetylators [74,75]. The geographical distribution of NAT2 phenotype is not uniform, with a higher frequency of more rapid acetylators in East Asian populations and more slow acetylators in the European populations [74]. Pharmacokinetic differences of oral hydralazine between rapid and slow acetylator phenotypes (non-pregnant) have been reported to be up to 15-fold in plasma

concentration [76–80]. This is a potential clinical concern, as slow hydralazine acetylators have a higher risk of severe adverse outcomes, including systemic lupus erythematosus, after high dose exposure to hydralazine in non-pregnant patients [77]. Currently, there is no FDA guidance or drug labeling that requires genotyping of patients prior to prescription of hydralazine, and doses are titrated at the clinician's discretion.

Of relevance to this issue, Hardman et al. found in non-pregnant patients that oral hydralazine bioavailability can vary up to two-fold based on NAT2 phenotype [81]. There was also a study that reported a small decrease of 13% in NAT2 activity in early gestation [82]. Taken together, this could pose a potential risk for slow acetylating pregnant women. However, no pharmacokinetic studies of oral hydralazine disposition in pregnancy have been conducted. Thus, in **Chapter 3**, we investigate and characterize NAT2 dependent kinetics of steady-state oral hydralazine in pregnant hypertensive women. We showed that NAT2 genotype significantly impacts hydralazine pharmacokinetic parameters such as apparent oral clearance, apparent volume of distribution (and by inference, oral bioavailability), area under the curve, parent to metabolite ratio.

## 1.5 ROLE OF GUT MICROBIOME ON DRUG DISPOSITION DURING PREGNANCY

The gut microbiome has come into the spotlight in recent years due to increasing evidence and awareness of its ability to metabolize certain drugs and modulate various metabolic pathways of its human host [83]. It has often been said that the gut microbiome is the "second human genome" due to the abundance of gut bacterial cells relative to human host's cells throughout the body [83,84]. At birth, the initial gut microbiome takes hold and colonizes the

infant's gastrointestinal tract and lives symbiotically with the human host for the rest of his/her life [83,85]. The gut microbiome is flexible and can respond to lifestyle, diet, disease, physiological change, and environment changes [83]. Pregnancy is one condition in which the gut microbiome has been found to shift in response to the host's physiological changes. Koren et al. compared the gut microbiome from 91 pregnant women and showed that the abundance of *Actinobacteria* and *Proteobacteria* was increased in the third trimester compared to non-pregnancy [86,87].

The gut microbiome can influence host drug disposition. Intestinal bacteria can directly metabolize, inactivate, or deconjugate compounds [88]. In addition, bacteria can produce metabolites that activate nuclear receptors which subsequently regulate drug metabolizing enzymes and transporters [88]. One explanation of this indirect regulation mechanism is related to the role of bacteria in production of secondary bile acids [89,90]. As primary bile acids are synthesized in the liver and enter the intestines via the bile duct. In the intestine, primary bile acids could be converted by intestinal bacteria, such as *Firmicutes*, through deconjugation, dihydroxylation or epimerization into secondary bile acids. Primary bile acids cholic acid, chenodeoxycholic acid, and secondary deoxycholic acids have been shown to be ligands for the nuclear receptor farnesoid X receptor (FXR) [91]. Secondary bile acid lithocholic acid have been reported to be ligands for the nuclear receptors pregnane X receptor (PXR) and vitamin D receptor [92,93]. Activation of these nuclear receptors leads to downstream upregulation of CYPs and transporters. Under dysbiosis, or disruption of normal gut microbiome, changes in bacteria composition and their ability to produce metabolites also change. Studies using germ-free mice revealed that the lack of gut microbiome resulted in accumulation of primary bile acids which are antagonist of FXRs and PXRs [89,94]. Therefore, the gut microbiome could play an

important role in drug disposition. However, how the gut microbiome influences drug disposition in pregnancy has not been investigated.

In **Chapter 4**, we use germ-free mice to determine the effect of the gut microbiome on hepatic drug processing gene expressions during pregnancy. We have demonstrated that not only are many enzymes and transporters including the Cyp3a isoforms influenced by pregnancy, they can be further modulated by the gut microbiome during pregnancy.

To further understand the global effect of the gut microbiome on drug metabolism pathways, we performed untargeted transcriptomics and untargeted plasma metabolomics on the same mice. In **Chapter 5**, we describe the changes in overall metabolic pathways observed as the result of pregnancy alone, and how the gut microbiome influenced some key pathways in addition to pregnancy effects. These data establish a basis for further investigation of the potential of gut microbiome in determining interindividual variability of drug disposition during pregnancy. In addition, knowledge of effects of the gut microbiome on hepatic drug metabolizing enzymes, transporters, and overall metabolic pathways, helps us better understand what processes are most vulnerable to microbial effects during pregnancy.

## 1.6 REFERENCES


1. Centers for Disease Control and Prevention. Treating for Two: Medicine and Pregnancy [Internet]. 2019.
2. Mitchell AA, Gilboa SM, Werler MM, et al. Medication use during pregnancy, with particular focus on prescription drugs: 1976-2008. *Am. J. Obstet. Gynecol.* 2011;205:51.e1-51.e8.
3. Trønnes JN, Lupattelli A, Nordeng H. Safety profile of medication used during pregnancy: results of a multinational European study. *Pharmacoepidemiol. Drug Saf.* 2017;26:802–811.
4. Food and Drug Administration. Pregnancy and Lactation Labeling Final Rule. 2014;1–3.
5. Thomas SHL, Yates LM. Prescribing without evidence - pregnancy. *Br. J. Clin. Pharmacol.* 2012;74:691–697.
6. Ross EJ, Graham DL, Money KM, et al. Developmental consequences of fetal exposure to drugs: what we know and what we still must learn. *Neuropsychopharmacology*. 2015;40:61–87.
7. Joshi AA, Vaidya SS, St-Pierre M V., et al. Placental ABC Transporters: Biological Impact and Pharmaceutical Significance. *Pharm. Res.* 2016;33:2847–2878.
8. Loebstein R, Lalkin A, Koren G. Pharmacokinetic changes during pregnancy and their clinical relevance [Internet]. Clin. Pharmacokinet. Springer International Publishing; 1997. p. 328–343.
9. Parry E, Shields R, Turnbull AC. Transit Time in the Small Intestine in Pregnancy. *BJOG An Int. J. Obstet. Gynaecol.* 1970;77:900–901.
10. Aguree S, Gernand AD. Plasma volume expansion across healthy pregnancy: a systematic review and meta-analysis of longitudinal studies. *BMC Pregnancy Childbirth*. 2019;19:508.
11. Soma-Pillay P, Nelson-Piercy C, Tolppanen H, et al. Physiological changes in pregnancy. *Cardiovasc. J. Afr.* 2016;27:89–94.
12. Sanghavi M, Rutherford JD. Cardiovascular physiology of pregnancy. *Circulation*. 2014;130:1003–1008.
13. Zanger UM, Schwab M. Cytochrome P450 enzymes in drug metabolism: Regulation of gene expression, enzyme activities, and impact of genetic variation. Pharmacol. Ther. Pergamon; 2013. p. 103–141.
14. Tracy TS, Venkataramanan R, Glover DD, et al. Temporal changes in drug metabolism (CYP1A2, CYP2D6 and CYP3A Activity) during pregnancy. *Am. J. Obstet. Gynecol.* 2005;192:633–639.
15. Andrew MA, Hebert MF, Vicini P. Physiologically based pharmacokinetic model of midazolam disposition during pregnancy. *Conf. Proc. ... Annu. Int. Conf. IEEE Eng. Med.*

*Biol. Soc. IEEE Eng. Med. Biol. Soc. Annu. Conf.* 2008;2008:5454–5457.

16. Isoherranen N, Thummel KE. Drug metabolism and transport during pregnancy: how does drug disposition change during pregnancy and what are the mechanisms that cause such changes? *Drug Metab. Dispos.* 2013;41:256–262.

17. Hebert M, Easterling T, Kirby B, et al. Effects of Pregnancy on CYP3A and P-glycoprotein Activities as Measured by Disposition of Midazolam and Digoxin: A University of Washington Specialized Center of Research Study. *Clin. Pharmacol. Ther.* 2008;84:248–253.

18. Dickinson RG, Hooper WD, Wood B, et al. The effect of pregnancy in humans on the pharmacokinetics of stable isotope labelled phenytoin. *Br. J. Clin. Pharmacol.* 1989;28:17–27.

19. Tomson T, Lindbom U, Ekqvist B, et al. Epilepsy and pregnancy: a prospective study of seizure control in relation to free and total plasma concentrations of carbamazepine and phenytoin. *Epilepsia*. 35:122–130.

20. Roth M, Obaidat A, Hagenbuch B. OATPs, OATs and OCTs: the organic anion and cation transporters of the SLCO and SLC22A gene superfamilies. *Br. J. Pharmacol.* 2012;165:1260–1287.

21. Hussein W, Lafayette RA. Renal function in normal and disordered pregnancy. Curr. Opin. Nephrol. Hypertens. NIH Public Access; 2014. p. 46–53.

22. Pearlstein T. Depression during Pregnancy. *Best Pract. Res. Clin. Obstet. Gynaecol.* 2015;29:754–764.

23. Melville JL, Gavin A, Guo Y, et al. Depressive disorders during pregnancy: prevalence and risk factors in a large urban sample. *Obstet. Gynecol.* 2010;116:1064–1070.

24. Nulman I, Rovet J, Stewart DE, et al. Neurodevelopment of children exposed in utero to antidepressant drugs. *N. Engl. J. Med.* 1997;336:258–262.

25. Oberlander TF, Misri S, Fitzgerald CE, et al. Pharmacologic factors associated with transient neonatal symptoms following prenatal psychotropic medication exposure. *J. Clin. Psychiatry*. 2004;65:230–237.

26. Källen B. Neonate Characteristics after Maternal Use of Antidepressants in Late Pregnancy [Internet]. Arch. Pediatr. Adolesc. Med. 2004. p. 312–316.

27. Zeskind PS, Stephens LE. Maternal Selective Serotonin Reuptake Inhibitor Use during Pregnancy and Newborn Neurobehavior. *Pediatrics*. 2004;113:368–375.

28. Laine K, Heikkinen T, Ekblad U, et al. Effects of exposure to selective serotonin reuptake inhibitors during pregnancy on serotonergic symptoms in newborns and cord blood monoamine and prolactin concentrations. *Arch. Gen. Psychiatry*. 2003;60:720–726.

29. Heikkinen T, Ekblad U, Palo P, et al. Pharmacokinetics of fluoxetine and norfluoxetine in pregnancy and lactation. *Clin. Pharmacol. Ther.* 2003;73:330–337.

30. Centers for Disease Control and Prevention. Smoking During Pregnancy. 2019.

31. Abraham M, Alramadhan S, Iniguez C, et al. A systematic review of maternal smoking during pregnancy and fetal measurements with meta-analysis. PLoS One. Public Library of Science; 2017.

32. Lockhart F, Liu A, Champion BL, et al. The Effect of Cigarette Smoking during Pregnancy on Endocrine Pancreatic Function and Fetal Growth: A Pilot Study. *Front. Public Heal.* 2017;5.

33. Kataoka MC, Carvalheira APP, Ferrari AP, et al. Smoking during pregnancy and harm reduction in birth weight: A cross-sectional study. *BMC Pregnancy Childbirth*. 2018;18.

34. Mund M, Louwen F, Klingelhoefer D, et al. Smoking and pregnancy - A review on the first major environmental risk factor of the unborn. Int. J. Environ. Res. Public Health. Multidisciplinary Digital Publishing Institute (MDPI); 2013. p. 6485–6499.

35. Slemmer JE, Martin BR, Damaj MI. Bupropion is a nicotinic antagonist. *J. Pharmacol. Exp. Ther.* 2000;295:321–327.

36. Ferris RM, Cooper BR, Maxwell RA. Studies of bupropion's mechanism of antidepressant activity. *J. Clin. Psychiatry*. 1983;44:74–78.

37. Cooper BR, Hester TJ, Maxwell RA. Behavioral and biochemical effects of the antidepressant bupropion (Wellbutrin): evidence for selective blockade of dopamine uptake in vivo. *J. Pharmacol. Exp. Ther.* 1980;215:127–134.

38. Findlay JWA, Van Wyck Fleet J, Smith PG, et al. Pharmacokinetics of bupropion, a novel antidepressant agent, following oral administration to healthy subjects. *Eur. J. Clin. Pharmacol.* 1981;21:127–135.

39. Benowitz NL, Zhu AZX, Tyndale RF, et al. Influence of CYP2B6 genetic variants on plasma and urine concentrations of bupropion and metabolites at steady state. *Pharmacogenet. Genomics*. 2013;23:135–141.

40. Schroeder DH. Metabolism and kinetics of bupropion. *J. Clin. Psychiatry*. 1983;44:79–81.

41. Bondarev ML, Bondareva TS, Young R, et al. Behavioral and biochemical investigations of bupropion metabolites. *Eur. J. Pharmacol.* 2003;474:85–93.

42. Jefferson JW, Pradko JF, Muir KT. Bupropion for major depressive disorder: Pharmacokinetic and formulation considerations. *Clin. Ther.* 2005;27:1685–1695.

43. Wang X, Abdelrahman DR, Zharikova OL, et al. Bupropion metabolism by human placenta. *Biochem. Pharmacol.* 2010;79:1684–1690.

44. Meyer A, Vuorinen A, Zielinska AE, et al. Formation of threohydrobupropion from bupropion is dependent on 11β-hydroxysteroid dehydrogenase 1. *Drug Metab. Dispos.* 2013;41:1671–1678.

45. Skarydova L, Tomanova R, Havlikova L, et al. Deeper Insight into the Reducing Biotransformation of Bupropion in the Human Liver. *Drug Metab. Pharmacokinet.* 2014;29:177–184.

46. Turpeinen M, Tolonen A, Uusitalo J, et al. Effect of clopidogrel and ticlopidine on

cytochrome P450 2B6 activity as measured by bupropion hydroxylation. *Clin. Pharmacol. Ther.* 2005;77:553–559.

47. Telles-Correia D, Barbosa A, Cortez-Pinto H, et al. Psychotropic drugs and liver disease: A critical review of pharmacokinetics and liver toxicity. *World J. Gastrointest. Pharmacol. Ther.* 2017;8:26–38.

48. Luethi D, Liechti ME, Krähenbühl S. Mechanisms of hepatocellular toxicity associated with new psychoactive synthetic cathinones. *Toxicology*. 2017;387:57–66.

49. Folk DM. Hypertensive Disorders of Pregnancy: Overview and Current Recommendations. *J. Midwifery Womens. Health*. 2018;

50. Lo JO, Mission JF, Caughey AB. Hypertensive disease of pregnancy and maternal mortality. *Curr. Opin. Obstet. Gynecol.* 2013;25:124–132.

51. Leffert LR, Clancy CR, Bateman BT, et al. Hypertensive Disorders and Pregnancy-Related Stroke. *Obstet. Gynecol.* 2015;125:124–131.

52. Centers for Disease Control and Prevention. Data on Pregnancy Complications. 2019.

53. Centers for Disease Control and Prevention. ICD-9-CM. 2019.

54. American College of Obstetricians and Gynecologists, Task Force on Hypertension in Pregnancy. Hypertension in Pregnancy. *Obstet. Gynecol.* 2013;122:1122–1131.

55. Redman CWG. Hypertension in pregnancy: the NICE guidelines. *Heart*. 2011;97:1967–1969.

56. Hypertension in pregnancy: diagnosis and management clinical guideline [Internet]. Natl. Inst. Heal. Care Excell. 2011.

57. Easterling TR. Pharmacological management of hypertension in pregnancy. *Semin. Perinatol.* 2014;38:487–495.

58. Kattah AG, Garovic VD. The Management of Hypertension in Pregnancy. Adv. Chronic Kidney Dis. NIH Public Access; 2013. p. 229–239.

59. Easterling TR, Benedetti TJ, Schmucker BC, et al. Antihypertensive therapy in pregnancy directed by noninvasive hemodynamic monitoring. *Am. J. Perinatol.* 1989;6:86–89.

60. Talseth T. Clinical Pharmacokinetics of Hydrallazine. *Clin. Pharmacokinet.* 1977;2:317–329.

61. Zak SB, Lukas G, Gilleran TG. Plasma levels of real and “apparent” hydralazine in man and rat. *Drug Metab. Dispos.* 5:116–121.

62. Reece PA, Stanley PE, Zacest R. Interference in assays for hydralazine in humans by a major plasma metabolite, hydralazine pyruvic acid hydrazone. *J. Pharm. Sci.* 1978;67:1150–1153.

63. Shepherd AM, Ludden TM, Haegele KD, et al. Pharmacokinetics of hydralazine, apparent hydralazine and hydralazine pyruvic acid hydrazone in humans. *Res. Commun. Chem. Pathol. Pharmacol.* 1979;26:129–144.

64. Lesser JM, Israili ZH, Davis DC, et al. Metabolism and Disposition of Hydralazine-14C in Man and Dog. *Drug Metab. Dispos.* 1974;2.

65. Wagner J, Faigle JW, Imhof P, et al. Metabolism of hydralazine in man. *Arzneimittelforschung.* 1977;27:2388–2395.

66. Barron K, Carrier O, Haegele KD, et al. Comparative evaluation of the in vitro effects of hydralazine and hydralazine acetonide on arterial smooth muscle. *Br. J. Pharmacol.* 1977;61:345–349.

67. McLean AJ, du Souich P, Barron K, et al. Study of in vitro effects of hydralazine metabolites--comparative evaluation of products of hydroxylation, hydrolysis and conjugation. *Arch. Int. Pharmacodyn. Ther.* 1978;235:19–25.

68. Iwaki M, Ogiso T, Ito Y. In vitro kinetic studies of the reaction of hydralazine and its acetone hydrazone with pyruvic acid. *J. Pharm. Sci.* 1988;77:280–283.

69. Zimmer H, Glaser R, Kokosa J, et al. 3-Hydroxymethyl-s-triazolo[3,4-a]phthalazine, a novel urinary hydralazine metabolite in man. *J. Med. Chem.* 1975;18:1031–1033.

70. Dubois JP, Schmid K, Riess W, et al. Metabolism of hydralazine in man. Part II: Investigation of features relevant to drug safety. *Arzneimittelforschung.* 1987;37:189–193.

71. Jenne JW. Studies of human patterns of isoniazid metabolism using an intravenous fall-off technique with a chemical method. *Am. Rev. Respir. Dis.* 1960;81:1–8.

72. Evans DA, White TA. Human Acetylation Polymorphism. *J Lab Clin Med*. 1964;63:394–403.

73. Windmill KF, Gaedigk A, de la M. Hall P, et al. Localization of N-Acetyltransferases NAT1 and NAT2 in Human Tissues. *Toxicol. Sci.* 2000;54:19–29.

74. Mortensen HM, Froment A, Lema G, et al. Characterization of genetic variation and natural selection at the arylamine *N* -acetyltransferase genes in global human populations. *Pharmacogenomics*. 2011;12:1545–1558.

75. Zang Y, Doll MA, Zhao S, et al. Functional characterization of single-nucleotide polymorphisms and haplotypes of human N-acetyltransferase 2. *Carcinogenesis*. 2007;28:1665–1671.

76. Shepherd AM, McNay JL, Ludden TM, et al. Plasma concentration and acetylator phenotype determine response to oral hydralazine. *Hypertens. (Dallas, Tex. 1979)*. 3:580–585.

77. Spinasse LB, Santos AR, Suffys PN, et al. Different phenotypes of the NAT2 gene influences hydralazine antihypertensive response in patients with resistant hypertension. *Pharmacogenomics*. 2014;15:169–178.

78. Lemke LE, McQueen CA. Acetylation and its role in the mutagenicity of the antihypertensive agent hydralazine. *Drug Metab. Dispos.* 1995;23:559–565.

79. Timbrell JA, Harland SJ, Facchini V. Polymorphic acetylation of hydralazine. *Clin. Pharmacol. Ther.* 1980;28:350–355.

80. Allen CE, Doll MA, Hein DW. N-Acetyltransferase 2 Genotype-Dependent N-Acetylation of Hydralazine in Human Hepatocytes. *Drug Metab. Dispos.* 2017;45:1276–1281.

81. Hardman J, Limbird L, Gilman A. Goodman and Gilman's The Pharmacological Basis of Therapeutics. 10th ed. McGraw Hill; 2001.

82. Tsutsumi K, Kotegawa T, Matsuki S, et al. The effect of pregnancy on cytochrome P4501A2, xanthine oxidase, and N -acetyltransferase activities in humans. *Clin. Pharmacol. Ther.* 2001;70:121–125.

83. Nicholson JK, Holmes E, Kinross J, et al. Host-gut microbiota metabolic interactions. Science (80-. ). American Association for the Advancement of Science; 2012. p. 1262–1267.

84. Gordon JI. Honor thy gut symbionts redux. *Science*. 2012;336:1251–1253.

85. Dominguez-Bello MG, Costello EK, Contreras M, et al. Delivery mode shapes the acquisition and structure of the initial microbiota across multiple body habitats in newborns. *Proc. Natl. Acad. Sci. U. S. A.* 2010;107:11971–11975.

86. Nuriel-Ohayon M, Neuman H, Koren O. Microbial changes during pregnancy, birth, and infancy. *Front. Microbiol.* 2016;7:1031.

87. Koren O, Goodrich JK, Cullender TC, et al. Host remodeling of the gut microbiome and metabolic changes during pregnancy. *Cell*. 2012;150:470–480.

88. Spanogiannopoulos P, Bess EN, Carmody RN, et al. The microbial pharmacists within us: a metagenomic view of xenobiotic metabolism. *Nat. Rev. Microbiol.* 2016;14:273–287.

89. Klaassen CD, Cui JY. Review: Mechanisms of How the Intestinal Microbiota Alters the Effects of Drugs and Bile Acids. *Drug Metab. Dispos.* 2015;43:1505–1521.

90. Claus SP, Ellero SL, Berger B, et al. Colonization-induced host-gut microbial metabolic interaction. *MBio*. 2011;2:e00271-10.

91. Wang H, Chen J, Hollister K, et al. Endogenous bile acids are ligands for the nuclear receptor FXR/BAR. *Mol. Cell*. 1999;3:543–553.

92. Staudinger JL, Goodwin B, Jones SA, et al. The nuclear receptor PXR is a lithocholic acid sensor that protects against liver toxicity. *Proc. Natl. Acad. Sci. U. S. A.* 2001;98:3369–3374.

93. Ishizawa M, Akagi D, Makishima M. Lithocholic acid is a vitamin D receptor ligand that acts preferentially in the ileum. *Int. J. Mol. Sci.* 2018;19.

94. Wahlström A, Kovatcheva-Datchary P, Ståhlman M, et al. Crosstalk between Bile Acids and Gut Microbiota and Its Impact on Farnesoid X Receptor Signalling. *Dig. Dis.* 2017;35:246–250.

# CHAPTER 2: TRANSPORT OF BUPROPION AND ITS METABOLITES BY THE MODEL CHO AND HEK293 CELL LINES

This work was previously published by Han et al. in *Drug Metabolism Letters* **2019**;13(1):25-35.



## 2.1 INTRODUCTION

Bupropion (BUP) is a dopamine-norepinephrine reuptake inhibitor and nicotinic receptor antagonist widely used as an antidepressant and to assist smoking cessation [1–3]. Recently, it has also been indicated for weight loss combination therapy, and is reportedly used off-label for the attention-deficit hyperactive and bipolar disorders [4–8].

Despite its wide applications, the factors that contribute to interindividual variability in BUP disposition and pharmacokinetics remain not well understood. Several studies have reported that only 1% of the BUP dose is excreted unchanged in urine, indicating extensive metabolism of the drug [9–11]. BUP is primarily metabolized in the liver by cytochrome P450 enzymes, 11β-hydroxysteroid dehydrogenase-1 (11β-HSD1), and aldoketoreductases [5,12,13]. The three resulting metabolites, hydroxybupropion (OHB), erythrohydrobupropion (EB) and threohydrobupropion (TB), are also pharmacologically active, with OHB being 50-100% and TB and EB being 20% as active as BUP [14,15]. OHB and TB, but not EB, circulate at 3 – 30-fold higher concentrations than the parent drug [10,13,16,17]. A detailed schematic of the current understanding of bupropion metabolic pathways was recently published [18].

Since the liver is the primary site of metabolism and elimination of xenobiotics, drugs must enter the liver in order for biotransformation and excretion to occur. Drugs may enter the liver by passive diffusion or transporter-mediated active uptake [19]. Organic anion-transporting polypeptide (OATP) uptake transporters are highly expressed in many organs such as the human liver, intestine, and placenta, and thus are critically important factors in drug disposition [19–22]. OATP1B1, OATP1B3 and OATP2B1 are located in the sinusoidal membrane of hepatocytes, facilitating drug uptake into the hepatocytes prior to metabolism or biliary excretion [19,23]. OATP2B1 is also expressed in the basal membrane of placental syncytiotrophoblasts, possibly transporting drugs and metabolites from the fetal compartment to the placenta, whereas OATP4A1 is highly expressed in the apical membrane of syncytiotrophoblasts and may mediate uptake of drugs from the maternal circulation into the placenta [24]. Hence, the systemic and local tissue exposure of OATP substrate drugs could be affected by drug-drug interactions (DDIs) through inhibition or induction of OATPs. Previous studies have shown that several drugs such as clopidogrel and ticlopidine significantly increase the systemic exposure (AUC) of BUP by 30-60% but disproportionately decreased metabolite OHB AUC by 60-89% [25]. This discordance may be due to inhibition of both hepatic CYP enzymes as well as uptake transporters. Clopidogrel is a known effective inhibitor of OATP1B1 and has been suggested to be involved in OATP1B1-mediated DDIs [26]. This led us to hypothesize that the entry of BUP into the hepatocytes is mediated by OATPs.

Furthermore, chronic BUP therapy has been linked to an increased risk of drug-induced liver injury (Alanine aminotransferase levels 3 times upper limit of normal in small number of patients) when co-prescribed with paroxetine [27,28]. Intracellular accumulation of some drugs has been associated with hepatic toxicity [29]. The concentration of drugs (such as BUP) in the

liver could be determined by uptake transporters in the sinusoidal membrane and accumulation of drug in the liver could be determined by the efflux transporters in the canalicular membrane of liver hepatocytes. Multidrug resistance-associated protein 2 (MRP2), P-glycoprotein (P-gp), breast cancer resistance protein (BCRP) are the three major ATP-binding cassette efflux transporters that are highly expressed in the canalicular membrane of liver hepatocytes [30], facilitating the elimination of endogenous substances and xenobiotics into the bile by actively transporting them against a concentration gradient [31]. MRP2, P-gp and BCRP are also the major efflux transporters at the blood-brain barrier and the placental barrier that limit drug exposure to the brain and fetus [32–38]. Whether these efflux transporters are important for biliary elimination and local tissue exposure of BUP and its metabolites are not known.

Therefore, in the present study, we investigated whether the major hepatic transporters important for drug disposition, including OATP1B1, OATP1B3, OATP2B1, MRP2, P-gp and BCRP, are capable of transporting BUP and its active metabolites. Transport of these compounds by OATP4A1, an uptake transporter in the apical membrane of placental syncytiotrophoblasts, was also evaluated. The data obtained will be important for understanding the roles of transporters in the overall disposition, local tissue (e.g., the liver and placenta) exposure, systemic clearance, and DDIs of BUP and its metabolites.

## 2.2 MATERIALS AND METHODS

### MATERIALS

BUP, OHB, TB, EB, BUP-$d_9$, OHB-$d_6$, TB-$d_9$, EB-$d_9$ were purchased from Toronto Research Chemicals (Ontario, Canada). Estrone-3-sulfate (E1-3-S), estradiol-17β-glucuronide ($E_2$-17β-G), rifampin (RIF), probenecid, decynium-22 (D-22), cyclosporin A (CsA), quinidine,

and N-methyl-quinidine (NMQ) were purchased from Sigma (St. Louis, MO). [$^3$H]-MPP$^+$ was purchased from Perkin Elmer (Waltham, MA). Hygromycin B and G418 were purchased from Fisher Scientific (Waltham, MA). All other chemicals and buffers used were of the highest commercial quality available. Dulbecco's Modified Eagle's Medium (DMEM), antibiotic-antimitotic solution, and Hank's balanced salt solution (HBSS) containing 1g/L D-glucose were purchased from Invitrogen (Carlsbad, CA). Fetal bovine serum (FBS) was purchased from Seradigm (Radnor, PA). Flp-In Human Embryonic Kidney (HEK)/OATP2B1, HEK/OCT1 and Flp-In HEK/pcDNA5 cells were developed in the laboratory of Dr. Joanne Wang by stable transfection. HEK/empty vector and HEK/OATP4A1 cells were kindly provided by Dr. Joerg Koenig in the Institute of Experimental and Clinical Pharmacology and Toxicology, University of Erlangen, Germany. Chinese Hamster Ovary (CHO) wild-type (WT), CHO/OATP1B1 and CHO/OATP1B3 cells were from Dr. Bruno Stieger in the Department of Clinical Pharmacology and Toxicology, University Hospital Zurich, Switzerland, through Dr. Bruno Hagenbuch in the Department of Pharmacology, Toxicology and Therapeutics at University of Kansas Medical Center. Multiscreen$^{TM}$ HTS Vacuum Manifold and 96-well filter plates with glass fiber filters were from Merck Millipore (Billerica, MA). HEK293 vesicular transport membranes overexpressing MRP2, P-gp or BCRP or mock control membrane vesicles were purchased from Solvo Biotechnology (Szeged, Hungary). All transporters investigated in this study are human transporters.

### CELL CULTURE

All cells were maintained in a humidified incubator at 37$^o$C with 5% $CO_2$. OATP-overexpressing CHO cells were cultured in phenol-red free, low glucose DMEM with 10% FBS, 100 U/mL penicillin, 100 μg/mL streptomycin, 0.2 μg/mL amphotericin B, 50 μg/mL L-proline,

and in the presence or absence of 500 μg/mL G418 (for OATP transfected or WT CHO cells, respectively). Flp-In HEK/pcDNA5, Flp-In HEK/OATP2B1 and Flp-In HEK/OCT1 cells were cultured in DMEM with 10% FBS, 100 U/mL penicillin, 100 μg/mL streptomycin, 0.2 μg/mL amphotericin B, and 500 μg/mL hygromycin B. HEK/empty vector and HEK/OATP4A1 were cultured under the same condition as HEK/pcDNA5, but in the presence of 500 μg/mL G418 instead of hygromycin B. Cells used in the experiments were between passages 8 and 25 to ensure good transporter expression and activity [39].

### CELLULAR UPTAKE TRANSPORT ASSAY

HEK cells were seeded onto Poly-D-Lysine-coated 96-well plates at a density of approximately 25,000 cells/well and cultured for 48 h prior to uptake experiments. CHO cells were seeded onto Collagen I-coated 96-well plates at a density of approximately 10,000 cells/well and cultured for 48 h and then induced by adding sodium butyrate to 5 mM in culture media for 24 h prior to uptake experiments. On the day of uptake experiments, each well was washed with 100 μL of HBSS (pH 7.4) and allowed to equilibrate in HBSS in 37°C water bath for 5 min. BUP or metabolite was then added to each well (0 – 300 μM) and incubation continued for 3 min (within linear range, Figure 2-1). After the incubation, cells were promptly washed three times with ice-cold HBSS to terminate uptake reactions. Cells were then lysed with ice-cold acetonitrile containing an internal standard, and drug compounds in cell lysates were quantified using a LC-MS assay as described below. Protein concentrations of cell lysates were determined using a Pierce BCA protein assay kit (Pierce Chemical, Rockford, IL) with bovine serum albumin as standard. Net transporter-mediated cellular uptake was calculated by subtracting intracellular accumulation in the parent or empty vector control cells from that in OATP/OCT-overexpressing cells and expressed as pmol of BUP, OHB, TB or EB/mg

protein/min. The concentration of vehicle (DMSO) used to dissolve test compounds was kept below 0.2% (v/v) in all assays. To assess potential nonspecific binding, we also performed three independent experiments comparing uptake of BUP using the methods described above, but washing the cells with either ice-cold HBSS, or ice-cold HBSS containing 3% bovine serum albumin (BSA).

### CELLULAR UPTAKE INHIBITION ASSAY

HEK and CHO cells were cultured and incubated under the same conditions as described above. During inhibition experiments, buffers containing the known OATP, OAT or OCT inhibitors (20 μM RIF and 20 μM CsA for OATP, 50 μM probenecid for OAT, 100 μM D-22 for OCT) were added to each well and the incubation continued for 5 min at 37°C. The inhibitor concentrations used were >10 fold above the reported $IC_{50}$ values for respective transporters. After the 5 min of pre-incubation, the buffers were aspirated and fresh buffers containing both the inhibitor and a test compound were added to each well. Then, the uptake reactions and sample extraction procedures were the same as described above.

### PLASMA MEMBRANE VESICLE TRANSPORT ASSAY

The rapid filtration method for vesicular transport membrane uptake assays was the same as previously described [40]. The plasma membrane vesicles (25 μg of protein per reaction) were incubated at 32°C (for BCRP or P-gp) or 37°C (for MRP2) with varying concentrations (1 – 10 μM) of a test compound in the presence of ATP or AMP (5 mM). The incubation buffer (pH 7.0) constituted of 10 mM Tris-HCl, 10 mM $MgCl_2$, and 250mM sucrose for the BCRP or P-gp membrane vesicles, or 50 mM MOPS-Tris, 10 mM $MgCl_2$, and 70 mM KCl for the MRP2 membrane vesicles. In addition, 2 mM glutathione was added to the assay mixtures containing MRP2 membrane vesicles to stimulate MRP-mediated transport. The assay mixtures (75 μL per

reaction) containing MRP2, P-gp or BCRP membrane vesicles were pre-incubated for 15 min at 32°C or 37°C in the presence of 5 mM ATP or AMP prior to the addition of test compound. After adding the test compound, the assay mixtures were further incubated for 1 min. Transport reactions were terminated by the addition of 200 μL of ice-cold incubation buffer containing 1.5% BSA. The reaction mixtures were quickly transferred to a 96-well glass fiber filter plate over the vacuum manifold and rapidly washed 5 times with 200 μL ice-cold buffer each time. Finally, the test compound trapped in the membrane vesicles was eluted from the filter by adding 200 μL of methanol containing internal standards and quantified using a LC-MS/MS assay as described below. The membrane vesicle systems were validated using known substrates as positive controls ($E_2$-17β-G for BCRP and MRP2; NMQ for P-gp). The concentration of vehicle (DMSO) used to dissolve test compounds was kept below 0.2% (v/v) in all assays. The ATP-dependent uptake of a test compound into plasma membrane vesicles was calculated by subtracting the uptake with AMP from that with ATP and expressed as pmol of BUP, OHB, TB or EB/mg protein/min.

### LC-MS/MS QUANTIFICATION

The extraction of BUP and metabolites from cell lysates or membrane vesicle eluents was conducted in 96-well plates with acetonitrile protein precipitation. Briefly, 100 μL of ice-cold acetonitrile containing 200 nM of an internal standard was added to each well, and then 100 μL of water was added for a final v/v ratio of 1:1 after 30 min. Samples were centrifuged at 4°C with 4,000 rpm for 5 min, and the supernatant was injected onto LC-MS/MS. Quantification of BUP and metabolites by LC-MS/MS was adapted and modified from previously published methods [18,41] on Agilent 1290 ultra-high-performance liquid chromatography interfaced with an Agilent 6410 B triple-quadrupole mass spectrometer (Agilent Technologies, Palo Alto, CA).

The mass spectrometer was operated in positive ion electrospray ionization mode. Chromatographic separation was performed on an Agilent Zorbax Extended-C18 column (2.1 × 50 mm, 5 μm) (Santa Clara, CA). The injection volume was 5 μL and the column temperature was 20°C. The mobile phases A and B were 0.1% formic acid and acetonitrile, respectively. The flow rate was 0.3 ml/min. The gradient started from 10% B, increased to 78% B at 2.8 min, decreased to 10% B at 3.8 min, and equilibrated at 10% B until 6 min. Under these conditions, retention times for BUP and metabolites were 2.0 – 2.2 min. Mass spectrometer conditions were optimized for each analyte to the following parameters: 300°C gas temperature, 11 L/min gas flow, 35 psi nebulizer, 4000 V capillary, 90 V fragmentor for all compounds; 25 V collision energy for BUP, OHB, BUP-$d_9$ and OHB-$d_6$; 12 V collision energy for TB-$d_9$, TB and EB. Multiple reaction monitoring transitions for each analyte and the internal standard were *m/z* 240 > 184 for BUP, *m/z* 256 > 139 for OHB, *m/z* 242 > 168 for TB and EB, *m/z* 249 > 185 for BUP-$d_9$, *m/z* 262 > 139 for OHB-$d_6$, and *m/z* 251 > 169 for TB-$d_9$. BUP-$d_9$, OHB-$d_6$, and TB-$d_9$ were used as internal standard for BUP, OHB, and TB/EB, respectively, with TB-$d_9$ serving as the internal standard for both TB and EB due to their identical *m/z* transitions. Drug compounds were quantified using peak area ratios of compounds to the respective internal standards with calibration curves and quality controls prepared using analytical grade BUP, OHB, TB and EB in matching matrix. The limit of quantification for all compounds was below 1 nM. Intraday variations for BUP, OHB, TB, and EB were 5%, 7%, 12%, and 6%, respectively. Inter-day variations in the same order were 3%, 3%, 5%, 2%, respectively.

### OCT1 Uptake and [$^3$H]-MPP$^+$ Quantification

HEK293 cells stably expressing OCT1 (HEK293/OCT1) or empty vector (HEK293/pcDNA5) were plated in 24 well plates at the density of 400,000 cells/well. Three days

after plating, cells were washed with pre-warmed HBSS (140 mM NaCl, 5 mM KCl, 1 mM $CaCl_2$, 0.4 mM $MgSO_4$, 0.5 mM $MgCl_2$, 0.3 mM $KH_2PO_4$, 6 mM glucose and 4 mM $NaHCO_3$) twice to remove residual medium. HBSS solution containing 1 µM $MPP^+$ (0.6 µCi/mL [$^3$H]-$MPP^+$) in the presence or absence of 100 µM quinone was then incubated with cells for 10 min at 37°C. Incubation was stopped by removing the solution and immediately washing with ice-cold HBSS 3 times. Cells were lysed with 500 µL of 1M NaOH for 1 h at 37°C, and neutralized with 500 µL of 1 M HCl. The lysates (500 µL each sample) were transferred and the radioactivity was counted with TRI-CARB Scintillation Counter. Twenty-five µL of lysate was used to measure protein concentration by BCA. The radioactivity uptake of each well was then normalized with protein concentration.

**DATA ANALYSIS**

All transport studies were performed with three independent experiments in triplicate for each experiment. Data shown were means ± SD of three independent experiments. The differences in cellular uptake between the transporter-overexpressing and the parent or empty control cells were analyzed using the unpaired Student *t*-test. Apparent $K_m$ and $V_{max}$ values were calculated by fitting the Michaelis-Menten kinetic equation to the net cellular uptake data. The effects of the OATP inhibitor rifampin and CsA, the OAT inhibitor probenecid or the OCT/PMAT/MATE inhibitor D-22 on cellular uptake were analyzed by two-way ANOVA analysis flowed by the Bonferroni correction for multiple comparison. Differences with *p* values of $< 0.05$ were considered statistically significant. All the analysis was performed using the GraphPad Prism software (GraphPad Prism 5.01, La Jolla, CA).

## 2.3 RESULTS

### UPTAKE OF BUP AND METABOLITES INTO OATP-OVEREXPRESSING CELLS

We first verified if OATPs overexpressed in CHO or HEK cells can mediate cellular uptake of known substrates, $E_1$-3-S and $E_2$-17β-G. $E_1$-3-S is a model substrate of OATP2B1 and OATP4A1, while $E_2$-17β-G is a known substrate of OATP1B1 and OATP1B3. Uptake of $E_1$-3-S at 5 μM into HEK/OATP2B1 and HEK/OATP4A1 cells were 42 and 20 times greater, respectively, than that into respective HEK vector control cells (Figure 2-2). Likewise, uptake of $E_2$-17β-G at 5 μM into CHO/OATP1B1 and CHO/OATP1B3 cells was approximately 6 and 2 times greater, respectively, than that into the CHO wild-type parent cells (Figure 2-2). These results confirmed that OATPs overexpressed in CHO or HEK cells were functional.

Next, we examined the uptake of BUP and metabolites into OATP-overexpressing and respective parent or empty vector control cells. We found that the uptake of all these compounds into the control cells was significantly lower than that into respective cells overexpressing OATP1B1, OATP1B3, or OATP2B1, over a concentration range of 0 – 300 μM (Figures 2-3 to 2-5), but no significant differences between OATP4A1-overexpressing and control cells were observed (Figure 2-6). These results suggest that OATP1B1, OATP1B3, and OATP2B1 could possibly mediate the cellular uptake of BUP and its metabolites, while OATP4A1 did not. We calculated the net cellular uptake by subtracting intracellular uptake associated with the parent or empty vector control cells from that associated with the OATP-overexpressing cells. The net cellular uptake appeared to be saturable (Figures 2-3 to 2-5). Hence, we estimated their "apparent $K_m$" values using the Michaelis-Menten kinetics (Table 2-1).

To further confirm whether OATPs can indeed mediate the cellular uptake of BUP, we performed cellular uptake experiments in the presence of 20 μM rifampin (RIF), a known potent,

general inhibitor of OATPs at concentrations well above its $IC_{50}$ values for respective transporter. The concentration of BUP (5 μM) used in the inhibition experiments was well below the estimated apparent $K_m$ values for respective OATPs. To first confirm the inhibitory activity of RIF and CsA, we assessed inhibition of prototypical substrates E1-S and $E_2$-17β-G in all cell lines, with 5 min and 60 min pre-incubations with inhibitor (Figure 2-7). Since no significant difference was observed with extended preincubation, we proceeded to perform inhibition study with 5 min preincubation only. The reported $IC_{50}$ values of RIF for OATP1B1, OATP1B3 and OATP2B1 were 1.5-3.25 μM, 1.5-2.6 μM, and 2.1 μM, respectively, so we chose 20 μM RIF to fully inhibit the transporters of interest [22,42–44]. Surprisingly, under these conditions, we showed that the cellular uptake of BUP into the OATP-overexpressing cells was not inhibited at all by RIF (Figure 2-8). We further confirmed this finding using another potent OATP inhibitor, CsA, which did not inhibit the cellular uptake of BUP into the OATP-overexpressing cells either (Figure 2-8). These results suggest that the observed cellular uptake of BUP into OATP-overexpressing cells is potentially mediated by other transporters, but not OATPs, or there is simultaneous inhibition of efflux by these substrates.

We also performed inhibition studies of the cellular uptake of metabolites by 20 μM RIF, with concentrations of each metabolite well below their estimated apparent $K_m$ values for each OATP-overexpressing cell line. For OATP1B1, 10 μM of OHB, 20 μM of TB and 30 μM of EB were used; for OATP1B3, 30 μM of OHB, 10 μM of TB and 5 μM of EB were used; for OATP2B1, 30 μM of OHB, 20 μM of TB and 100 μM of EB were used. Likewise, no statistically significant differences in the cellular uptake of the metabolites between the OATP-overexpressing and the parent or empty vector control cells were observed (Figure 2-9), suggesting that the cellular uptake of the metabolites is not mediated by OATPs either.

Lastly, we assessed the impact of non-specific binding of BUP to cell membranes on cellular uptake by comparing intracellular accumulation of BUP in each cell line after washing the cells with ice-cold HBSS in the presence or absence of 3% BSA. Although some non-specific binding was observed as washing the cells with BSA decreased cellular uptake of BUP, the uptake of BUP into transporter-transfected cells were still significantly higher than that in parent or vector control cells (Figure 2-10). Therefore, the higher cellular uptake of BUP into transporter-transfected cells is unlikely due to differential non-specific binding.

### CELLULAR UPTAKE OF BUP BY ENDOGENOUS TRANSPORTERS

The saturable uptake transport kinetics of BUP and metabolites into the parent or empty vector control cells or the OATP-overexpressing cells suggests that this cellular uptake is mediated by active transporters, rather than passive diffusion. Further, the inhibition studies showed that the uptake of BUP was not mediated by OATPs. This raised suspicions that endogenous transporters in these cell lines were responsible for the uptake. To test this possibility, we performed additional inhibition experiments using probenecid, a known OAT inhibitor, and D-22, a known inhibitor of OCT/PMAT/MATE transporters. The concentrations of the inhibitors used were kept at least 5-fold above their known $IC_{50}$ values for respective transporters to ensure full inhibition. The reported $IC_{50}$ values of probenecid and D-22 were 3.1-7.4 μM and 13.8-21.9 μM, respectively [45–48]. Therefore, probenecid and D-22 were used at 50 μM and 100 μM, respectively. Likewise, we used BUP at concentrations that were well below the apparent $K_m$ values where no saturation would occur. No inhibition of BUP uptake into both the OATP-overexpressing cells and their respective control cells by probenecid was observed (Figure 2-11), suggesting that the active BUP uptake is not mediated by OATs. However, a

significant decrease in the cellular uptake of BUP was seen in both the OATP-overexpressing and control cells when D-22, a known OCT/PMAT/MATE inhibitor, was used (Figure 2-11).

### CELLULAR UPTAKE OF BUP BY OCT1

To further test if the observed BUP uptake into the CHO and HEK cells is mediated by OCT1, an important hepatic transporter, we performed cellular uptake studies for BUP using the OCT1-overexpressing HEK cells and the empty vector control cells. We first verified that cellular uptake of the OCT1 model substrate [$^3$H]-MPP$^+$ into the OCT1-overexpressing cells was 15 times higher than that into the vector control cells (Figure 2-2), confirming that OCT1 overexpressed in the cells was fully functional. No significant differences in the cellular uptake of BUP at 0.1, 1 and 10 μM between the OCT1-overexpressing cells and the vector control cells were observed (Figure 2-12), suggesting that BUP is not a substrate of OCT1 at pharmacologically relevant concentrations.

### EFFLUX TRANSPORT OF BUP AND METABOLITES BY BCRP, MRP2, AND P-GP

Finally, we tested if BUP and metabolites are substrates of the major hepatic efflux transporters MRP2, P-gp and BCRP using (inside out?) membrane vesicle transport assays. We first verified the function of these transporters in the vesicular transport membranes using model substrates. $E_2$-17β-G at 5 μM was used as a model substrate for BCRP and MRP2. NMQ at 1 μM was used as a model substrate for P-gp. Uptake of the model substrates into the MRP2, P-gp or BCRP vesicles in the presence of ATP was 10-100 times greater than that in the presence of AMP (Figure 2-13), confirming that these transporters in the membrane vesicles were fully functional. We then examined ATP-dependent uptake of BUP and its metabolites at 1 and 10 μM by the three transporters, but did not observe significant differences in the vesicle uptake of any

of these compounds between the presence of ATP and AMP (Figure 2-14). Therefore, BUP and its metabolites are unlikely substrates of MRP2, P-gp and BCRP.

## 2.4 DISCUSSION

As aforementioned, the mechanisms underlying the overall disposition and systemic clearance of BUP and its active metabolites have not been well understood [10,13,16,17]. BUP is known to be extensively metabolized in the liver; however, little is known about whether transporters also play a role in the disposition of BUP and its metabolites.

Therefore, in this study, we investigated whether BUP, OHB, TB and EB are substrates of the major hepatic uptake and efflux transporters. BUP is mainly administered orally; metabolism in the liver is considered a major elimination pathway, and renal clearance seems to play a minor role [5,12,13,15,49]. The overall disposition of BUP in the body could be highly dependent on the efficiency of hepatic uptake of BUP from the portal blood and systemic circulation before being metabolized in the liver. Our *in vitro* transport studies showed that, although the OATP-overexpressing cells did exhibit a significantly greater and saturable cellular uptake of BUP and metabolites compared to the parent or empty vector control cells (Figures 2-3 to 2-5), this uptake could not be inhibited by two potent OATP inhibitors rifampin and CsA (Figures 2-8 & 2-9), suggesting that BUP and metabolites are not substrates of the major hepatic uptake transporters in the sinusoidal membrane, OATP1B1, OATP1B3 and OATP2B1. This raised an important question as to which transporters are responsible for cellular uptake of BUP into the OATP-overexpressing CHO and HEK cells. OAT2 and OCT1 are known to be expressed in the sinusoidal membrane of the liver hepatocyte, mediating uptake of xenobiotics and endogenous compounds into the liver [19]. Our further studies found that the cellular uptake

of BUP was not affected by the OAT inhibitor probenecid, but significantly inhibited by the OCT inhibitor D-22 in both the OATP-overexpressing and the control CHO or HEK cells (Figure 2-11), indicating that BUP is unlikely a substrate of OAT2. Direct uptake transport studies using OCT1-overexpressing cells demonstrated that BUP is not a substrate of OCT1 either (Figure 2-12). Taken together, based upon the results of the current study, we conclude that BUP is not a substrate of the major hepatic uptake transporters (OATP1B1, OATP1B1, OATP2B1, OCT1 and OAT2) in the sinusoidal membrane and thus these uptake transporters are not expected to play a role in the hepatic disposition of BUP. It is worth noting that D-22 is a general potent inhibitor of OCT/PMAT/MATE transporters. Endogenous expression of OCT/PMAT/MATE transporters in HEK cells would be expected considering HEK cells are originated from the human embryonic kidney, and previous studies have found low levels of mRNA and protein evidence of endogenous OCT expression in wild-type HEK293 cell line [50–52]. However, endogenous expression or activity in CHO cells was a surprise. Since PMAT, MATEs and other OCTs are not known to be highly expressed in the liver hepatocytes, we elected to not pursue PMAT, MATEs and other OCTs further. Identification of transporters that can transport BUP and its metabolites would be an interesting topic of future studies. We do not have explanations to the findings that the cellular uptake of BUP and metabolites into OATP-transfected cells is generally higher than that into the parent or empty control cells (Figures 2-3 to 2-5). It appears that cells transfected with target genes (OATPs) gain some additional transport properties as compared to the parent or mock transfected cells. This is possible as it has been shown that transfection of even empty vectors can promote intensive genome-level alternations beyond the function of target genes [53]. Nonetheless, this speculation is based on the assumption that only OATP genes are altered during the transfection process. A follow up study

using primary hepatocytes and the same inhibitors could be interesting to see whether the same holds true outside of an overexpressed cell system. Furthermore, although the substrate concentrations we chose for inhibition assays are at or below the apparent Km, it may be possible that there is potential saturation occurring. Future studies using lower substrate concentrations could also be considered to test this.

Alternatively, the lack of inhibition observed in our study might possibly be due to the fact that OATPs are known to have multiple-binding sites [54–57]. Other researchers have also observed low inhibitory effects of rifampicin on OATP2B1 uptake of hematoporphyrin monomethyl ether, even though significant uptake activity was observed in HEK293 cell lines and hepatocytes [58]. It is possible, though less likely, that BUP and metabolites occupy different binding sites from the two potent inhibitors we used as these two inhibitors seem to be commonly used general inhibitors of OATPs [59]. In all our transport experiments, we saw very low background noise in LC-MS/MS assays and peaks were well defined and clear, without any unidentified peaks, suggesting that no other analytes were present. Therefore, the data we present in this study cannot be explained by bupropion metabolism in these cells (CHO and HEK293) either.

Our results support the notion that the major hepatic uptake transporters are possibly not essential for mediating the entry of BUP into the liver. One clinical study had shown that clopidogrel and ticlopidine significantly increased the systemic exposure (AUC) of BUP by 36-61%, but disproportionally decreased the AUC of primary metabolite OHB by 60-89% [25]. Since clopidogrel is a known effective inhibitor of OATP1B1 and has been suggested to be involved in OATP1B1-mediated DDIs [26], we hypothesized that the interaction between clopidogrel and BUP could possibly be due to inhibition of OATP1B1-mediated hepatic uptake

of BUP by clopidogrel. However, the results of the current study do not support this hypothesis. The increase in the systemic exposure of BUP by co-administration of clopidogrel could be most likely caused by inhibition of drug-metabolizing enzyme-mediated BUP metabolism by clopidogrel. At the time of the clinical study, it was not known that BUP could also be metabolized by 11β-HSD1, a cytosolic enzyme extensively expressed in the liver, but not intestine or kidney [60]. Thus, in the presence of perpetrator drugs clopidogrel and ticlopidine, although the formation of OHB was heavily suppressed, BUP AUC did not increase proportionally because it was metabolized by 11β-HSD1. In order for this metabolism to occur, BUP must readily enter the hepatocytes by passive diffusion and/or other unknown uptake transporters to access the enzyme responsible. Furthermore, no significant difference was observed in the half-life of BUP. Taken together, the clinical study further suggested that the major hepatic OATP uptake transporters did not seem to play a significant role in this DDI.

We also explored the potential of interactions of the major hepatic efflux transporters with BUP and its metabolites, and did not observe any active transport activity of MRP2, P-gp or BCRP for these compounds (Figure 2-14). Consistent with our observation, He et al. also reported that BUP had no inhibitory effect on the transport of digoxin, a P-gp substrate, in LLC-PK1 cells overexpressing human P-gp [61]. However, our finding conflicts with another study showing that BUP is a substrate of BCRP and P-gp with $K_m$ of 3 μM and 0.5 μM, respectively [62]. One possible explanation is that the previous study used membrane vesicles isolated from human placenta which did not overexpress the transporters of interest, thus the vesicle uptake of BUP could be mediated by other endogenous transporters in the placental membrane vesicles.

BUP can be used by pregnant women. Previous studies have reported significant fetal exposure to BUP and its metabolites in pregnant women [17,63,64], suggesting that BUP and its

metabolites are able to cross the placental barrier and this is a safety concern for the developing fetus. In this study, we showed that BUP and its metabolites were not transported by OATP4A1 (Figure 2-6), an uptake transporter expressed in the apical membrane of placental syncytiotrophoblasts. Furthermore, P-gp and BCRP are known to be highly expressed in the apical membrane of placental syncytiotrophoblasts, limiting fetal exposure to drugs and xenobiotics. Results of this study suggest that P-gp, BCRP and OATP4A1 do not play a role in determining fetal exposure to BUP and its metabolites. Further studies are needed to investigate whether fetal exposure to these compounds is mediated by other placental transporters or passive diffusion.

Taken together, the significant active OATP uptake and lack of inhibition by prototypical inhibitors in CHO and HEK293 cell lines raises a concern that there may be endogenous transporters expressed that have not been identified. Caution should be taken when using these model cell lines to evaluate uptake transport activity of compounds. While our study does not support major hepatic transporters to be important in overall disposition of BUP and its metabolites, the active uptake in our study suggests that they are substrates of an unknown transporter. More studies are needed to identify their identities and potential drug-drug interactions.

Lastly, we recognize that BUP and its metabolites are racemic mixtures and previous metabolic studies have shown a stereoselectivity in *in vivo* disposition and *in vitro* metabolism [65]. Future studies are needed to verify if there is a stereoselectivity in the transport of BUP and its metabolites [66].

## 2.5 TABLES AND FIGURES

**Table 2-1. Apparent uptake transport kinetic parameters ($K_m$ and $V_{max}$) for BUP and its metabolites into OATP1B1-, OATP1B3- or OATP2B1-overexpressing cells**. Data shown are means ± SD estimated with the net cellular uptake data from three independent experiments. Units for $K_m$ and $V_{max}$ are μM and pmol/mg protein/min, respectively.

| | | BUP | OHB | TB | EB |
|---|---|---|---|---|---|
| CHO/OATP1B1-overexpressing cells | $K_m$ | 31 ± 7 | 18 ± 3 | 33 ± 5 | 82 ± 16 |
| | $V_{max}$ | 1407 ± 91 | 1423 ± 49 | 1351 ± 55 | 1806 ± 133 |
| CHO/OATP1B3-overexpressing cells | $K_m$ | 242 ± 64 | 76 ± 14 | 21 ± 3 | 14 ± 2 |
| | $V_{max}$ | 1312 ± 227 | 1258 ± 86 | 2536 ± 97 | 1026 ± 37 |
| HEK/OATP2B1-overexpressing cells | $K_m$ | 176 ± 20 | 74 ± 12 | 53 ± 9 | 192 ± 35 |
| | $V_{max}$ | 1697 ± 231 | 1641 ± 98 | 1368 ± 72 | 1752 ± 192 |

**Figure 2-1**

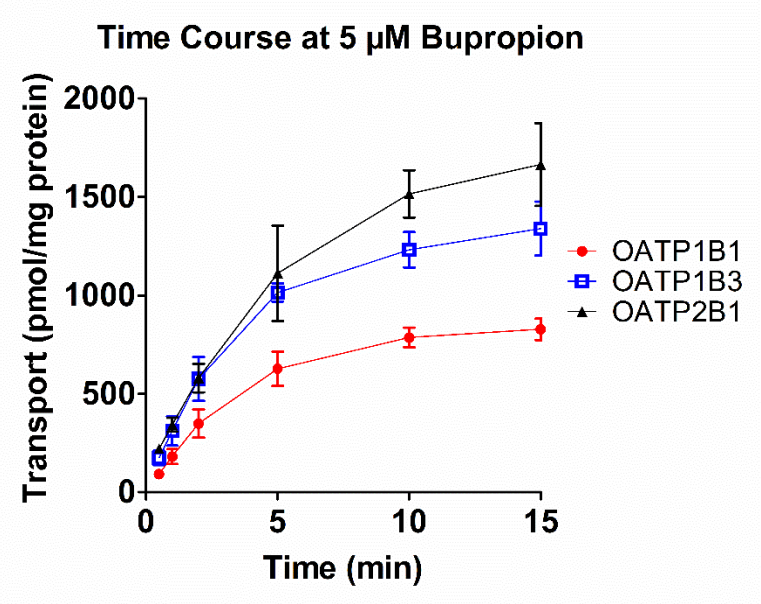


**Figure 2-1. Time course of 5 µM bupropion uptake in CHO/OATP1B1, CHO/OATP1B3, and HEK/OATP2B1 cell lines.** Cells were incubated in culture media with 5 µM bupropion for 0.5, 1, 2, 5, 10, and 15 min at 37°C. Reactions were terminated by removing solutions and washing with ice-cold HBSS 3 times. Cells were lysed and intracellular accumulation of compounds was quantified by LC-MS/MS. Data shown are means ± SD of three independent experiments. Linear range was observed to be between 0-5 min for most transporters, hence a 3 min time point was chosen for subsequent experiments.

**Figure 2-2**

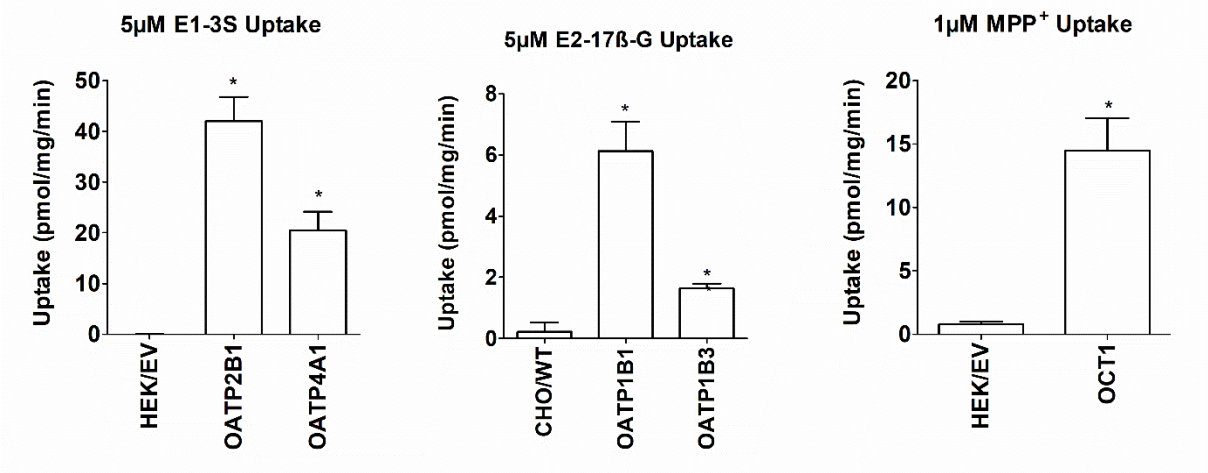


**Figure 2-2. Cellular accumulation of model substrates of CHO/OATP1B1, CHO/OATP1B3, CHO/OATP4A1, HEK/OATP2B1, and HEK/OCT1 cell lines.** Cells were incubated in culture media with 5 μM estrone-3-sulfate ($E_1$-3-S) or 5 μM estradiol-17β-glucuronide ($E_2$-17β-G) for 3 min, or 1 μM [$^3$H]-$MPP^+$ for 10 min at 37°C. Reactions were terminated by removing solutions and washing with ice-cold HBSS 3 times. Cells were lysed and intracellular accumulation of compounds was quantified by LC-MS/MS (estron-3-sulfate and estradiol-17β-glucuronide) or TRI-CARB scintillation counter ([$^3$H]-$MPP^+$). Data shown are means ± SD of three independent experiments. Significantly higher uptake of model substrates in cells overexpressing OATPs and OCT1 were observed compared to the uptake in their respective control cell lines. *$p < 0.05$

**Figure 2-3**

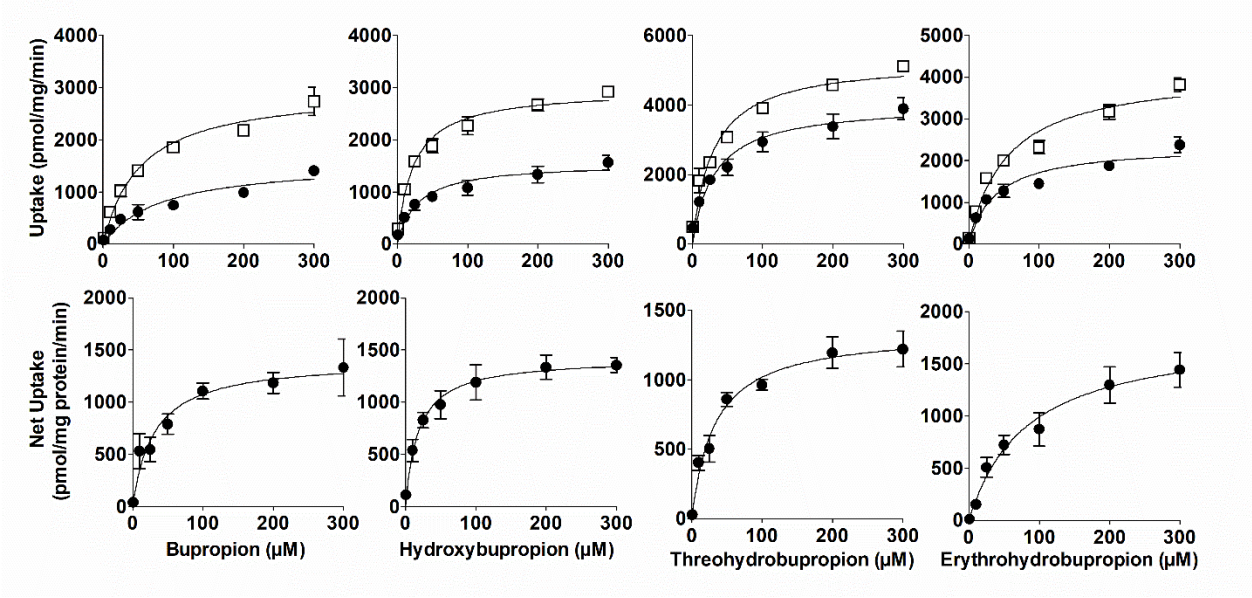


**Figure 2-3. Uptake (upper panels) and net uptake (lower panels) of BUP and metabolites by OATP1B1.** Cells were incubated in culture media with 1 – 300 μM bupropion (BUP), hydroxybupropion (OHB), therohydrobupropion (TB) or erythrohydrobupropion (EB) for 3 min. Uptake was terminated with adding ice-cold buffer and washed, intracellular concentrations were determined by LC-MS/MS. Data shown are means ± SD of three independent experiments. Circles indicate uptake by the parent wild-type CHO cells, and squares indicate uptake by the OATP1B1-overexpressing CHO cells.

**Figure 2-4**

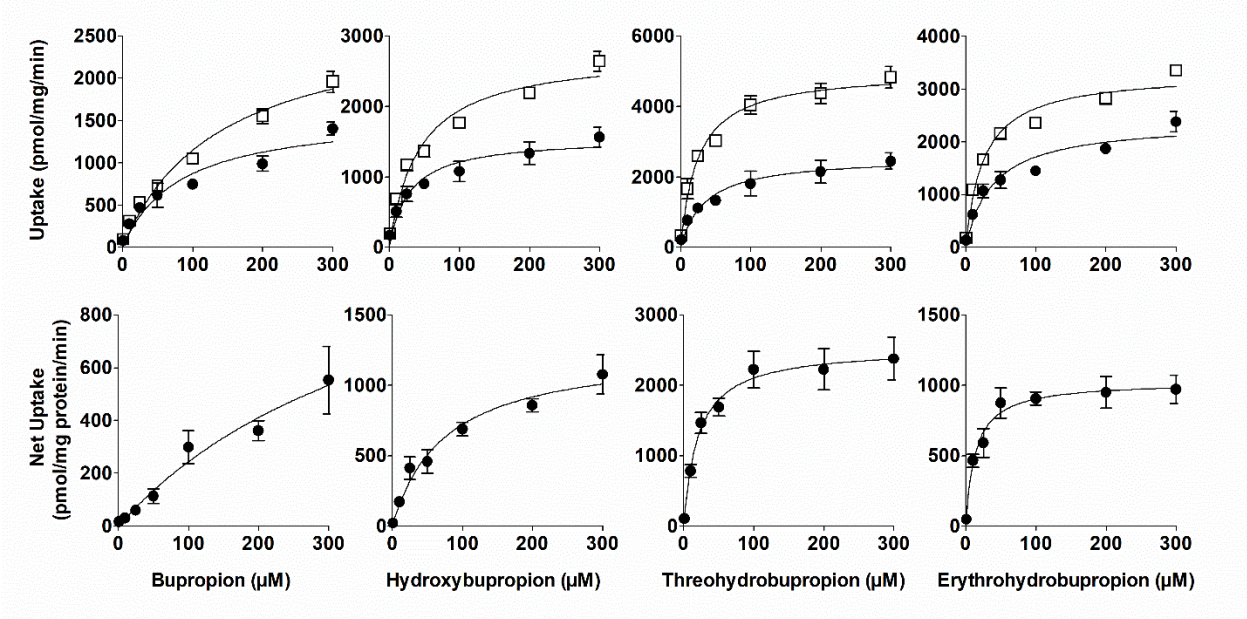


**Figure 2-4. Uptake (upper panels) and net uptake (lower panels) of BUP and metabolites by OATP1B3.** Cells were incubated in culture media with 1 – 300 μM bupropion (BUP), hydroxybupropion (OHB), therohydrobupropion (TB) or erythrohydrobupropion (EB) for 3 min. Uptake was terminated with adding ice-cold buffer and washed, intracellular concentrations were determined by LC-MS/MS. Data shown are means ± SD of three independent experiments. Circles indicate uptake by the wild-type CHO cells, and squares indicate uptake by the OATP1B3-overexpressing CHO cells.

**Figure 2-5**

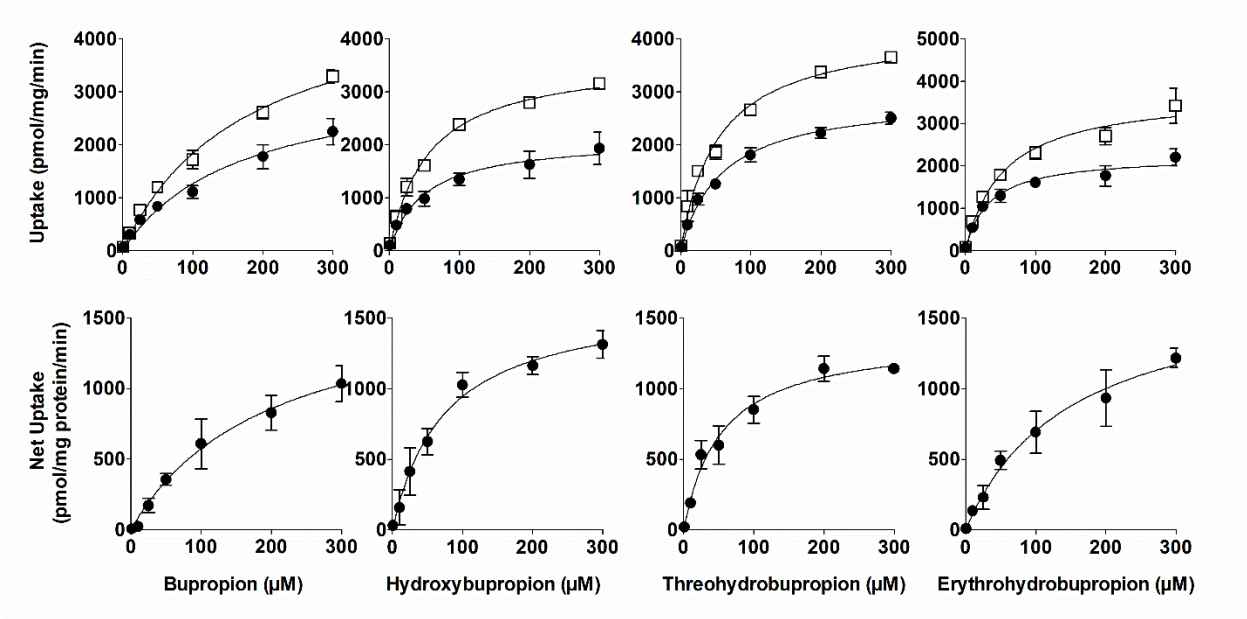


**Figure 2-5. Uptake (upper panels) and net uptake (lower panels) of BUP and metabolites by OATP2B1.** Cells were incubated in culture media with 1 – 300 μM bupropion (BUP), hydroxybupropion (OHB), therohydrobupropion (TB) or erythrohydrobupropion (EB) for 3 min. Uptake was terminated with adding ice-cold buffer and washed, intracellular concentrations were determined by LC-MS/MS. Data shown are means ± SD of three independent experiments. Circles indicate uptake by the empty vector control HEK cells, and squares indicate uptake by the OATP2B1-overexpressing HEK cells.

**Figure 2-6**

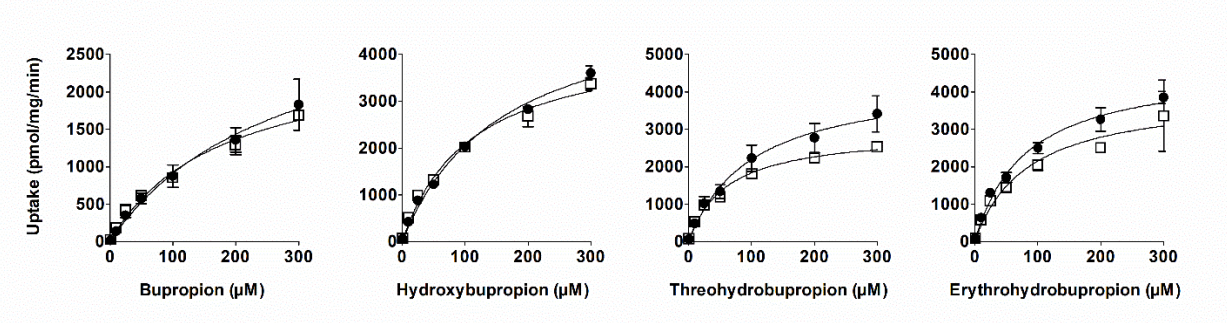


**Figure 2-6. Uptake of BUP and metabolites by OATP4A1**. Cells were incubated in culture media with 1 – 300 μM bupropion (BUP), hydroxybupropion (OHB), therohydrobupropion (TB) or erythrohydrobupropion (EB) for 3 min. Uptake was terminated with adding ice-cold buffer and washed, intracellular concentrations were determined by LC-MS/MS. Data shown are means ± SD of three independent experiments. Circles indicate uptake by the empty vector control HEK cells, and squares indicate uptake by the OATP4A1-overexpressing HEK cells.

**Figure 2-7**

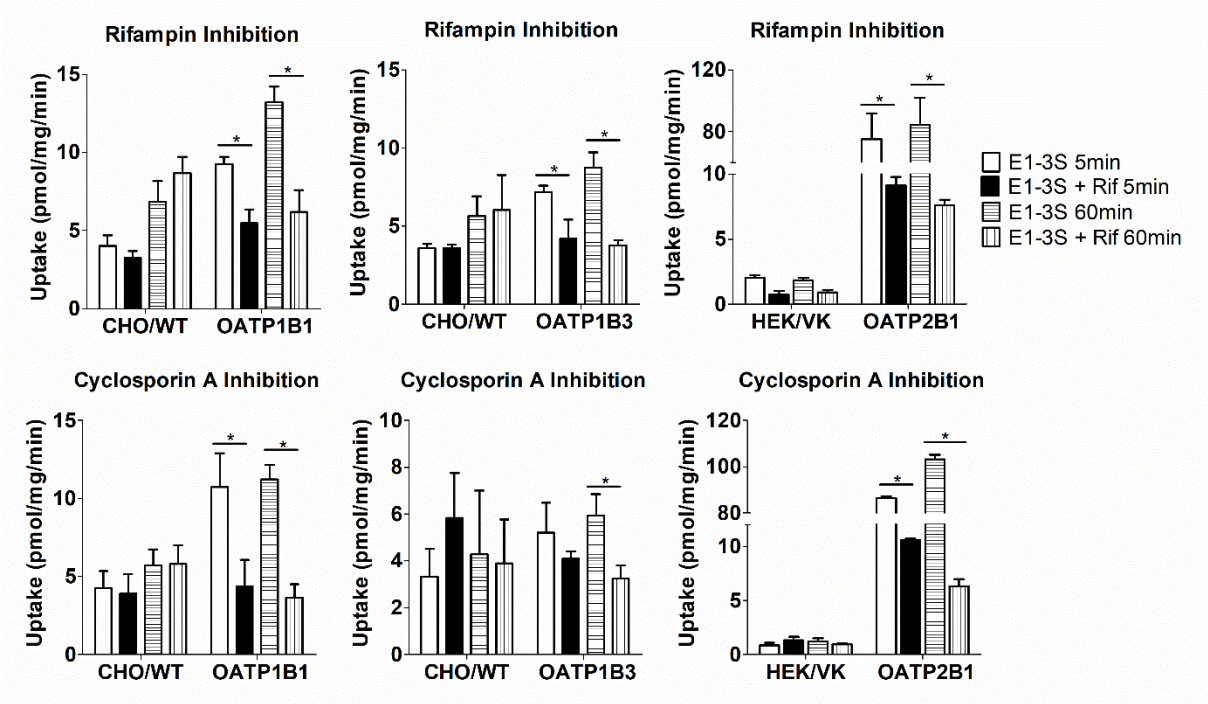


**Figure 2-7. Inhibition of model substrates of CHO/OATP1B1, CHO/OATP1B3, and HEK/OATP2B1 with prototypical inhibitors.** Cells were pre-incubated with 20 μM rifampin or 20 μM cyclosporin A for 5 or 60 min in HBSS at 37°C. The pre-incubation solution was then aspirated and replaced with HBSS containing 5 μM estrone-3-sulfate ($E_1$-3-S) and 20 μM inhibitor, and incubation was continued for 3 min at 37°C. Afterwards, solution was removed and cells were washed 3 times with ice-cold HBSS. Cells were then lysed and intracellular accumulation of estrone-3-sulfate was quantified by LC-MS/MS. Data shown are means ± SD of three independent experiments. Significant reduction in cellular uptake of model substrates was observed in the presence of rifampin or cyclosporin A. No significant difference was observed between 5 min and 60 min pre-incubation with inhibitor. *$p < 0.05$

**Figure 2-8**

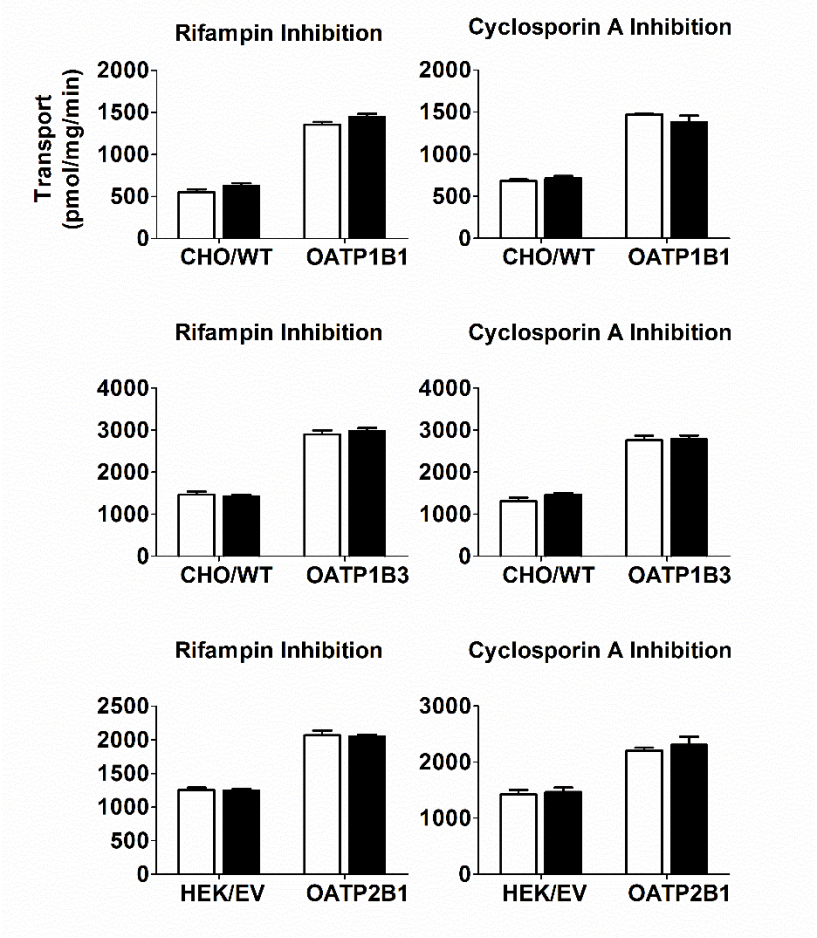


**Figure 2-8. No Inhibition of cellular uptake of BUP by rifampin (left panels) and cyclosporin A (right panels)**. Cells were pre-incubated with an inhibitor (20 μM rifampin or 20 μM cyclosporine A) for 10 min, and then bupropion (BUP) was added to a final concentration of 5 μM and incubation was continued for 3 min. Afterwards, transport was terminated and intracellular concentrations were determined by LC-MS/MS. Open bars indicate uptake of BUP in the absence of an inhibitor, and filled bars indicate uptake of BUP in the presence of an inhibitor. Data shown are means ± SD of three independent experiments. Cells overexpressing OATP1B1, OATP1B1 and OATP2B1 and their corresponding parent (CHO/WT) or empty vector (HEK/EV) control cell were used.

**Figure 2-9**

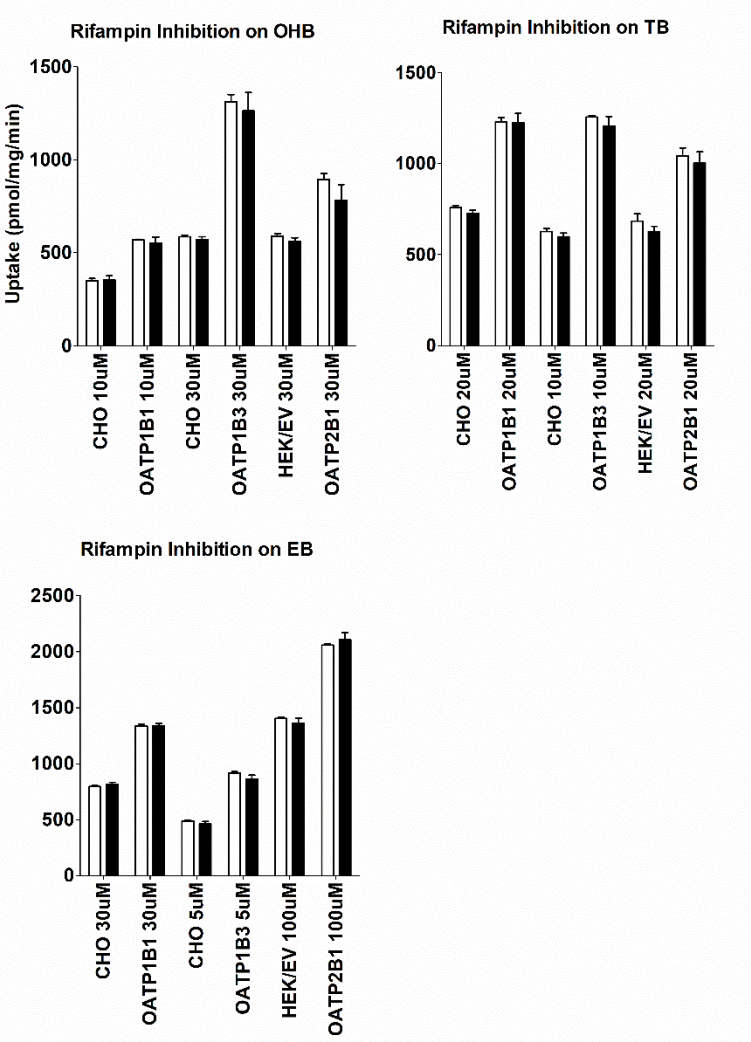


**Figure 2-9. No Inhibition of cellular uptake of OHB, TB, and EB by rifampin.** Cells were pre-incubated with 20 µM rifampin for 10 min, then hydroxybupropion (OHB), threohydrobupropion (TB) or erythrohydrobupropion (EB) was added to a final concentration (shown in the figure) lower than their respective apparent $K_m$. Incubation was continued for 3 min and then immediately terminated. Intracellular concentrations were determined by LC-MS/MS. Open bars indicate uptake of OHB, TB, or EB in the absence of rifampin, and filled bars indicate uptake in the presence of rifampin. Data shown are means ± SD of three

independent experiments. Cells overexpressing OATP1B1, OATP1B1 and OATP2B1 and their corresponding parent (CHO) or empty vector (HEK/EV) control cells were used.

**Figure 2-10**

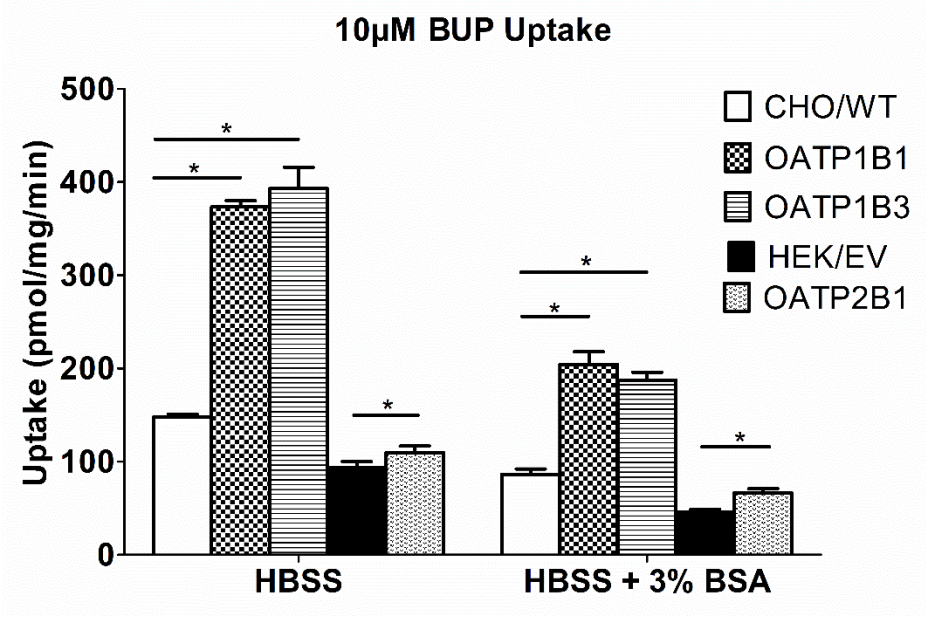


**Figure 2-10. Assessment of non-specific binding of bupropion in CHO/WT, CHO/OATP1B1, CHO/OATP1B3, HEK/EV, and HEK/OATP2B1 cell lines.** Cells were incubated in HBSS containing 10 μM bupropion (BUP) for 3 min at 37°C. Solution was then removed and cells were quickly washed with ice-cold HBSS with or without 3% BSA. Cells were then lysed with acetonitrile and intracellular accumulation of bupropion was quantified using LC-MS/MS. Data shown are means ± SD of three independent experiments. Reduction in cellular uptake was observed after washing in the presence of 3% BSA, indicating non-specific binding of bupropion to cell surface during the uptake process. However, significant net uptake was still observed after accounting for non-specific binding. *$p < 0.05$

**Figure 2-11**

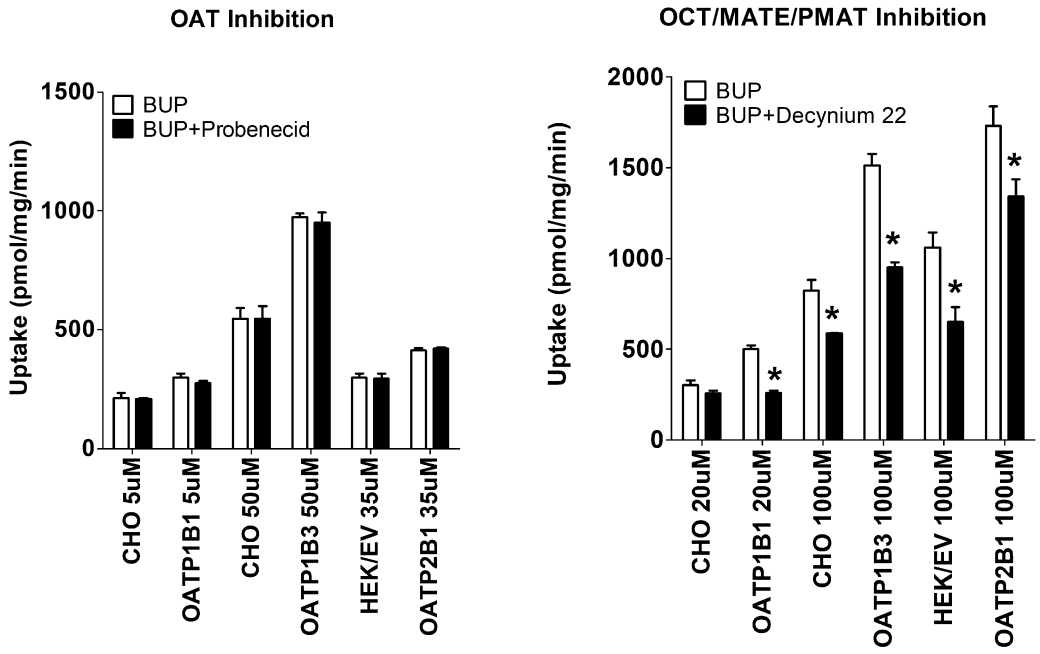


**Figure 2-11. No Inhibition of cellular uptake of BUP by probenecid and decynium-22.** Cells were pre-incubated with an inhibitor (50 μM probenecid or 100 μM decynium-22) for 10 min, and then BUP was added to a final concentration (shown in the figure) lower than their respective apparent $K_{m.}$ Incubation was continued for 3 min. Afterwards, transport was terminated and intracellular concentrations of BUP were determined by LC-MS/MS. Open bars indicate uptake of BUP in the absence of an inhibitor, and filled bars indicate uptake of BUP in the presence of an inhibitor. Data shown are means ± SD of three independent experiments. Differences in uptake of BUP between with and without D-22 were statistically significant with * $p < 0.05$ by one-way ANOVA analysis. Cells overexpressing OATP1B1, OATP1B1 and OATP2B1 and their corresponding parent (CHO) or empty vector (HEK/EV) control cells were used.

**Figure 2-12**

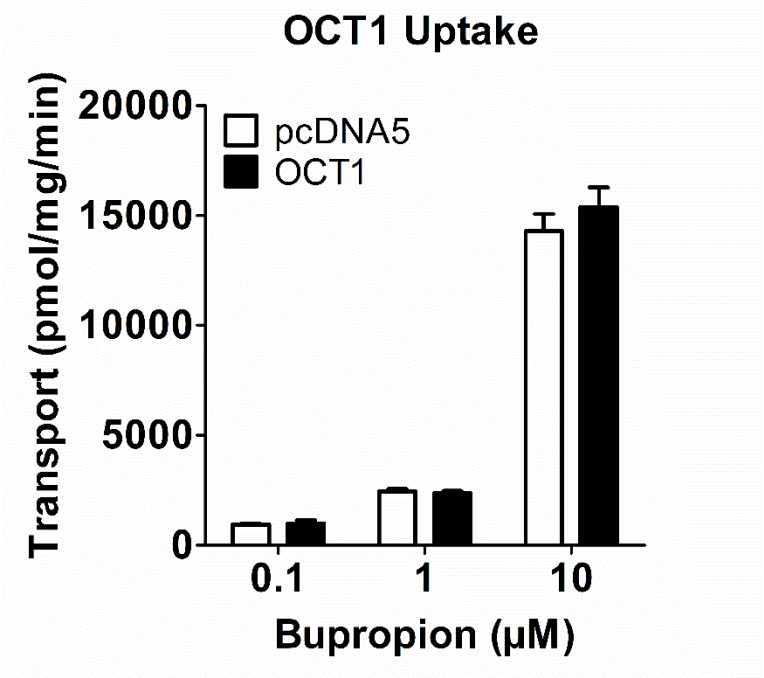


**Figure 2-12. Uptake and net cellular uptake of bupropion and metabolites by OCT1.** Cells were incubated in culture media with 0.1, 1 and 10 μM BUP for 3 min. Uptake was terminated with adding ice-cold buffer and washed, intracellular concentrations were determined by LC-MS/MS. Data shown are means ± SD of three independent experiments. Open bars indicate uptake by the empty vector control HEK cells, and filled bars indicate uptake by the OCT1-overexpressing HEK cells. No statically significant differences in uptake of BUP between the OCT1-oveerexpressing cells and the empty vector control cells were observed.

**Figure 2-13**

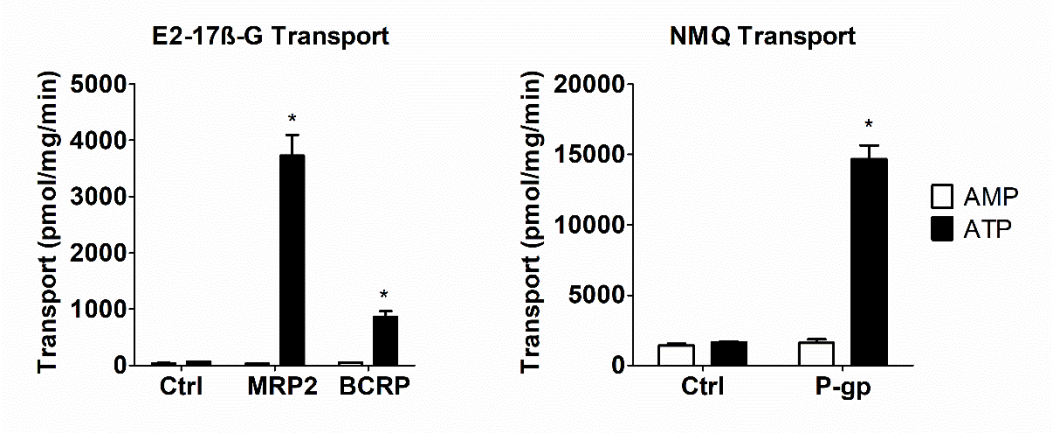


**Figure 2-13. Validation of ATP-dependent uptake of model substrates into the control, MRP2-, BCRP-, and P-gp-overexpressing plasma membrane vesicles.** Membrane vesicles were pre-incubated for 15 min in the absence of ATP or AMP prior to the addition of 50 μM estradiol-17β-glucuronide (model substrate of MRP2 and BCRP) or 1 μM N-methyl-quinidine (model substrate of P-gp). Incubation was continued for 5 min. Transport reactions were then terminated and the assay mixtures were transferred to glass fiber filter plates and rapidly washed over vacuum manifold. Estradiol-17β-glucuronide ($E_2$-17β-G) or N-methyl-quinidine (NMQ) trapped in the membrane vesicles was eluted and quantified by LC-MS/MS. Data shown are means ± SD of three independent experiments. Open bars indicate the vesicle uptake in the presence of AMP. Filled bars indicate the vesicle uptake in the presence of ATP. Significantly higher transport between the presence of ATP and AMP in vesicles overexpressing MRP2, BCRP, and P-gp were observed. *$p < 0.05$

**Figure 2-14**

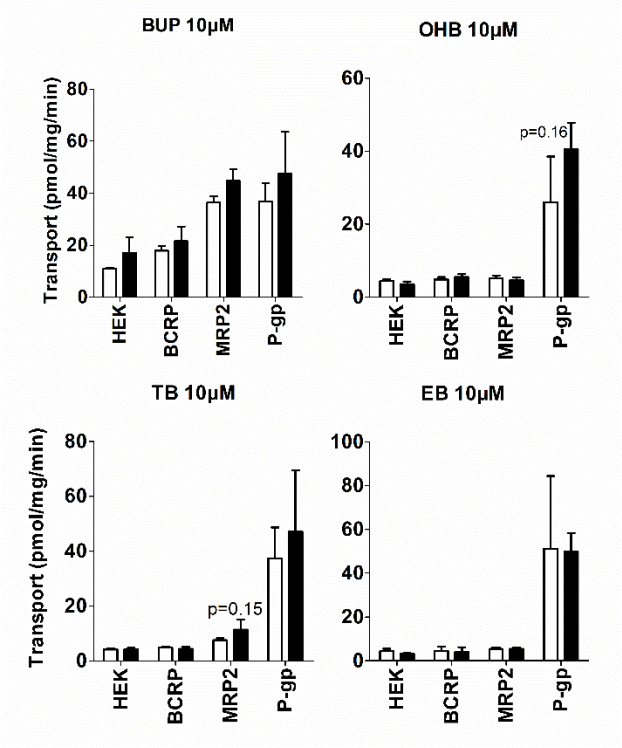


**Figure 2-14. ATP-dependent uptake of BUP and metabolites vesicular transport membrane vesicles overexpressing MRP2, P-gp or BCRP.** Membrane vesicles were pre-incubated for 15 min in the presence of ATP or AMP prior to the addition of BUP, OHB, TB or EB to 1 or 10 µM, and incubation was continued for 1 min. Transport reactions were then terminated and the assay mixtures were transferred to glass fiber filter plates and rapidly washed over vacuum manifold. BUP, OHB, TB or EB trapped in the membrane vesicles was eluted and quantified by LC-MS/MS. Data shown are means ± SD of three independent experiments. Open bars indicate the vesicle uptake of BUP, OHB, TB or EB in the presence of AMP, and filled bars indicate the vesicle uptake in the presence of ATP. No significant differences in vesicle uptake between ATP and AMP were observed.

## 2.6 REFERENCES


1. Slemmer JE, Martin BR, Damaj MI. Bupropion is a nicotinic antagonist. *J. Pharmacol. Exp. Ther.* 2000;295:321–327.

2. Cooper BR, Hester TJ, Maxwell RA. Behavioral and biochemical effects of the antidepressant bupropion (Wellbutrin): evidence for selective blockade of dopamine uptake in vivo. *J. Pharmacol. Exp. Ther.* 1980;215:127–134.

3. Ferris RM, Cooper BR, Maxwell RA. Studies of bupropion's mechanism of antidepressant activity. *J. Clin. Psychiatry*. 1983;44:74–78.

4. Gadde KM, Parker CB, Maner LG, et al. Bupropion for Weight Loss: An Investigation of Efficacy and Tolerability in Overweight and Obese Women. *Obes. Res.* 2001;9:544–551.

5. Skarydova L, Tomanova R, Havlikova L, et al. Deeper Insight into the Reducing Biotransformation of Bupropion in the Human Liver. *Drug Metab. Pharmacokinet.* 2014;29:177–184.

6. Li D-J, Tseng P-T, Chen Y-W, et al. Significant Treatment Effect of Bupropion in Patients With Bipolar Disorder but Similar Phase-Shifting Rate as Other Antidepressants. *Medicine (Baltimore).* 2016;95:e3165.

7. Ng QX. A Systematic Review of the Use of Bupropion for Attention-Deficit/Hyperactivity Disorder in Children and Adolescents. *J. Child Adolesc. Psychopharmacol.* 2016;cap.2016.0124.

8. Verbeeck W, Bekkering GE, Van den Noortgate W, et al. Bupropion for attention deficit hyperactivity disorder (ADHD) in adults. *Cochrane Database Syst. Rev.*

2017;10:CD009504.

9. Findlay JWA, Van Wyck Fleet J, Smith PG, et al. Pharmacokinetics of bupropion, a novel antidepressant agent, following oral administration to healthy subjects. *Eur. J. Clin. Pharmacol.* 1981;21:127–135.

10. Benowitz NL, Zhu AZX, Tyndale RF, et al. Influence of CYP2B6 genetic variants on plasma and urine concentrations of bupropion and metabolites at steady state. *Pharmacogenet. Genomics*. 2013;23:135–141.

11. Schroeder DH. Metabolism and kinetics of bupropion. *J. Clin. Psychiatry*. 1983;44:79–81.

12. Wang X, Abdelrahman DR, Zharikova OL, et al. Bupropion metabolism by human placenta. *Biochem. Pharmacol.* 2010;79:1684–1690.

13. Meyer A, Vuorinen A, Zielinska AE, et al. Formation of threohydrobupropion from bupropion is dependent on 11β-hydroxysteroid dehydrogenase 1. *Drug Metab. Dispos.* 2013;41:1671–1678.

14. Bondarev ML, Bondareva TS, Young R, et al. Behavioral and biochemical investigations of bupropion metabolites. *Eur. J. Pharmacol.* 2003;474:85–93.

15. Jefferson JW, Pradko JF, Muir KT. Bupropion for major depressive disorder: Pharmacokinetic and formulation considerations. *Clin. Ther.* 2005;27:1685–1695.

16. Masters AR, Gufford BT, Lu JBL, et al. Chiral Plasma Pharmacokinetics and Urinary Excretion of Bupropion and Metabolites in Healthy Volunteers. *J. Pharmacol. Exp. Ther.* 2016;358.

17. Fokina VM, West H, Oncken C, et al. Bupropion therapy during pregnancy: the drug and

its major metabolites in umbilical cord plasma and amniotic fluid. *Am. J. Obstet. Gynecol.* 2016;

18. Sager JE, Price LSL, Isoherranen N. Stereoselective Metabolism of Bupropion to OH-bupropion, Threohydrobupropion, Erythrohydrobupropion and 4'-OH-bupropion in vitro. *Drug Metab. Dispos.* 2016;

19. Roth M, Obaidat A, Hagenbuch B. OATPs, OATs and OCTs: the organic anion and cation transporters of the SLCO and SLC22A gene superfamilies. *Br. J. Pharmacol.* 2012;165:1260–1287.

20. Wang H, Yan Z, Dong M, et al. Alteration in placental expression of bile acids transporters OATP1A2, OATP1B1, OATP1B3 in intrahepatic cholestasis of pregnancy. *Arch. Gynecol. Obstet.* 2012;285:1535–1540.

21. Kullak-Ublick GA, Ismair MG, Stieger B, et al. Organic anion-transporting polypeptide B (OATP-B) and its functional comparison with three other OATPs of human liver. *Gastroenterology*. 2001;120:525–533.

22. Hagenbuch B, Gui C. Xenobiotic transporters of the human organic anion transporting polypeptides (OATP) family. *Xenobiotica*. 2008;38:778–801.

23. Ronaldson P, Bauer B, El-Kattan A, et al. Highlights From the American Association of Pharmaceutical Scientists/ International Transporter Consortium Joint Workshop on Drug Transporters in Absorption, Distribution, Metabolism, and Excretion: From the Bench to the Bedside - Clinical Pharmacology C. *Clin. Pharmacol. Ther.* 2016;100:419–422.

24. Mao Q, Ganapathy V, Unadkat JD. Drug Transport in the Placenta. *Drug Transp.*

Hoboken, NJ: John Wiley & Sons, Inc.; 2014. p. 341–353.

25. Turpeinen M, Tolonen A, Uusitalo J, et al. Effect of clopidogrel and ticlopidine on cytochrome P450 2B6 activity as measured by bupropion hydroxylation. *Clin. Pharmacol. Ther.* 2005;77:553–559.

26. Tamraz B, Fukushima H, Wolfe AR, et al. OATP1B1-related drug-drug and drug-gene interactions as potential risk factors for cerivastatin-induced rhabdomyolysis. *Pharmacogenet. Genomics*. 2013;23:355–364.

27. Telles-Correia D, Barbosa A, Cortez-Pinto H, et al. Psychotropic drugs and liver disease: A critical review of pharmacokinetics and liver toxicity. *World J. Gastrointest. Pharmacol. Ther.* 2017;8:26–38.

28. Voican CS, Corruble E, Naveau S, et al. Antidepressant-induced liver injury: A review for clinicians [Internet]. Am. J. Psychiatry. American Psychiatric Association; 2014. p. 404–415.

29. Luethi D, Liechti ME, Krähenbühl S. Mechanisms of hepatocellular toxicity associated with new psychoactive synthetic cathinones. *Toxicology*. 2017;387:57–66.

30. Köck K, Brouwer KLR. A perspective on efflux transport proteins in the liver. *Clin. Pharmacol. Ther.* 2012;92:599–612.

31. Choi YH, Yu A-M. ABC transporters in multidrug resistance and pharmacokinetics, and strategies for drug development. *Curr. Pharm. Des.* 2014;20:793–807.

32. Joshi AA, Vaidya SS, St-Pierre M V., et al. Placental ABC Transporters: Biological Impact and Pharmaceutical Significance. *Pharm. Res.* 2016;33:2847–2878.

33. Mason CW, Buhimschi IA, Buhimschi CS, et al. ATP-Binding Cassette Transporter Expression in Human Placenta as a Function of Pregnancy Condition. *Drug Metab. Dispos.* 2011;39:1000–1007.

34. Ni Z, Mao Q. ATP-binding cassette efflux transporters in human placenta. *Curr. Pharm. Biotechnol.* 2011;12:674–685.

35. Mao Q. BCRP/ABCG2 in the Placenta: Expression, Function and Regulation. *Pharm. Res.* 2008;25:1244–1255.

36. Begley DJ. ABC transporters and the blood-brain barrier. *Curr. Pharm. Des.* 2004;10:1295–1312.

37. Miller D. Regulation of ABC transporters at the blood-brain barrier. *Clin. Pharmacol. Ther.* 2015;97:395–403.

38. Mahringer A, Fricker G. ABC transporters at the blood–brain barrier. *Expert Opin. Drug Metab. Toxicol.* 2016;12:499–508.

39. Beckmann TF, Krämer O, Klausing S, et al. Effects of high passage cultivation on CHO cells: a global analysis. *Appl. Microbiol. Biotechnol.* 2012;94:659–671.

40. Gao C, Liao MZ, Han LW, et al. Hepatic transport of 25-hydroxyvitamin D 3 conjugates: a mechanism of 25-hydroxyvitamin D 3 delivery to the intestinal tract. *Drug Metab. Dispos.* 2018;dmd.117.078881.

41. Wang X, Abdelrahman DR, Fokina VM, et al. Metabolism of bupropion by baboon hepatic and placental microsomes. *Biochem. Pharmacol.* 2011;82:295–303.

42. Lau YY, Huang Y, Frassetto L, et al. Effect of OATP1B Transporter Inhibition on the

Pharmacokinetics of Atorvastatin in Healthy Volunteers. *Clin. Pharmacol. Ther.* 2007;81:194–204.

43. Treiber A, Schneiter R, Hausler S, et al. Bosentan Is a Substrate of Human OATP1B1 and OATP1B3: Inhibition of Hepatic Uptake as the Common Mechanism of Its Interactions with Cyclosporin A, Rifampicin, and Sildenafil. *Drug Metab. Dispos.* 2007;35:1400–1407.

44. Annaert P, Ye ZW, Stieger B, et al. Interaction of HIV protease inhibitors with OATP1B1, 1B3, and 2B1. *Xenobiotica*. 2010;40:163–176.

45. Okuda M, Urakami Y, Saito H, et al. Molecular mechanisms of organic cation transport in OCT2-expressing Xenopus oocytes. *Biochim. Biophys. Acta*. 1999;1417:224–231.

46. Ho ES, Lin DC, Mendel DB, et al. Cytotoxicity of antiviral nucleotides adefovir and cidofovir is induced by the expression of human renal organic anion transporter 1. *J. Am. Soc. Nephrol.* 2000;11:383–393.

47. Chu X-Y, Bleasby K, Yabut J, et al. Transport of the Dipeptidyl Peptidase-4 Inhibitor Sitagliptin by Human Organic Anion Transporter 3, Organic Anion Transporting Polypeptide 4C1, and Multidrug Resistance P-glycoprotein. *J. Pharmacol. Exp. Ther.* 2007;321:673–683.

48. Mulato AS, Ho ES, Cihlar T. Nonsteroidal anti-inflammatory drugs efficiently reduce the transport and cytotoxicity of adefovir mediated by the human renal organic anion transporter 1. *J. Pharmacol. Exp. Ther.* 2000;295:10–15.

49. Turpeinen M, Koivuviita N, Tolonen A, et al. Effect of renal impairment on the

pharmacokinetics of bupropion and its metabolites. *Br. J. Clin. Pharmacol.* 2007;64:165–173.

50. Hayer-Zillgen M, Brüss M, Bönisch H. Expression and pharmacological profile of the human organic cation transporters hOCT1, hOCT2 and hOCT3. *Br. J. Pharmacol.* 2002;136:829–836.

51. Ahlin G, Karlsson J, Pedersen JM, et al. Structural Requirements for Drug Inhibition of the Liver Specific Human Organic Cation Transport Protein 1. *J. Med. Chem.* 2008;51:5932–5942.

52. Ahlin G, Hilgendorf C, Karlsson J, et al. Endogenous gene and protein expression of drug-transporting proteins in cell lines routinely used in drug discovery programs. *Drug Metab. Dispos.* 2009;37:2275–2283.

53. Stepanenko AA, Heng HH. Transient and stable vector transfection: Pitfalls, off-target effects, artifacts. *Mutat. Res. Mutat. Res.* 2017;773:91–103.

54. Karlgren M, Vildhede A, Norinder U, et al. Classification of inhibitors of hepatic organic anion transporting polypeptides (OATPs): influence of protein expression on drug-drug interactions. *J. Med. Chem.* 2012;55:4740–4763.

55. Tamai I, Nozawa T, Koshida M, et al. Functional characterization of human organic anion transporting polypeptide B (OATP-B) in comparison with liver-specific OATP-C. *Pharm. Res.* 2001;18:1262–1269.

56. Noe J, Portmann R, Brun M-E, et al. Substrate-Dependent Drug-Drug Interactions between Gemfibrozil, Fluvastatin and Other Organic Anion-Transporting Peptide (OATP)

Substrates on OATP1B1, OATP2B1, and OATP1B3. *Drug Metab. Dispos.* 2007;35:1308–1314.

57. Sai Y, Kaneko Y, Ito S, et al. Predominant contribution of organic anion transporting polypeptide OATP-B (OATP2B1) to apical uptake of estrone-3-sulfate by human intestinal Caco-2 cells. *Drug Metab. Dispos.* 2006;34:1423–1431.

58. Li X, Guo Z, Wang Y, et al. Potential role of organic anion transporting polypeptide 1B1 (OATP1B1) in the selective hepatic uptake of hematoporphyrin monomethyl ether isomers. *Acta Pharmacol. Sin.* 2015;36:268–280.

59. Kalliokoski A, Niemi M. Impact of OATP transporters on pharmacokinetics. *Br. J. Pharmacol.* 2009;158:693–705.

60. Yang X, Hua W, Ryu S, et al. 11 $\beta$ -Hydroxysteroid Dehydrogenase 1 Human Tissue Distribution, Selective Inhibitor, and Role in Doxorubicin Metabolism. *Drug Metab. Dispos.* 2018;46:1023–1029.

61. He J, Yu Y, Prasad B, et al. Mechanism of an unusual, but clinically significant, digoxin-bupropion drug interaction. *Biopharm. Drug Dispos.* 2014;35:253–263.

62. Hemauer SJ, Patrikeeva SL, Wang X, et al. Role of transporter-mediated efflux in the placental biodisposition of bupropion and its metabolite, OH-bupropion. *Biochem. Pharmacol.* 2010;80:1080–1086.

63. Earhart AD, Patrikeeva S, Wang X, et al. Transplacental transfer and metabolism of bupropion. *J. Matern. Fetal. Neonatal Med.* 2010;23:409–416.

64. Nishikawa M, Iwano H, Yanagisawa R, et al. Placental transfer of conjugated bisphenol A

and subsequent reactivation in the rat fetus. *Environ. Health Perspect.* 2010;118:1196–1203.

65. Sager JE, Price LSL, Isoherranen N. Stereoselective Metabolism of Bupropion to OH-bupropion, Threohydrobupropion, Erythrohydrobupropion, and 4'-OH-bupropion in vitro. *Drug Metab. Dispos.* 2016;44:1709–1719.

66. Zhou Q, Yu L-S, Zeng S. Stereoselectivity of chiral drug transport: a focus on enantiomer–transporter interaction. *Drug Metab. Rev.* 2014;46:283–290.

# CHAPTER 3: EFFECT OF *N*-ACETYLTRANSFERASE 2 (NAT2) GENOTYPE ON THE PHARMACOKINETICS OF HYDRALAZINE DURING PREGNANCY

This work was previously published by Han et al. in *Journal of Clinical Pharmacology* **2019**;59(12):1678-1689.



## 3.1 INTRODUCTION

Hypertensive disorders during pregnancy include gestational hypertension, chronic hypertension, preeclampsia, and chronic hypertension with superimposed preeclampsia. These disorders have been on the rise over the past two decades and affect up to 10% of pregnant women [1–3]. Some of the complications associated with severe hypertensive disorders in pregnancy includes placental abruption, kidney injury, liver injury, cerebral hemorrhage, seizures, fetal growth restriction, preterm birth, and in some cases maternal or fetal demise [4]. Treatment initiation criteria and hypertension management approaches vary [4–7]. Among other drugs, hydralazine is one of the antihypertensive drugs recommended by The American College of Obstetricians and Gynecologists for pregnant women due to its efficacy in lowering total peripheral resistance (TPR) and relative safety for the mother and fetus [4].

The parent compound, hydralazine, is responsible for the significant decrease in systemic vascular resistance, mean arterial pressure, compensatory increase in cardiac output, and stroke volume [8]. It is extensively metabolized and only 10% of unchanged drug is recovered in the urine [9]. Hydralazine is highly protein bound and unstable in blood under physiological

conditions [10]. The predominate circulating form (>90%) is the acid-labile inactive metabolite hydralazine pyruvic acid hydrazone (HPH) [11–13]. However, only 6% of an oral dose is recovered in the urine as HPH [14]. In addition, hydralazine readily forms another acetone hydrazone (HAH) that is reportedly equipotent as the parent compound [15,16]. Iwaki et al. reported that HAH is capable of reacting with pyruvic acid and forming HPH [17]. Despite being pharmacologically active, HAH does not circulate abundantly due to its instability *in vivo* and thus is generally considered a minor contributor to the overall anti-hypertensive effect [9,17,18]. Descriptions of hydralazine PK have varied over time due to lack of specificity of early hydralazine assays, which failed to avoid the acid-catalyzed hydrolysis of HPH to release hydralazine during derivatization reactions; as a result, earlier quantification of plasma hydralazine concentrations were, in reality, a combination of the parent compound and the acid-labile hydrazones [11,12]. This was later referred to as "apparent" hydralazine. The majority of the dose was recovered in the urine as the inactive sequential metabolites of 3-methyl-1,2,4-triazolo[3,4-a]phthalazine (MTP) [9]. MTP formation occurs via *N*-acetyltransferase 2 (NAT2) [19,20]. MTP is further hydroxylated and eliminated as glucuronide conjugates. A summary of the metabolic pathway schematic is shown in Figure 3-1. NAT2 is a genetically determined polymorphic enzyme. In non-pregnant subjects, hydralazine plasma concentrations reportedly varied up to 15-fold between slow and rapid acetylator phenotypes [21–25]. Higher frequency of hydralazine induced adverse effects, including systemic lupus erythematosus, has been reported in non-pregnant NAT2 slow acetylators compared to rapid acetylators [22]. In the same study, NAT2 rapid acetylators failed to achieve adequate blood pressure reduction with hydralazine [22]. Both increased risk of adverse effects in slow acetylators and reduced efficacy in rapid

acetylators suggest a significant role of NAT2 genotype in hydralazine PK and variation in response.

As a result of NAT2-mediated polymorphic first-pass metabolism, the systemic oral bioavailability of parent drug is ~16% for rapid acetylators and ~35% for slow acetylators in non-pregnant individuals [26]. This difference in first-pass metabolism can be explained by genetically determined differential expression of NAT2 in the intestines and liver [27–29]. In non-pregnant adults, the peak plasma concentration of hydralazine occurs within an hour after dose, and the elimination half-life typically ranges from 1 to 4 hours [13,30,31].

Earlier studies of hydralazine exposure during gestation were limited to blood samples collected at the time of delivery or postpartum [32,33]. These studies demonstrated trans-placental fetal exposure to hydralazine with mean umbilical cord-to-maternal plasma concentration ratio of 2 ± 2.5 at the time of birth. Postpartum studies have reported the presence of hydralazine in the breast milk with mean breast milk-to-maternal plasma concentration ratio of 0.8 ± 0.5[32,33]. Rigorous intensive sampling PK studies of hydralazine and its metabolites during pregnancy have not been reported. Although the impact of NAT2 genotype on hydralazine PK has been studied in the non-pregnant population, little is known regarding the effect of NAT2 on hydralazine and its metabolites during pregnancy. The main objective of our study was to describe the PK of hydralazine during pregnancy and evaluate the effects of NAT2 genotype on steady-state PK of hydralazine and its metabolite MTP during pregnancy.

## 3.2 MATERIALS AND METHODS

### SUBJECTS

The study was approved by the institutional review board at the University of Washington and was conducted in accordance with its guidelines. Written informed consent was obtained from all subjects. We examined steady-state, whole blood hydralazine and plasma MTP PK in 12 pregnant women receiving hydralazine for therapeutic reasons. Women who had a hematocrit less than 28% were excluded from the study.

### DOSING REGIMENS

Oral hydralazine hydrochloride (5 – 25 mg four times daily) was prescribed to women with hypertension, and dosages titrated according to clinical need without regard to the study. As previously described, a validated, noninvasive, Doppler technique (Ultracom Cardiac Output Monitor, Laurence Medical, Redmond WA) was utilized to measure hemodynamics prior to and during oral hydralazine treatment for clinical titration of antihypertensive agents [34]. Hemodynamic measurements were collected for clinical purposes. The timing relative to dosing was variable and not specified. The oral hydralazine tablets [Teva Pharmaceutical Industries (Petah Tikva, Israel)] were provided by the investigators for the 3 days prior to the study day and dosing times were recorded on a calendar during this time period. Calendar checks and pill counts were conducted to assess adherence. Hydralazine was taken every 6 hours for the 3 days prior to the study. As food is known to increase the absorption of hydralazine [35–39], subjects were asked to fast for at least 5 hours prior to study dose administration on the day of the PK study, and for another hour post-dosing to minimize food interaction effects. Participants were encouraged to drink clear liquids during the fasting period.

### SAMPLE COLLECTION AND ANALYSIS

Serial blood samples were collected from an indwelling venous catheter over one dosing interval (pre-dose, then 0.5, 1, 1.5, 2, 3, 4 and 6 hours after dosing) to determine hydralazine and MTP steady-state concentrations. Five subjects completed mid- (22-26 weeks gestation) and 8 subjects completed late-pregnancy (30-38 weeks gestation) study days. Of these participants, one subject completed both mid- and late-pregnancy studies. Concomitant medications were also recorded. One subject's samples had to be collected over three dosing intervals due to the subject's clinical situation, but dosing every 6 hour was maintained throughout the study period.

Semple et al. previously reported an HPLC-UV assay for hydralazine in blood as its stable *p*-nitrobenzaldehyde hydrazine, with the distinct advantages of avoiding hydrolysis of acid-labile hydrazone metabolites by achieving rapid and quantitative derivatization at physiological pH, and having a stable hydrazine derivative that allowed derivatized blood samples to be stored at -80 ℃ for long periods of time pending further processing and analysis [40]. We improved the specificity and sensitivity of the assay by deploying mass spectrometric detection. Furthermore, all blood samples were derivatized immediately upon their collection to minimize instability of hydralazine in blood. The *N*-acetylated metabolite MTP in plasma was analyzed by adapting the procedure described by Reece et al. to an LC-MS/MS method. Handling, processing and analysis of blood and plasma samples for the respective measurement of hydralazine and MTP are briefly described below [41].

Whole blood was collected in EDTA vacutainer tubes, which stabilizes the chemical integrity of hydralazine, and placed into wet ice. Immediately after collection, 1 mL of the whole blood was added to a 15 mL polypropylene centrifuge tube containing 1 mL of 0.1 M sodium citrate (pH 6) and 75 μL of 0.1 mg/mL *p*-nitrobenzaldehyde in dioxane [40]. Duplicate tubes

were prepared. Internal standard (40 ng 1-hydrazino-4-methyl phthalazine in acidified methanol) was added to each tube. The samples were then vortexed vigorously, placed on a horizontal rocker-shaker and mixed gently at room temperature for 45 min. The samples were then immediately frozen on dry ice. Samples were stored at -80° C for 4-14 months for 9 subjects and 2.5-3 years for 4 subjects until extraction and analysis. Stability testing over two years showed minimal to no degradation. Remaining whole blood was centrifuged at 1500 x g for 5 min at 4° C. Calibration and quality assurance samples were prepared by spiking plasma with MTP (5 – 250 ng/mL) and treating in the same fashion as a subject sample.

Buccal swab samples were collected from each subject and frozen at -80$^{o}$ C for 2-6 years until DNA extraction and analysis.

**SAMPLE EXTRACTION**

For hydralazine, 5 mL of 98.5:1.5 heptane:isoamyl alcohol was added to each calibration, quality assurance and subject sample. They were placed on a reciprocating shaker set at 250 cycles per minute for 20 minutes at room temperature, and centrifuged at 2000 x g for 5 minutes. Tubes were then frozen on dry ice, and organic layer decanted to 12 x 75 mm culture tubes. Another 3 mL of 98.5:1.5 heptane:isoamyl alcohol was added to the frozen aqueous layer, allowed to thaw either at room temperature or in a tepid water bath, and the extraction procedure was repeated. Combined heptane:isoamyl alcohol extracts were evaporated under a gentle stream of air at 35-40° C, and reconstituted in 100 μL acetonitrile. Reconstituted extracts were transferred to 96-well plate, and 2 μL was injected onto the high-performance liquid chromatography (LC) system with mass spectrometry (MS) detection.

For MTP, internal standard (40 ng 3-trifluoromethyl-s-triazolo[3,4α]phthalazine or MTP-F3) in 0.25 mL of 0.1 M borate buffer (pH 8.9) and 3 mL ethyl acetate was added to calibration,

quality assurance, and subject samples. Samples were extracted in a similar manner as with hydralazine, but the residue reconstituted in 125 µL of 50:50 0.1% formic acid in water:methanol. The extract was transferred to a 0.5 mL micro-centrifuge tube and centrifuged at 14,000 x g for 10 minutes at 4° C. The extract was then transferred to 96-well plate, and 2 µL was injected onto the LC-MS/MS.

### WHOLE BLOOD HYDRALAZINE AND PLASMA MTP LC-MS ANALYSIS

Hydralazine concentrations and internal standards were detected and quantified as *p*-nitrobenzaldehyde hydrazones, and analyzed using an AB Sciex QTRAP 6500 LC-MS/MS (Concord, ON Canada). HPLC separation was achieved on an Agilent SB-Phenyl column (150mm x 2.1mm x 5 µm; Agilent Technologies, Santa Clara, CA) maintained at 30° C. The mobile phase consisted of A) 30% 20 mM ammonium formate (pH 3.3), and B) 70% methanol delivered isocratically in a proportion of 30:70; flow rate was set at 0.3 mL/min. Total run time was 6 minutes, and sample tray was kept at 4° C. The mass spectrometer was operated in positive API-ES mode. Multiple reaction monitoring transitions for hydralazine and internal standard (1-hydrazino-4-methyl phthalazine) were *m/z* 294.0 > 145.1 and *m/z* 308.2 > 158.9, respectively. Mass spectrometer conditions were optimized to the following conditions: 350° C drying gas temperature, 100° C quadrupole temperature, 10 L/min nitrogen drying gas flow rate, 35 psi nebulizer pressure, 3200 V capillary voltage. Fragmentor voltage was 135 V for hydralazine and 125 V for the internal standard. Collision energy was 20 V for hydralazine and 24 V for the internal standard. Dwell time was 100 msec for both. Retention time for hydralazine was 3.7 min and for internal standard was 4.0 min. The relationship between peak area ratio for hydralazine to 1-hydrazino-4-methyl phthalazine and hydralazine concentration was analyzed by second order polynomial regression that included origin and 1/x weighting to determine the

respective coefficients of the calibration curve. The limit of detection was 0.02 ng/mL and limit of quantification was 0.04 ng/mL. The coefficient of variance for both were under 20% at respective signal-to-noise ratio of 24:1 and 49.2:1.

For MTP LC-MS/MS analysis, an Agilent Technologies (Santa Clara, CA) 1100 series HPLC coupled to a model G1946D mass spectrometer was used. Agilent Chemstation (version B.03.02) was used for instrument control. HPLC was performed on an Advanced Chromatography Technologies (Aberdeen, Scotland) ACE C8 column (150 mm x 2.1 mm x 3 μm) maintained at 3° C. The mobile phase consisted of A) 0.1% formic acid in water and B) methanol delivered isocratically at a 50:50 proportion. The flow rate was 0.25 mL/min, and the autosampler tray was kept at 4° C. Total run time was 8.5 min. The mass spectrometer was operated in positive electrospray mode and selected ion monitoring (SIM) was used in unit resolution. The transition ions monitored for MTP and its internal standard (MTP-F3) were *m/z* 185.0 and *m/z* 239.0, respectively. Mass spectrometer conditions were identical to that of hydralazine analysis method, except that capillary voltage was 1000 V. The fragmentor voltage for MTP was 160 V and for internal standard was 60 V. Dwell time was 289 msec for both. Retention time for MTP was 3.1 min, and for MTP-F3 was 5.1 min. Quantification of MTP was performed in the same fashion as hydralazine. Limit of detection and quantification for MTP was 1.5 ng/mL, with coefficient of variance under 5% at respective signal-to-noise ratio of 6.6:1 and 19.8:1.

For MTP LC-MS/MS analysis, an Agilent Technologies (Santa Clara, CA) 1100 series HPLC coupled to a model G1946D mass spectrometer was used. Agilent Chemstation (version B.03.02) was used for instrument control. HPLC was performed on an Advanced Chromatography Technologies (Aberdeen, Scotland) ACE C8 column (150 mm x 2.1 mm x 3

μm) maintained at 3° C. The mobile phase consisted of A) 0.1% formic acid in water and B) methanol delivered isocratically at a 50:50 proportion. The flow rate was 0.25 mL/min, and the autosampler tray was kept at 4° C. Total run time was 8.5 min. The mass spectrometer was operated in positive electrospray mode and selected ion monitoring (SIM) was used in unit resolution. The transition ions monitored for MTP and its internal standard (MTP-F3) were *m/z* 185.0 and *m/z* 239.0, respectively. Mass spectrometer conditions were identical to that of hydralazine analysis method, except that capillary voltage was 1000 V. The fragmentor voltage for MTP was 160 V and for internal standard was 60 V. Dwell time was 289 msec for both. Retention time for MTP was 3.1 min, and for MTP-F3 was 5.1 min. Quantification of MTP was performed in the same fashion as hydralazine. Limit of detection and quantification for MTP was 1.5 ng/mL, with coefficient of variance under 5% at respective signal-to-noise ratio of 6.6:1 and 19.8:1.

### NAT2 Genotyping Analysis and Inferred Phenotype

Buccal cell DNA was isolated using QIAGEN DNeasy Blood & Tissue Kit (Hilden, Germany) according to manufacturer's instructions. Single nucleotide polymorphisms (SNP) in the *NAT2* coding region and their corresponding haplotypes were determined using four-SNP assays, i.e., rs181280, c.341T>C; rs1799930, c.590G>A; rs1799931, c.857G>A; rs1801279, c.191G>A, with TaqMan Assays from Thermo Fisher Scientific (Waltham, MA). Subjects were classified as slow acetylators (SA) if they had 2 reduced-activity *NAT2* alleles (**5, *6, *7,* or **14*), or rapid acetylators (RA) if they carried 1 reduced-activity allele and 1 fully functional allele (**4*), or 2 fully functional alleles [42]

### PHARMACOKINETIC ANALYSIS

Non-compartmental, steady-state PK parameters were estimated using Phoenix WinNonlin (Princeton, NJ). Steady-state area under the concentration-time curve ($AUC_{\tau}^{ss}$) was calculated using linear trapezoidal method for ascending concentrations and log trapezoidal method for descending concentrations over one dosing interval (0-6 hours). Apparent oral clearance was determined by $CL/F = dose/AUC_{\tau}^{ss}$ and apparent oral volume of distribution by $V_z/F = (CL/F)/k_{el}$, in which $k_{el}$ was the elimination rate constant estimated using log-linear regression of terminal decline in concentration and F was bioavailability. The terminal elimination half-life was determined by $t_{1/2,z} = \ln(2)/k_{el}$. $T_{max}$ and $C_{max}$ were determined directly from the concentration-time profiles. The metabolite to parent area under the concentration-time curve ratio was calculated using $AUC_{\tau}^{ss}$(MTP)/$AUC_{\tau}^{ss}$(hydralazine). Actual body weight for each participant was used for weight adjusted parameter estimates. For comparison purposes, AUC and $C_{max}$ were dose-normalized to 10-mg every 6 hours. For one subject with a measured concentration just below the limit of quantification, group PK analyses were performed including and excluding the data point. Because inclusion of the measured concentration below limit of quantification did not alter group PK means, we included this data point in the final analysis.

### STATISTICAL ANALYSIS

Mann-Whitney *U* tests were performed to compare PK parameter estimates between RAs and SAs. Linear regression with multiple variables was used to analyze the relationship between PK estimates and the subjects' NAT2 status, gestational age and dose. Only one subject had repeat measurements in mid- and late- pregnancy. Her PK estimates were considered independently for gestational age-dependent PK comparisons. In addition, the average of both of her mid- and late- pregnancy PK estimates was used for NAT2 genotype-dependent PK

comparison. All data analyses were performed with GraphPad Prism (La Jolla, CA) and R[43]. Results are reported as means ± SD unless otherwise stated, and $p < .05$ was considered significant.

## 3.3 RESULTS

### DEMOGRAPHICS

A total of 13 pregnant women consented, but only 12 (7 non-Hispanic White, 3 Asian, and 2 Native Hawaiian/other Pacific Islander) completed at least 1 study day. Among the 12 subjects, 6 were identified as RAs (*NAT2* genotypes **4/*5* in 2, **4/*6* in 3, and **4/*7* in 1) and 6 were identified as SAs (*NAT2* genotypes **5/*5* in 1, **5/*6* in 2, **5/*7* in 1, and **6/*6* in 2). Five subjects were mid-pregnancy at the time of study, and eight were late-pregnancy. Table 3-1 presents the demographics for subjects studied in mid- and late-pregnancy. There were no significant differences in age, height, weight, or wrist circumferences between RAs and SAs. There was no significant difference between mid-pregnancy and late-pregnancy in body weight (122 ± 41 kg vs 108 ± 38 kg) or age (32 ± 5.9 yrs vs 35 ± 8.3 yrs). The average height, weight and wrist circumference of all subjects were 163 ± 6 cm, 113 ± 38 kg and 6.3 ± 0.8 inches, respectively. The hydralazine dosage ranged from 5 to 25 mg orally every 6 hours. There was no statistical difference between doses taken by RAs versus SAs (10.7 ± 6.7 mg vs 17.5 ± 8.2 mg, $p = .1$). All subjects were also taking atenolol as a part of their hypertension management. Similarly, there was no difference in atenolol dosage taken by RAs compared to SAs, when considered alone or in combination with hydralazine dose ($p = .7$ and $p = 1$, respectively) (see Table 3-1 for doses). None of the concomitant medication or supplements taken by the subjects had known drug interactions with hydralazine PK, and a list of concomitant medications are

included in Table 3-2. No significant difference was seen based on acetylator status in total peripheral resistance at baseline (RA: 1074 ± 192 dyne•sec•cm$^{-5}$ vs SA: 1232 ± 253 dyne•sec•cm$^{-5}$, $p$ = .3) or with hydralazine (RA: 949 ± 237 dyne•sec•cm$^{-5}$ vs SA: 1209 ± 295 dyne•sec•cm$^{-5}$, $p$ = .1). There was also no difference in the change in TPR with hydralazine (RA: -125 ± 272 dyne•sec•cm$^{-5}$ vs SA: -23 ± 130 dyne•sec•cm$^{-5}$, $p$ = .5). No significant difference was seen based on acetylator status in mean arterial pressure (MAP) at baseline (RA: 101 ± 9 mm Hg vs SA: 100 ± 8 mm Hg, $p$ = .8) or with hydralazine (RA: 92 ± 6 mm Hg vs SA: 99 ± 10 mm Hg, $p$ = .2). There was also no difference in change in MAP with hydralazine (RA: -9 ± 12 mm Hg vs SA: -1 ± 9 mm Hg, $p$ = .3). No difference was observed based on acetylator status in heart rate (HR) at baseline (RA: 77 ± 4 BPM vs SA: 73 ± 8 BPM, $p$ = .4) or with hydralazine (RA: 69 ± 9 BPM vs SA: 77 ± 6 BPM, $p$ = .1). There was also no significant difference in change in HR with hydralazine (RA: -8 ± 10 BPM vs SA: 5 ± 13 BPM, $p$ = .1).

### PLASMA HYDRALAZINE AND MTP CONCENTRATIONS AND KINETICS

Mean steady-state, concentration-time profiles for hydralazine comparing RAs and SAs are depicted in Figure 3-2, and all PK parameter estimates are summarized in Table 3-3. In SAs, mean hydralazine dose-normalized $AUC_{\tau}^{ss}$ was 408% larger ($p$ < .05), dose-normalized $C_{max}$ 525% higher ($p$ < .05), weight-adjusted CL/F 71% slower ($p$ < .05), and weight-adjusted $V_z$/F was 68% smaller ($p$ < .05) than in RAs.

Figure 3-3 depicts the mean, dose-normalized, steady-state plasma MTP concentration-time profiles for RAs and SAs. In SAs, mean MTP dose-normalized Cmax was 53% lower ($p$ < .05), and steady-state, dose-normalized AUC was 52% smaller ($p$ < .05) than in RAs. Mean MTP/hydralazine AUC ratio among the SAs was 10% that of the RAs ($p$ < .05). Terminal half-life was similar in SAs and RAs ($p$ = .6), and comparable to that of parent hydralazine.

### GESTATIONAL AGE EFFECTS

Blood or plasma concentration-time curves for the subject that completed mid- and late-pregnancy study days are depicted in Figure 3-4A for hydralazine and in Figure 3-4B for MTP. This subject took the same hydralazine dose (10 mg every 6 hours) during both mid- and late-pregnancy studies. Hydralazine apparent oral clearance adjusted for weight in mid- and late pregnancy were 85.4 and 81.3 L/h/kg, respectively. Hydralazine area under the concentration-time curve was 0.6 ng•h/mL for both mid- and late pregnancy. Elimination half-life was 3.7 and 3.0 h, and metabolite-to-parent ratio was 100 and 76 for mid- and late pregnancy, respectively.

The influence of NAT2 genotype and gestational age on weight-adjusted apparent oral clearance (Figure 3-5A), apparent oral volume of distribution (Figure 3-5B), and MTP/hydralazine AUC ratio (Figure 3-5C) were analyzed by multiple linear regression. There was a significant effect of NAT2 genotype on weight-adjusted CL/F ($\beta$ = -50.3, SE = 6.6, $p$ < .001), weight-adjusted $V_z/F$, ($\beta$ = -191.2, SE = 52.1, $p$ < .01) and MTP/hydralazine AUC ratio ($\beta$ = -67.8, SE = 13, $p$ < .001). However, gestational age did not affect weight-adjusted CL/F ($\beta$ = 1.9, SE = 6.7, $p$ = .8), weight-adjusted $V_z/F$ ($\beta$ = 26.2, SE = 53.3, $p$ = .6) or MTP/hydralazine AUC ratio ($\beta$ = -11.0, SE = 13.3, $p$ = .4). In addition, dose did not significantly affect any of these parameters (CL/F, $\beta$ = -0.8, SE = 0.4, $p$ = 0.09; $V_z/F$, $\beta$ = -2.9, SE = 3.6, $p$ = .4; and $AUC_{MTP}/AUC_{hydralzine}$, $\beta$ = -0.6, SE = 0.9, $p$ = .5).

## 3.4 DISCUSSION

Hydralazine is an antihypertensive agent commonly prescribed during pregnancy. However, its PK and impact of NAT2 genotype during gestation have not been investigated. In this study we characterized for the first time the PK of oral hydralazine and its metabolite MTP

during pregnancy. Similar to previous reports in the non-pregnant population, oral hydralazine PK during pregnancy exhibited dependence upon NAT2 genotype [13,30,44,45]. Pregnant subjects with NAT2 RA genotypes exhibited significantly higher apparent oral clearance and apparent oral volume of distribution of hydralazine compared to women with SA genotypes. In addition, MTP-to-hydralazine AUC ratio was significantly higher in pregnant subjects with NAT2 RA genotypes.

The marked distinction in PK between NAT2 rapid and slow acetylators is likely in part due to a difference in the oral bioavailability of hydralazine as a result of disparity in rate and extent of acetylation during first pass. Oral bioavailability (F) of a drug is governed by the percentage of parent drug that passes from the gut lumen into the mucosa (Fa), through the gut mucosa into the vasculature (Fg), and finally through the liver (Fh) into systemic circulation. NAT2 is known to be abundantly expressed in the small intestine and liver [29]. In non-pregnant subjects, the bioavailability of hydralazine was reportedly 2.2-fold lower in RA than SA subjects [26]. We report a 2.5-fold difference in apparent oral volume of distribution (V/F), and nearly 3.5-fold difference in apparent oral clearance (CL/F) between RA and SA pregnant subjects. Small changes in NAT2 activity during pregnancy have been described [46]. Furthermore, the ~10-fold difference in MTP/hydralazine AUC ratio in pregnant subjects matched that of a previous study that found a 10-fold difference in urinary MTP/hydralazine ratio between RA and SA non-pregnant subjects [47]. This result is consistent with the current knowledge that MTP is primarily formed by *N*-acetylation via NAT2 [48]. While it is possible that there are compensatory mechanisms that would increase elimination of hydralazine by other pathways, any such effect is expected to be minor as metabolism to MTP is the dominant pathway for hydralazine elimination [9,49].

While there was a marked difference in hydralazine AUC between NAT2 genotypes, we did not find an association with genotype and hydralazine dosage needed for therapeutic reasons. In fact, contrary to what we expected, we saw a non-significant but numerically higher average dosage in the SA group. We explored gestational age, body weights, demographics, baseline hemodynamics and concomitant medication dosage, but did not find an explanation for this unexpected finding. A study in healthy non-pregnant volunteers demonstrated that higher hydralazine dose was needed for NAT2 RAs to achieve comparable hydralazine AUC as with the SAs [50]. A large study in non-pregnant subjects showed that RAs did not achieve adequate therapeutic effect with oral hydralazine, suggesting that NAT2 acetylation status might be important in pharmacodynamic response to oral hydralazine [22]. This too was not observed in our study. The lack of difference in dosage as well as pharmacodynamic response seen in our study between NAT2 RAs and SAs is likely multifactorial. First, this study was not adequately powered to assess these outcomes. Second, the hemodynamic measurements reported in this study were not performed for research purposes and not controlled for timing relative to dosing. Therefore, the ability to interpret these outcomes is confounded. Third, the patients participating in this study had their hydralazine titrated based on clinical response without regard to the study. Physician discretion on target endpoint for blood pressure control likely contributed to variability in dosage and pharmacodynamic response. Fourth, hydralazine was administered as part of combination therapy, which included atenolol for blood pressure management. Therefore, interpretation of hemodynamic changes were confounded by concomitant treatment. Lastly, intersubject variability likely contributed to our inability to detect differences.

Nevertheless, the increased exposure of hydralazine among pregnant SAs may still be of clinical concern. Earlier studies in the non-pregnant population demonstrate that *N*-acetylation is

a saturable process for hydralazine and other NAT2 drug substrates (e.g., procainamide and isoniazid) [9,51–53]. Although we did not see a significant dose-dependent effect in our study, our sample size was relatively small and dosage range was limited to 5-25 mg. Previous hydralazine PK studies reported nonlinearity with single doses higher than 100-150 mg [9]. Since both pharmacological activity as well as toxicity are attributed to parent drug exposure, caution is suggested with high-dose hydralazine during pregnancy [54–56]. Adverse effects and complications when parenteral hydralazine is needed during pregnancy include placental abruption, increased risk of surgical delivery, maternal oliguria, altered fetal heart rate, and low Apgar scores at one minute[57]. NAT2 SAs, especially in female patients, have been found to have increased risk of developing severe adverse events (e.g. systemic lupus erythematosus) with high-dose hydralazine (> 200 mg/day) [54]. While the current study did not address the extent of fetal exposure to hydralazine, previous studies have reported trans-placental passage of hydralazine through measurement of umbilical cord hydralazine concentrations at the time of delivery [32,33]. Thus, high inter-individual variability in maternal hydralazine PK during pregnancy due to NAT2 polymorphism may not only affect maternal efficacy with low concentrations in RAs, but in SAs there may be increased maternal and fetal exposure to hydralazine and potential toxicity. Furthermore, NAT2 protein and activity were detected in term placentas, suggesting potential for placental metabolism of hydralazine [58]. Fetal metabolism of hydralazine has not been shown, but a pediatric study using isoniazid (another NAT2 substrate) reported lower NAT2 activity in neonates compared to older children [59]. While fetal metabolism contribution to overall maternal hydralazine PK is expected to be small, fetal metabolism can play a role in enhancing toxicity or minimizing adverse effects of drugs and toxins in the fetus. Although published data is conflicting [60], Shi et al. reported that following

*in utero* exposure to maternal smoking, there was a decreased risk of orofacial clefts in fetuses that expressed low activity NAT2 variants [61]. Additional studies are needed to explore hydralazine maternal and fetal safety in NAT2 SAs.

Since pregnancy results in gestational age dependent effects on numerous drug-metabolizing enzymes, we explored the effects of gestational age on hydralazine PK while accounting for NAT2 genotype. Among our subjects, we did not observe any significant difference in hydralazine PK (apparent oral clearance, apparent volume of distribution and MTP/hydralazine AUC ratio) between mid- and late pregnancy. In the one subject who completed both mid- and late-pregnancy study days, the subject's hydralazine concentration-time profiles were very similar during both gestational windows. Previous work utilizing caffeine as a probe for NAT2 activity reported a 13% lower NAT2 activity in early pregnancy, which returned to baseline by mid-pregnancy. There was no difference in NAT2 activity between mid-pregnancy, late-pregnancy, or postpartum [46].

In evaluating previously published studies on hydralazine PK, there are some key technical problems. For years, quantification of hydralazine and its acid-labile metabolites has been a challenge for researchers due to chemical instability of hydralazine and potential interference from its pyruvate hydrazone metabolite. The present study adapted a previously developed derivatization technique at pH 6 that avoids release of apparent hydralazine from the acid-labile hydrazine metabolites (mainly HPH) and minimized hydralazine instability by performing the derivatization reaction immediately after blood collection [40,62]. Therefore, the present study measured the pharmacologically active parent hydralazine concentrations.

In non-pregnant subjects, the elimination half-life of parent hydralazine was reported in the literature to be 0.7 ± 0.1 h in SA and 0.3 ± 0.1 h in RA after oral administration of

hydralazine in solution [44]; this is rather different from what we found in pregnant RA and SA subjects (3.0 ± 0.9 vs 4.0 ± 1.1, $p$ = .1). The discrepancy is not surprising because the previous study by Shepherd et al. only sampled blood for 3 hours after hydralazine administration. Furthermore, their assay had limited sensitivity (LOQ of 2 ng/mL vs 0.04 ng/mL in our study). IV hydralazine exhibits multi-compartmental pharmacokinetics [63]. It is likely that, with rapid oral absorption from a solution formulation and brief duration of blood sampling, the short half-life observed by Shepherd et al. reflected the distribution phase of hydralazine disposition. By comparison, previously reported hydralazine Cmax and apparent oral clearance in non-pregnant subjects were close to what we found in our study in pregnant women. In non-pregnant RAs, the dose-normalized (to 10 mg) Cmax range was 4 – 5 ng/mL, and in SAs the range was 7 – 50 ng/mL, compared to the range of 0.3 – 1.8 ng/mL in pregnant RAs, and 1.4 – 9.4 ng/mL in pregnant SAs that we reported in our study [44,64,65]. Similarly, earlier studies report hydralazine CL/F ranging from 18,750 – 37,500 L/h in RAs and 3260 – 7500 L/h in SAs in non-pregnant subjects, whereas we report CL/F ranging from 3903 – 16,292 L/h in RAs and 800 – 2849 L/h in SA pregnant subjects [44,64]. It should be noted these two publications reported plasma hydralazine concentrations instead of whole blood concentrations; hence, we adjusted reported dose-normalized Cmax and CL/F values by the known whole blood-to-plasma ratio of 1.65 [63]. Comparison of apparent oral volume of distribution (V/F) is not meaningful as calculation of V/F is dependent on an estimate of the elimination rate constant. As stated previously, earlier studies were not able to capture the true terminal elimination half-life. Based on aforementioned PK parameter estimates, hydralazine PK during pregnancy is reasonably comparable to that of non-pregnant subjects considering differences in study design, study population, assay methodologies, and hydralazine formulation (tablet vs. solution).

Lastly, we were not able to quantify the many known hydralazine metabolites in urine to establish a mass-balance recovery of the dose administered. We expect that future studies will overcome the formidable analytical challenges and allow for a more comprehensive understanding of hydralazine's complex metabolic pathways and fraction metabolized by each metabolic enzyme.

## 3.5 TABLES AND FIGURES

**Table 3-1. Subject Characteristics.**

| | **Weight** (kg) | **Height** (cm) | **Wrist Circ.** (inch) | ***NAT2* Inferred Phenotype[1]** | **Hydralazine dose every 6 hours (mg)** | **Atenolol dose twice daily (mg)** |
|---|---|---|---|---|---|---|
| Mid-pregnancy (22-26 weeks) | 102.8 | 161.0 | 6.4 | Slow | 25 | 50 |
| | 183.4 | 168.5 | 6.6 | Rapid | 10 | 25 |
| | 75.0 | 160.0 | 6.0 | Rapid | 10 | 25 |
| | 113.3 | 166.5 | 6.5 | Slow | 10 | 50 |
| | 133.9 | 173.3 | 8.0 | Slow | 10 | 25 |
| Mean (SD) | 121.7 (40.5) | 165.9 (5.5) | 6.7 (0.8) | | 13.0 (6.7) | 35 (14) |
| Late-pregnancy (30-38 weeks) | 87.8 | 157.7 | 6.5 | Rapid | 10 | 100 |
| | 92.4 | 163.9 | 5.9 | Slow | 25 | 12.5 |
| | 114.8 | 163.1 | 6.9 | Rapid | 5 | 12.5 |
| | 79.5 | 151.5 | 6.1 | Rapid | 25 | 25 |
| | 77.0 | 160.0 | 4.5 | Slow | 25 | 25 |
| | 192.6 | 167.0 | 6.6 | Rapid | 10 | 25 |
| | 118.8 | 173.3 | 7.0 | Rapid | 5 | 25 |
| | 98.8 | 162.4 | 6.8 | Slow | 10 | 12.5 |
| Mean (SD) | 107.7 (37.5) | 162.4 (6.4) | 6.3 (0.8) | | 14.4 (9.0) | 30 (30) |

[1]Rapid acetylators consists of subjects with genotypes *4/*5, *4/*6, or *4/*7; slow acetylators consists of subjects with genotypes *5/*5, *5/*6, *5/*7, or *6/*6.

**Table 3-2. Concomitant medications taken within 48 hours prior to hydralazine study dose**

| Subject | Concomitant Medications |
|---|---|
| Rapid Acetylator 1 | atenolol, multivitamin with minerals, omeprazole, ibuprofen, acetaminophen + dextromethorphan + phenylephrine, folic acid, venlafaxine, betamethasone, lactated ringers, magnesium sulfate with lactated ringers |
| Rapid Acetylator 2 | atenolol, loratadine, prenatal vitamin with DHA, triamcinolone cream |
| Rapid Acetylator 3 | atenolol, prenatal vitamin with DHA, levothyroxine, cetirizine, cough drops |
| Rapid Acetylator 4 | atenolol, furosemide, potassium, prenatal multivitamin, decongestant |
| Rapid Acetylator 5 | atenolol, acetaminophen, azathioprine, clonidine, diphenhydramine, furosemide |
| Rapid Acetylator 6 | atenolol, cetirizine, prenatal vitamin, acetaminophen, calcium carbonate |
| Slow Acetylator 1 | atenolol, prenatal vitamin, vitamin D, calcium carbonate |
| Slow Acetylator 2 | atenolol, acetaminophen, insulin glargine, insulin isophane, insulin lispro, metformin, prenatal vitamin, omeprazole |
| Slow Acetylator 3 | atenolol, prenatal vitamin |
| Slow Acetylator 4 | atenolol, cetirizine, vitamin D, omeprazole, CoQ10, fish oil, prenatal vitamin |
| Slow Acetylator 5 | atenolol, acetylsalicylic acid, prenatal vitamin, fluoxetine, diphenhydramine |
| Slow Acetylator 6 | atenolol, prenatal vitamin, escitalopram |

Rapid acetylator = *N*-acetyltransferase 2 (*NAT2)* rapid acetylator genotypes: *4/*5, *4/*5, *4/*6, *4/*6, *4/*6, *4/*7
Slow acetylator = *NAT2* slow acetylator genotypes: *5/*5, *5/*6, *5/*6, *5/*7, *6/*6, *6/*6

**Table 3-3. Estimated whole blood hydralazine and plasma MTP steady-state pharmacokinetic parameters throughout gestation in subjects treated with 5 – 25 mg of oral hydralazine every 6 hours.**

| Parameter | Hydralazine | | MTP | |
|---|---|---|---|---|
| | Rapid Acetylators (n = 6) | Slow Acetylators (n = 6) | Rapid Acetylators (n = 6) | Slow Acetylators (n = 6) |
| $AUC_{dose\text{-}normalized}$ (ng•h/mL) | 1.5 ± 0.8 | 5.9 ± 3.7 ($p < .05$) | 118.1 ± 64.9 | 56.4 ± 40.7 ($p < .05$) |
| $T_{max}$ (h) | 0.8 ± 0.4 | 0.6 ± 0.1 (*N.S.*) | 1.2 ± 0.6 | 0.7 ± 0.2 (*N.S.*) |
| $C_{max,\ dose\text{-}normalized}$ (ng/mL) | 0.8 ± 0.5 | 4.0 ± 3.2 ($p < .05$) | 32.3 ± 11.7 | 15.0 ± 8.8 ($p < .05$) |
| CL/F (L/h) | 8999 ± 4981 | 2129 ± 883 ($p < .05$) | *N.A.* | *N.A.* |
| CL/F (L/h/kg) | 70.01 ± 13.55 | 20.1 ± 6.9 ($p < .05$) | *N.A.* | *N.A.* |
| $V_z$/F (L) | 39483 ± 26369 | 12617 ± 6353 ($p < .05$) | *N.A.* | *N.A.* |
| $V_z$/F (L/kg) | 302 ± 112 | 116 ± 45 ($p < .05$) | *N.A.* | *N.A.* |
| Elimination half-life (h) | 2.96 ± 0.92 | 4.0 ± 1.1 (*N.S.*) | 2.6 ± 1.1 | 3.2 ± 1.4 (*N.S.*) |
| Elimination rate constant (1/h) | 0.3 ± 0.1 | 0.2 ± 0.1 (*N.S.*) | 0.3 ± 0.1 | 0.3 ± 0.1 (*N.S.*) |
| MTP/hydralazine AUC ratio | 78 ± 30 | 8 ± 3 ($p < .05$) | | |

Estimated pharmacokinetic parameters compared between NAT2 rapid and slow acetylators. Area under the concentration-time curve ($AUC_{dose\text{-}normalized}$) and maximal concentration ($C_{max,\ dose\text{-}normalized}$) are dose-normalized to 10 mg for comparison purposes. CL/F=apparent oral clearance, $V_z$/F=apparent oral volume of distribution, $T_{max}$=time to peak concentration, Cmax=peak concentration, *N.S.* = not significant and *N.A.* = not applicable, Data reported as mean ± SD.

**Figure 3-1**

**Figure 1.**

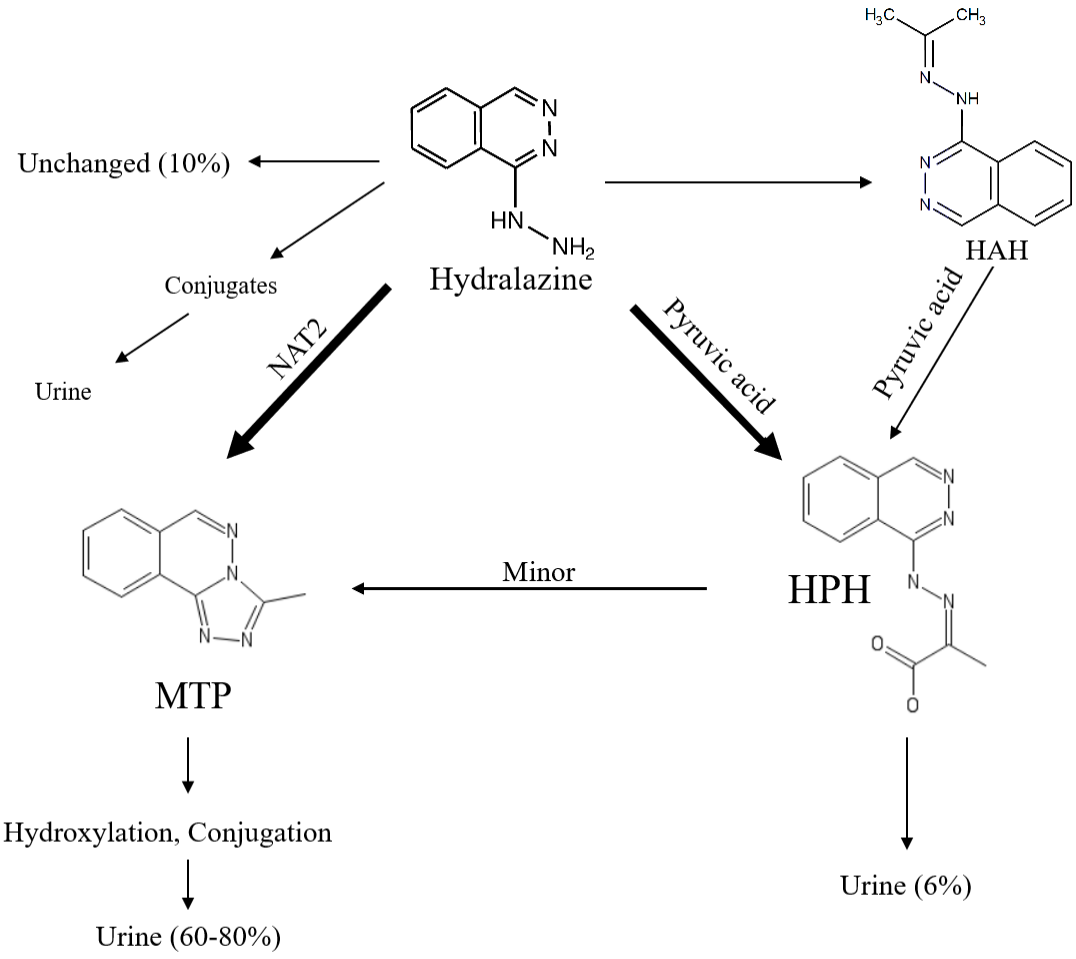


Hydralazine acetone hydrazone (HAH), hydralazine pyruvic acid hydrazone (HPH), 3-methyl-1,2,4-triazolo[3,4-a]phthalazine (MTP), *N*-acetyltransferase 2 (NAT2).

**Figure 3-1.** Hydralazine metabolic pathway.

**Figure 3-2**

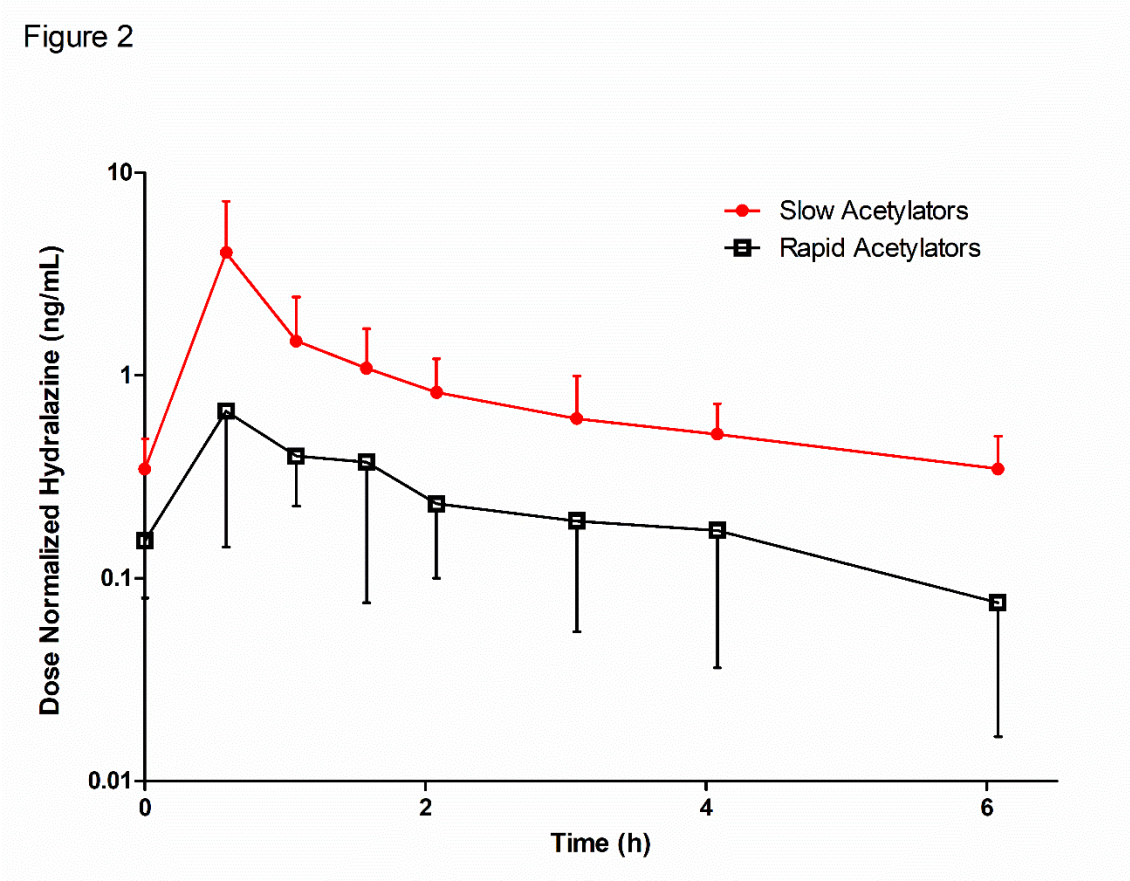


**Figure 3-2.** Mean (± SD), dose normalized, steady-state, whole blood oral hydralazine concentration versus time profiles for *N*-acetyltransferase 2 rapid (*NAT2* genotypes *4/*5, *4/*5, *4/*6, *4/*6, *4/*6, *4/*7) and slow (*NAT2* genotypes *5/*5, *5/*6, *5/*6, *5/*7, *6/*6, *6/*6) acetylators in pregnant women. Concentrations were dose normalized to oral hydralazine 10 mg every 6 hours. Closed circles and red line indicate slow acetylators. Open squares and black line indicate rapid acetylators.

**Figure 3-3**

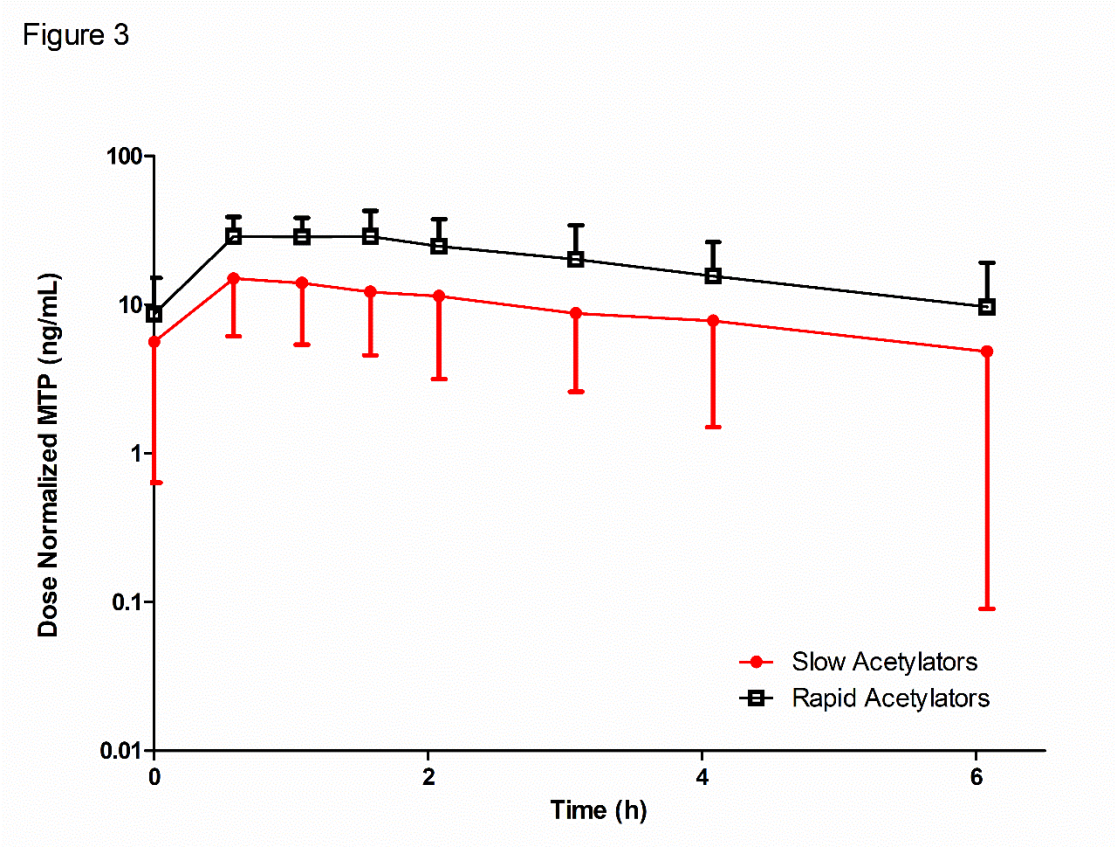


**Figure 3-3.** Mean (± SD), dose normalized, steady-state, plasma MTP concentration versus time profiles for *N*-acetyltransferase 2 rapid (*NAT2* genotypes *4/*5, *4/*5, *4/*6, *4/*6, *4/*6, *4/*7) and slow (*NAT2* genotypes *5/*5, *5/*6, *5/*6, *5/*7, *6/*6, *6/*6) acetylators in pregnant women. Concentrations were dose normalized to oral hydralazine 10 mg every 6 hours. Closed circles and red line indicate slow acetylators. Open squares and black line indicate rapid acetylators.

**Figure 3-4**

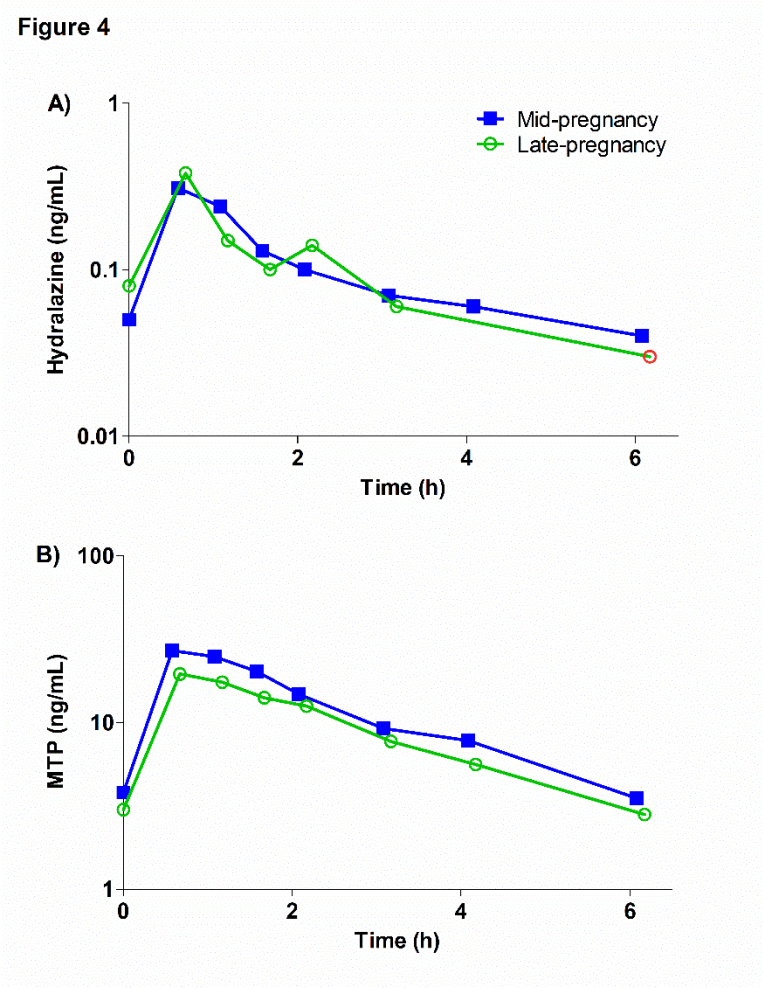


**Figure 3-4.** Steady-state A) whole blood hydralazine concentration and B) plasma MTP concentration versus time profile of the subject that completed both mid- (closed squares, blue line) and late-pregnancy (open circles, green line) study days. Red open circle indicates measured concentration, which was just below the limit of quantification. A 10 mg dose every 6 hours was administered during both study days. This subject was identified as a NAT2 rapid acetylator.

**Figure 3-5**

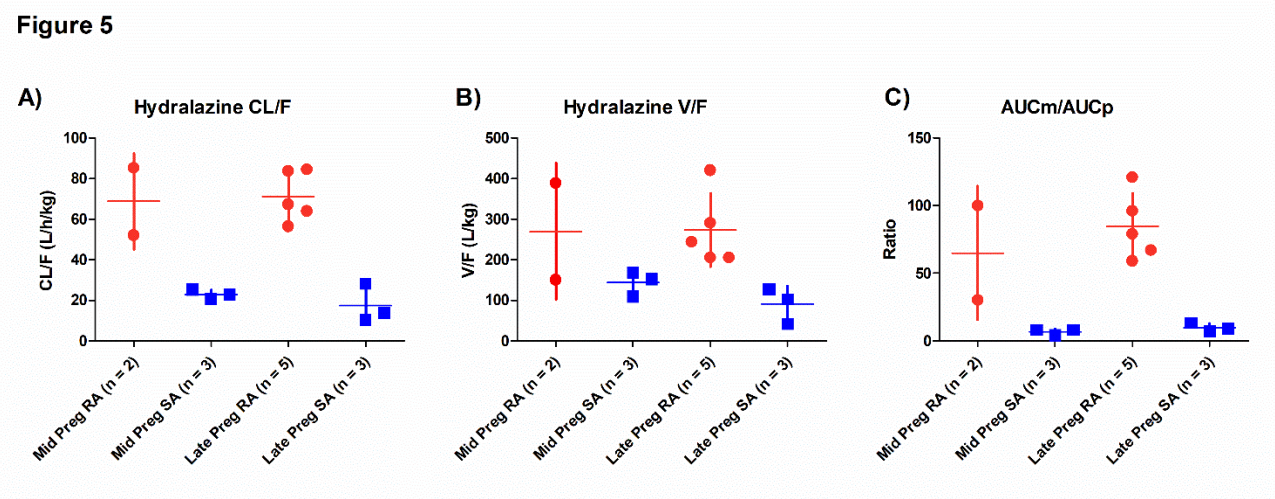


**Figure 3-5.** The effects of NAT2 status and gestational age on A) apparent oral clearance, B) apparent volume of distribution, and C) metabolite to parent AUC ratio. Red circle indicates rapid acetylators and blue squares indicate slow acetylators. Mid-pregnancy was defined as 22 – 26 weeks gestation, and late-pregnancy as 30 – 38 weeks gestation. NAT2 acetylation status was categorized as rapid (RA, *NAT2* *4/*5, *4/*6, *4/*7) and slow (SA, *NAT2* *5/*5, *5/*6, *5/*7, *6/*6) acetylators based on genotype. No gestational age effects were observed on these key pharmacokinetic parameters after adjusting for subjects' NAT2 phenotype.

## 3.6 REFERENCES


1. Folk DM. Hypertensive Disorders of Pregnancy: Overview and Current Recommendations. *J. Midwifery Womens. Health*. 2018;

2. Lo JO, Mission JF, Caughey AB. Hypertensive disease of pregnancy and maternal mortality. *Curr. Opin. Obstet. Gynecol.* 2013;25:124–132.

3. Leffert LR, Clancy CR, Bateman BT, et al. Hypertensive Disorders and Pregnancy-Related Stroke. *Obstet. Gynecol.* 2015;125:124–131.

4. American College of Obstetricians and Gynecologists, Task Force on Hypertension in Pregnancy. Hypertension in Pregnancy. *Obstet. Gynecol.* 2013;122:1122–1131.

5. Redman CWG. Hypertension in pregnancy: the NICE guidelines. *Heart*. 2011;97:1967–1969.

6. Hypertension in pregnancy: diagnosis and management clinical guideline [Internet]. Natl. Inst. Heal. Care Excell. 2011.

7. Easterling TR. Pharmacological management of hypertension in pregnancy. *Semin. Perinatol.* 2014;38:487–495.

8. Easterling TR, Benedetti TJ, Schmucker BC, et al. Antihypertensive therapy in pregnancy directed by noninvasive hemodynamic monitoring. *Am. J. Perinatol.* 1989;6:86–89.

9. Talseth T. Clinical Pharmacokinetics of Hydrallazine. *Clin. Pharmacokinet.* 1977;2:317–329.

10. Lesser JM, Israili ZH, Davis DC, et al. Metabolism and Disposition of Hydralazine-14C in Man and Dog. *Drug Metab. Dispos.* 1974;2.

11. Zak SB, Lukas G, Gilleran TG. Plasma levels of real and “apparent” hydralazine in man and rat. *Drug Metab. Dispos.* 5:116–121.

12. Reece PA, Stanley PE, Zacest R. Interference in assays for hydralazine in humans by a major plasma metabolite, hydralazine pyruvic acid hydrazone. *J. Pharm. Sci.* 1978;67:1150–1153.

13. Shepherd AM, Ludden TM, Haegele KD, et al. Pharmacokinetics of hydralazine, apparent hydralazine and hydralazine pyruvic acid hydrazone in humans. *Res. Commun. Chem. Pathol. Pharmacol.* 1979;26:129–144.

14. Wagner J, Faigle JW, Imhof P, et al. Metabolism of hydralazine in man. *Arzneimittelforschung.* 1977;27:2388–2395.

15. Barron K, Carrier O, Haegele KD, et al. Comparative evaluation of the in vitro effects of hydralazine and hydralazine acetonide on arterial smooth muscle. *Br. J. Pharmacol.* 1977;61:345–349.

16. McLean AJ, du Souich P, Barron K, et al. Study of in vitro effects of hydralazine metabolites--comparative evaluation of products of hydroxylation, hydrolysis and conjugation. *Arch. Int. Pharmacodyn. Ther.* 1978;235:19–25.

17. Iwaki M, Ogiso T, Ito Y. In vitro kinetic studies of the reaction of hydralazine and its acetone hydrazone with pyruvic acid. *J. Pharm. Sci.* 1988;77:280–283.

18. Reece PA. Hydralazine and related compounds: chemistry, metabolism, and mode of action. *Med. Res. Rev.* 1981;1:73–96.

19. Zimmer H, Glaser R, Kokosa J, et al. 3-Hydroxymethyl-s-triazolo[3,4-a]phthalazine, a

novel urinary hydralazine metabolite in man. *J. Med. Chem.* 1975;18:1031–1033.

20. Dubois JP, Schmid K, Riess W, et al. Metabolism of hydralazine in man. Part II: Investigation of features relevant to drug safety. *Arzneimittelforschung.* 1987;37:189–193.

21. Shepherd AM, McNay JL, Ludden TM, et al. Plasma concentration and acetylator phenotype determine response to oral hydralazine. *Hypertens. (Dallas, Tex. 1979)*. 3:580–585.

22. Spinasse LB, Santos AR, Suffys PN, et al. Different phenotypes of the NAT2 gene influences hydralazine antihypertensive response in patients with resistant hypertension. *Pharmacogenomics*. 2014;15:169–178.

23. Lemke LE, McQueen CA. Acetylation and its role in the mutagenicity of the antihypertensive agent hydralazine. *Drug Metab. Dispos.* 1995;23:559–565.

24. Timbrell JA, Harland SJ, Facchini V. Polymorphic acetylation of hydralazine. *Clin. Pharmacol. Ther.* 1980;28:350–355.

25. Allen CE, Doll MA, Hein DW. N-Acetyltransferase 2 Genotype-Dependent N-Acetylation of Hydralazine in Human Hepatocytes. *Drug Metab. Dispos.* 2017;45:1276–1281.

26. Hardman J, Limbird L, Gilman A. Goodman and Gilman's The Pharmacological Basis of Therapeutics. 10th ed. McGraw Hill; 2001.

27. Jenne JW. Studies of human patterns of isoniazid metabolism using an intravenous fall-off technique with a chemical method. *Am. Rev. Respir. Dis.* 1960;81:1–8.

28. Evans DA, White TA. Human Acetylation Polymorphism. *J Lab Clin Med*. 1964;63:394–403.

29. Windmill KF, Gaedigk A, de la M. Hall P, et al. Localization of N-Acetyltransferases NAT1 and NAT2 in Human Tissues. *Toxicol. Sci.* 2000;54:19–29.

30. Shen DD, Hosler JP, Schroder RL, et al. Pharmacokinetics of hydralazine and its acid-labile hydrazone metabolites in relation to acetylator phenotype. *J. Pharmacokinet. Biopharm.* 1980;8:53–68.

31. Ludden TM, Shepherd AM, McNay JL, et al. Effect of intravenous dose on hydralazine kinetics after administration. *Clin. Pharmacol. Ther.* 1983;34:148–152.

32. Liedholm H, Wåhlin-Boll E, Hanson A, et al. Transplacental passage and breast milk concentrations of hydralazine. *Eur. J. Clin. Pharmacol.* 1982;21:417–419.

33. Lamont RF, Elder MG. Transfer of hydralazine across the placenta and into breast milk. *J. Obstet. Gynaecol. (Lahore).* 1986;7:47–48.

34. Hebert MF, Carr DB, Anderson GD, et al. Pharmacokinetics and Pharmacodynamics of Atenolol During Pregnancy and Postpartum. *J. Clin. Pharmacol.* 2005;45:25–33.

35. Shepherd AM, Irvine NA, Ludden TM. Effect of food on blood hydralazine levels and response in hypertension. *Clin. Pharmacol. Ther.* 1984;36:14–18.

36. Liedholm H, Wåhlin-Boll E, Hanson A, et al. Influence of food on the bioavailability of "real" and "apparent" hydralazine from conventional and slow-release preparations. *Drug. Nutr. Interact.* 1982;1:293–302.

37. Melander A, Danielson K, Hanson A, et al. Enhancement of hydralazine bioavailability by food. *Clin. Pharmacol. Ther.* 1977;22:104–107.

38. Melander A, Liedholm H, McLean A. Concomitant food intake does enhance the

bioavailability and effect of hydralazine. *Clin. Pharmacol. Ther.* 1985;38:475–476.

39. Walden RJ, Hernandez R, Witts D, et al. Effect of food on the absorption of hydralazine in man. *Eur. J. Clin. Pharmacol.* 1981;20:53–58.

40. Semple HA, Tam YK, Tin S, et al. Assay for hydralazine as its stable p-nitrobenzaldehyde hydrazone. *Pharm. Res.* 1988;5:383–386.

41. Reece PA, Cozamanis I, Zacest R. Selective high-performance liquid chromatographic assays for hydralazine and its metabolites in plasma of man. *J. Chromatogr.* 1980;181:427–440.

42. Hein DW, Doll MA. Accuracy of various human *NAT2* SNP genotyping panels to infer rapid, intermediate and slow acetylator phenotypes. *Pharmacogenomics*. 2012;13:31–41.

43. R Development Core Team. R: A language and environment for statistical computing [Internet]. Vienna, Austria: R Foundation for Statistical Computing; 2008.

44. Shepherd AM, Ludden TM, McNay JL, et al. Hydralazine kinetics after single and repeated oral doses. *Clin. Pharmacol. Ther.* 1980;28:804–811.

45. Talseth T. Kinetics of hydralazine elimination. *Clin. Pharmacol. Ther.* 1977;21:715–720.

46. Tsutsumi K, Kotegawa T, Matsuki S, et al. The effect of pregnancy on cytochrome P4501A2, xanthine oxidase, and N -acetyltransferase activities in humans. *Clin. Pharmacol. Ther.* 2001;70:121–125.

47. Rashid JR, Kofi-Tsepko, Juma FD. Acetylation status using hydralazine in African hypertensives at Kenyatta National Hospital. *East Afr. Med. J.* 1992;69:406–408.

48. Reece PA, Stafford I, Prager RH, et al. Synthesis, formulation, and clinical

pharmacological evaluation of hydralazine pyruvic acid hydrazone in two healthy volunteers. *J. Pharm. Sci.* 1985;74:193–196.

49. Haegele KD, Talseth T, Skrdlant HB, et al. Determination of hydralazine pyruvic acid hydrazone and its correlation with "apparent" hydralazine. *Arzneimittelforschung.* 1981;31:357–362.

50. Garcés-Eisele SJ, Cedillo-Carvallo B, Reyes-Núñez V, et al. Genetic selection of volunteers and concomitant dose adjustment leads to comparable hydralazine/valproate exposure. *J. Clin. Pharm. Ther.* 2014;39:368–375.

51. Drucker MM, Blondheim SH, Wislicki L. Factors affecting the acetylation in-vivo of para-aminobenzoic acid by human subjects. *Clin. Sci.* 1964;27:133–141.

52. Talseth T, Landmark KH. Polymorphic acetylation of sulphadimidine in normal and uraemic man. *Eur. J. Clin. Pharmacol.* 1977;11:33–36.

53. Graffner C. Elimination rate of N-acetylprocainamide after a single intravenous dose of procainamide hydrochloride in man. *J. Pharmacokinet. Biopharm.* 1975;3:69–76.

54. Cameron HA, Ramsay LE. The lupus syndrome induced by hydralazine: a common complication with low dose treatment. *Br. Med. J. (Clin. Res. Ed).* 1984;289:410–412.

55. Hofstra AH. Metabolism of Hydralazine: Relevance to Drug-Induced Lupus. *Drug Metab. Rev.* 1994;26:485–505.

56. Iyer P, Dirweesh A, Zijoo R. Hydralazine Induced Lupus Syndrome Presenting with Recurrent Pericardial Effusion and a Negative Antinuclear Antibody. *Case Rep. Rheumatol.* 2017;2017:5245904.

57. Magee LA, Cham C, Waterman EJ, et al. Hydralazine for treatment of severe hypertension in pregnancy: meta-analysis. *BMJ*. 2003;327:955–0.

58. Smelt VA, Mardon HJ, Sim E. Placental Expression of Arylamine N-Acetyltransferases: Evidence for Linkage Disequilibrium between *NAT1* 10* and *NAT2* 4* Alleles of the Two Human Arylamine N-Acetyltransferase Loci *NAT1* and *NAT2*. *Pharmacol. Toxicol.* 1998;83:149–157.

59. Rogers Z, Hiruy H, Pasipanodya JG, et al. The Non-Linear Child: Ontogeny, Isoniazid Concentration, and NAT2 Genotype Modulate Enzyme Reaction Kinetics and Metabolism. *EBioMedicine*. 2016;11:118–126.

60. Lammer EJ, Shaw GM, Iovannisci DM, et al. Maternal smoking and the risk of orofacial clefts: Susceptibility with NAT1 and NAT2 polymorphisms. *Epidemiology*. 2004;15:150–156.

61. Shi M, Christensen K, Weinberg CR, et al. Orofacial Cleft Risk Is Increased with Maternal Smoking and Specific Detoxification-Gene Variants. *Am. J. Hum. Genet.* 2007;80:76.

62. Ludden TM, Goggin LK, McNay JL, et al. High-pressure liquid chromatographic assay for hydralazine in human plasma. *J. Pharm. Sci.* 1979;68:1423–1425.

63. Ludden TM, Shepherd AM, McNay JL, et al. Hydralazine kinetics in hypertensive patients after intravenous administration. *Clin. Pharmacol. Ther.* 1980;28:736–742.

64. Ludden TM, McNay JL, Shepherd AM, et al. Variability of plasma hydralazine concentrations in male hypertensive patients. *Arthritis Rheum.* 1981;24:987–993.

65. Ludden TM, Rotenberg KS, Ludden LK, et al. Relative bioavailability of immediate- and sustained-release hydralazine formulations. *J. Pharm. Sci.* 1988;77:1026–1032.

# CHAPTER 4: IMPACT OF THE GUT MICROBIOME ON HEPATIC DRUG PROCESSING GENES IN MICE DURING PREGNANCY

## 4.1 INTRODUCTION

Drug safety in vulnerable populations, such as pregnant women, has been a priority for drug development and regulatory agencies due to changes observed in efficacy and toxicity profiles [1,2]. Understanding how drug disposition is changed in these populations is therefore of utmost importance. However, due to the vulnerable nature of these populations, it is often difficult or impossible to study them directly. Therefore, surrogate models must be used to elucidate mechanisms by which pharmacokinetic and pharmacodynamic changes occur. One of the challenges that drug development faces today is the understanding and prediction of inter-individual variability. Influence of pharmacogenomics on drug metabolism during pregnancy has been explored [3]. However, there remains gaps in knowledge of other factors that can affect drug disposition in this population. Pharmacomicrobiomics or the impact of microbiome on drug disposition is one such example [4].

Pregnancy changes the maternal body in numerous ways to accommodate the developing fetus. Changes such as increased total body volume, decreased plasma albumin, increased cardiac output and renal glomerular filtration rate, and altered expression or activity of drug-metabolizing enzymes and transporters profoundly alter drug disposition in pregnant women as compared to non-pregnant women or men [3,5–8]. Previous studies have shown increased activity of CYP3A4, CYP2D6, and CYP2C9, and decreased activity of CYP2C19 and CYP1A2, by using respective probe substrates prescribed to women during pregnancy [9]. Drug

transporters such as P-glycoprotein (P-gp/Abcb1), organic anion-transporting polypeptide 1B1 (OATP1B1/Slco1b1), multidrug resistance protein 3 (Mrp3/Abcc3), and organic cation transporters (OCTs) were also found to have dynamic activity or mRNA expression changes throughout pregnancy [5,6,10]. Together, these changes in expression or activity of drug-metabolizing enzymes and transporters highlight the importance of mechanistic understanding of such changes so that dosing regimens of drugs for pregnant woman could be optimized with better efficacy and safety for both the mother and her fetus. It has been proposed that pregnancy-related hormones such as progesterone, estradiol, and cortisol which are ligands of nuclear receptors such as glucocorticoid receptor (GR) and pregnane X receptor (PXR) mediate induction of drug metabolizing enzymes and transporters (DMET) during pregnancy [11–13].

The microbiome is often referred to as the second human genome due to their abundance throughout the GI tract. Recently, it has come to light that the maternal gut microbiome changes as pregnancy progresses in humans [14], for example, with a shift to higher abundance of *Actinobacteria* and *Proteobacteria* [14]. The gut microbiome can directly metabolize and inactivate compounds, thereby changing drug disposition and toxicity profiles [15]. Gut bacteria also can indirectly alter drug disposition by changing expression or activity of host DMET [15]. The predominant mechanism by which bacteria modulate DMET expression is thought to be due to altered secondary bile acid profiles in the host [16,17]. Primary bile acids are synthesized in the liver from cholesterol and subsequently transported into the bile duct by efflux transporters, such as the bile salt export pump (BSEP). The bile duct leads primary bile acids into the duodenum, where intestinal bacteria deconjugate, dehydroxylate, and epimerize them into secondary bile acids. Intestinal bacteria such as *Clostridia* from Firmicutes phylum express the enzymes (e.g. hydroxysteroid dehydrogenase and 7-dehydratase) necessary for these

biotransformation reactions. Primary bile acids cholic acid (CA) and chenodeoxycholic acid (CDCA), as well as secondary bile acid deoxycholic acid (DCA) and their taurine conjugated forms have been shown to activate farnesoid X receptor (FXR) [18]; and lithocholic acid (LCA) has been shown to activate PXR [19], which in turn up-regulates expression of certain CYPs. In mice, it has been demonstrated that the primary muricholic acids are antagonists of FXR, thus the lack of transformation of primary bile acids into secondary bile acids in GF mice would result in accumulation of FXR antagonists (primary bile acids) and reduction of PXR agonists (secondary bile acids); ultimately, this decreases FXR and PXR signaling in the intestine and the liver [16,20].

Although both pregnancy and the gut microbiome individually have been shown to have a profound impact on drug disposition, no studies to date have investigated their combined effects. The objective of this study was to explore the combined effects of pregnancy and microbiome on the expression and/or activity of hepatic DMET using CV and GF pregnant mouse models. We will test the hypothesis that the magnitude and direction of expression changes reflect the combined effects of pregnancy and gut microbiome. Understanding how pregnancy and the microbiome interplay to influence DMET will help us better predict drug disposition and its inter-individual variability in pregnancy.

## 4.2 MATERIALS AND METHODS

### CHEMICALS

Liquid chromatography-mass spectrometry grade methanol, water, and acetonitrile were purchased from Fisher Scientific (Fair Lawn, NJ). Steroid hormone standards and deuterated internal standards for bile acids (lithocholic acid, deoxycholic acid, cholic acid, glycochenodeoxycholic acid, and glycocholic acid) were purchased from Cerilliant Corporation

(Round Rock, TX) and Steraloids Inc. (Newport, RI). All other chemicals were obtained from Thermo Fisher Scientific (Rockford, IL) unless stated otherwise.

### ANIMAL STUDIES

Conventional C57BL/6J mice (JAX stock #000664) were from The Jackson Laboratory (Bar Habor, ME) and given one week to adjust to new animal facility prior to experiments. Germ-free C57BL/6 colony was originated from mice purchased from the National Gnotobiotic Rodent Resource Center of the University of North Carolina at Chapel Hill. All animals were cared for in accordance with the Guide for the Care and Use of Laboratory Animals published by the National Research Council. This animal protocol was approved by the Institutional Animal Care and Use Committee of the University of Washington (protocol# 4035-04).

Both CV and GF mice were maintained on 12-h light/dark cycles, and the same autoclaved Breeder Chow #5021 (LabDiet, St. Louis, MO), autoclaved non-acidified water, and autoclaved Enrich-N'Pure bedding (The Andersons Inc., Maumee, OH) were provided *ad libitum*. CV female mice of 8 weeks of age were mated with CV male mice overnight, and male mice were promptly separated from female mice in the morning. The day with the overnight housing was defined as gestation day (gd) 0. Due to difficulties in achieving pregnancies in GF mice, GF female mice of 11-15 weeks of age were mated with male mice for 72 h prior to separation from GF male mice. Day 2 after introduction of male mice to the cage was assumed to be gd 0. All pregnant mouse tissues were collected on gd 15, which was previously shown to be the optimal time point to observe peak levels of gene expression changes [10]. On the day of tissue collection, mice were anesthetized with isoflurane, and blood was collected via cardiac puncture and immediately centrifuged (1,500 × *g* for 10 min at 4°C) to isolate plasma. Tissues (e.g., the liver) were removed, washed in cold saline, and immediately snap-frozen in liquid $N_2$.

In total, plasma samples and tissues from 6 CVNP, 5 CVP, 6 GFNP, and 5 GFP mice were collected. All samples were then stored at -80°C until analysis.

### RNA-SEQ ANALYSIS

Total RNA was extracted from liver tissues using Qiagen RNeasy Mini Kit (Qiagen, Hilden, Germany) following the manufacturer's instructions. The concentration of total RNA was determined by using a Synergy HTX Multi-mode Plate Reader (BioTek, Winooski, VT) at 260 nm. Paired end RNA sequencing (2 × 150 bp) was performed by Novogene Bioinformatics Technology Co., Ltd. (Sacramento, CA) using the Illumina NovaSeq 6000 (GEO accession GSE143391) with average 20 million reads. The library was prepared using NEBNext® Ultra™ RNA Library Prep Kit from Illumina®. We aligned reads to the mouse GRCm38.p6 transcriptome (Gencode release M19) using the *Salmon* aligner (v0.11.3) [21] and then the transcript-level counts were imported into R and summarized at the gene level using the Bioconductor tximport package (v1.10.1) [22]. Data was subsequently filtered to remove genes that had consistently low expression levels to improve the signal-to-noise ratio using filterByExpr function in the edgeR package (v3.24.3), implemented in R (v3.5.1). After filtering, 18849 genes remained. Differential gene expression analysis between groups was performed using the edgeR package with a negative binomial generalized linear model (GLM), and quasi-likelihood F-tests for a given contrast [23,24]. A false discovery rate (FDR) of 10% was selected to limit the number of false positives[25].

### QUANTITATIVE REAL-TIME PCR

Quantitative real-time polymerase chain reaction (qRT-PCR) was performed to determine the mRNA levels of selected genes, as previously described, to validate RNA sequencing data [10]. Aliquots from the same total RNA samples used for RNA-seq analysis were transcribed to

cDNAs using random primers from High-Capacity cDNA Reverse Transcription Kit (Applied Biosystems, Foster City, CA). We selected 4 enzyme genes coding (*Cyp2b13, Cyp2c50, Cyp3a16, and Sult4a1*) and 2 transporter genes (*Abcc3* and *Slco1a4*) for validation. The genes were selected based on the large magnitude of change in mRNA abundance observed from RNA-seq analysis. The cDNAs were amplified using SsoAdvanced Universal SYBR Green Supermix and the Bio-Rad CFX384 Real-Time PCR Detection System (Hercules, CA). PCR primers were synthesized by Integrated DNA Technologies (Coralville, IA). *Gapdh* was used as a housekeeping gene for normalization of the gene expression data.

### TARGETED PROTEOMIC ANALYSIS OF HEPATIC METABOLIC ENZYMES AND TRANSPORTERS BY LC-MS/MS

Quantification of relative protein abundance of major metabolic enzymes and transporters in the liver tissues of CV and GF mice was done by quantitative LC-MS/MS proteomic analysis using methods previously described [26–28]. For CYP enzymes, changes in protein levels of CYP2C37, CYP2C50, CYP2C54, CYP2D22, CYP2D40, CYP3A11, CYP3A16, and CYP3A41 were quantified. For transporters, changes in protein levels of ABCB11, ABCB1A, ABCB1B, ABCC3, ABCG2, SLC22A2, SLC22A7, SLCO1A1, and SLCO1A4 were determined. We used the same procedures for protein isolation and digestion as previously published [28]. Briefly, approximately 50 mg of frozen liver tissue per mouse was homogenized in 2 ml of permeabilization buffer (the permeabilization and protease inhibitor solution mix) using hand homogenizer. All steps were carried out on ice to minimize protein degradation. The resulting liver homogenate was shaken for 30 min at 4°C then centrifuged at 16,000 × *g* for 15 min. The resulting supernatant was aliquoted for protein quantification via BCA analysis and diluted to 2 mg/ml prior to trypsin digestion. To 80 µl of post-treatment supernatant, 30 µl of ammonium

bicarbonate buffer (100 mM, pH 7.8), 10 µl of human serum albumin (HSA), 20 µl of bovine serum albumin (BSA), and 10 µl of dithiothreitol (DTT) were added and incubated at 95°C for 10 min. After cooling, 20 µl of iodoacetamide (500 mM) was added to incubate at room temperature for 30 min in the dark. Then, ice-cold methanol (0.5 ml), chloroform (0.1ml), and water (0.4ml) was added to desalt the samples. After centrifugation at 16,000 × $g$ for 5 min at 4°C, the pellet was washed with ice-cold methanol (0.5 ml) and centrifuged at 8000 × $g$ for 5 min at 4°C.Trypsin (20 µl, 1:10 trypsin: protein ratio (w/w)) was added and incubated for 16 h at 37°C while shaking at 300 rpm. The reaction was quenched with dry ice and internal standards were added. The relative levels of protein abundance of CYP enzymes and transporter were quantified using surrogate peptides for respective CYP enzymes or transporters as standards (Table 4-1). Chromatographic and mass spectrometric conditions were the same as previously described [28]. Previous studies [27] found that it was necessary to perform various normalization steps in order to minimize batch-to-batch and sample-to-sample variation. Therefore, bovine serum albumin (BSA) and a stable-isotope labeled heavy peptide cocktail were added as normalization controls. The quality of peptide signal was verified by plotting the correlation between two or more peptide fragments or transitions derived from different samples with the same total protein concentration. Ion suppression was assessed with multiple peptides from the same protein. This approach measures whether the variability in peak responses reflect the biological variability. In addition, by adding BSA, an exogenous protein, into the homogenized sample before protein denaturation, the sample loss during subsequent processing steps was addressed. Moreover, the use of heavy isotope-labeled peptides as internal standard provided adjustment for possible matrix effects and sample concentration changes due to evaporation and nonspecific binding to the vials. Relative protein abundance of each enzyme or

transporter was calculated by taking the average signal for all peptides that passed linearity test for each enzyme or transporter in each individual liver sample and dividing it by the average signal of the corresponding heavy isotope-labeled peptide. The ratio was subsequently normalized to BSA and the group mean (pool of all samples) of each surrogate peptide. The resulting ratio-of-ratio (ROR) estimates reflect relative protein abundance of each individual enzyme or transporter. The samples used for proteomic analysis were essentially the same as those used for RNA-seq analysis or activity assay (see below) except that the number of samples used for proteomic analysis in the CVP and GFNP groups was 4 instead of 5 or 6, due to a lack of sufficient tissue homogenates.

### LIVER MICROSOME ISOLATION AND ACTIVITY ASSAY

Liver microsomes were prepared from individual mouse livers, as previously described [29–31]. All steps were carried out at 4°C to minimize protein degradation. Approximately 750 mg of frozen mouse liver tissue was homogenized in 2 ml homogenization buffer (50 mM KPi buffer containing 0.25 M sucrose and 1 mM EDTA) using Omni Bead Ruptor Homogenizer (Omni International, Kennesaw, GA). The homogenate was then centrifuged for 30 min at 15,000 × *g*, and the resulting supernatant was centrifuged for 70 min at 120,000 × *g*. The pellet containing microsomes was washed once with the buffer (10 mM KPi, 0.1 mM KCl, 1 mM EDTA, pH 7.4) before a final centrifugation for 70 min at 120,000 × *g*. The final pellet was resuspended in 1 ml of the storage buffer (50 mM KPi, 0.25 M sucrose, 10 mM EDTA, pH 7.4) and stored in 200 μl aliquots at -80°C until analysis. Microsomal protein concentration was determined using the Pierce BCA Protein Assay Kit (Thermo Scientific, Rockford, IL).

Cyp3a activities in individual liver microsomal preparations were determined using the Promega P450-Glo Screening Kit (Promega Corporation, Madison, WI) according to the

manufacturer's instruction. Briefly, liver microsomes (7 μg per reaction) from CV and GF mice were pre-incubated with 3 μM luminogenic P450-Glo Luciferin-IPA for 10 min at 37°C. In the case of the inhibition assay, ketoconazole was added to the reaction mixture to a final concentration of 5 μM as described in previous studies [32]. Then, NADPH regeneration system was added to the mixture to initiate reaction. Total reaction volume was 75 μl. After incubation of 10 min at 37°C, reaction was stopped by the addition of equal volume of the luciferin detection reagent at room temperature and let the mixture sit for 20 min. Cyp3a-mediated reaction results in generation of a luciferin product, which was measured by a Glomax 96 Microplate Luminometer (Promega Corporation, Madison, WI). Light signal detected reflects the magnitude of Cyp3a activity. Both the substrate concentration and time of incubation were optimized to fall within the linear range of human CYP3A activity, as reported by Promega and described in its instruction. Control incubations using recombinant CYP3A4 microsomes were also performed in parallel as positive control. Incubations were done in triplicates and repeated once. The same assay kit has previously been used to measure mouse Cyp3a activity [33–35].

#### QUANTIFICATION OF PLASMA BILE ACIDS AND STEROID HORMONES

Bile acids were extracted from mouse plasma as previously described [36]. Briefly, 50 μl of plasma sample was mixed with 10 μl of internal standard solution (20 μg/ml d4-G-CDCA, 10 μg/ml d4-G-CDCA in 50% MeOH) and vortexed well. Protein was precipitated by adding 500 μl ice-cold methanol. The mixture was centrifuged at 12,000 × *g* for 10 min at 4°C. The resulting supernatant was kept in a new tube and the pellet was put through the same steps. The resulting supernatant was combined with the previous one, dried under vacuum (30°C) and reconstitute in100 μl of 1:1 methanol/water (v/v). The suspension was centrifuged again at 12,000 × *g* for 10 min at 4°C and 50 μl was subjected into the ultra-performance liquid chromatography coupled

with mass spectrometry in tandem (UPLC-MS/MS) for analysis. Chromatographic conditions and instrument settings were the same as described [36] with modifications. Samples were eluted using mobile phases (A) consisted of 20% acetonitrile and 10 mmol/L ammonium acetate in aqueous solutions and (B) consisted of 80% acetonitrile and 10 mmol/L ammonium acetate in aqueous solutions, at a flow rate of 0.400 ml/min. 5 µl of each sample was injected on column for analysis using negative ionization mode.

Primary bile acids cholic acid (CA), chenodeoxycholic acid (CDCA), ursodeoxycholic acid (UDCA), alpha/beta-murine cholic acid (α/βMCA), and their respective taurine conjugates (TCA, T-CDCA, TUDCA, T-α/βMCA) as well as secondary bile acids deoxycholic acid (DCA), hyodeoxycholic acid (HDCA), lithocholic acid (LCA), murideoxycholic acid (MDCA), omega-muricholic acid (ωMCA), and their respective taurine conjugates (T-ωMCA, T-DCA, T-HDCA, and T-LCA) were quantified. Calibrator and different quality control (QCs) samples were prepared by adding the appropriate amount of the different standard stock solutions and were extracted using the similar sample preparation procedure described above.

Steroid hormones were extracted from mouse plasma as previously described [37]. Briefly, 200 µl of methanol containing an internal standard cocktail (10 µg/ml estrone-d4, 10 µg/ml cortisol-d4, 10 µg/ml 11-deoxycortisol-d5, 10 µg/ml DHEA-d5, 10 µg/ml progesterone-d9, 10 µg/ml 17OH-progesterone-d8, and 10 µg/ml 17OH-pregnenolone-d3) was added to 50 µl of plasma samples, and the mixture was mixed vigorously for 1 min followed by a centrifugation at 3,500 × *g* for 10 min at 4°C. The supernatant was moved to a new micro centrifuge tube and dried down under $N_2$. Samples were reconstituted in 50% methanol and analyzed by LC-MS/MS using the same instrument and conditions as described [37].

### STATISTICAL ANALYSES FOR PLASMA METABOLITE QUANTIFICATION AND MICROSOME ACTIVITY

Data are presented as means ± SE (or SD) of independent samples from 4 – 6 different mice. Statistical significance of the difference between two groups was determined by Wilcoxon T test, with $p < 0.05$ to be considered as significant. Data analyses were performed using R (v3.5.1 & v3.6.1) and GraphPad Prism (GraphPad Prism 5.01, La Jolla, CA).

## 4.3 RESULTS

### VALIDATION OF RNA-SEQ DATA BY QRT-PCR

A direct comparison of the two approaches (RNA-seq and qRT-PCR) is shown in Fig. 4-1 for 6 selected genes (*Cyp3a16, Cyp2b13, Cyp2c50, Sult4a1, Abcc3, and Slco1a4*). Overall, gene expression levels determined by the two approaches showed the same pattern of pregnancy-induced changes in both CV and GF mice (upregulation or downregulation). More specifically, *Cyp2b13, Cyp2c50, Sult4a1, Abcc3,* and *Slco1a4* demonstrated downregulation by both RNA-seq and qRT-PCR analyses. As for *Cyp3a16,* downregulation in GFNP group, and upregulation in CVNP, CVP, and GFP groups were observed. The consistency of these results established the accuracy and reliability of the more comprehensive RNA-seq data.

### RNA-SEQ ANALYSIS OF HEPATIC DMET

To determine whether pregnancy and the microbiome interact to affect the expression of host hepatic DMET, we performed RNA-seq analysis of liver tissues from conventional non-pregnant (CVNP, n = 6), conventional pregnant (CVP, n = 5), germ-free non-pregnant (GFNP, n = 6), and germ-free pregnant (GFP, n = 5) C57BL/6 mice. Specifically, we examined the mRNA expression profiles of genes important for xenobiotic, bile acid, and steroid hormone disposition,

including phase I enzymes (cytochrome P450 (*Cyp*) enzymes), phase II enzymes (UDP-glucuronosyltransferases (*Ugt*), sulfotransferases (*Sult*), and glutathione *S*-transferases (*Gst*)), and transporters (ATP-binding cassette (*Abc*) transporters, solute carrier (*Slc*) transporters, and solute carrier organic anion (*Slco*) transporters). Differential changes in the expression of key DMET by pregnancy in CV and GF mice are shown in Table 4-2. A complete list of DMET as determined by RNA-seq analysis can be found in Table 4-3.

First, we did not observe significant differences in the expression of DMET between CVNP and GFNP mice, with either no change or slight trend of down-regulation for most of the DMET listed in Table 4-2 in GFNP mice compared to CVNP mice. When CVP was compared with GFP, we found that the mRNA levels of only two genes, *Cyp2b13 and Cyp2c38,* were higher, 5.3-fold (*FDR* < 0.1) and 3-fold (*FDR* < 0.1), respectively, in GFP mice, as compared to CVP mice (Table 4-2). The expression of other DMET genes was not significantly different between CVP and GFP mice (Table 4-2).

In both CV and GF mice, pregnancy induced significant changes in the expression of many DMET in phase I (Fig. 4-2) and phase II (Fig. 4-3) enzymes, as well as transporters (Fig. 4-4). We noticed that pregnancy altered the expression of DMET with an overall similar trend, but with different magnitudes of changes, in CV and GF mice. For example, pregnancy decreased the mRNA levels of *Cyp2c37, Cyp2c38, Cyp2c50* and *Cyp2c54* by 3.3-fold (*FDR* < 0.01), 2.5-fold (*FDR* < 0.01), 5-fold (*FDR* < 0.001) and 2.5-fold (*FDR* < 0.01), respectively, in CV mice, whereas in GF mice, no significant changes in pregnancy was observed for the same genes (Table 4-2). Similarly, *Cyp2d40* was induced 3.9-fold (*FDR* < 0.001) and 5.4-fold (*FDR* < 0.001) by pregnancy, respectively, in CV and GF mice (Table 4-2 and Fig. 4-2). Among all the *Cyp* isoforms analyzed, CV and GF mice showed most differences in *Cyp3a* isoforms gene

expressions in response to pregnancy (Table 4-2 and Fig. 4-2). We observed a 0.3-fold down-regulation of *Cyp3a11* by pregnancy in GF mice (*FDR* < 0.1), but non-significant down-regulation in CV mice by pregnancy. The mRNA levels of *Cyp3a16* were induced 20.6-fold (*FDR* < 0.1) by pregnancy in CV mice versus 128-fold (*FDR* < 0.001) in GF mice. Likewise, *Cyp3a41a* and *Cyp3a41b* were induced by pregnancy 4.8-fold and 74.2- fold (*FDR* < 0.1), respectively, in CV mice, compared to 10.8-fold and 181.7-fold (*FDR* < 0.01), respectively, in GF mice. *Cyp3a44* was up-regulated by 14.3-fold (*FDR* < 0.001) by pregnancy in CV mice versus 30.5-fold (*FDR* < 0.001) in GF mice.

Of all phase II enzymes that were differentially expressed during pregnancy, we noted that the most significant changes induced by pregnancy were associated with *Sult3a2* and *Sult4a1* in both CV and GF mice. We observed a 53.9-fold (*FDR* < 0.001) induction by pregnancy in CV mice versus a 226.7-fold (*FDR* < 0.001) induction in GF mice for *Sult3a2*, and a 287.7-fold (*FDR* < 0.001) induction in CV mice versus only a non-significant induction in GF mice for *Sult4a1* (Table 4-2 and Fig. 4-3).

For transporters, *Abcc3* and *Slco1a4* were down-regulated by pregnancy to a similar extent in CV and GF mice (Table 4-2 and Fig. 4-4). *Abcc3* was down-regulated by pregnancy by 70% (*p* < 0.05) and 90% (*FDR* < 0.001), respectively, in CV and GF mice. *Slco1a4* was decreased 60% by pregnancy in CV mice (*FDR* < 0.1), but non-significantly in GF mice. Pregnancy induced *Slc22a2* and *Slc22a7* by 561.5-fold (*FDR* < 0.001) and 3.1-fold (*FDR* < 0.1), respectively, in GF mice, versus 260.5-fold (*FDR* < 0.001) induction of *Slc22a2* and non-significant induction of *Slc22a7* in CV mice (Table 4-2 and Fig. 4-4).

### QUANTIFICATION OF RELATIVE PROTEIN ABUNDANCE OF SELECTED HEPATIC DMET BY TARGETED PROTEOMICS

To investigate and compare how protein levels of hepatic enzymes and transporters were changed by pregnancy in CV and GF mice, we performed quantitative proteomics of hepatic DMET in liver tissues. Due to the limited amount of isolated liver membrane proteins available, we performed targeted proteomics only on a set of selected DMET. Selection of DMET was based on *a priori* knowledge of their importance in overall xenobiotic disposition [38]. Relative protein abundance of theses DMET was quantified by LC-MS/MS-based proteomics and results are shown in Fig. 4-5 and Fig. 4-6.

Of the phase I enzymes, we opted to quantify mouse isoforms homologous to human CYP2C19 (CYP2C37, CYP2C50 and CYP2C54), human CYP2D6 (CYP2D22 and CYP2D40), and human CYP3A4 (CYP3A11, CYP3A16, CYP3A41A and CYP3A41B) . Because there are no distinct methods to separate CYP3A41A and CYP3A41B, the results for these two enzymes were combined as CYP3A41. Overall, the effects of pregnancy on protein expression profiles of these Cyp enzymes in CV and GF mice were notably different from the effects of pregnancy on respective mRNA expression profiles. Specifically, we found that pregnancy significantly increased the protein levels of CYP3A11 approximately 2-fold in both CV and GF mice (Fig. 4-5), whereas the mRNA levels of *Cyp3a11* were down-regulated by pregnancy in CV and GF mice (Fig. 4-2). There were no significant differences in the protein levels of CYP3A16 between CVNP and CVP or between GFNP and GFP; however, the protein levels of CYP3A16 in CVP mice were significantly higher by ~25% than those in GFP mice ($0.95 \pm 0.04$ vs. $0.72 \pm 0.03$, $p < 0.05$) (Fig. 4-5). The effect of pregnancy on protein expression of CYP3A41 was similar to its effect on mRNA expression, with a trend of higher abundance in pregnancy for both CV and GF

mice; however, a statistically significant increase by pregnancy was observed only in CV mice (Fig. 4-5). No significant differences in the protein levels of CYP2C and CYP2D isoforms between CVNP and CVP or between GFNP and GFP were observed (Fig. 4-5). Like CYP3A16, the protein levels of CYP2D22 in CVP mice were significantly higher by ~40% than those in GFP mice (0.98 ± 0.03 vs. 0.58 ± 0.02, $p < 0.05$) (Fig. 4-5).

We also quantified various transporters due to their importance in drug disposition, including ABCB11 (Bsep), ABCB1A/B (P-gp), ABCC3 (Mrp3), ABCG2 (Bcrp), SLC22A2 (Oct2), SLC22A7 (Oat2), SLCO1A1 (Oatp1a1), and SLCO1A4 (Oatp1a4). Similar to CYP3A16 and CYP2D22, there were no significant differences in the protein levels of ABCB11 between CVNP and CVP or between GFNP and GFP; however, the protein levels of ABCB11 in CVP mice were significantly greater by ~37% than those in GFP mice (1.3 ± 0.07 vs. 0.82 ± 0.03, $p < 0.05$) (Fig. 4-6). We also observed significantly decreased protein abundance of Slco1a1 in GFP mice compared to CVP mice (1.20 ± 0.03 vs. 2.20 ± 0.03, $p < 0.001$). On the other hand, the protein levels of SLCO1A4 in GFP mice were significantly higher than those in CVP mice (0.71 ± 0.03 vs. 0.42 ± 0.03, $p < 0.05$), but there were no significant differences between GFNP and CVNP mice (Fig. 4-6). Pregnancy significantly increased the protein levels of SLC22A7 ~60% in GF mice (0.87 ± 0.04 vs. 0.55 ± 0.02, $p < 0.05$), but not in CV mice. No significant changes were observed in the abundance of ABCB1A/B, ABCC3 and ABCG2 proteins due to pregnancy or the microbiome.

### ACTIVITY OF HEPATIC CYP3A ENZYMES DETERMINED BY LIVER MICROSOMAL INCUBATIONS

To confirm pregnancy-induced changes in protein expression of Cyp3a enzymes, microsomal incubations were performed to determine Cyp3a activity. We used a luciferin

CYP3A probe to measure the amount of metabolite formed at a single incubation time point, which all fell within the linear range of product formation. Liver microsomes from CVP mice exhibited ~30-fold higher Cyp3a activities ($p < 0.05$) than those from CVNP mice, whereas liver microsomes from GFP mice showed only a ~3-fold induction ($p < 0.05$) of Cyp3a activity compared to GFNP mice (Fig. 4-7). Furthermore, the addition of ketoconazole (a potent, known CYP3A inhibitor) at 5 μM completely abolished metabolite formation with microsomes from both CV and GF mice (Fig. 4-7), suggesting that the enzymatic activity we measured was due to Cyp3a enzymes. Blank control and human recombinant CYP3A4 controls were also assayed in parallel to verify assay functionality (data not shown).

#### QUANTIFICATION OF PLASMA BILE ACIDS AND STEROID HORMONES

Because secondary bile acids generated by gut microbiome may play an important role in regulating the expression of certain key DMET including Cyp3a enzymes [38,39], we quantified plasma concentrations of primary and secondary bile acids in all mice by LC-MS/MS.

The plasma concentrations of the primary bile acids, αMCA and βMCA, in GFNP and GFP mice were lower than those in CVNP and CVP mice (Fig. 4-8). Pregnancy significantly increased the plasma concentrations of β-MCA in CV mice, but had no effect in GF mice. The microbiome had the opposite effect on taurine conjugates, with higher plasma concentrations of T-α-MCA and T-β-MCA in GF mice than in CV mice, regardless of pregnancy. The plasma concentrations of CA were increased ~14-fold by pregnancy in CV mice, with no significant changes between GFP and GFNP mice. Moreover, the plasma concentrations of CA in GF mice were significantly lower than those in CV mice regardless of pregnancy (Fig. 4-8). The pattern of plasma concentrations of UDCA in all mice was similar to that of CA. Neither pregnancy nor the microbiome significantly affected the plasma concentrations of taurine conjugates of CA, CDCA

and UDCA (TCA, TCDCA, and TUDCA, respectively), with the exception that the plasma concentrations of TCA in GFNP mice were 55 times greater than those in CVNP mice (Fig. 4-8).

As expected, the plasma concentrations of most of secondary bile acids were lower in GF mice versus CV mice, likely due to the lack of gut bacteria to synthesize them from primary bile acids (Fig. 4-9). The plasma concentrations of DCA, HDCA, LCA, ωMCA, T-ωMCA, TDCA, and TLCA in GF mice were all significantly decreased versus those in CV mice, regardless of pregnancy (Fig. 4-9). Interestingly, in addition to a decrease in plasma concentrations of LCA in GFNP mice compared to CVNP mice (~11-fold decrease, $p < 0.05$), there was a further decrease of ~5-fold by pregnancy from GFNP to GFP mice ($p < 0.05$). Pregnancy also seemed to affect the production of some secondary bile acids. For example, pregnancy increased the plasma concentrations of DCA ~7-fold ($p < 0.05$) in CV mice, but had no effects in GF mice. Pregnancy also significantly increased the plasma concentrations of HDCA in CV mice (9-fold, $p < 0.05$), but caused a 4-fold reduction ($p < 0.05$) in GF mice. Neither pregnancy nor microbiome significantly affected the plasma concentrations of MDCA and THDCA (Fig. 4-9).

Pregnancy-related steroid hormones have been shown to regulate the expression of drug-metabolizing enzymes and transporters. Therefore, we also determined plasma concentrations of steroid hormones in all mice. As expected, pregnancy significantly increased the plasma concentrations of various steroid hormones, including 11-deoxycorticosterone, 17-OH-pregnenolone, 17-OH-progesterone, corticosterone, cortisol and progesterone, 38- to 125-fold in both CV and GF mice (Fig. 4-20). The lack of microbiome did not seem to alter pregnancy-induced levels of these hormones. The plasma concentrations of aldosterone and cortisone were significantly elevated by pregnancy in GF mice, but not in CV mice (Fig. 4-20). On the other

hand, we did not observe significant effects of pregnancy or microbiome on pregnenolone, estradiol, estrone and DHEA.

## 4.4 DISCUSSION

In this study, we performed the first comprehensive analysis of hepatic DMET expression in pregnant and non-pregnant CV and GF mice using RNA-seq analysis. Six genes were selected for validation by qRT-PCR based on their robust changes and/or importance in drug metabolism or transport. Fold changes in the qRT-PCR data were generally higher than those in the RNA-seq data, but the direction of changes was essentially the same for the two approaches (Fig. 4-1).

Because pregnancy or gut microbiota can separately regulate hepatic DMET [5,40–42], we aimed at investigating whether an interplay of the two physiological factors affects hepatic DMET. To achieve this goal, we utilized CV and GF pregnant and non-pregnant mouse models. The C57BL/6 strain used in this study was also used in previous studies to investigate the effects of the gut microbiome on hepatic DMET expression in non-pregnant mice by RNA-seq analysis [35,43]. This allowed us to compare our results with previously published data. Both the present and previous studies showed a trend of down-regulation of *Cyp3a* isoforms in GF mice compared to CV mice [43] (Table 4-2 and Fig. 4-2); however, the magnitude of down-regulation observed in this study was much less pronounced than that reported previously. This could be due to a sex-difference, as we used female mice whereas the previous studies used male mice. The previous studies, using immunoblotting, also showed a marked decrease in the protein levels of hepatic *Cyp3a11* by the microbiome knockout [43]; however, we did not observe any significant differences in the CYP3A11 protein levels between GFNP and CVNP mice using LC-MS/MS-based proteomics analysis. This could be due to gender-divergent protein expression of

CYP3A11 and/or lower detection specificity of antibody recognition in immunoblotting versus targeted proteomics analysis. The previous studies also reported a significant induction of the *Cyp4a* cluster genes by the microbiome knockout [43], whereas we did not observe any significant changes in *Cyp4a* gene expression (Table 4-1 and Table 4-2). Again, this could be due to the fact that the *Cyp4a* genes, like most other mice Cyps, are sex-divergent [44], and regulation of *Cyp4a14* was reported to be strongly influenced by androgen concentrations [45], which is expectedly low in our female mice.

We have shown that pregnancy alters hepatic DMET in a gestational-age dependent manner in CV FVB mice [10]. Thus, we also compared results of this study with published data as a secondary validation of our RNA-seq data. Overall, our results are in agreement with data from the previous studies. For example, we previously reported that the mRNA levels of hepatic *Cyp3a11* were decreased, while those of *Cyp3a16* and *Cyp3a41* were increased during pregnancy [10]. Consistently, this study also showed down-regulation and induction of *Cyp3a11* and *Cyp3a16/Cyp3a41*, respectively, by pregnancy in CV mice (Table 4-2 and Fig. 4-2). We also reported significant down-regulation of *Cyp2c* cluster genes and *Abcc3* by pregnancy just as we showed in this study in CV mice (Table 4-2 and Fig. 4-2) [10]. Nevertheless, there are some inconsistencies in the magnitude of pregnancy-induced changes for some DMET between this and our previous studies. For example, this study showed a 20.6-fold induction of *Cyp3a16* by pregnancy, while the previous studies reported an induction of only 60% on the same gestation day 15 [10]. The previous studies used FVB mice, while this study used C57BL/6. It is known that the two different mouse strains possess significantly different basal microbiota [46]. It has also been acknowledged that the husbandry environment of the facility in which mice are housed plays a crucial role in bacterial composition [47–51]. Thus, the difference in husbandry

environment could alter bacterial composition in FVB and C57BL/6 mice. These factors may contribute to the different magnitude of pregnancy-induced changes for some DMET between the present and our previous studies, as we have shown in this study that microbiome can alter the magnitude of pregnancy-induced changes for some DMET (detailed below).

The *Cyp3a* isoforms (*Cyp3a11, Cyp3a16, Cyp3a41* and *Cyp3a44*) were of particular interest to us because of the prominent role of their human CYP3A4 homolog in drug metabolism [52]. Therefore, we systemically examined their expression profiles, with quantitation of mRNA, protein and catalytic activity, to see how well changes in the mRNA or protein expression induced by pregnancy and the microbiome predicted alterations in CYP3A activity. We found that the mRNA levels of *Cyp3a11* were significantly decreased by pregnancy in both CV and GF mice, but with a much greater magnitude of down-regulation in GF mice versus CV mice (Table 4-2 and Fig. 4-2). Down-regulation of *Cyp3a11* mRNA by pregnancy has been reported in our previous studies in CV mice [10,53]. The reason of such down-regulation is not known; however, the much greater magnitude of down-regulation of *Cyp3a11* mRNA by pregnancy in GF mice could be due to the combined effects of the lack of secondary bile acids, which would otherwise compensate for the decreased *Cyp3a11* gene expression during pregnancy in CV mice. Yet, targeted proteomics analysis revealed an opposite effect of pregnancy on the protein levels of CYP3A11, with a comparable 2-fold induction of CYP3A11 protein in both CV and GF mice (Fig. 4-5). In contrast to *Cyp3a11*, the mRNA levels of all other *Cyp3a* isoforms were induced by pregnancy in both CV and GF mice. Although the mRNA levels of these *Cyp3a* isoforms in CVP and GFP mice were comparable, the fold-induction in GF mice was generally much greater than that in CV mice (e.g., 128-fold in GF mice versus 20.6-fold in CV mice for *Cyp3a16*) (Table 4-2). This was due to the lower baseline levels of these

*Cyp3a* genes in GFNP mice compared with CVNP mice which were likely caused by the lack of secondary bile acids. Surprisingly, pregnancy induced the protein levels of CYP3A16 and CYP3A41 in CV mice, but had not much effect in GF mice (Fig. 4-5). Although circadian patterns of Cyp mRNA transcripts have been reported, all our mice were sacrificed around the same time of day, and thus the contribution of time of tissue collection is unlikely to be the source of changes observed [54]. Next, we examined the effects of pregnancy and microbiome on the overall CYP3A activity. At present, it is not possible to determine activities of individual CYP3A isoforms due to the lack of specific probes or selective inhibitors for each individual mouse CYP3A isoform. Thus, the CYP3A activities we measured in this study reflected the overall, combined activities of all CYP3A isoforms. We found that the CYP3A activities were significantly induced by pregnancy in both CV and GF mice, but with a much greater induction in CV mice versus GF mice (Fig. 4-7). The activity data agreed with the overall trend of pregnancy-induced increase in Cyp3a protein (Fig. 4-5) and are also consistent with previous studies showing that the metabolic activities of mouse CYP3A for various substrates such as testosterone and glyburide were significantly induced by pregnancy [53,55]. However, for the first time, we showed that microbiome can significantly alter the magnitude of pregnancy-induction of CYP3A activity. The lower fold of pregnancy induction of the CYP3A activity in GF mice could reflect only the activities of the CYP3A isoforms other than CYP3A11 that were not induced by pregnancy at the protein levels (Fig. 4-5). Future studies are needed to explore the mechanisms of microbiome-induced changes in CYP3A activity.

Looking closer at our mRNA and protein expression data, we noted a disconnection between the two sets of data for many DMET in addition to *Cyp3a11* described above. For example, pregnancy drastically decreased the mRNA levels of *Cyp2c50* and *Cyp2c54* (Table 4-

2), but had no significant impact on the protein levels of the two enzymes (Fig. 4-5) in both CV and GF mice. Likewise, the mRNA levels of *Abcc3* were significantly decreased by pregnancy in CV and GF mice (Fig. 4-4), but its protein levels were not affected by pregnancy at all (Fig. 4-6). Although we cannot exclude the possibility that such inconsistencies could possibly be due to the relatively small sample size and large variations in analysis (e.g., proteomics) for certain DMET, the data for CYP3A isoforms seem to be reliable because both the mRNA and/or activity data for the CYP3A isoforms are fully consistent with previous studies. This disconnection between mRNA and protein expression could possibly be due to post-transcriptional or epigenomic regulation of gene expression as what has been shown in numerous studies [56–59]. One of the possible explanations could be the effects of mRNA methylation. Recent studies showed that the gut bacteria *Akkermansia muciniphila* can affect N6-methyladenosine (m6A) in both the intestines and the liver, and m6A methylation can greatly alter RNA transcription processes, leading to epitranscriptomic changes that may explain the gap between mRNA and protein data [60,61]. MicroRNA (miRNA) modification is another possibility to consider. A recent study reported bacteria such as *Firmicutes*, *Bacteroidetes*, and *Proteobacteria* have significant effect on miRNA expression in human [62]. Changes in miRNA expression due to bacteria shift could also lead to changes in downstream gene regulation and result in variations in gene translation. However, contradicting findings exist as to which direction these bacteria regulate miRNA. While the aforementioned human study showed positive correlation in miRNA with *Firmicutes*, another study reported negative correlation with hepatic miRNA expression with relative abundance of the same bacteria in C57BL/6 male mice [63,64]. These changes may be species- and tissue-dependent and should be investigated further.

Another possibility is that our limited sampling time (same time of the day for all mice) restricted our ability to see dynamic changes in mRNA and protein expression relative to the circadian rhythm. Moreover, such post-transcriptional or epigenomic regulation could be altered by microbiota-derived metabolites, which might explain why the protein levels of certain DMET (e.g., CYP3A41 and SLCO1A1) were significantly induced by pregnancy in CV, but not in GF mice (Fig. 4-5 and Fig. 4-6).

Cortisol has previously been shown to induce the expression of CYP3A through activation of GR which in turn induces PXR and then PXR induces transcription of CYP3A gene expression [65]. This could be the potential mechanism by which hepatic human CYP3A abundance is increased during pregnancy. Our data support this hypothesis as we showed that the plasma concentrations of cortisol were markedly increased by pregnancy in both CV and GF mice (Fig. 4-20) and the mRNA levels of all *Cyp3a* isoforms but *Cyp3a11* were induced by pregnancy (Fig. 4-2). *Cyp3a11* is an exception, with its mRNA levels reduced during pregnancy possibly due to post-transcriptional or epigenomic regulation. On the other hand, secondary bile acids have been shown to be PXR ligands that can induce CYP3A [66]. This explains our findings showing that the baseline mRNA levels of all *Cyp3a* isoforms in GFNP mice were generally lower than those in CVNP mice (Fig. 4-2). However, the absence of secondary bile acids did not affect the induction of *Cyp3a16* and *Cyp3a41* mRNA by pregnancy (Fig. 4-2), which is consistent with the notion that pregnancy-induced hormone production was generally not affected by the microbiome knockout (Fig. 4-20). This suggests that the lack of microbiome does not interfere with pregnancy-mediated induction of *Cyp3a* gene transcription, which is mediated by increased production of steroid hormones during pregnancy. Nevertheless, the microbiome can alter the magnitude of induction during pregnancy by changing the baseline

expression of *Cyp3a* genes (Fig. 4-2) or influence pregnancy-induced Cyp3a protein expression (Fig. 4-5) and hence activity (Fig. 4-7) possibly through microbiota-derived metabolites by altering post-transcriptional or epigenomic regulation.

## 4.5 TABLES AND FIGURES

**Table 4-1. Surrogate peptides of cytochrome P450s and transporters and their MS/MS parameters** for detection

| Protein Name | Surrogate Peptide | Peptide Type | Parent Ion (m/z) | Fragment Ion (m/z) |
|---|---|---|---|---|
| Cyp2c37 | DICQSFTNLSK | Light | 656.8 | 796.4 |
| Cyp2c37 | DICQSFTNLSK | Light | 656.8 | 709.4 |
| Cyp2c50 | YAILLLLK | Light | 473.8 | 712.5 |
| Cyp2c50 | YAILLLLK | Light | 473.8 | 599.4 |
| Cyp2c54 | ATNGMGIGFSNGSVWK | Light | 813.4 | 1151.6 |
| Cyp2c54 | ATNGMGIGFSNGSVWK | Light | 813.4 | 1094.6 |
| Cyp2c54 | ESLDVTIPR | Light | 343.9 | 407.2 |
| Cyp2c54 | ESLDVTIPR | Light | 343.9 | 350.7 |
| Cyp2d22 | MPYTNAVIHEVQR | Light | 390.2 | 476.3 |
| Cyp2d22 | MPYTNAVIHEVQR | Light | 390.2 | 476.2 |
| Cyp2d40 | GNPESSFNEANLR | Light | 717.8 | 950.5 |
| Cyp2d40 | GNPESSFNEANLR | Light | 717.8 | 863.4 |
| Cyp3a11 | ALLSPTFTSGK | Light | 561.3 | 937.5 |
| Cyp3a11 | ALLSPTFTSGK | Light | 561.3 | 824.4 |
| Cyp3a11 | ALLSPTFTSGK | Light | 561.3 | 737.4 |
| Cyp3a16 | QDFFPVGIMSK | Light | 423.5 | 731.4 |
| Cyp3a16 | QDFFPVGIMSK | Light | 423.5 | 366.2 |
| Cyp3a41 | VDFLQLMMNAHNNSK | Light | 441.2 | 599.3 |
| Cyp3a41 | VDFLQLMMNAHNNSK | Light | 441.2 | 516.6 |
| Cyp3a41 | LQEEIDETLPNK | Light | 476.9 | 701.4 |
| Cyp3a41 | LQEEIDETLPNK | Light | 476.9 | 572.3 |
| Cyp3a41 | LQEEIDETLPNK | Light | 476.9 | 120.1 |
| BSA | LVNELTEFAK | Light | 582.3 | 708.4 |
| BSA | LVNELTEFAK | Light | 582.3 | 951.5 |
| BSA | AEFVEVTK | Light | 461.7 | 722.4 |
| BSA | AEFVEVTK | Light | 461.7 | 347.2 |
| BSA | AEFVEVTK | Heavy | 465.8 | 859.5 |
| BSA | AEFVEVTK | Heavy | 465.8 | 730.4 |
| BSA | AEFVEVTK | Heavy | 465.8 | 583.4 |
| BSA | AEFVEVTK | Heavy | 465.8 | 484.3 |
| Abcc3 | HIFDQVIGPEGVLAGK | Light | 840.5 | 1429.8 |
| Abcc3 | HIFDQVIGPEGVLAGK | Light | 840.5 | 1282.7 |
| Abcc3 | HIFDQVIGPEGVLAGK | Heavy | 844.5 | 1437.8 |
| Abcc3 | HIFDQVIGPEGVLAGK | Heavy | 844.5 | 1290.7 |
| Abcc3 | HIFDQVIGPEGVLAGK | Heavy | 844.5 | 1175.7 |
| Abcc3 | HIFDQVIGPEGVLAGK | Heavy | 844.5 | 948.6 |
| Abcc3 | HIFDQVIGPEGVLAGK | Heavy | 844.5 | 778.5 |
| Abcb11 | LSTALSGLLLGFYR | Light | 504.3 | 655.4 |
| Abcb11 | LSTALSGLLLGFYR | Light | 504.3 | 699.3 |
| Abcb11 | LSTALSGLLLGFYR | Light | 504.3 | 605.4 |
| Abcb11 | FYDPCEGMVTLDGHDIR | Light | 507.0 | 825.4 |
| Abcb11 | FYDPCEGMVTLDGHDIR | Light | 507.0 | 712.3 |

| | | | | |
|---|---|---|---|---|
| Abcb11 | FYDPCEGMVTLDGHDIR | Light | 507.0 | 597.3 |
| Abcg2 | GEKPVIENLSEFYINSAIYGETK | Light | 867.8 | 982.5 |
| Abcg2 | GEKPVIENLSEFYINSAIYGETK | Light | 867.8 | 989.5 |
| Mdr1a | ATVSASHIIR | Light | 527.8 | 983.6 |
| Mdr1a | ATVSASHIIR | Light | 527.8 | 783.4 |
| Mdr1b | GIYFSMVQAGAK | Light | 636.3 | 791.4 |
| Mdr1b | GIYFSMVQAGAK | Light | 636.3 | 704.4 |
| Slco1a1 | YLEQQYGK | Light | 514.8 | 623.3 |
| Slco1a1 | YLEQQYGK | Light | 514.8 | 662.3 |
| Slco1a1 | YLEQQYGK | Heavy | 518.8 | 873.5 |
| Slco1a1 | YLEQQYGK | Heavy | 518.8 | 631.3 |
| Slco1a1 | YLEQQYGK | Heavy | 518.8 | 662.3 |
| Slc22a2 | YEVDWNQSTLDCVDPLSSLAANR | Light | 885.1 | 1043.5 |
| Slc22a2 | YEVDWNQSTLDCVDPLSSLAANR | Light | 885.1 | 1131.5 |
| Slc22a2 | YEVDWNQSTLDCVDPLSSLAANR | Heavy | 889.1 | 1043.5 |
| Slc22a2 | YEVDWNQSTLDCVDPLSSLAANR | Heavy | 889.1 | 928.5 |
| Slc22a2 | LNPSFLDLVR | Light | 587.3 | 946.5 |
| Slc22a2 | LNPSFLDLVR | Light | 587.3 | 473.8 |
| Slc22a2 | LNPSFLDLVR | Heavy | 592.3 | 956.5 |
| Slc22a2 | LNPSFLDLVR | Heavy | 592.3 | 859.5 |
| Slc22a2 | LNPSFLDLVR | Heavy | 592.3 | 772.4 |
| Slc22a2 | LNPSFLDLVR | Heavy | 592.3 | 625.3 |
| Slc22a2 | LNPSFLDLVR | Heavy | 592.3 | 478.8 |
| Slc22a7 | WLLLAATLPCVPGIISIWWVPESAR | Light | 950.2 | 1343.7 |
| Slc22a7 | WLLLAATLPCVPGIISIWWVPESAR | Light | 950.2 | 1230.6 |
| Slco1a4 | MYDINSFR | Light | 349.2 | 409.2 |
| Slco1a4 | MYDINSFR | Light | 349.2 | 457.7 |
| Slco1a4 | MYDINSFR | Light | 349.2 | 376.2 |

**Table 4-2**. **Pregnancy and microbiome alter mRNA expression of key DMET in female C57BL/6 liver.** This list of genes was generated using the following filtration criteria: fold-change > 1.5 or < 0.65 and $p < 0.01$, on at least one comparison group between CVP and CVNP, GFP and GFNP, GFNP and CVNP, or GFP and CVP.

| Gene Symbol | CVP vs. CVNP | | GFP vs. GFNP | | GFNP vs. CVNP | | GFP vs. CVP | |
|---|---|---|---|---|---|---|---|---|
| | Fold Change | *FDR* | Fold Change | *FDR* | Fold Change | *FDR* | Fold Change | *FDR* |
| ***Cyp17a1*** | 1.7 | 0.28 | 2.9 | 0.01 | 0.9 | 1 | 1.6 | 0.704 |
| ***Cyp26a1*** | 3.2 | 0.076 | 4.2 | 0.02 | 0.9 | 1 | 1.1 | 0.996 |
| ***Cyp26b1*** | <0.1 | <0.001 | 0.1 | <0.001 | 1.9 | 0.982 | 5 | 0.289 |
| ***Cyp2b13*** | 0.1 | <0.001 | 0.3 | <0.001 | 1.2 | 1 | 5.3 | <0.001 |
| ***Cyp2c37*** | 0.3 | 0.002 | 0.6 | 0.152 | 1 | 1 | 1.8 | 0.401 |
| ***Cyp2c38*** | 0.4 | 0.007 | 1 | 0.965 | 1.3 | 1 | 3 | 0.013 |
| ***Cyp2c39*** | 1 | 0.983 | 2.4 | 0.022 | 1.1 | 1 | 2.7 | 0.154 |
| ***Cyp2c50*** | 0.2 | <0.001 | 0.5 | 0.001 | 1 | 1 | 2 | 0.066 |
| ***Cyp2c54*** | 0.4 | 0.001 | 0.8 | 0.561 | 1 | 1 | 2.2 | 0.074 |
| ***Cyp2c55*** | 0.5 | 0.216 | 0.1 | <0.001 | 2.8 | 0.319 | 0.8 | 0.974 |
| ***Cyp2c67*** | 0.4 | 0.012 | 0.6 | 0.279 | 1.4 | 1 | 2.3 | 0.238 |
| ***Cyp2c69*** | 1 | 0.998 | 2.6 | 0.02 | 0.6 | 0.982 | 1.6 | 0.708 |
| ***Cyp2d40*** | 3.9 | <0.001 | 5.4 | <0.001 | 0.7 | 1 | 1 | 1 |
| ***Cyp2d9*** | 0.3 | 0.025 | 0.2 | 0.002 | 1.8 | 1 | 1.1 | 1 |
| ***Cyp2g1*** | 2.8 | 0.047 | 3.6 | 0.01 | 0.6 | 1 | 0.8 | 0.964 |
| ***Cyp39a1*** | 0.4 | 0.031 | 0.3 | 0.017 | 1 | 1 | 0.9 | 0.999 |
| ***Cyp3a11*** | 0.6 | 0.29 | 0.3 | 0.005 | 0.6 | 0.953 | 0.3 | 0.131 |
| ***Cyp3a16*** | 20.6 | 0.001 | 128 | <0.001 | 0.2 | 0.578 | 1.4 | 0.953 |
| ***Cyp3a41a*** | 4.8 | 0.047 | 10.8 | 0.002 | 0.6 | 1 | 1.4 | 0.941 |
| ***Cyp3a41b*** | 74.2 | <0.001 | 181.7 | <0.001 | 0.5 | 1 | 1.3 | 0.989 |
| ***Cyp3a44*** | 14.3 | <0.001 | 30.5 | <0.001 | 0.8 | 1 | 1.7 | 0.816 |
| ***Cyp3a63-ps*** | 5.1 | 0.047 | 8.5 | 0.007 | 0.9 | 1 | 1.5 | 0.926 |
| ***Cyp4a14*** | 0.4 | 0.021 | 0.3 | 0.002 | 1.2 | 1 | 0.9 | 0.958 |
| ***Cyp4a31*** | 4.6 | <0.001 | 5.3 | <0.001 | 1.1 | 1 | 1.3 | 0.909 |
| ***Cyp4f13*** | 0.6 | 0.042 | 0.8 | 0.329 | 0.8 | 1 | 1.1 | 0.987 |
| ***Cyp4f15*** | 0.5 | 0.033 | 0.5 | 0.052 | 1 | 1 | 1.1 | 0.976 |
| ***Ugt1a10*** | 0.9 | 0.977 | 9.6 | 0.004 | 0.2 | 0.439 | 2.4 | 0.689 |
| ***Ugt1a5*** | 2.6 | 0.062 | 3.3 | 0.016 | 0.5 | 0.949 | 0.7 | 0.833 |
| ***Ugt1a6b*** | 0.3 | 0.042 | 0.3 | 0.023 | 1 | 1 | 0.9 | 0.999 |
| ***Ugt2b38*** | 0.2 | 0.139 | <0.1 | 0.013 | 0.5 | 1 | 0.1 | 0.408 |
| ***Sult2a7*** | 0.2 | 0.061 | 0.2 | 0.031 | 0.9 | 1 | 0.7 | 0.964 |
| ***Sult3a1*** | 3.6 | 0.056 | 12.9 | <0.001 | 0.3 | 0.359 | 1 | 1 |
| ***Sult3a2*** | 53.9 | <0.001 | 226.7 | <0.001 | 0.2 | 0.605 | 0.9 | 1 |
| ***Sult4a1*** | 287.7 | <0.001 | 3.5 | 0.333 | 5.2 | 1 | 0.1 | 0.129 |
| ***Gsta2*** | 0.6 | 0.215 | 0.4 | 0.033 | 2 | 0.605 | 1.5 | 0.782 |

| | | | | | | | | |
|---|---|---|---|---|---|---|---|---|
| ***Gstk1*** | 0.5 | 0.005 | 0.5 | 0.018 | 1.1 | 1 | 1.2 | 0.901 |
| ***Gstm2*** | 1.8 | 0.041 | 1.4 | 0.248 | 1.4 | 1 | 1.1 | 0.984 |
| ***Gstm3*** | 3.1 | 0.044 | 0.6 | 0.456 | 2.5 | 0.564 | 0.5 | 0.625 |
| ***Gstp1*** | 3.4 | 0.002 | 2.2 | 0.039 | 0.9 | 1 | 0.6 | 0.635 |
| ***Gstp2*** | 5.9 | 0.016 | 1.8 | 0.505 | 0.9 | 1 | 0.3 | 0.386 |
| ***Gstt1*** | 0.4 | 0.005 | 0.4 | 0.017 | 0.8 | 1 | 0.9 | 0.976 |
| ***Gstt3*** | 1.5 | 0.177 | 2 | 0.005 | 0.8 | 1 | 1.1 | 0.951 |
| ***Abca17*** | 103.3 | <0.001 | 1779 | <0.001 | 0.1 | 0.757 | 1.2 | 0.989 |
| ***Abca5*** | 2 | 0.025 | 3.3 | <0.001 | 0.8 | 1 | 1.3 | 0.768 |
| ***Abca7*** | 0.9 | 0.851 | 0.5 | 0.006 | 1.1 | 1 | 0.6 | 0.298 |
| ***Abcb6*** | 0.6 | 0.019 | 0.7 | 0.129 | 1 | 1 | 1.2 | 0.83 |
| ***Abcc3*** | 0.3 | 0.025 | 0.1 | <0.001 | 1 | 1 | 0.5 | 0.613 |
| ***Abcg5*** | 0.4 | 0.003 | 0.4 | 0.009 | 1.3 | 1 | 1.4 | 0.696 |
| ***Abcg8*** | 0.5 | 0.008 | 0.6 | 0.061 | 1.2 | 1 | 1.4 | 0.613 |
| ***Slc10a1*** | 0.4 | 0.02 | 0.5 | 0.045 | 0.8 | 1 | 1 | 1 |
| ***Slc16a1*** | 2 | 0.018 | 1.6 | 0.142 | 0.9 | 1 | 0.7 | 0.625 |
| ***Slc16a6*** | 16.2 | <0.001 | 14.4 | <0.001 | 1.1 | 1 | 1 | 1 |
| ***Slc17a2*** | 0.3 | 0.057 | 0.2 | 0.009 | 0.9 | 1 | 0.6 | 0.816 |
| ***Slc22a15*** | 0.5 | 0.008 | 0.5 | 0.028 | 1.1 | 1 | 1.2 | 0.869 |
| ***Slc22a2*** | 260.5 | <0.001 | 561.5 | <0.001 | 0.4 | 1 | 0.8 | 0.984 |
| ***Slc22a7*** | 1.3 | 0.713 | 3.1 | 0.004 | 0.5 | 0.437 | 1.1 | 0.975 |
| ***Slc24a3*** | 9.5 | <0.001 | 6.6 | <0.001 | 1.3 | 1 | 0.9 | 0.969 |
| ***Slc25a19*** | 0.8 | 0.291 | 0.6 | 0.015 | 1.1 | 1 | 0.9 | 0.857 |
| ***Slc25a28*** | 0.6 | 0.007 | 0.7 | 0.024 | 0.9 | 1 | 0.9 | 0.953 |
| ***Slc25a30*** | 1.7 | 0.128 | 2.2 | 0.01 | 0.5 | 0.315 | 0.7 | 0.639 |
| ***Slc25a37*** | 0.5 | 0.012 | 0.6 | 0.027 | 0.9 | 1 | 1 | 1 |
| ***Slc25a51*** | 0.6 | 0.026 | 0.3 | <0.001 | 1.8 | 0.181 | 1.1 | 0.951 |
| ***Slc26a10*** | 0.4 | 0.079 | 0.3 | 0.006 | 1.3 | 1 | 0.9 | 0.988 |
| ***Slc26a4*** | 0.1 | 0.009 | 0.2 | 0.016 | 1.2 | 1 | 1.6 | 0.947 |
| ***Slc27a1*** | 0.7 | 0.21 | 0.6 | 0.018 | 1.3 | 1 | 1 | 1 |
| ***Slc35b1*** | 1.8 | 0.006 | 2.5 | <0.001 | 1 | 1 | 1.3 | 0.617 |
| ***Slc35c1*** | 1.3 | 0.254 | 1.6 | 0.029 | 0.9 | 1 | 1.1 | 0.953 |
| ***Slc35c2*** | 1.7 | 0.003 | 2 | <0.001 | 0.9 | 1 | 1 | 1 |
| ***Slc36a1*** | 2.3 | 0.001 | 2.7 | <0.001 | 0.9 | 1 | 1 | 1 |
| ***Slc37a1*** | 11.6 | <0.001 | 6.2 | <0.001 | 1.5 | 1 | 0.8 | 0.946 |
| ***Slc38a4*** | 0.3 | <0.001 | 0.3 | <0.001 | 1.1 | 1 | 1.2 | 0.951 |
| ***Slc39a11*** | 1.4 | 0.18 | 2 | <0.001 | 0.9 | 1 | 1.3 | 0.626 |
| ***Slc39a14*** | 2.3 | 0.013 | 2.1 | 0.022 | 1.5 | 0.978 | 1.4 | 0.775 |
| ***Slc41a2*** | 30.2 | <0.001 | 28.1 | <0.001 | 1.1 | 1 | 1 | 1 |
| ***Slc41a3*** | 4.3 | 0.001 | 3.5 | 0.002 | 1.9 | 0.781 | 1.5 | 0.753 |
| ***Slc43a1*** | 2.6 | 0.037 | 3.1 | 0.01 | 1.1 | 1 | 1.3 | 0.934 |
| ***Slc45a3*** | 3 | 0.001 | 2.1 | 0.027 | 1.2 | 1 | 0.9 | 0.948 |
| ***Slc4a1*** | 8 | 0.002 | 24 | <0.001 | 0.9 | 1 | 2.6 | 0.415 |
| ***Slc4a9*** | 0.1 | 0.025 | 0.1 | 0.001 | 3.9 | 0.359 | 1.9 | 0.914 |
| ***Slc6a9*** | 6.1 | <0.001 | 9 | <0.001 | 0.7 | 1 | 1.1 | 1 |
| ***Slc7a15*** | 5 | 0.102 | 19.1 | 0.01 | 0.1 | 0.554 | 0.4 | 0.786 |
| ***Slc7a2*** | 0.4 | 0.013 | 0.5 | 0.058 | 1.3 | 1 | 1.6 | 0.625 |
| ***Slc7a7*** | 5 | <0.001 | 2.9 | 0.003 | 1.1 | 1 | 0.6 | 0.601 |
| ***Slc8b1*** | 0.5 | 0.023 | 0.6 | 0.055 | 0.8 | 1 | 0.9 | 0.958 |
| ***Slc9a3*** | 0.4 | 0.766 | 74.3 | 0.005 | 0.1 | 1 | 23.5 | 0.238 |

| | | | | | | | | |
|---|---|---|---|---|---|---|---|---|
| ***Slco1a4*** | 0.4 | 0.045 | 0.4 | 0.063 | 1.1 | 1 | 1.2 | 0.945 |
| ***Slco4c1*** | 4.8 | 0.519 | 17.8 | 0.035 | 2.6 | 1 | 9.6 | 0.376 |

**Table 4-3.** P**regnancy and microbiome alter the mRNA expression of DMET in female C57BL/6 liver.** This list of genes was generated by comparing mRNA expression in groups between CVP and CVNP, GFP and GFNP, GFNP and CVNP, and GFP and CVP.

| Gene Symbol | CVP vs. CVNP | | GFP vs. GFNP | | GFNP vs. CVNP | | GFP vs. CVP | |
|---|---|---|---|---|---|---|---|---|
| | Fold Change | *FDR* | Fold Change | *FDR* | Fold Change | *FDR* | Fold Change | *FDR* |
| ***Cyp11a1*** | 1.0 | 1.000 | 0.4 | 0.505 | 1.6 | 1.000 | 0.6 | 0.968 |
| ***Cyp11b1*** | 1.0 | 1.000 | 0.4 | 0.628 | 2.8 | 1.000 | 1.0 | 1.000 |
| ***Cyp17a1*** | 1.7 | 0.280 | 2.9 | 0.010 | 0.9 | 1.000 | 1.6 | 0.704 |
| ***Cyp1a1*** | 0.4 | 0.088 | 0.7 | 0.570 | 1.0 | 1.000 | 1.8 | 0.635 |
| ***Cyp1a2*** | 0.6 | 0.322 | 0.8 | 0.594 | 1.0 | 1.000 | 1.2 | 0.930 |
| ***Cyp1b1*** | 1.1 | 0.959 | 1.9 | 0.462 | 1.0 | 1.000 | 1.7 | 0.859 |
| ***Cyp20a1*** | 0.9 | 0.702 | 0.9 | 0.738 | 0.9 | 1.000 | 0.9 | 0.941 |
| ***Cyp21a1*** | 2.5 | 0.729 | 0.7 | 0.896 | 2.7 | 1.000 | 0.8 | 1.000 |
| ***Cyp21a2-ps*** | 0.7 | 0.797 | 0.9 | 0.932 | 0.8 | 1.000 | 1.0 | 1.000 |
| ***Cyp24a1*** | 1.0 | 1.000 | 1.0 | 1.000 | 1.0 | 1.000 | 1.0 | 1.000 |
| ***Cyp26a1*** | 3.2 | 0.076 | 4.2 | 0.020 | 0.9 | 1.000 | 1.1 | 0.996 |
| ***Cyp26b1*** | 0.0 | <0.001 | 0.1 | <0.001 | 1.9 | 0.982 | 5.0 | 0.289 |
| ***Cyp26c1*** | 0.8 | 0.920 | 0.7 | 0.814 | 0.8 | 1.000 | 0.7 | 0.969 |
| ***Cyp27a1*** | 0.5 | 0.077 | 0.6 | 0.121 | 0.7 | 1.000 | 0.8 | 0.857 |
| ***Cyp2a12*** | 1.0 | 0.975 | 1.3 | 0.641 | 1.0 | 1.000 | 1.4 | 0.824 |
| ***Cyp2a21-ps*** | 1.6 | 0.693 | 1.9 | 0.484 | 1.1 | 1.000 | 1.3 | 0.965 |
| ***Cyp2a22*** | 0.7 | 0.466 | 0.7 | 0.531 | 1.8 | 0.811 | 2.0 | 0.467 |
| ***Cyp2a4*** | 2.2 | 0.052 | 1.5 | 0.323 | 0.7 | 1.000 | 0.5 | 0.413 |
| ***Cyp2a5*** | 0.6 | 0.381 | 0.6 | 0.436 | 1.1 | 1.000 | 1.2 | 0.985 |
| ***Cyp2ab1*** | 0.5 | 0.709 | 0.6 | 0.813 | 1.2 | 1.000 | 1.7 | 0.969 |
| ***Cyp2b10*** | 1.2 | 0.828 | 0.8 | 0.837 | 1.0 | 1.000 | 0.6 | 0.840 |
| ***Cyp2b13*** | 0.1 | <0.001 | 0.3 | <0.001 | 1.2 | 1.000 | 5.3 | <0.001 |
| ***Cyp2b9*** | 0.6 | 0.136 | 1.0 | 0.992 | 0.8 | 1.000 | 1.3 | 0.799 |
| ***Cyp2c23*** | 0.7 | 0.504 | 0.9 | 0.874 | 1.1 | 1.000 | 1.4 | 0.768 |
| ***Cyp2c29*** | 0.7 | 0.261 | 0.7 | 0.241 | 1.4 | 0.953 | 1.4 | 0.639 |
| ***Cyp2c37*** | 0.3 | 0.002 | 0.6 | 0.152 | 1.0 | 1.000 | 1.8 | 0.401 |
| ***Cyp2c38*** | 0.4 | 0.007 | 1.0 | 0.965 | 1.3 | 1.000 | 3.0 | 0.013 |
| ***Cyp2c39*** | 1.0 | 0.983 | 2.4 | 0.022 | 1.1 | 1.000 | 2.7 | 0.154 |
| ***Cyp2c40*** | 0.6 | 0.141 | 0.9 | 0.900 | 0.8 | 1.000 | 1.2 | 0.902 |
| ***Cyp2c50*** | 0.2 | <0.001 | 0.5 | 0.001 | 1.0 | 1.000 | 2.0 | 0.066 |
| ***Cyp2c54*** | 0.4 | 0.001 | 0.8 | 0.561 | 1.0 | 1.000 | 2.2 | 0.074 |
| ***Cyp2c55*** | 0.5 | 0.216 | 0.1 | <0.001 | 2.8 | 0.319 | 0.8 | 0.974 |
| ***Cyp2c67*** | 0.4 | 0.012 | 0.6 | 0.279 | 1.4 | 1.000 | 2.3 | 0.238 |
| ***Cyp2c68*** | 0.7 | 0.527 | 1.1 | 0.930 | 0.9 | 1.000 | 1.3 | 0.841 |
| ***Cyp2c69*** | 1.0 | 0.998 | 2.6 | 0.020 | 0.6 | 0.982 | 1.6 | 0.708 |
| ***Cyp2c70*** | 1.9 | 0.317 | 2.3 | 0.162 | 0.9 | 1.000 | 1.0 | 1.000 |

| | | | | | | | | |
|---|---|---|---|---|---|---|---|---|
| ***Cyp2d10*** | 0.8 | 0.540 | 1.2 | 0.566 | 0.9 | 1.000 | 1.4 | 0.729 |
| ***Cyp2d12*** | 0.9 | 0.965 | 0.5 | 0.204 | 1.4 | 1.000 | 0.8 | 0.912 |
| ***Cyp2d22*** | 0.7 | 0.249 | 0.7 | 0.250 | 1.2 | 1.000 | 1.2 | 0.884 |
| ***Cyp2d26*** | 0.8 | 0.658 | 1.2 | 0.711 | 1.0 | 1.000 | 1.5 | 0.689 |
| ***Cyp2d34*** | 1.0 | 0.993 | 0.7 | 0.641 | 1.3 | 1.000 | 1.0 | 1.000 |
| ***Cyp2d35-ps*** | 1.6 | 0.742 | 0.9 | 0.934 | 2.2 | 1.000 | 1.2 | 0.995 |
| ***Cyp2d36-ps*** | 2.1 | 0.280 | 2.3 | 0.175 | 1.0 | 1.000 | 1.1 | 1.000 |
| ***Cyp2d37-ps*** | 1.6 | 0.342 | 1.2 | 0.754 | 1.0 | 1.000 | 0.8 | 0.898 |
| ***Cyp2d38-ps*** | 2.2 | 0.088 | 1.8 | 0.241 | 1.1 | 1.000 | 0.9 | 0.977 |
| ***Cyp2d40*** | 3.9 | <0.001 | 5.4 | <0.001 | 0.7 | 1.000 | 1.0 | 1.000 |
| ***Cyp2d41-ps*** | 1.2 | 0.831 | 0.9 | 0.907 | 1.0 | 1.000 | 0.7 | 0.904 |
| ***Cyp2d9*** | 0.3 | 0.025 | 0.2 | 0.002 | 1.8 | 1.000 | 1.1 | 1.000 |
| ***Cyp2e1*** | 0.4 | 0.141 | 0.7 | 0.474 | 1.1 | 1.000 | 1.6 | 0.799 |
| ***Cyp2f2*** | 0.6 | 0.182 | 0.8 | 0.507 | 0.7 | 1.000 | 0.9 | 0.977 |
| ***Cyp2g1*** | 2.8 | 0.047 | 3.6 | 0.010 | 0.6 | 1.000 | 0.8 | 0.964 |
| ***Cyp2j5*** | 0.8 | 0.627 | 0.9 | 0.901 | 1.0 | 1.000 | 1.1 | 0.985 |
| ***Cyp2j6*** | 0.8 | 0.543 | 1.1 | 0.808 | 0.9 | 1.000 | 1.3 | 0.774 |
| ***Cyp2j9*** | 0.4 | 0.153 | 0.4 | 0.103 | 0.8 | 1.000 | 0.7 | 0.894 |
| ***Cyp2r1*** | 1.0 | 0.962 | 1.2 | 0.622 | 0.6 | 0.439 | 0.7 | 0.722 |
| ***Cyp2s1*** | 0.3 | 0.222 | 4.5 | 0.072 | 0.5 | 1.000 | 7.1 | 0.238 |
| ***Cyp2u1*** | 0.8 | 0.720 | 0.9 | 0.902 | 0.7 | 1.000 | 0.8 | 0.869 |
| ***Cyp39a1*** | 0.4 | 0.031 | 0.3 | 0.017 | 1.0 | 1.000 | 0.9 | 0.999 |
| ***Cyp3a11*** | 0.6 | 0.290 | 0.3 | 0.005 | 0.6 | 0.953 | 0.3 | 0.131 |
| ***Cyp3a13*** | 1.0 | 1.000 | 1.6 | 0.478 | 0.9 | 1.000 | 1.5 | 0.874 |
| ***Cyp3a16*** | 20.6 | 0.001 | 128.0 | <0.001 | 0.2 | 0.578 | 1.4 | 0.953 |
| ***Cyp3a25*** | 0.7 | 0.235 | 0.8 | 0.374 | 0.7 | 0.873 | 0.8 | 0.762 |
| ***Cyp3a41a*** | 4.8 | 0.047 | 10.8 | 0.002 | 0.6 | 1.000 | 1.4 | 0.941 |
| ***Cyp3a41b*** | 74.2 | <0.001 | 181.7 | <0.001 | 0.5 | 1.000 | 1.3 | 0.989 |
| ***Cyp3a44*** | 14.3 | <0.001 | 30.5 | <0.001 | 0.8 | 1.000 | 1.7 | 0.816 |
| ***Cyp3a59*** | 1.4 | 0.352 | 1.1 | 0.802 | 0.7 | 0.953 | 0.6 | 0.321 |
| ***Cyp3a63-ps*** | 5.1 | 0.047 | 8.5 | 0.007 | 0.9 | 1.000 | 1.5 | 0.926 |
| ***Cyp46a1*** | 0.6 | 0.547 | 0.4 | 0.117 | 1.0 | 1.000 | 0.6 | 0.816 |
| ***Cyp4a10*** | 0.7 | 0.494 | 0.8 | 0.721 | 1.2 | 1.000 | 1.4 | 0.782 |
| ***Cyp4a12a*** | 1.0 | 1.000 | 0.2 | 0.239 | 1.5 | 1.000 | 0.3 | 0.756 |
| ***Cyp4a14*** | 0.4 | 0.021 | 0.3 | 0.002 | 1.2 | 1.000 | 0.9 | 0.958 |
| ***Cyp4a31*** | 4.6 | <0.001 | 5.3 | <0.001 | 1.1 | 1.000 | 1.3 | 0.909 |
| ***Cyp4a32*** | 0.6 | 0.389 | 1.0 | 0.999 | 1.0 | 1.000 | 1.5 | 0.725 |
| ***Cyp4b1*** | 0.8 | 0.655 | 0.6 | 0.378 | 0.9 | 1.000 | 0.8 | 0.909 |
| ***Cyp4f13*** | 0.6 | 0.042 | 0.8 | 0.329 | 0.8 | 1.000 | 1.1 | 0.987 |
| ***Cyp4f14*** | 0.8 | 0.624 | 1.0 | 0.925 | 0.9 | 1.000 | 1.1 | 0.977 |
| ***Cyp4f15*** | 0.5 | 0.033 | 0.5 | 0.052 | 1.0 | 1.000 | 1.1 | 0.976 |
| ***Cyp4f16*** | 1.0 | 0.976 | 0.7 | 0.364 | 0.9 | 1.000 | 0.6 | 0.553 |
| ***Cyp4f17*** | 0.9 | 0.949 | 1.0 | 0.971 | 0.8 | 1.000 | 0.8 | 0.924 |
| ***Cyp4f18*** | 1.0 | 1.000 | 0.4 | 0.364 | 0.9 | 1.000 | 0.4 | 0.656 |
| ***Cyp4v3*** | 0.6 | 0.095 | 0.9 | 0.697 | 1.0 | 1.000 | 1.4 | 0.703 |
| ***Cyp4x1*** | 1.2 | 0.887 | 1.4 | 0.747 | 0.9 | 1.000 | 1.1 | 1.000 |
| ***Cyp51*** | 0.7 | 0.477 | 1.4 | 0.486 | 0.5 | 0.359 | 0.9 | 0.999 |
| ***Cyp7a1*** | 1.1 | 0.883 | 1.4 | 0.614 | 0.9 | 1.000 | 1.1 | 0.993 |

| | | | | | | | | |
|---|---|---|---|---|---|---|---|---|
| ***Cyp7b1*** | 1.3 | 0.732 | 2.2 | 0.064 | 0.6 | 1.000 | 1.1 | 0.981 |
| ***Cyp8b1*** | 1.4 | 0.751 | 2.9 | 0.123 | 0.2 | 0.145 | 0.4 | 0.546 |
| ***Ugt1a1*** | 0.8 | 0.784 | 1.2 | 0.770 | 1.0 | 1.000 | 1.5 | 0.828 |
| ***Ugt1a10*** | 0.9 | 0.977 | 9.6 | 0.004 | 0.2 | 0.439 | 2.4 | 0.689 |
| ***Ugt1a2*** | 0.4 | 0.681 | 0.8 | 0.920 | 0.7 | 1.000 | 1.3 | 1.000 |
| ***Ugt1a5*** | 2.6 | 0.062 | 3.3 | 0.016 | 0.5 | 0.949 | 0.7 | 0.833 |
| ***Ugt1a6a*** | 1.3 | 0.698 | 1.3 | 0.674 | 0.9 | 1.000 | 0.9 | 0.976 |
| ***Ugt1a6b*** | 0.3 | 0.042 | 0.3 | 0.023 | 1.0 | 1.000 | 0.9 | 0.999 |
| ***Ugt1a7c*** | 0.8 | 0.893 | 1.8 | 0.449 | 0.8 | 1.000 | 1.8 | 0.799 |
| ***Ugt1a8*** | 0.3 | 0.496 | 0.2 | 0.230 | 2.9 | 1.000 | 1.6 | 0.974 |
| ***Ugt1a9*** | 0.9 | 0.970 | 1.8 | 0.237 | 1.1 | 1.000 | 2.1 | 0.440 |
| ***Ugt2a2*** | 0.7 | 0.836 | 0.9 | 0.938 | 0.9 | 1.000 | 1.1 | 1.000 |
| ***Ugt2a3*** | 0.8 | 0.364 | 0.9 | 0.869 | 0.9 | 1.000 | 1.1 | 0.943 |
| ***Ugt2b1*** | 0.8 | 0.435 | 0.8 | 0.360 | 1.2 | 1.000 | 1.1 | 0.924 |
| ***Ugt2b34*** | 0.8 | 0.709 | 0.9 | 0.884 | 0.9 | 1.000 | 1.1 | 1.000 |
| ***Ugt2b35*** | 1.3 | 0.522 | 1.2 | 0.648 | 0.9 | 1.000 | 0.9 | 0.954 |
| ***Ugt2b36*** | 1.2 | 0.815 | 1.5 | 0.447 | 1.1 | 1.000 | 1.4 | 0.833 |
| ***Ugt2b37*** | 0.7 | 0.800 | 0.8 | 0.876 | 0.5 | 1.000 | 0.5 | 0.797 |
| ***Ugt2b38*** | 0.2 | 0.139 | 0.0 | 0.013 | 0.5 | 1.000 | 0.1 | 0.408 |
| ***Ugt2b5*** | 0.9 | 0.841 | 0.9 | 0.799 | 1.1 | 1.000 | 1.0 | 1.000 |
| ***Ugt3a1*** | 0.7 | 0.510 | 1.0 | 0.973 | 1.0 | 1.000 | 1.4 | 0.809 |
| ***Ugt3a2*** | 0.9 | 0.957 | 1.4 | 0.579 | 0.9 | 1.000 | 1.3 | 0.915 |
| ***Ugt8a*** | 0.9 | 0.968 | 1.0 | 0.998 | 2.5 | 1.000 | 2.7 | 0.764 |
| ***Sult1a1*** | 0.9 | 0.863 | 1.1 | 0.936 | 1.3 | 1.000 | 1.6 | 0.769 |
| ***Sult1b1*** | 1.2 | 0.761 | 1.4 | 0.428 | 1.3 | 1.000 | 1.5 | 0.690 |
| ***Sult1c2*** | 1.0 | 0.981 | 2.1 | 0.067 | 0.9 | 1.000 | 1.9 | 0.467 |
| ***Sult1d1*** | 0.3 | 0.277 | 0.4 | 0.342 | 1.4 | 1.000 | 1.7 | 0.916 |
| ***Sult1e1*** | 0.2 | 0.417 | 0.2 | 0.255 | 9.9 | 0.411 | 13.6 | 0.454 |
| ***Sult2a1*** | 1.1 | 0.966 | 1.5 | 0.801 | 0.4 | 1.000 | 0.6 | 0.938 |
| ***Sult2a2*** | 0.6 | 0.750 | 0.5 | 0.557 | 1.0 | 1.000 | 0.8 | 0.989 |
| ***Sult2a3*** | 0.5 | 0.697 | 0.2 | 0.239 | 1.7 | 1.000 | 0.6 | 0.975 |
| ***Sult2a5*** | 0.2 | 0.122 | 0.2 | 0.066 | 1.0 | 1.000 | 0.7 | 0.978 |
| ***Sult2a7*** | 0.2 | 0.061 | 0.2 | 0.031 | 0.9 | 1.000 | 0.7 | 0.964 |
| ***Sult2a8*** | 1.1 | 0.934 | 1.5 | 0.548 | 0.9 | 1.000 | 1.2 | 0.982 |
| ***Sult2b1*** | 3.9 | 0.440 | 2.3 | 0.415 | 8.6 | 0.555 | 5.0 | 0.412 |
| ***Sult3a1*** | 3.6 | 0.056 | 12.9 | <0.001 | 0.3 | 0.359 | 1.0 | 1.000 |
| ***Sult3a2*** | 53.9 | <0.001 | 226.7 | <0.001 | 0.2 | 0.605 | 0.9 | 1.000 |
| ***Sult4a1*** | 287.7 | <0.001 | 3.5 | 0.333 | 5.2 | 1.000 | 0.1 | 0.129 |
| ***Sult5a1*** | 0.7 | 0.632 | 0.5 | 0.291 | 0.2 | 0.134 | 0.1 | 0.081 |
| ***Gsta1*** | 7.4 | 0.160 | 0.1 | 0.086 | 9.5 | 0.564 | 0.1 | 0.444 |
| ***Gsta2*** | 0.6 | 0.215 | 0.4 | 0.033 | 2.0 | 0.605 | 1.5 | 0.782 |
| ***Gsta3*** | 0.9 | 0.942 | 1.0 | 0.964 | 0.9 | 1.000 | 1.0 | 1.000 |
| ***Gsta4*** | 0.5 | 0.181 | 0.5 | 0.098 | 1.2 | 1.000 | 1.1 | 0.989 |
| ***Gstcd*** | 1.6 | 0.311 | 1.0 | 0.966 | 1.0 | 1.000 | 0.7 | 0.763 |
| ***Gstk1*** | 0.5 | 0.005 | 0.5 | 0.018 | 1.1 | 1.000 | 1.2 | 0.901 |
| ***Gstm1*** | 1.0 | 0.984 | 0.7 | 0.498 | 1.1 | 1.000 | 0.7 | 0.838 |
| ***Gstm2*** | 1.8 | 0.041 | 1.4 | 0.248 | 1.4 | 1.000 | 1.1 | 0.984 |
| ***Gstm3*** | 3.1 | 0.044 | 0.6 | 0.456 | 2.5 | 0.564 | 0.5 | 0.625 |

| | | | | | | | | |
|---|---|---|---|---|---|---|---|---|
| ***Gstm4*** | 1.1 | 0.800 | 0.8 | 0.503 | 0.8 | 1.000 | 0.5 | 0.289 |
| ***Gstm5*** | 1.1 | 0.948 | 1.2 | 0.635 | 0.7 | 1.000 | 0.8 | 0.884 |
| ***Gstm6*** | 0.9 | 0.908 | 0.9 | 0.892 | 1.3 | 1.000 | 1.3 | 0.922 |
| ***Gstm7*** | 0.8 | 0.809 | 0.8 | 0.797 | 1.0 | 1.000 | 1.1 | 1.000 |
| ***Gsto1*** | 0.8 | 0.496 | 1.1 | 0.882 | 0.9 | 1.000 | 1.3 | 0.822 |
| ***Gsto2*** | 1.0 | 1.000 | 1.1 | 0.938 | 0.5 | 1.000 | 0.6 | 0.817 |
| ***Gstp1*** | 3.4 | 0.002 | 2.2 | 0.039 | 0.9 | 1.000 | 0.6 | 0.635 |
| ***Gstp2*** | 5.9 | 0.016 | 1.8 | 0.505 | 0.9 | 1.000 | 0.3 | 0.386 |
| ***Gstp3*** | 1.9 | 0.190 | 1.4 | 0.516 | 1.1 | 1.000 | 0.8 | 0.951 |
| ***Gstt1*** | 0.4 | 0.005 | 0.4 | 0.017 | 0.8 | 1.000 | 0.9 | 0.976 |
| ***Gstt2*** | 0.6 | 0.182 | 0.7 | 0.380 | 0.9 | 1.000 | 1.0 | 1.000 |
| ***Gstt3*** | 1.5 | 0.177 | 2.0 | 0.005 | 0.8 | 1.000 | 1.1 | 0.951 |
| ***Abca1*** | 1.3 | 0.494 | 1.4 | 0.365 | 1.0 | 1.000 | 1.0 | 1.000 |
| ***Abca13*** | 10.9 | 0.144 | 0.2 | 0.365 | 5.3 | 1.000 | 0.1 | 0.451 |
| ***Abca17*** | 103.3 | <0.001 | 1779.0 | <0.001 | 0.1 | 0.757 | 1.2 | 0.989 |
| ***Abca2*** | 1.2 | 0.873 | 1.4 | 0.579 | 0.8 | 1.000 | 1.0 | 1.000 |
| ***Abca3*** | 1.1 | 0.896 | 1.8 | 0.112 | 0.6 | 0.873 | 1.0 | 1.000 |
| ***Abca4*** | 2.0 | 0.383 | 0.7 | 0.702 | 1.1 | 1.000 | 0.4 | 0.526 |
| ***Abca5*** | 2.0 | 0.025 | 3.3 | <0.001 | 0.8 | 1.000 | 1.3 | 0.768 |
| ***Abca6*** | 1.1 | 0.951 | 1.4 | 0.512 | 1.0 | 1.000 | 1.3 | 0.859 |
| ***Abca7*** | 0.9 | 0.851 | 0.5 | 0.006 | 1.1 | 1.000 | 0.6 | 0.298 |
| ***Abca8a*** | 0.7 | 0.493 | 0.5 | 0.158 | 1.4 | 1.000 | 1.0 | 1.000 |
| ***Abca8b*** | 1.2 | 0.650 | 1.4 | 0.308 | 0.9 | 1.000 | 1.1 | 0.999 |
| ***Abca9*** | 1.5 | 0.328 | 1.3 | 0.495 | 1.1 | 1.000 | 1.0 | 1.000 |
| ***Abcb10*** | 0.9 | 0.586 | 1.0 | 0.964 | 0.8 | 0.817 | 0.9 | 0.856 |
| ***Abcb11*** | 0.7 | 0.438 | 0.9 | 0.794 | 0.9 | 1.000 | 1.2 | 0.950 |
| ***Abcb1a*** | 0.6 | 0.333 | 0.7 | 0.438 | 0.9 | 1.000 | 1.0 | 1.000 |
| ***Abcb1b*** | 1.7 | 0.553 | 1.8 | 0.465 | 1.2 | 1.000 | 1.2 | 0.986 |
| ***Abcb4*** | 0.6 | 0.214 | 0.7 | 0.424 | 0.9 | 1.000 | 1.0 | 1.000 |
| ***Abcb6*** | 0.6 | 0.019 | 0.7 | 0.129 | 1.0 | 1.000 | 1.2 | 0.830 |
| ***Abcb7*** | 1.0 | 0.939 | 1.3 | 0.387 | 0.8 | 1.000 | 1.0 | 1.000 |
| ***Abcb8*** | 0.6 | 0.057 | 0.6 | 0.091 | 0.9 | 1.000 | 1.0 | 1.000 |
| ***Abcb9*** | 1.2 | 0.650 | 1.0 | 0.973 | 1.2 | 1.000 | 1.0 | 1.000 |
| ***Abcc1*** | 1.6 | 0.344 | 0.9 | 0.890 | 1.6 | 0.978 | 0.9 | 0.998 |
| ***Abcc10*** | 0.8 | 0.667 | 0.7 | 0.303 | 1.1 | 1.000 | 0.9 | 0.985 |
| ***Abcc12*** | 0.8 | 0.840 | 0.5 | 0.456 | 0.9 | 1.000 | 0.6 | 0.876 |
| ***Abcc2*** | 0.8 | 0.803 | 0.8 | 0.768 | 1.0 | 1.000 | 1.0 | 1.000 |
| ***Abcc3*** | 0.3 | 0.025 | 0.1 | <0.001 | 1.0 | 1.000 | 0.5 | 0.613 |
| ***Abcc4*** | 1.4 | 0.698 | 1.0 | 0.977 | 1.5 | 1.000 | 1.2 | 0.978 |
| ***Abcc5*** | 1.4 | 0.635 | 0.9 | 0.863 | 1.1 | 1.000 | 0.7 | 0.816 |
| ***Abcc6*** | 0.6 | 0.364 | 0.7 | 0.395 | 1.1 | 1.000 | 1.2 | 0.955 |
| ***Abcc8*** | 0.7 | 0.928 | 1.4 | 0.901 | 1.3 | 1.000 | 2.5 | 0.914 |
| ***Abcc9*** | 1.0 | 0.979 | 1.2 | 0.667 | 0.9 | 1.000 | 1.2 | 0.941 |
| ***Abcd1*** | 1.0 | 0.959 | 1.2 | 0.426 | 0.8 | 1.000 | 1.0 | 1.000 |
| ***Abcd2*** | 1.1 | 0.947 | 1.4 | 0.650 | 0.7 | 1.000 | 0.9 | 1.000 |
| ***Abcd3*** | 0.8 | 0.328 | 0.8 | 0.538 | 0.8 | 0.877 | 0.8 | 0.801 |
| ***Abcd4*** | 0.8 | 0.406 | 0.6 | 0.078 | 1.2 | 1.000 | 1.0 | 1.000 |
| ***Abce1*** | 1.1 | 0.715 | 1.2 | 0.477 | 1.0 | 1.000 | 1.0 | 1.000 |

| | | | | | | | | |
|---|---|---|---|---|---|---|---|---|
| ***Abcf1*** | 0.9 | 0.652 | 1.0 | 0.983 | 0.9 | 1.000 | 1.0 | 1.000 |
| ***Abcf2*** | 0.9 | 0.817 | 1.0 | 0.893 | 0.9 | 1.000 | 1.0 | 0.997 |
| ***Abcf3*** | 0.7 | 0.151 | 0.8 | 0.377 | 0.8 | 1.000 | 0.9 | 0.988 |
| ***Abcg1*** | 1.3 | 0.734 | 0.9 | 0.880 | 0.9 | 1.000 | 0.7 | 0.773 |
| ***Abcg2*** | 1.1 | 0.762 | 1.1 | 0.800 | 0.9 | 1.000 | 0.9 | 0.969 |
| ***Abcg3*** | 1.5 | 0.459 | 1.0 | 0.975 | 0.9 | 1.000 | 0.6 | 0.678 |
| ***Abcg4*** | 3.2 | 0.693 | 0.4 | 0.581 | 9.4 | 0.917 | 1.1 | 1.000 |
| ***Abcg5*** | 0.4 | 0.003 | 0.4 | 0.009 | 1.3 | 1.000 | 1.4 | 0.696 |
| ***Abcg8*** | 0.5 | 0.008 | 0.6 | 0.061 | 1.2 | 1.000 | 1.4 | 0.613 |
| ***Slc10a1*** | 0.4 | 0.020 | 0.5 | 0.045 | 0.8 | 1.000 | 1.0 | 1.000 |
| ***Slc10a2*** | 0.9 | 0.947 | 1.2 | 0.693 | 1.0 | 1.000 | 1.3 | 0.878 |
| ***Slc10a3*** | 0.9 | 0.681 | 1.0 | 1.000 | 0.8 | 1.000 | 1.0 | 1.000 |
| ***Slc10a5*** | 1.2 | 0.821 | 1.1 | 0.915 | 0.9 | 1.000 | 0.8 | 0.972 |
| ***Slc10a6*** | 0.2 | 0.249 | 0.6 | 0.650 | 1.0 | 1.000 | 2.4 | 0.830 |
| ***Slc10a7*** | 1.0 | 0.978 | 0.8 | 0.495 | 1.3 | 1.000 | 1.0 | 1.000 |
| ***Slc11a1*** | 1.5 | 0.567 | 1.2 | 0.836 | 0.7 | 1.000 | 0.6 | 0.689 |
| ***Slc11a2*** | 1.4 | 0.314 | 0.9 | 0.855 | 1.0 | 1.000 | 0.7 | 0.514 |
| ***Slc12a2*** | 0.9 | 0.888 | 1.1 | 0.725 | 1.3 | 0.962 | 1.5 | 0.314 |
| ***Slc12a3*** | 0.8 | 0.900 | 0.7 | 0.697 | 1.7 | 1.000 | 1.4 | 0.945 |
| ***Slc12a4*** | 0.9 | 0.914 | 0.8 | 0.408 | 1.0 | 1.000 | 0.8 | 0.820 |
| ***Slc12a5*** | 0.7 | 0.792 | 0.5 | 0.446 | 0.9 | 1.000 | 0.7 | 0.916 |
| ***Slc12a6*** | 1.1 | 0.789 | 0.9 | 0.662 | 1.1 | 1.000 | 0.9 | 0.901 |
| ***Slc12a7*** | 0.6 | 0.153 | 0.6 | 0.066 | 0.8 | 1.000 | 0.8 | 0.768 |
| ***Slc12a8*** | 1.2 | 0.909 | 1.0 | 1.000 | 1.3 | 1.000 | 1.1 | 1.000 |
| ***Slc12a9*** | 0.7 | 0.472 | 0.9 | 0.883 | 1.1 | 1.000 | 1.4 | 0.768 |
| ***Slc13a2*** | 1.4 | 0.779 | 2.6 | 0.158 | 0.5 | 1.000 | 1.0 | 1.000 |
| ***Slc13a3*** | 0.4 | 0.068 | 0.5 | 0.244 | 0.7 | 1.000 | 0.9 | 0.997 |
| ***Slc13a4*** | 0.3 | 0.250 | 0.6 | 0.672 | 0.6 | 1.000 | 1.2 | 1.000 |
| ***Slc13a5*** | 0.4 | 0.216 | 0.2 | 0.070 | 0.8 | 1.000 | 0.5 | 0.788 |
| ***Slc14a1*** | 1.4 | 0.878 | 6.5 | 0.066 | 0.5 | 1.000 | 2.5 | 0.768 |
| ***Slc14a2*** | 1.4 | 0.947 | 3.9 | 0.479 | 0.2 | 1.000 | 0.5 | 0.941 |
| ***Slc15a1*** | 1.2 | 0.915 | 0.9 | 0.938 | 1.2 | 1.000 | 0.8 | 0.995 |
| ***Slc15a2*** | 1.5 | 0.736 | 0.3 | 0.229 | 2.3 | 1.000 | 0.5 | 0.809 |
| ***Slc15a3*** | 1.8 | 0.316 | 1.0 | 0.994 | 0.9 | 1.000 | 0.5 | 0.550 |
| ***Slc15a4*** | 0.9 | 0.761 | 0.6 | 0.072 | 1.2 | 1.000 | 0.8 | 0.874 |
| ***Slc15a5*** | 0.5 | 0.404 | 0.7 | 0.786 | 0.5 | 1.000 | 0.8 | 0.986 |
| ***Slc16a1*** | 2.0 | 0.018 | 1.6 | 0.142 | 0.9 | 1.000 | 0.7 | 0.625 |
| ***Slc16a10*** | 0.5 | 0.051 | 0.7 | 0.283 | 1.1 | 1.000 | 1.5 | 0.635 |
| ***Slc16a11*** | 0.9 | 0.897 | 1.0 | 0.995 | 0.6 | 0.953 | 0.7 | 0.768 |
| ***Slc16a12*** | 0.5 | 0.088 | 0.7 | 0.401 | 0.9 | 1.000 | 1.2 | 0.945 |
| ***Slc16a13*** | 2.2 | 0.136 | 1.6 | 0.408 | 0.5 | 0.940 | 0.4 | 0.347 |
| ***Slc16a2*** | 0.7 | 0.628 | 1.0 | 0.974 | 0.8 | 1.000 | 1.1 | 0.999 |
| ***Slc16a3*** | 3.3 | 0.107 | 1.1 | 0.959 | 2.2 | 1.000 | 0.7 | 0.945 |
| ***Slc16a4*** | 0.9 | 0.900 | 0.6 | 0.341 | 1.2 | 1.000 | 0.8 | 0.946 |
| ***Slc16a5*** | 1.0 | 0.978 | 1.2 | 0.781 | 1.1 | 1.000 | 1.2 | 0.917 |
| ***Slc16a6*** | 16.2 | <0.001 | 14.4 | <0.001 | 1.1 | 1.000 | 1.0 | 1.000 |
| ***Slc16a7*** | 0.7 | 0.458 | 0.8 | 0.633 | 1.1 | 1.000 | 1.2 | 0.854 |
| ***Slc16a9*** | 1.1 | 0.908 | 1.2 | 0.752 | 0.9 | 1.000 | 1.0 | 1.000 |

| | | | | | | | | |
|---|---|---|---|---|---|---|---|---|
| ***Slc17a1*** | 0.7 | 0.687 | 0.6 | 0.507 | 1.0 | 1.000 | 0.9 | 0.993 |
| ***Slc17a2*** | 0.3 | 0.057 | 0.2 | 0.009 | 0.9 | 1.000 | 0.6 | 0.816 |
| ***Slc17a3*** | 0.7 | 0.336 | 0.9 | 0.685 | 0.9 | 1.000 | 1.1 | 0.987 |
| ***Slc17a4*** | 1.7 | 0.415 | 1.5 | 0.493 | 1.3 | 1.000 | 1.1 | 0.996 |
| ***Slc17a5*** | 0.9 | 0.930 | 1.1 | 0.872 | 1.0 | 1.000 | 1.2 | 0.930 |
| ***Slc17a8*** | 1.9 | 0.375 | 0.6 | 0.519 | 1.0 | 1.000 | 0.4 | 0.383 |
| ***Slc17a9*** | 1.4 | 0.593 | 1.2 | 0.757 | 0.9 | 1.000 | 0.8 | 0.950 |
| ***Slc18a1*** | 1.4 | 0.575 | 1.1 | 0.845 | 1.3 | 1.000 | 1.1 | 1.000 |
| ***Slc18a2*** | 1.0 | 0.977 | 1.0 | 0.984 | 1.0 | 1.000 | 0.9 | 1.000 |
| ***Slc18b1*** | 0.9 | 0.915 | 1.1 | 0.939 | 0.8 | 1.000 | 1.0 | 1.000 |
| ***Slc19a1*** | 0.6 | 0.178 | 0.8 | 0.557 | 1.1 | 1.000 | 1.4 | 0.761 |
| ***Slc19a2*** | 0.7 | 0.156 | 0.7 | 0.198 | 0.9 | 1.000 | 0.9 | 0.996 |
| ***Slc19a3*** | 0.4 | 0.650 | 3.7 | 0.483 | 0.4 | 1.000 | 3.7 | 0.816 |
| ***Slc1a1*** | 1.2 | 0.900 | 1.4 | 0.800 | 0.9 | 1.000 | 1.1 | 1.000 |
| ***Slc1a2*** | 1.5 | 0.699 | 2.1 | 0.313 | 1.4 | 1.000 | 2.0 | 0.756 |
| ***Slc1a3*** | 1.5 | 0.825 | 0.6 | 0.660 | 1.4 | 1.000 | 0.5 | 0.895 |
| ***Slc1a4*** | 1.8 | 0.140 | 1.0 | 1.000 | 1.1 | 1.000 | 0.6 | 0.533 |
| ***Slc1a5*** | 0.7 | 0.616 | 0.5 | 0.141 | 1.3 | 1.000 | 0.9 | 0.987 |
| ***Slc1a6*** | 0.5 | 0.714 | 0.3 | 0.475 | 0.9 | 1.000 | 0.5 | 0.951 |
| ***Slc20a1*** | 0.6 | 0.059 | 0.7 | 0.141 | 1.1 | 1.000 | 1.2 | 0.832 |
| ***Slc20a2*** | 1.4 | 0.188 | 1.5 | 0.113 | 1.0 | 1.000 | 1.0 | 1.000 |
| ***Slc22a1*** | 0.8 | 0.595 | 0.9 | 0.847 | 1.0 | 1.000 | 1.2 | 0.953 |
| ***Slc22a13b-ps*** | 0.4 | 0.487 | 0.5 | 0.528 | 0.9 | 1.000 | 1.0 | 1.000 |
| ***Slc22a15*** | 0.5 | 0.008 | 0.5 | 0.028 | 1.1 | 1.000 | 1.2 | 0.869 |
| ***Slc22a17*** | 1.0 | 0.990 | 0.9 | 0.906 | 0.9 | 1.000 | 0.8 | 0.975 |
| ***Slc22a18*** | 0.7 | 0.294 | 0.9 | 0.810 | 1.0 | 1.000 | 1.4 | 0.768 |
| ***Slc22a2*** | 260.5 | <0.001 | 561.5 | <0.001 | 0.4 | 1.000 | 0.8 | 0.984 |
| ***Slc22a21*** | 0.3 | 0.083 | 1.9 | 0.337 | 0.5 | 0.889 | 2.8 | 0.433 |
| ***Slc22a23*** | 1.4 | 0.270 | 1.6 | 0.080 | 1.0 | 1.000 | 1.1 | 0.967 |
| ***Slc22a26*** | 0.6 | 0.352 | 1.0 | 1.000 | 0.7 | 1.000 | 1.1 | 0.985 |
| ***Slc22a27*** | 0.5 | 0.126 | 0.5 | 0.101 | 0.6 | 0.992 | 0.6 | 0.665 |
| ***Slc22a28*** | 2.9 | 0.100 | 2.8 | 0.102 | 1.3 | 1.000 | 1.2 | 0.976 |
| ***Slc22a29*** | 0.2 | 0.075 | 0.2 | 0.072 | 0.9 | 1.000 | 0.9 | 1.000 |
| ***Slc22a3*** | 0.9 | 0.930 | 0.9 | 0.890 | 1.6 | 1.000 | 1.6 | 0.767 |
| ***Slc22a30*** | 1.1 | 0.852 | 1.3 | 0.317 | 0.9 | 1.000 | 1.1 | 0.996 |
| ***Slc22a4*** | 0.5 | 0.194 | 0.8 | 0.825 | 0.8 | 1.000 | 1.3 | 0.917 |
| ***Slc22a5*** | 0.8 | 0.566 | 0.9 | 0.709 | 1.0 | 1.000 | 1.1 | 0.951 |
| ***Slc22a6*** | 0.4 | 0.654 | 0.2 | 0.449 | 1.7 | 1.000 | 1.0 | 1.000 |
| ***Slc22a7*** | 1.3 | 0.713 | 3.1 | 0.004 | 0.5 | 0.437 | 1.1 | 0.975 |
| ***Slc22a8*** | 0.3 | 0.567 | 0.0 | 0.108 | 1.9 | 1.000 | 0.3 | 0.890 |
| ***Slc23a1*** | 1.0 | 1.000 | 1.2 | 0.682 | 0.7 | 1.000 | 0.9 | 0.969 |
| ***Slc23a2*** | 0.6 | 0.194 | 0.7 | 0.336 | 0.9 | 1.000 | 1.0 | 1.000 |
| ***Slc23a3*** | 1.1 | 0.975 | 0.6 | 0.764 | 2.7 | 1.000 | 1.5 | 0.974 |
| ***Slc23a4*** | 1.6 | 0.654 | 0.4 | 0.269 | 1.7 | 1.000 | 0.4 | 0.681 |
| ***Slc24a3*** | 9.5 | <0.001 | 6.6 | <0.001 | 1.3 | 1.000 | 0.9 | 0.969 |
| ***Slc24a5*** | 0.7 | 0.690 | 0.9 | 0.920 | 0.6 | 1.000 | 0.8 | 0.962 |
| ***Slc25a1*** | 0.7 | 0.153 | 0.8 | 0.343 | 0.7 | 0.811 | 0.8 | 0.786 |
| ***Slc25a10*** | 0.7 | 0.080 | 0.8 | 0.336 | 0.9 | 1.000 | 1.0 | 1.000 |

| | | | | | | | | |
|---|---|---|---|---|---|---|---|---|
| ***Slc25a11*** | 0.7 | 0.016 | 0.7 | 0.029 | 1.0 | 1.000 | 1.0 | 1.000 |
| ***Slc25a12*** | 1.0 | 0.989 | 0.9 | 0.845 | 0.9 | 1.000 | 0.8 | 0.901 |
| ***Slc25a13*** | 0.7 | 0.220 | 0.8 | 0.529 | 1.0 | 1.000 | 1.2 | 0.880 |
| ***Slc25a14*** | 1.1 | 0.944 | 0.7 | 0.420 | 1.1 | 1.000 | 0.7 | 0.768 |
| ***Slc25a15*** | 0.8 | 0.688 | 0.9 | 0.833 | 1.3 | 1.000 | 1.4 | 0.713 |
| ***Slc25a16*** | 1.0 | 0.995 | 1.1 | 0.796 | 1.1 | 1.000 | 1.2 | 0.857 |
| ***Slc25a17*** | 1.0 | 0.943 | 0.9 | 0.500 | 0.9 | 1.000 | 0.8 | 0.654 |
| ***Slc25a18*** | 1.4 | 0.820 | 0.4 | 0.257 | 2.5 | 0.940 | 0.7 | 0.945 |
| ***Slc25a19*** | 0.8 | 0.291 | 0.6 | 0.015 | 1.1 | 1.000 | 0.9 | 0.857 |
| ***Slc25a20*** | 1.0 | 0.975 | 1.0 | 0.908 | 1.0 | 1.000 | 0.9 | 0.946 |
| ***Slc25a21*** | 0.7 | 0.286 | 0.6 | 0.182 | 1.0 | 1.000 | 0.9 | 0.978 |
| ***Slc25a22*** | 1.0 | 0.990 | 0.7 | 0.221 | 1.4 | 0.757 | 1.0 | 0.999 |
| ***Slc25a23*** | 0.7 | 0.245 | 1.0 | 1.000 | 0.8 | 1.000 | 1.2 | 0.924 |
| ***Slc25a24*** | 1.1 | 0.862 | 1.2 | 0.703 | 1.1 | 1.000 | 1.2 | 0.945 |
| ***Slc25a25*** | 1.1 | 0.885 | 1.1 | 0.861 | 1.6 | 1.000 | 1.6 | 0.701 |
| ***Slc25a26*** | 1.1 | 0.849 | 1.1 | 0.732 | 0.9 | 1.000 | 1.0 | 1.000 |
| ***Slc25a27*** | 0.8 | 0.836 | 0.4 | 0.229 | 1.8 | 1.000 | 1.0 | 1.000 |
| ***Slc25a28*** | 0.6 | 0.007 | 0.7 | 0.024 | 0.9 | 1.000 | 0.9 | 0.953 |
| ***Slc25a29*** | 0.8 | 0.585 | 1.0 | 0.977 | 1.0 | 1.000 | 1.3 | 0.816 |
| ***Slc25a3*** | 0.8 | 0.504 | 0.8 | 0.231 | 1.0 | 1.000 | 0.9 | 0.947 |
| ***Slc25a30*** | 1.7 | 0.128 | 2.2 | 0.010 | 0.5 | 0.315 | 0.7 | 0.639 |
| ***Slc25a31*** | 0.4 | 0.521 | 0.4 | 0.589 | 1.0 | 1.000 | 1.2 | 1.000 |
| ***Slc25a32*** | 0.8 | 0.457 | 0.8 | 0.381 | 1.3 | 1.000 | 1.3 | 0.722 |
| ***Slc25a33*** | 1.4 | 0.250 | 1.5 | 0.147 | 0.9 | 1.000 | 0.9 | 0.999 |
| ***Slc25a34*** | 1.0 | 1.000 | 1.1 | 0.936 | 1.0 | 1.000 | 1.1 | 0.998 |
| ***Slc25a35*** | 0.7 | 0.608 | 0.9 | 0.890 | 0.9 | 1.000 | 1.2 | 0.985 |
| ***Slc25a36*** | 1.2 | 0.683 | 1.5 | 0.299 | 1.1 | 1.000 | 1.3 | 0.837 |
| ***Slc25a37*** | 0.5 | 0.012 | 0.6 | 0.027 | 0.9 | 1.000 | 1.0 | 1.000 |
| ***Slc25a38*** | 0.9 | 0.631 | 0.9 | 0.609 | 1.1 | 1.000 | 1.1 | 0.869 |
| ***Slc25a39*** | 0.7 | 0.070 | 0.8 | 0.298 | 0.9 | 1.000 | 1.0 | 0.994 |
| ***Slc25a4*** | 1.0 | 0.948 | 0.8 | 0.628 | 1.0 | 1.000 | 0.8 | 0.799 |
| ***Slc25a40*** | 1.1 | 0.943 | 0.9 | 0.833 | 0.9 | 1.000 | 0.8 | 0.854 |
| ***Slc25a42*** | 0.8 | 0.396 | 0.7 | 0.320 | 0.9 | 1.000 | 0.9 | 0.912 |
| ***Slc25a43*** | 0.8 | 0.876 | 0.5 | 0.329 | 0.8 | 1.000 | 0.4 | 0.625 |
| ***Slc25a44*** | 1.1 | 0.895 | 1.1 | 0.701 | 1.0 | 1.000 | 1.0 | 1.000 |
| ***Slc25a45*** | 0.9 | 0.916 | 1.0 | 0.983 | 0.8 | 1.000 | 0.9 | 0.913 |
| ***Slc25a46*** | 0.9 | 0.787 | 1.1 | 0.728 | 1.0 | 1.000 | 1.2 | 0.800 |
| ***Slc25a47*** | 0.9 | 0.746 | 0.9 | 0.861 | 1.2 | 1.000 | 1.3 | 0.817 |
| ***Slc25a48*** | 0.6 | 0.189 | 0.7 | 0.387 | 1.2 | 1.000 | 1.4 | 0.753 |
| ***Slc25a5*** | 0.8 | 0.388 | 0.8 | 0.271 | 0.9 | 1.000 | 0.9 | 0.886 |
| ***Slc25a51*** | 0.6 | 0.026 | 0.3 | <0.001 | 1.8 | 0.181 | 1.1 | 0.951 |
| ***Slc25a53*** | 1.2 | 0.893 | 0.7 | 0.703 | 1.4 | 1.000 | 0.8 | 0.979 |
| ***Slc26a1*** | 0.8 | 0.793 | 1.1 | 0.903 | 0.9 | 1.000 | 1.1 | 0.988 |
| ***Slc26a10*** | 0.4 | 0.079 | 0.3 | 0.006 | 1.3 | 1.000 | 0.9 | 0.988 |
| ***Slc26a11*** | 0.9 | 0.864 | 0.7 | 0.206 | 1.1 | 1.000 | 0.8 | 0.833 |
| ***Slc26a2*** | 1.2 | 0.580 | 1.0 | 0.994 | 1.1 | 1.000 | 0.9 | 0.961 |
| ***Slc26a3*** | 1.4 | 0.899 | 7.5 | 0.104 | 0.9 | 1.000 | 4.8 | 0.601 |
| ***Slc26a4*** | 0.1 | 0.009 | 0.2 | 0.016 | 1.2 | 1.000 | 1.6 | 0.947 |

| | | | | | | | | |
|---|---|---|---|---|---|---|---|---|
| ***Slc26a6*** | 1.1 | 0.955 | 1.9 | 0.062 | 0.5 | 0.536 | 1.0 | 1.000 |
| ***Slc26a7*** | 0.1 | 0.150 | 3.3 | 0.516 | 0.1 | 0.615 | 3.3 | 0.838 |
| ***Slc26a8*** | 0.4 | 0.450 | 0.7 | 0.800 | 0.9 | 1.000 | 1.6 | 0.950 |
| ***Slc27a1*** | 0.7 | 0.210 | 0.6 | 0.018 | 1.3 | 1.000 | 1.0 | 1.000 |
| ***Slc27a2*** | 0.7 | 0.547 | 0.7 | 0.530 | 1.0 | 1.000 | 1.0 | 1.000 |
| ***Slc27a3*** | 1.9 | 0.334 | 0.8 | 0.754 | 2.7 | 0.438 | 1.1 | 0.998 |
| ***Slc27a4*** | 1.0 | 0.934 | 1.2 | 0.517 | 0.9 | 1.000 | 1.1 | 0.945 |
| ***Slc27a5*** | 0.6 | 0.242 | 0.9 | 0.837 | 0.8 | 1.000 | 1.2 | 0.943 |
| ***Slc27a6*** | 1.8 | 0.632 | 0.8 | 0.920 | 1.5 | 1.000 | 0.7 | 0.951 |
| ***Slc28a1*** | 0.4 | 0.347 | 0.6 | 0.572 | 0.8 | 1.000 | 1.2 | 1.000 |
| ***Slc28a2*** | 1.3 | 0.804 | 1.3 | 0.788 | 1.0 | 1.000 | 1.0 | 1.000 |
| ***Slc28a3*** | 0.4 | 0.702 | 0.7 | 0.837 | 4.2 | 0.875 | 7.3 | 0.597 |
| ***Slc29a1*** | 0.7 | 0.137 | 0.7 | 0.166 | 1.1 | 1.000 | 1.2 | 0.888 |
| ***Slc29a2*** | 0.6 | 0.285 | 0.4 | 0.075 | 1.0 | 1.000 | 0.7 | 0.888 |
| ***Slc29a3*** | 1.2 | 0.806 | 1.5 | 0.321 | 0.8 | 1.000 | 1.1 | 0.993 |
| ***Slc29a4*** | 0.9 | 0.996 | 0.2 | 0.287 | 2.8 | 1.000 | 0.7 | 0.983 |
| ***Slc2a1*** | 1.0 | 0.990 | 0.9 | 0.940 | 0.9 | 1.000 | 0.8 | 0.946 |
| ***Slc2a10*** | 0.9 | 0.977 | 1.4 | 0.800 | 0.8 | 1.000 | 1.2 | 0.999 |
| ***Slc2a12*** | 0.7 | 0.737 | 3.2 | 0.106 | 0.4 | 0.761 | 1.6 | 0.847 |
| ***Slc2a13*** | 1.3 | 0.817 | 0.6 | 0.495 | 1.9 | 0.995 | 1.0 | 1.000 |
| ***Slc2a2*** | 0.5 | 0.233 | 0.6 | 0.438 | 1.1 | 1.000 | 1.4 | 0.911 |
| ***Slc2a3*** | 1.9 | 0.495 | 3.4 | 0.116 | 2.8 | 0.873 | 5.0 | 0.242 |
| ***Slc2a4*** | 0.3 | 0.257 | 0.4 | 0.296 | 2.0 | 1.000 | 2.3 | 0.739 |
| ***Slc2a4rg-ps*** | 0.6 | 0.453 | 0.4 | 0.071 | 1.2 | 1.000 | 0.8 | 0.914 |
| ***Slc2a5*** | 0.9 | 0.948 | 1.2 | 0.796 | 0.9 | 1.000 | 1.1 | 0.991 |
| ***Slc2a6*** | 4.4 | 0.144 | 0.6 | 0.668 | 1.7 | 1.000 | 0.2 | 0.478 |
| ***Slc2a7*** | 1.0 | 1.000 | 1.0 | 1.000 | 1.0 | 1.000 | 1.0 | 1.000 |
| ***Slc2a8*** | 1.0 | 0.919 | 1.0 | 0.970 | 0.9 | 1.000 | 1.0 | 0.998 |
| ***Slc2a9*** | 0.7 | 0.404 | 0.8 | 0.550 | 0.9 | 1.000 | 1.0 | 1.000 |
| ***Slc30a1*** | 1.3 | 0.505 | 1.6 | 0.051 | 1.0 | 1.000 | 1.3 | 0.799 |
| ***Slc30a10*** | 1.7 | 0.622 | 1.3 | 0.854 | 1.1 | 1.000 | 0.8 | 0.984 |
| ***Slc30a2*** | 2.0 | 0.661 | 2.1 | 0.775 | 0.3 | 1.000 | 0.3 | 0.747 |
| ***Slc30a3*** | 0.4 | 0.499 | 0.4 | 0.533 | 0.5 | 1.000 | 0.6 | 0.946 |
| ***Slc30a4*** | 1.4 | 0.351 | 1.4 | 0.333 | 1.1 | 1.000 | 1.1 | 0.985 |
| ***Slc30a5*** | 1.1 | 0.870 | 1.0 | 0.975 | 1.0 | 1.000 | 1.0 | 1.000 |
| ***Slc30a6*** | 1.2 | 0.552 | 1.2 | 0.454 | 1.0 | 1.000 | 1.0 | 1.000 |
| ***Slc30a7*** | 1.0 | 0.973 | 0.9 | 0.921 | 0.8 | 1.000 | 0.8 | 0.901 |
| ***Slc30a9*** | 0.8 | 0.245 | 0.8 | 0.181 | 1.0 | 1.000 | 1.0 | 1.000 |
| ***Slc31a1*** | 0.9 | 0.851 | 1.1 | 0.739 | 0.9 | 1.000 | 1.1 | 0.960 |
| ***Slc31a2*** | 1.1 | 0.797 | 1.1 | 0.751 | 0.9 | 1.000 | 0.9 | 0.971 |
| ***Slc33a1*** | 1.4 | 0.280 | 1.5 | 0.076 | 1.0 | 1.000 | 1.1 | 0.943 |
| ***Slc34a2*** | 2.6 | 0.176 | 2.0 | 0.403 | 0.6 | 1.000 | 0.5 | 0.694 |
| ***Slc34a3*** | 1.0 | 1.000 | 1.0 | 1.000 | 1.0 | 1.000 | 1.0 | 1.000 |
| ***Slc35a1*** | 0.9 | 0.827 | 1.1 | 0.578 | 0.8 | 0.999 | 1.0 | 1.000 |
| ***Slc35a2*** | 1.0 | 0.930 | 1.0 | 0.947 | 1.0 | 1.000 | 1.1 | 0.988 |
| ***Slc35a3*** | 1.0 | 0.937 | 1.1 | 0.709 | 1.0 | 1.000 | 1.1 | 0.978 |
| ***Slc35a4*** | 0.9 | 0.938 | 1.3 | 0.506 | 1.0 | 1.000 | 1.5 | 0.689 |
| ***Slc35a5*** | 1.1 | 0.800 | 1.0 | 1.000 | 1.1 | 1.000 | 1.0 | 1.000 |

| | | | | | | | | |
|---|---|---|---|---|---|---|---|---|
| ***Slc35b1*** | 1.8 | 0.006 | 2.5 | <0.001 | 1.0 | 1.000 | 1.3 | 0.617 |
| ***Slc35b2*** | 1.0 | 0.977 | 1.5 | 0.089 | 0.9 | 1.000 | 1.3 | 0.629 |
| ***Slc35b3*** | 1.1 | 0.771 | 1.3 | 0.272 | 0.8 | 1.000 | 1.0 | 0.996 |
| ***Slc35b4*** | 1.0 | 0.984 | 1.4 | 0.288 | 0.9 | 1.000 | 1.4 | 0.753 |
| ***Slc35c1*** | 1.3 | 0.254 | 1.6 | 0.029 | 0.9 | 1.000 | 1.1 | 0.953 |
| ***Slc35c2*** | 1.7 | 0.003 | 2.0 | <0.001 | 0.9 | 1.000 | 1.0 | 1.000 |
| ***Slc35d1*** | 1.2 | 0.546 | 1.1 | 0.735 | 0.8 | 1.000 | 0.8 | 0.595 |
| ***Slc35d2*** | 1.2 | 0.542 | 1.5 | 0.131 | 0.8 | 1.000 | 1.0 | 1.000 |
| ***Slc35d3*** | 3.5 | 0.641 | 5.8 | 0.488 | 0.4 | 1.000 | 0.6 | 0.984 |
| ***Slc35e1*** | 1.1 | 0.628 | 1.0 | 0.919 | 1.1 | 1.000 | 1.0 | 0.997 |
| ***Slc35e2*** | 1.0 | 0.944 | 1.0 | 0.964 | 1.3 | 0.817 | 1.3 | 0.702 |
| ***Slc35e3*** | 0.8 | 0.483 | 0.7 | 0.158 | 0.9 | 1.000 | 0.8 | 0.745 |
| ***Slc35e4*** | 1.8 | 0.451 | 1.3 | 0.794 | 1.2 | 1.000 | 0.9 | 0.988 |
| ***Slc35f1*** | 1.8 | 0.798 | 0.8 | 0.937 | 1.7 | 1.000 | 0.7 | 0.994 |
| ***Slc35f2*** | 1.1 | 0.979 | 1.0 | 0.995 | 0.9 | 1.000 | 0.8 | 0.999 |
| ***Slc35f3*** | 1.0 | 1.000 | 2.3 | 0.532 | 0.8 | 1.000 | 1.8 | 0.917 |
| ***Slc35f5*** | 1.3 | 0.458 | 1.1 | 0.781 | 1.0 | 1.000 | 0.9 | 0.951 |
| ***Slc35f6*** | 1.0 | 0.942 | 1.1 | 0.876 | 1.0 | 1.000 | 1.1 | 0.971 |
| ***Slc35g1*** | 0.9 | 0.742 | 1.0 | 0.946 | 1.1 | 1.000 | 1.2 | 0.876 |
| ***Slc35g2*** | 0.7 | 0.754 | 0.7 | 0.684 | 1.6 | 1.000 | 1.5 | 0.865 |
| ***Slc36a1*** | 2.3 | 0.001 | 2.7 | <0.001 | 0.9 | 1.000 | 1.0 | 1.000 |
| ***Slc36a2*** | 0.1 | 0.266 | 0.8 | 0.915 | 0.9 | 1.000 | 4.6 | 0.756 |
| ***Slc36a4*** | 1.1 | 0.901 | 1.2 | 0.598 | 0.9 | 1.000 | 1.0 | 1.000 |
| ***Slc37a1*** | 11.6 | <0.001 | 6.2 | <0.001 | 1.5 | 1.000 | 0.8 | 0.946 |
| ***Slc37a2*** | 1.2 | 0.832 | 0.7 | 0.424 | 0.8 | 1.000 | 0.5 | 0.350 |
| ***Slc37a3*** | 1.4 | 0.227 | 1.4 | 0.208 | 1.0 | 1.000 | 1.0 | 1.000 |
| ***Slc37a4*** | 0.5 | 0.094 | 0.6 | 0.135 | 1.3 | 1.000 | 1.4 | 0.809 |
| ***Slc38a1*** | 1.0 | 0.988 | 1.3 | 0.605 | 1.1 | 1.000 | 1.3 | 0.835 |
| ***Slc38a10*** | 1.3 | 0.351 | 1.6 | 0.062 | 0.8 | 1.000 | 1.0 | 1.000 |
| ***Slc38a11*** | 0.5 | 0.595 | 0.7 | 0.791 | 0.9 | 1.000 | 1.3 | 0.991 |
| ***Slc38a2*** | 1.1 | 0.704 | 1.3 | 0.202 | 1.4 | 0.322 | 1.6 | 0.107 |
| ***Slc38a3*** | 0.8 | 0.551 | 0.9 | 0.715 | 1.0 | 1.000 | 1.1 | 0.971 |
| ***Slc38a4*** | 0.3 | <0.001 | 0.3 | <0.001 | 1.1 | 1.000 | 1.2 | 0.951 |
| ***Slc38a5*** | 1.2 | 0.955 | 0.4 | 0.465 | 2.8 | 1.000 | 1.0 | 1.000 |
| ***Slc38a6*** | 0.9 | 0.914 | 0.9 | 0.751 | 1.1 | 1.000 | 1.0 | 1.000 |
| ***Slc38a7*** | 0.7 | 0.149 | 0.9 | 0.609 | 0.9 | 1.000 | 1.1 | 0.945 |
| ***Slc38a8*** | 1.2 | 0.967 | 0.9 | 0.958 | 3.3 | 1.000 | 2.5 | 0.865 |
| ***Slc38a9*** | 1.0 | 0.963 | 0.9 | 0.742 | 1.1 | 1.000 | 0.9 | 0.973 |
| ***Slc39a1*** | 1.0 | 0.998 | 1.2 | 0.507 | 0.9 | 1.000 | 1.1 | 0.965 |
| ***Slc39a10*** | 1.3 | 0.439 | 0.7 | 0.344 | 1.4 | 1.000 | 0.7 | 0.722 |
| ***Slc39a11*** | 1.4 | 0.180 | 2.0 | <0.001 | 0.9 | 1.000 | 1.3 | 0.626 |
| ***Slc39a13*** | 1.1 | 0.728 | 1.1 | 0.853 | 1.0 | 1.000 | 1.0 | 1.000 |
| ***Slc39a14*** | 2.3 | 0.013 | 2.1 | 0.022 | 1.5 | 0.978 | 1.4 | 0.775 |
| ***Slc39a2*** | 0.6 | 0.522 | 0.5 | 0.208 | 1.1 | 1.000 | 0.9 | 0.988 |
| ***Slc39a3*** | 1.1 | 0.749 | 1.0 | 0.877 | 0.9 | 1.000 | 0.9 | 0.794 |
| ***Slc39a4*** | 0.9 | 0.817 | 0.7 | 0.358 | 0.8 | 1.000 | 0.6 | 0.603 |
| ***Slc39a5*** | 1.5 | 0.680 | 1.2 | 0.878 | 1.1 | 1.000 | 0.9 | 0.998 |
| ***Slc39a6*** | 1.0 | 0.990 | 1.0 | 1.000 | 1.3 | 1.000 | 1.3 | 0.843 |

| | | | | | | | | |
|---|---|---|---|---|---|---|---|---|
| ***Slc39a7*** | 1.1 | 0.762 | 1.2 | 0.461 | 0.9 | 1.000 | 0.9 | 0.975 |
| ***Slc39a8*** | 1.0 | 0.996 | 1.1 | 0.817 | 1.0 | 1.000 | 1.2 | 0.949 |
| ***Slc39a9*** | 1.1 | 0.707 | 1.2 | 0.579 | 1.0 | 1.000 | 1.1 | 0.978 |
| ***Slc3a1*** | 1.0 | 1.000 | 1.8 | 0.469 | 0.7 | 1.000 | 1.2 | 0.985 |
| ***Slc3a2*** | 0.8 | 0.448 | 0.9 | 0.719 | 1.0 | 1.000 | 1.1 | 0.936 |
| ***Slc40a1*** | 1.5 | 0.292 | 1.6 | 0.180 | 0.7 | 1.000 | 0.8 | 0.837 |
| ***Slc41a1*** | 1.0 | 0.997 | 1.2 | 0.671 | 0.7 | 1.000 | 0.9 | 0.943 |
| ***Slc41a2*** | 30.2 | <0.001 | 28.1 | <0.001 | 1.1 | 1.000 | 1.0 | 1.000 |
| ***Slc41a3*** | 4.3 | 0.001 | 3.5 | 0.002 | 1.9 | 0.781 | 1.5 | 0.753 |
| ***Slc43a1*** | 2.6 | 0.037 | 3.1 | 0.010 | 1.1 | 1.000 | 1.3 | 0.934 |
| ***Slc43a2*** | 1.1 | 0.895 | 1.0 | 0.982 | 0.9 | 1.000 | 0.9 | 0.967 |
| ***Slc43a3*** | 0.8 | 0.493 | 0.8 | 0.334 | 1.0 | 1.000 | 0.9 | 0.962 |
| ***Slc44a1*** | 1.1 | 0.751 | 1.2 | 0.425 | 0.9 | 1.000 | 1.0 | 1.000 |
| ***Slc44a2*** | 0.9 | 0.721 | 0.8 | 0.477 | 1.0 | 1.000 | 0.9 | 0.943 |
| ***Slc44a3*** | 0.9 | 0.908 | 0.6 | 0.416 | 0.9 | 1.000 | 0.7 | 0.803 |
| ***Slc44a4*** | 0.6 | 0.844 | 2.6 | 0.389 | 1.6 | 1.000 | 6.9 | 0.404 |
| ***Slc45a3*** | 3.0 | 0.001 | 2.1 | 0.027 | 1.2 | 1.000 | 0.9 | 0.948 |
| ***Slc45a4*** | 1.2 | 0.706 | 1.4 | 0.343 | 0.7 | 1.000 | 0.8 | 0.912 |
| ***Slc46a1*** | 0.9 | 0.608 | 1.1 | 0.570 | 0.7 | 0.593 | 1.0 | 0.995 |
| ***Slc46a3*** | 0.5 | 0.090 | 0.9 | 0.866 | 0.7 | 1.000 | 1.4 | 0.844 |
| ***Slc47a1*** | 0.9 | 0.922 | 1.0 | 0.975 | 0.9 | 1.000 | 1.0 | 1.000 |
| ***Slc48a1*** | 1.1 | 0.749 | 1.0 | 1.000 | 1.0 | 1.000 | 0.9 | 0.914 |
| ***Slc4a1*** | 8.0 | 0.002 | 24.0 | <0.001 | 0.9 | 1.000 | 2.6 | 0.415 |
| ***Slc4a11*** | 0.6 | 0.755 | 0.6 | 0.742 | 0.6 | 1.000 | 0.6 | 0.944 |
| ***Slc4a1ap*** | 0.8 | 0.268 | 0.7 | 0.074 | 1.0 | 1.000 | 0.9 | 0.869 |
| ***Slc4a2*** | 0.9 | 0.818 | 0.8 | 0.433 | 1.0 | 1.000 | 0.9 | 0.938 |
| ***Slc4a3*** | 0.6 | 0.469 | 0.9 | 0.856 | 0.9 | 1.000 | 1.3 | 0.930 |
| ***Slc4a4*** | 0.7 | 0.439 | 0.8 | 0.517 | 1.1 | 1.000 | 1.1 | 0.967 |
| ***Slc4a5*** | 1.3 | 0.926 | 0.3 | 0.436 | 2.9 | 1.000 | 0.6 | 0.984 |
| ***Slc4a7*** | 1.1 | 0.862 | 1.1 | 0.699 | 1.0 | 1.000 | 1.1 | 0.982 |
| ***Slc4a8*** | 1.1 | 0.978 | 0.3 | 0.272 | 0.9 | 1.000 | 0.3 | 0.557 |
| ***Slc4a9*** | 0.1 | 0.025 | 0.1 | 0.001 | 3.9 | 0.359 | 1.9 | 0.914 |
| ***Slc50a1*** | 0.6 | 0.144 | 0.8 | 0.703 | 0.9 | 1.000 | 1.3 | 0.816 |
| ***Slc51a*** | 0.3 | 0.381 | 0.3 | 0.424 | 0.4 | 1.000 | 0.4 | 0.795 |
| ***Slc51b*** | 1.4 | 0.835 | 0.9 | 0.943 | 0.8 | 1.000 | 0.5 | 0.820 |
| ***Slc52a2*** | 0.6 | 0.178 | 0.6 | 0.112 | 0.8 | 1.000 | 0.7 | 0.762 |
| ***Slc52a3*** | 0.9 | 0.931 | 1.6 | 0.605 | 1.1 | 1.000 | 2.0 | 0.762 |
| ***Slc5a1*** | 0.6 | 0.551 | 0.8 | 0.856 | 1.1 | 1.000 | 1.6 | 0.897 |
| ***Slc5a11*** | 0.5 | 0.758 | 0.5 | 0.734 | 0.4 | 1.000 | 0.3 | 0.868 |
| ***Slc5a3*** | 1.2 | 0.779 | 0.9 | 0.861 | 1.1 | 1.000 | 0.8 | 0.949 |
| ***Slc5a4b*** | 0.7 | 0.821 | 0.9 | 0.966 | 1.2 | 1.000 | 1.7 | 0.938 |
| ***Slc5a5*** | 1.8 | 0.786 | 2.1 | 0.703 | 0.6 | 1.000 | 0.7 | 0.999 |
| ***Slc5a6*** | 0.5 | 0.130 | 0.6 | 0.166 | 1.2 | 1.000 | 1.3 | 0.912 |
| ***Slc5a9*** | 8.5 | 0.247 | 0.4 | 0.685 | 8.4 | 0.908 | 0.4 | 0.912 |
| ***Slc6a1*** | 2.1 | 0.629 | 0.9 | 0.971 | 0.7 | 1.000 | 0.3 | 0.739 |
| ***Slc6a12*** | 1.1 | 0.952 | 1.6 | 0.137 | 0.9 | 1.000 | 1.4 | 0.718 |
| ***Slc6a13*** | 0.8 | 0.699 | 0.9 | 0.818 | 0.9 | 1.000 | 1.0 | 1.000 |
| ***Slc6a14*** | 0.5 | 0.769 | 3.5 | 0.348 | 0.8 | 1.000 | 5.4 | 0.575 |

| | | | | | | | | |
|---|---|---|---|---|---|---|---|---|
| ***Slc6a15*** | 0.5 | 0.809 | 1.1 | 0.997 | 0.5 | 1.000 | 1.2 | 1.000 |
| ***Slc6a16*** | 0.3 | 0.253 | 0.4 | 0.249 | 1.4 | 1.000 | 1.5 | 0.941 |
| ***Slc6a17*** | 0.9 | 0.993 | 0.6 | 0.731 | 2.4 | 1.000 | 1.5 | 0.978 |
| ***Slc6a18*** | 2.9 | 0.637 | 7.4 | 0.293 | 1.0 | 1.000 | 2.6 | 0.901 |
| ***Slc6a19*** | 0.1 | 0.369 | 0.2 | 0.320 | 1.6 | 1.000 | 2.0 | 0.975 |
| ***Slc6a2*** | 4.6 | 0.452 | 0.9 | 0.953 | 6.0 | 0.979 | 1.1 | 1.000 |
| ***Slc6a20b*** | 1.6 | 0.646 | 0.6 | 0.525 | 1.5 | 1.000 | 0.6 | 0.799 |
| ***Slc6a4*** | 1.8 | 0.513 | 1.4 | 0.783 | 0.6 | 1.000 | 0.5 | 0.744 |
| ***Slc6a6*** | 1.2 | 0.713 | 1.6 | 0.159 | 0.8 | 1.000 | 1.0 | 1.000 |
| ***Slc6a8*** | 0.9 | 0.836 | 1.3 | 0.616 | 0.9 | 1.000 | 1.4 | 0.856 |
| ***Slc6a9*** | 6.1 | <0.001 | 9.0 | <0.001 | 0.7 | 1.000 | 1.1 | 1.000 |
| ***Slc7a1*** | 1.4 | 0.606 | 1.1 | 0.915 | 1.6 | 1.000 | 1.2 | 0.956 |
| ***Slc7a10*** | 0.3 | 0.619 | 0.4 | 0.559 | 2.8 | 1.000 | 4.4 | 0.763 |
| ***Slc7a11*** | 2.0 | 0.478 | 1.2 | 0.861 | 2.2 | 1.000 | 1.4 | 0.950 |
| ***Slc7a14*** | 0.6 | 0.680 | 0.3 | 0.273 | 1.5 | 1.000 | 0.7 | 0.978 |
| ***Slc7a15*** | 5.0 | 0.102 | 19.1 | 0.010 | 0.1 | 0.554 | 0.4 | 0.786 |
| ***Slc7a2*** | 0.4 | 0.013 | 0.5 | 0.058 | 1.3 | 1.000 | 1.6 | 0.625 |
| ***Slc7a3*** | 1.8 | 0.779 | 0.6 | 0.776 | 2.5 | 1.000 | 0.8 | 1.000 |
| ***Slc7a4*** | 1.1 | 0.933 | 1.0 | 1.000 | 0.9 | 1.000 | 0.8 | 0.971 |
| ***Slc7a5*** | 0.8 | 0.833 | 0.9 | 0.848 | 1.1 | 1.000 | 1.2 | 0.969 |
| ***Slc7a6*** | 0.5 | 0.451 | 2.3 | 0.214 | 1.0 | 1.000 | 4.6 | 0.262 |
| ***Slc7a6os*** | 0.9 | 0.658 | 0.8 | 0.243 | 1.0 | 1.000 | 0.9 | 0.947 |
| ***Slc7a7*** | 5.0 | <0.001 | 2.9 | 0.003 | 1.1 | 1.000 | 0.6 | 0.601 |
| ***Slc7a8*** | 1.6 | 0.380 | 1.3 | 0.649 | 0.9 | 1.000 | 0.7 | 0.841 |
| ***Slc7a9*** | 8.0 | 0.255 | 14.3 | 0.138 | 0.6 | 1.000 | 1.1 | 1.000 |
| ***Slc8a1*** | 3.1 | 0.236 | 2.1 | 0.486 | 0.7 | 1.000 | 0.5 | 0.803 |
| ***Slc8b1*** | 0.5 | 0.023 | 0.6 | 0.055 | 0.8 | 1.000 | 0.9 | 0.958 |
| ***Slc9a1*** | 0.9 | 0.792 | 0.8 | 0.421 | 1.1 | 1.000 | 1.0 | 1.000 |
| ***Slc9a2*** | 0.8 | 0.965 | 13.0 | 0.056 | 0.3 | 1.000 | 4.9 | 0.575 |
| ***Slc9a3*** | 0.4 | 0.766 | 74.3 | 0.005 | 0.1 | 1.000 | 23.5 | 0.238 |
| ***Slc9a3r1*** | 0.6 | 0.055 | 0.7 | 0.229 | 0.9 | 1.000 | 1.1 | 0.951 |
| ***Slc9a3r2*** | 0.6 | 0.067 | 0.6 | 0.102 | 0.9 | 1.000 | 1.0 | 1.000 |
| ***Slc9a5*** | 1.0 | 0.998 | 0.7 | 0.518 | 1.2 | 1.000 | 0.8 | 0.951 |
| ***Slc9a6*** | 1.1 | 0.872 | 1.0 | 1.000 | 1.0 | 1.000 | 0.9 | 0.997 |
| ***Slc9a7*** | 1.7 | 0.429 | 2.3 | 0.141 | 0.6 | 1.000 | 0.9 | 0.979 |
| ***Slc9a8*** | 0.7 | 0.197 | 0.8 | 0.267 | 0.9 | 1.000 | 0.9 | 0.943 |
| ***Slc9a9*** | 1.3 | 0.567 | 1.1 | 0.861 | 0.9 | 1.000 | 0.8 | 0.855 |
| ***Slc9b1*** | 3.2 | 0.335 | 5.5 | 0.152 | 0.5 | 1.000 | 0.8 | 1.000 |
| ***Slc9b2*** | 1.3 | 0.734 | 1.2 | 0.795 | 1.1 | 1.000 | 1.0 | 1.000 |
| ***Slco1a1*** | 1.6 | 0.585 | 2.0 | 0.319 | 0.5 | 1.000 | 0.6 | 0.856 |
| ***Slco1a4*** | 0.4 | 0.045 | 0.4 | 0.063 | 1.1 | 1.000 | 1.2 | 0.945 |
| ***Slco1a6*** | 3.9 | 0.339 | 5.1 | 0.192 | 0.9 | 1.000 | 1.2 | 1.000 |
| ***Slco1b2*** | 0.5 | 0.316 | 0.6 | 0.375 | 1.1 | 1.000 | 1.2 | 0.964 |
| ***Slco2a1*** | 1.1 | 0.883 | 1.3 | 0.562 | 0.9 | 1.000 | 1.0 | 1.000 |
| ***Slco2b1*** | 0.9 | 0.806 | 1.1 | 0.859 | 1.0 | 1.000 | 1.2 | 0.869 |
| ***Slco3a1*** | 1.0 | 0.983 | 0.8 | 0.635 | 1.0 | 1.000 | 0.8 | 0.894 |
| ***Slco4a1*** | 0.5 | 0.475 | 0.6 | 0.524 | 1.1 | 1.000 | 1.3 | 0.976 |
| ***Slco4c1*** | 4.8 | 0.519 | 17.8 | 0.035 | 2.6 | 1.000 | 9.6 | 0.376 |

| | | | | | | | | |
|---|---|---|---|---|---|---|---|---|
| ***Slco5a1*** | 1.8 | 0.479 | 0.3 | 0.180 | 2.1 | 0.982 | 0.4 | 0.636 |

**Figure 4-1**

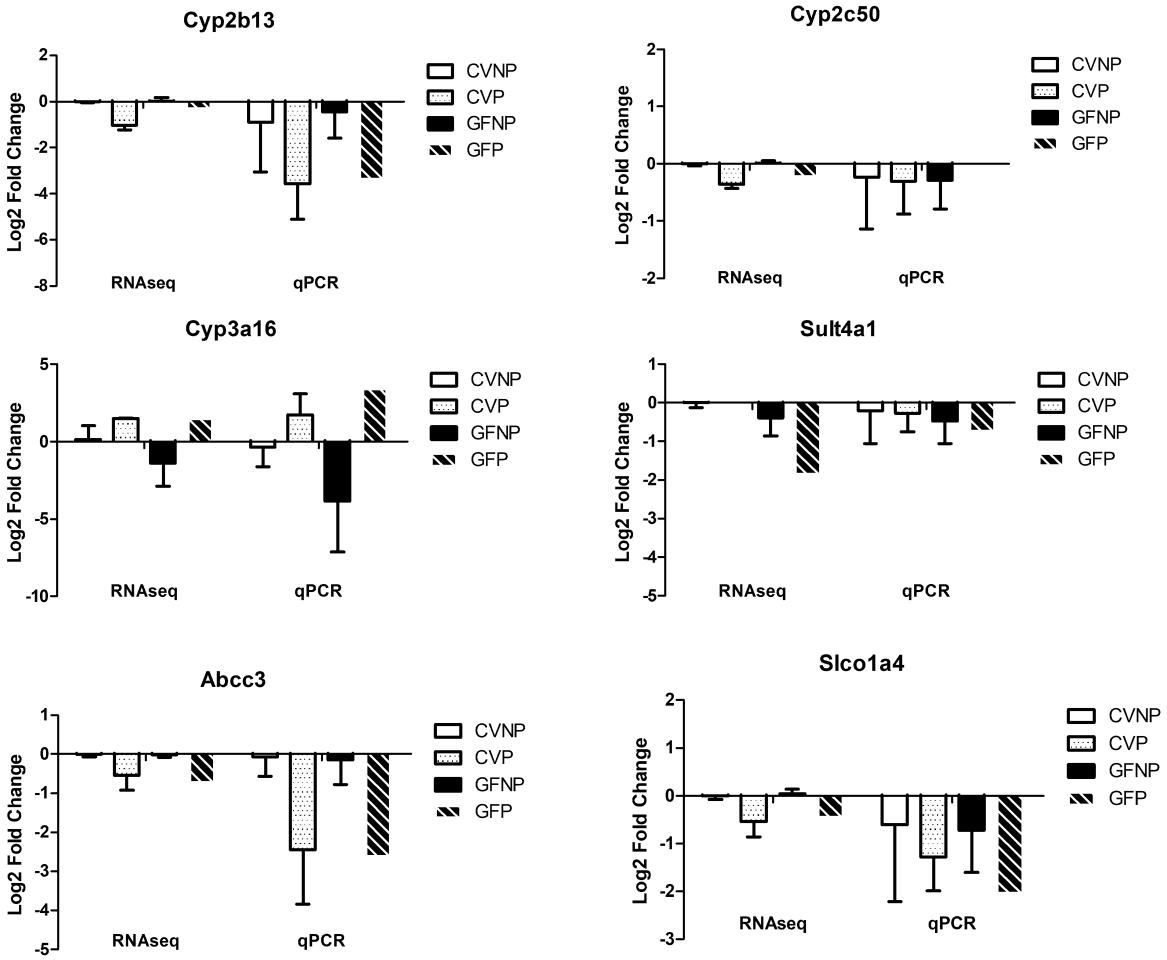


**Figure 4-1. Comparison of RNA-seq and qRT-PCR gene expression data in the liver.** Log2 fold-change is relative to the CVNP group for both RNA-seq and qRT-PCR data. Shown are means ± SD of gene expression data from 5 – 6 different mouse liver tissues.

**Figure 4-2**

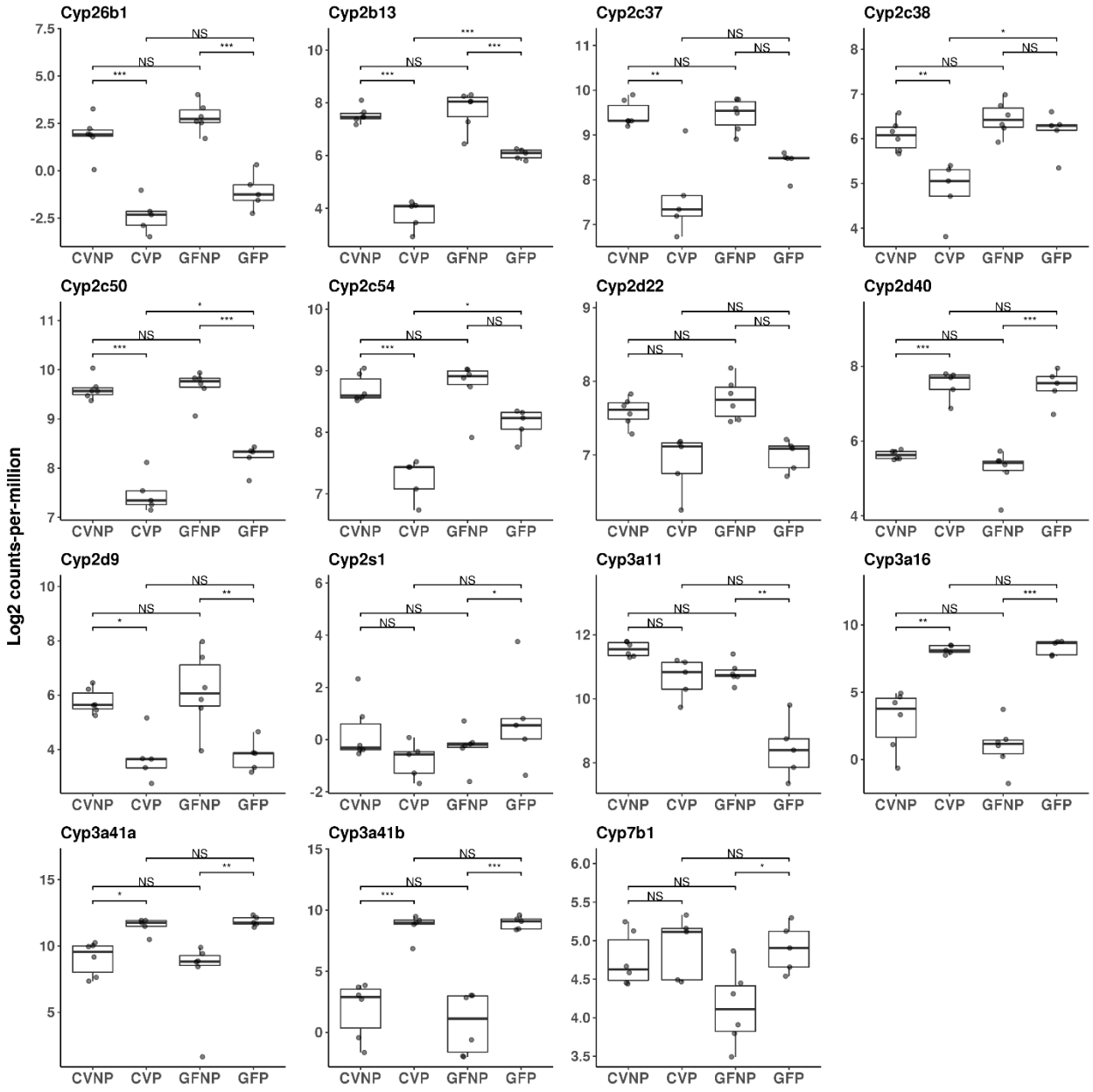


**Figure 4-2. Effect of pregnancy and microbiome on mRNA expression of hepatic Phase I enzymes.** Shown are boxplots with individual scatters of RNA-seq analysis data of hepatic phase I enzymes from female C57BL/6 mice. Data illustrates individual log2 counts-per-million for each DMET. All pregnant mice used were on gestation day 15. *$FDR < 0.1$; **$FDR < 0.01$;

***$FDR < 0.001$. CVNP, conventional non-pregnant mice; CVP, conventional pregnant mice; GFNP, germ-free non-pregnant mice; GFP, germ-free pregnant mice.

**Figure 4-3**

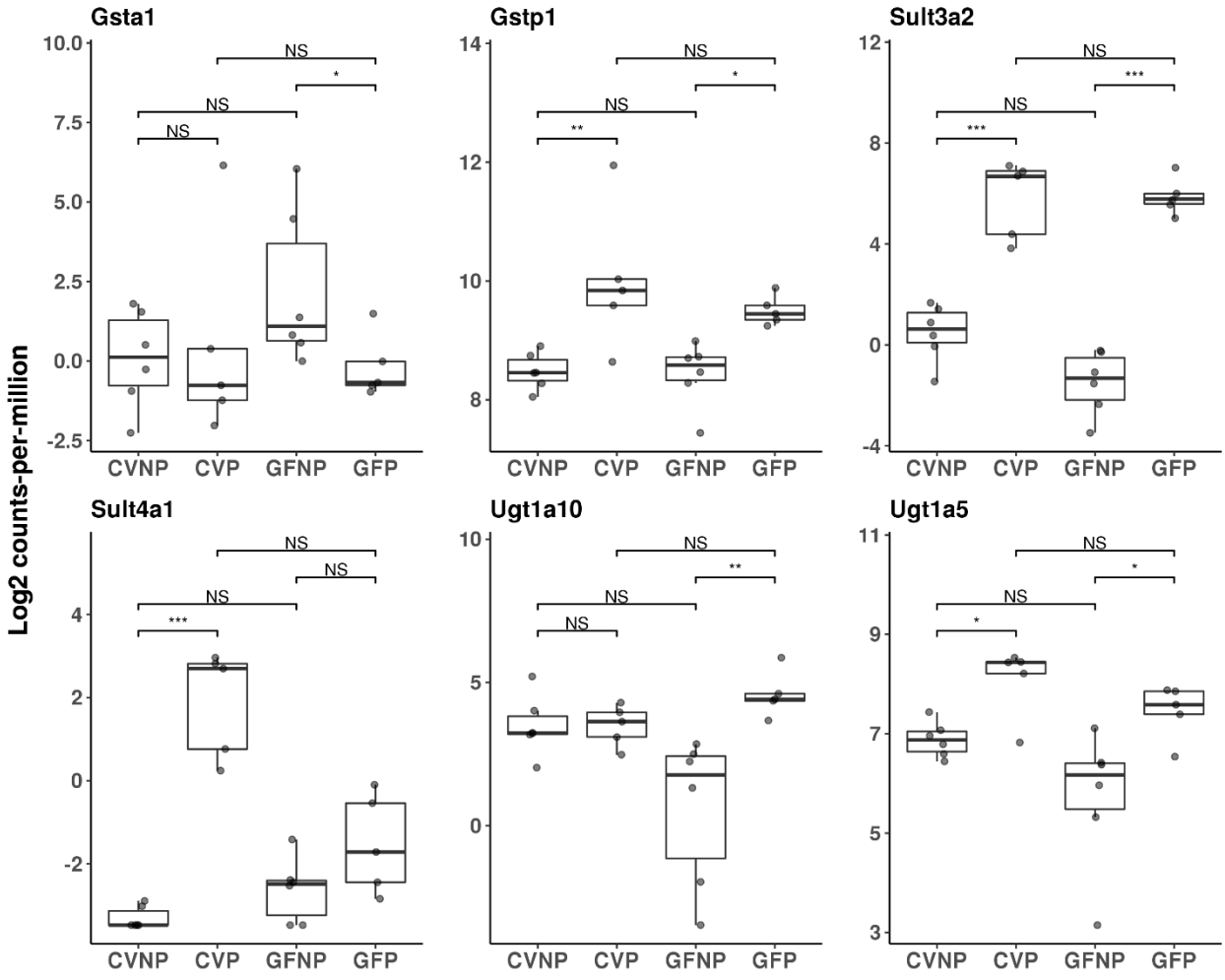


**Figure 4-3. Effect of pregnancy and microbiome on mRNA expression of hepatic Phase II enzymes**. Shown are boxplots with individual scatters of RNA-seq analysis data of hepatic phase II enzymes from female C57BL/6 mice. Data illustrates individual log2 counts-per-million for each DMET. All pregnant mice used were on gestation day 15. *$FDR < 0.1$; **$FDR < 0.01$; ***$FDR < 0.001$. CVNP, conventional non-pregnant mice; CVP, conventional pregnant mice; GFNP, germ-free non-pregnant mice; GFP, germ-free pregnant mice.

**Figure 4-4**

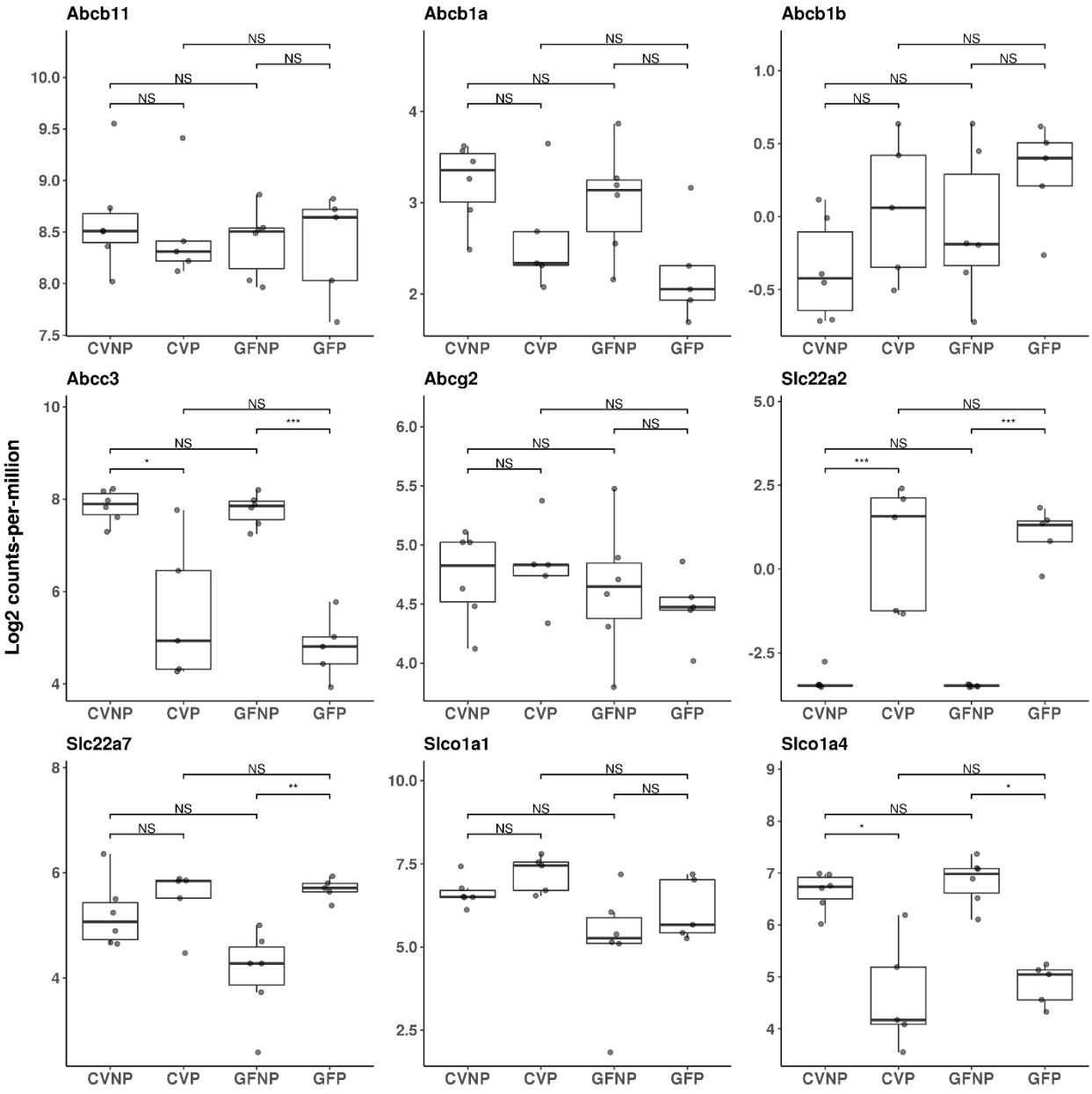


**Figure 4-4. Effect of pregnancy and microbiome on mRNA expression of hepatic transporters**. Shown are boxplots with individual scatters of RNA-seq analysis data of hepatic transporters from female C57BL/6 mice. Data illustrates individual log2 counts-per-million for each DMET. All pregnant mice used were on gestation day 15. *$FDR < 0.1$; **$FDR < 0.01$;

***$FDR < 0.001$. CVNP, conventional non-pregnant mice; CVP, conventional pregnant mice; GFNP, germ-free non-pregnant mice; GFP, germ-free pregnant mice.

**Figure 4-5**

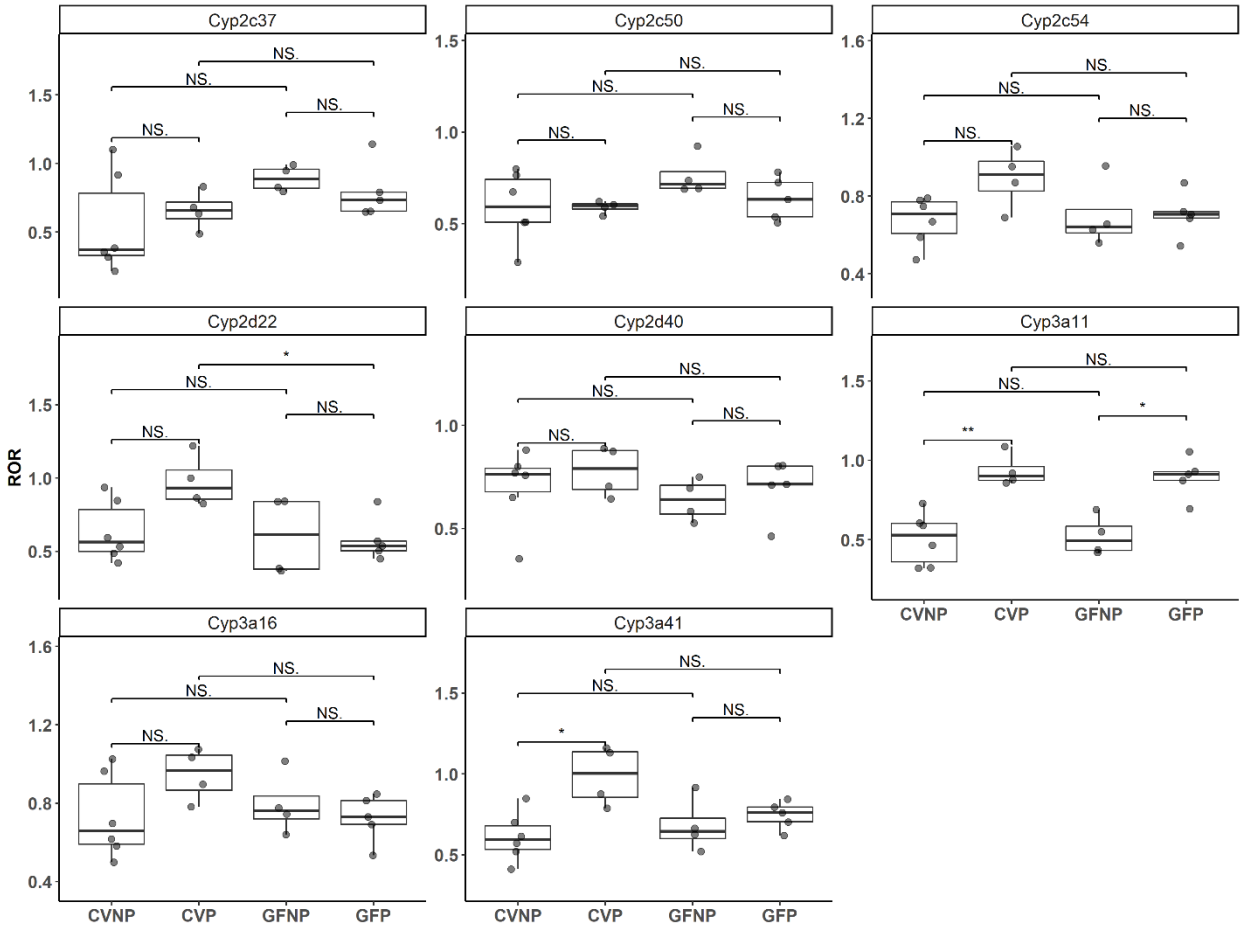


**Figure 4-5. Effect of pregnancy and microbiome on protein expression of hepatic Cyp enzymes.** Shown are boxplots with individual data points of relative protein levels of hepatic Cyp enzymes in C57BL/6 female mice. Shown are means ± SE for selected enzymes or transporters in the liver from 4-6 mice. Data illustrates ratio-of-ratio estimates for each DMET. All pregnant mice used were on gestation day 15. *$p < 0.05$; **$p < 0.01$; ***$p < 0.001$ by Wilcoxon signed-rank test. CVNP, conventional non-pregnant mice; CVP, conventional pregnant mice; GFNP, germ-free non-pregnant mice; GFP, germ-free pregnant mice.

**Figure 4-6**

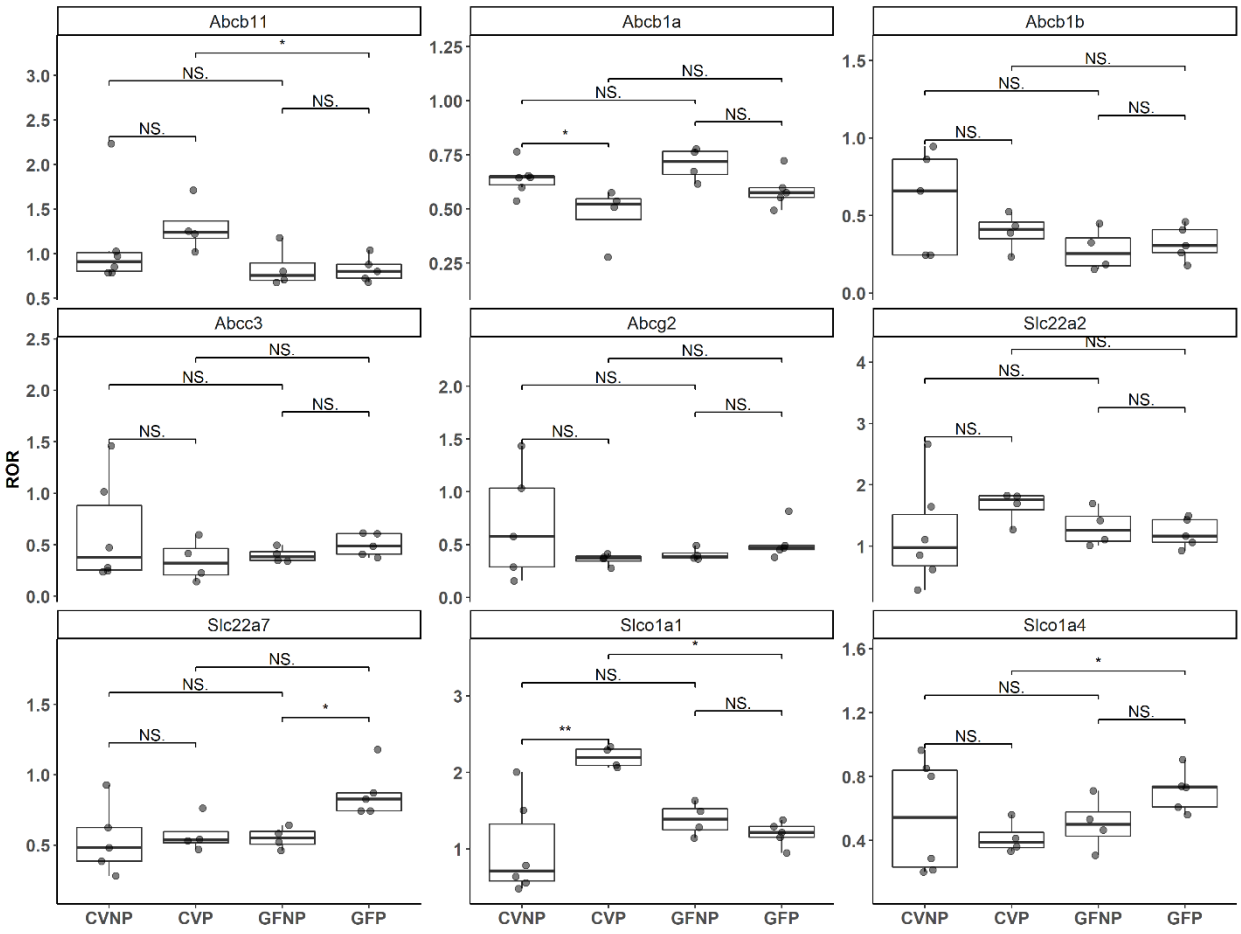


**Figure 4-6. Effect of pregnancy and microbiome on protein expression of hepatic transporters.** Shown are boxplots with individual data points of relative protein levels of hepatic transporters in C57BL/6 female mice. Shown are means ± SE for selected enzymes or transporters in the liver from 4-6 mice. Data illustrates ratio-of-ratio estimates for each DMET. All pregnant mice used were on gestation day 15. *$p < 0.05$; **$p < 0.01$; ***$p < 0.001$ by Wilcoxon signed-rank test. CVNP, conventional non-pregnant mice; CVP, conventional pregnant mice; GFNP, germ-free non-pregnant mice; GFP, germ-free pregnant mice.

**Figure 4-7**

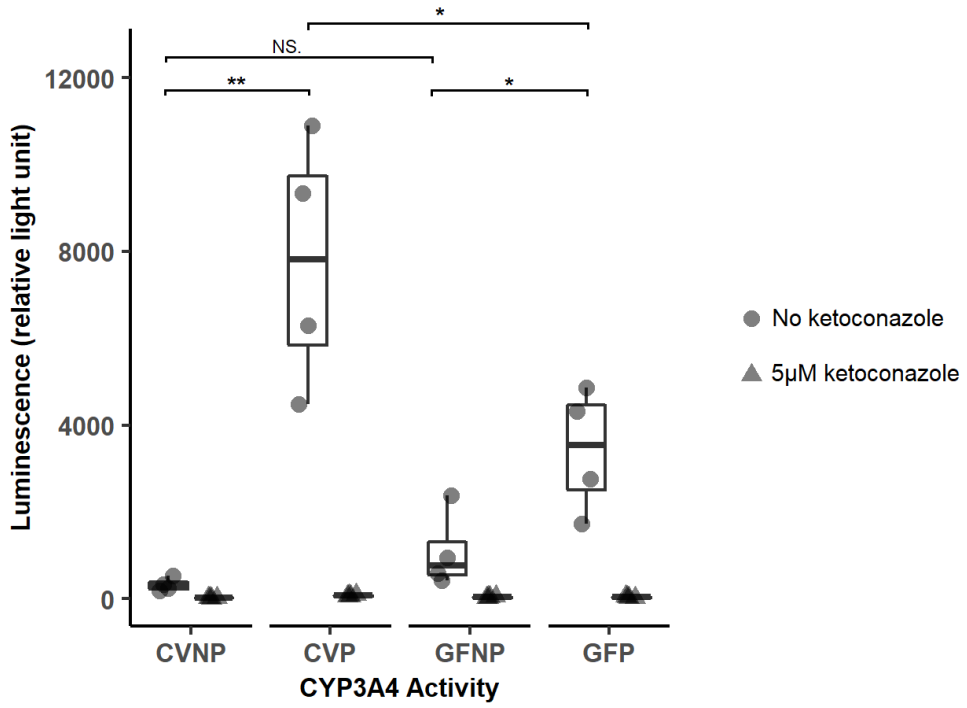


**Figure 4-7. Effect of pregnancy and microbiome on hepatic Cyp3a activity.** Shown are boxplots of individual data points of hepatic Cyp3a activity which is presented as relative light unit. Circles represent incubations without an inhibitor, and triangles indicate incubations in the presence of the inhibitor ketoconazole at 5 μM. Data shown are means ± SE of hepatic Cyp3a activity in liver microsomes isolated from 4-6 mice from one representative experiment. The experiment was done in triplicate and repeated, and similar results were obtained. All pregnant mice used were on gestation day 15. *$p < 0.05$; **$p < 0.01$; ***$p < 0.001$ by Wilcoxon signed-rank test. CVNP, conventional non-pregnant mice; CVP, conventional pregnant mice; GFNP, germ-free non-pregnant mice; GFP, germ-free pregnant mice.

**Figure 4-8**

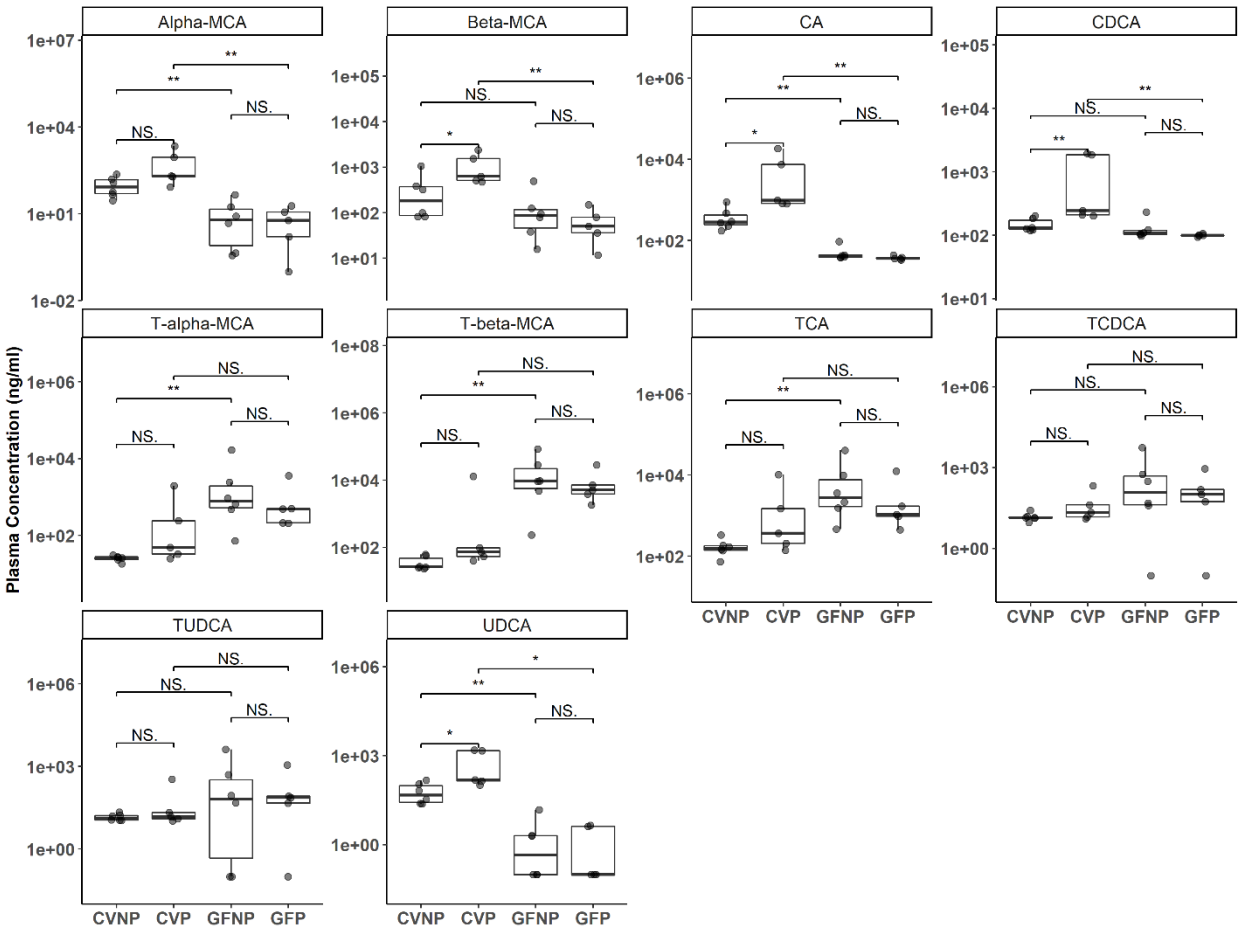


**Figure 4-8**. **Effect of pregnancy and microbiome on plasma concentrations of primary bile acids.** Shown are boxplots with individual data points of plasma concentrations of primary bile acids in C57BL/6 female mice. Concentrations were determined using targeted LC-MS/MS quantification and reported as ng/ml. Shown are means ± SE for selected bile acids or steroid hormones in the plasma from 5-6 mice. All pregnant mice used were on gestation day 15. *$p$ < 0.05; **$p$ < 0.01; ***$p$ < 0.001 by Wilcoxon signed-rank test. CVNP, conventional non-pregnant mice; CVP, conventional pregnant mice; GFNP, germ-free non-pregnant mice; GFP, germ-free pregnant mice.

**Figure 4-9**

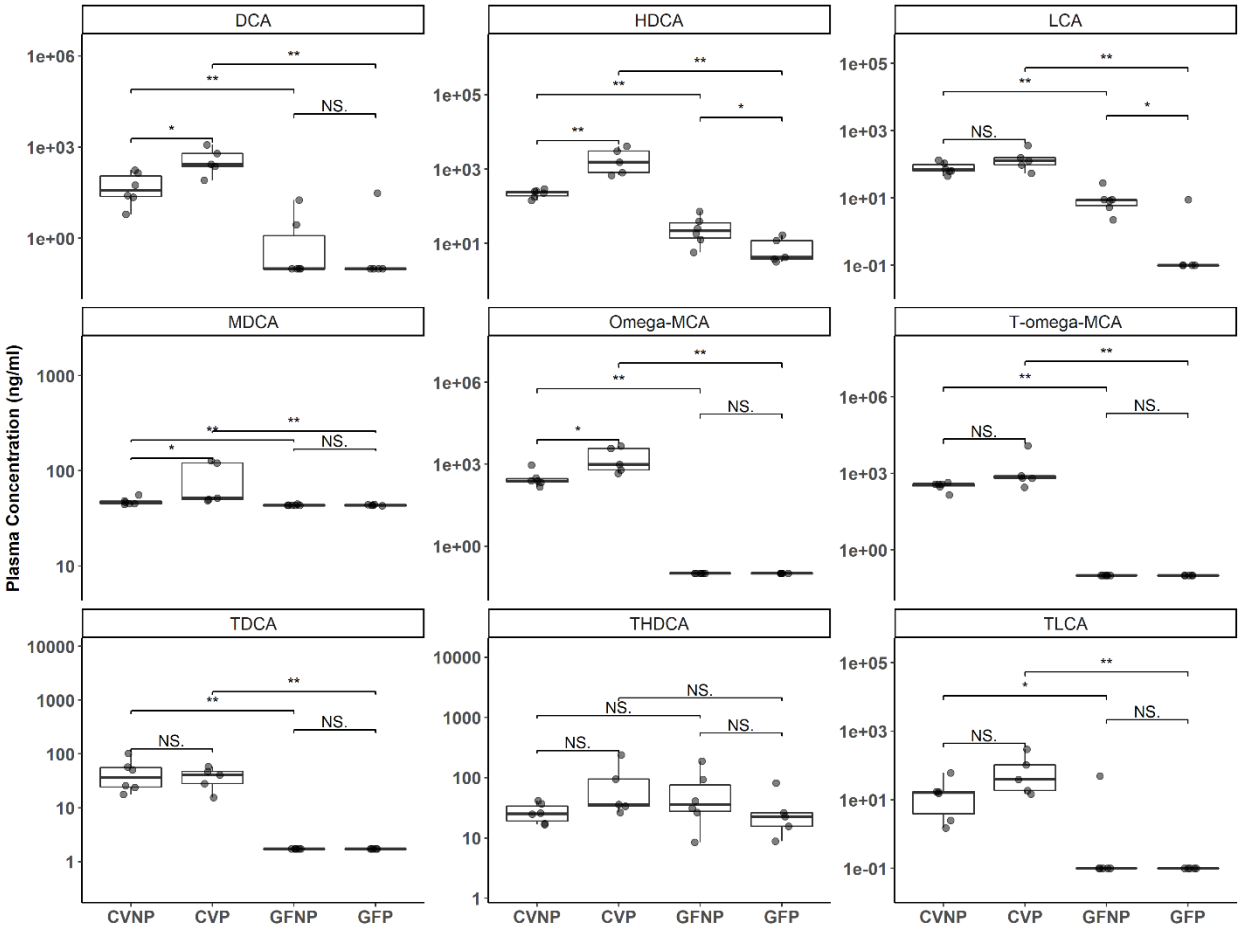


**Figure 4-9**. **Effect of pregnancy and microbiome on plasma concentrations of secondary bile acids.** Shown are boxplots with individual data points of plasma concentrations of secondary bile acids in C57BL/6 female mice. Concentrations were determined using targeted LC-MS/MS quantification and reported as ng/ml. Shown are means ± SE for selected bile acids or steroid hormones in the plasma from 5-6 mice. All pregnant mice used were on gestation day 15. *$p <$ 0.05; **$p < 0.01$; ***$p < 0.001$ by Wilcoxon signed-rank test. CVNP, conventional non-pregnant mice; CVP, conventional pregnant mice; GFNP, germ-free non-pregnant mice; GFP, germ-free pregnant mice.

**Figure 4-10**

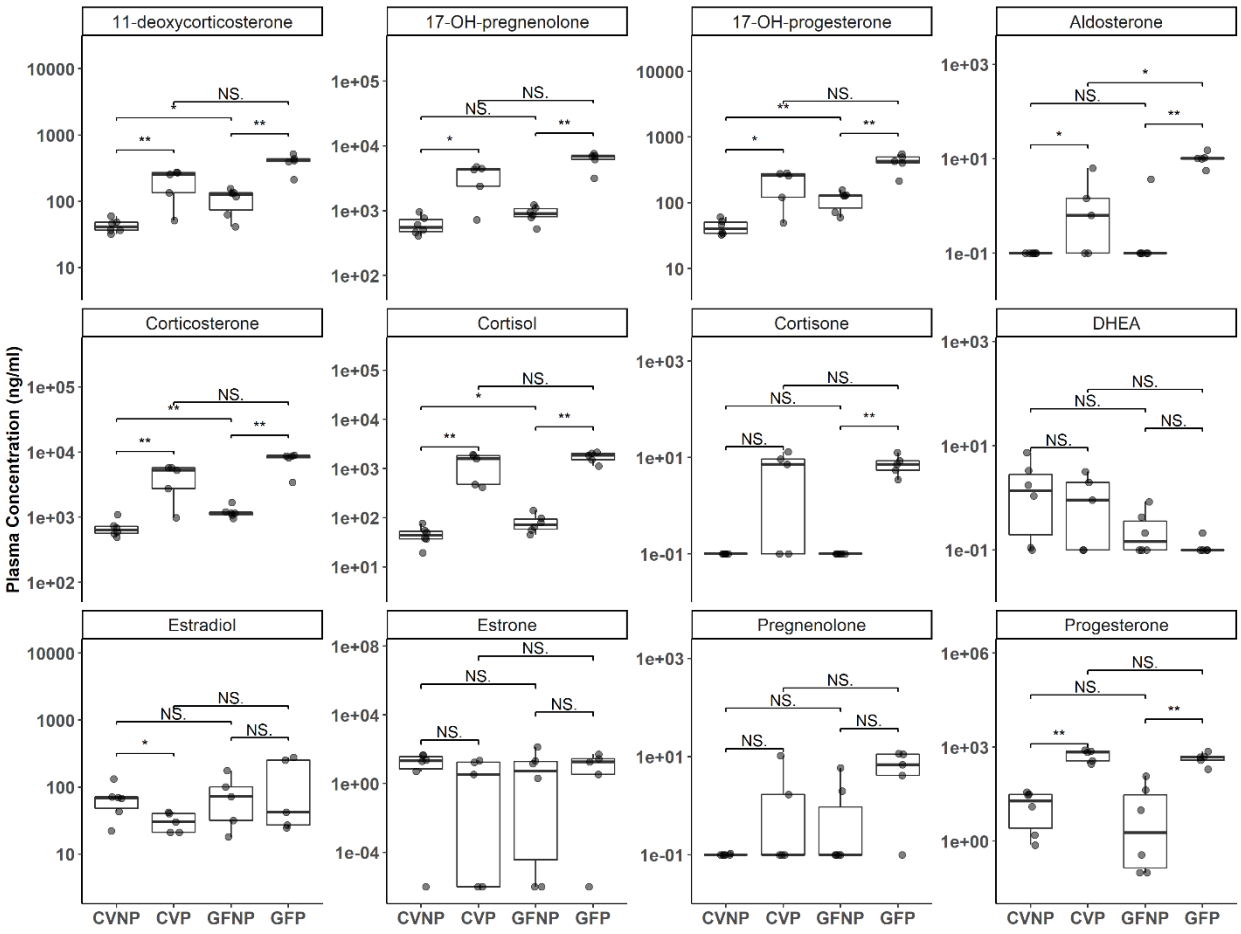


**Figure 4-10**. **Effect of pregnancy and microbiome on plasma concentrations of steroid hormones.** Shown are boxplots with individual data points of plasma concentrations of steroid hormones in C57BL/6 female mice. Concentrations were determined using targeted LC-MS/MS quantification and reported as ng/ml. Shown are means ± SE for selected bile acids or steroid hormones in the plasma from 5-6 mice. All pregnant mice used were on gestation day 15. *$p$ < 0.05; **$p$ < 0.01; ***$p$ < 0.001 by Wilcoxon signed-rank test. CVNP, conventional non-pregnant mice; CVP, conventional pregnant mice; GFNP, germ-free non-pregnant mice; GFP, germ-free pregnant mice.

## 4.6 REFERENCES


1. Beigi RH, Noguchi L, Brown G, et al. Performing drug safety research during pregnancy and lactation: Biomedical HIV prevention research as a template. *J. Women's Heal.* 2016;25:761–766.

2. FDA. Drug Safety Priorities 2018 [Internet]. 2018.

3. Helldén A, Madadi P. Pregnancy and pharmacogenomics in the context of drug metabolism and response. Pharmacogenomics. Future Medicine Ltd.; 2013. p. 1779–1791.

4. Sharma A, Buschmann MM, Gilbert JA. Pharmacomicrobiomics: The Holy Grail to Variability in Drug Response? Clin. Pharmacol. Ther. Nature Publishing Group; 2019. p. 317–328.

5. Isoherranen N, Thummel KE. Drug metabolism and transport during pregnancy: how does drug disposition change during pregnancy and what are the mechanisms that cause such changes? *Drug Metab. Dispos.* 2013;41:256–262.

6. Lee N, Hebert MF, Prasad B, et al. Effect of gestational age on mRNA and protein expression of polyspecific organic cation transporters during pregnancy. *Drug Metab. Dispos.* 2013;41:2225–2232.

7. Pariente G, Leibson T, Carls A, et al. Pregnancy-Associated Changes in Pharmacokinetics: A Systematic Review. *PLoS Med.* 2016;13.

8. Tasnif Y, Morado J, Hebert M. Pregnancy-related pharmacokinetic changes. *Clin. Pharmacol. Ther.* 2016;100:53–62.

9. Feghali M, Venkataramanan R, Caritis S. Pharmacokinetics of drugs in pregnancy. *Semin.*

*Perinatol.* 2015;39:512–519.

10. Shuster DL, Bammler TK, Beyer RP, et al. Gestational age-dependent changes in gene expression of metabolic enzymes and transporters in pregnant mice. *Drug Metab. Dispos.* 2013;41:332–342.

11. Papacleovoulou G, Abu-Hayyeh S, Williamson C. Nuclear receptor-driven alterations in bile acid and lipid metabolic pathways during gestation. Biochim. Biophys. Acta - Mol. Basis Dis. 2011. p. 879–887.

12. Kliewer SA, Moore JT, Wade L, et al. An orphan nuclear receptor activated by pregnanes defines a novel steroid signaling pathway. *Cell*. 1998;92:73–82.

13. Dussault I, Yoo HD, Lin M, et al. Identification of an endogenous ligand that activates pregnane X receptor-mediated sterol clearance. *Proc. Natl. Acad. Sci. U. S. A.* 2003;100:833–838.

14. Nuriel-Ohayon M, Neuman H, Koren O. Microbial changes during pregnancy, birth, and infancy. *Front. Microbiol.* 2016;7:1031.

15. Spanogiannopoulos P, Bess EN, Carmody RN, et al. The microbial pharmacists within us: a metagenomic view of xenobiotic metabolism. *Nat. Rev. Microbiol.* 2016;14:273–287.

16. Klaassen CD, Cui JY. Review: Mechanisms of How the Intestinal Microbiota Alters the Effects of Drugs and Bile Acids. *Drug Metab. Dispos.* 2015;43:1505–1521.

17. Claus SP, Ellero SL, Berger B, et al. Colonization-induced host-gut microbial metabolic interaction. *MBio*. 2011;2:e00271-10.

18. Wang H, Chen J, Hollister K, et al. Endogenous bile acids are ligands for the nuclear

receptor FXR/BAR. *Mol. Cell*. 1999;3:543–553.

19. Staudinger JL, Goodwin B, Jones SA, et al. The nuclear receptor PXR is a lithocholic acid sensor that protects against liver toxicity. *Proc. Natl. Acad. Sci. U. S. A.* 2001;98:3369–3374.

20. Wahlström A, Kovatcheva-Datchary P, Ståhlman M, et al. Crosstalk between Bile Acids and Gut Microbiota and Its Impact on Farnesoid X Receptor Signalling. *Dig. Dis.* 2017;35:246–250.

21. Patro R, Duggal G, Love M, et al. Salmon provides accurate, fast, and bias-aware transcript expression estimates using dual-phase inference. *bioRxiv*. 2015;021592.

22. Soneson C, Love MI, Robinson MD. Differential analyses for RNA-seq: transcript-level estimates improve gene-level inferences. *F1000Research*. 2015;4:1521.

23. Chen Y, Lun ATL, Smyth GK. From reads to genes to pathways: Differential expression analysis of RNA-Seq experiments using Rsubread and the edgeR quasi-likelihood pipeline [version 2; referees: 5 approved]. *F1000Research*. 2016;5.

24. Robinson MD, McCarthy DJ, Smyth GK. edgeR: A Bioconductor package for differential expression analysis of digital gene expression data. *Bioinformatics*. 2009;26:139–140.

25. Benjamini Y, Hochberg Y. Controlling the False Discovery Rate: A Practical and Powerful Approach to Multiple Testing. *J. R. Stat. Soc. B.* 1995;57:289–300.

26. Liao MZ, Gao C, Phillips BR, et al. Quantitative Proteomics Reveals Changes in Transporter Protein Abundance in Liver, Kidney and Brain of Mice by Pregnancy. *Drug Metab. Lett.* 2018;12:145–152.

27. Bhatt DK, Prasad B. Critical Issues and Optimized Practices in Quantification of Protein Abundance Level to Determine Interindividual Variability in DMET Proteins by LC-MS/MS Proteomics. Clin. Pharmacol. Ther. Nature Publishing Group; 2018. p. 619–630.

28. Prasad B, Bhatt DK, Johnson K, et al. Abundance of phase 1 and 2 drug-metabolizing enzymes in alcoholic and hepatitis C cirrhotic livers: A quantitative targeted proteomics study. *Drug Metab. Dispos.* 2018;46:943–952.

29. Shuster D, Risler L, Prasad B, et al. Identification of CYP3A7 for glyburide metabolism in human fetal livers. *Biochem. Pharmacol.* 2014;92:690–700.

30. Thummel KE, Kharasch ED, Podoll T, et al. Human liver microsomal enflurane defluorination catalyzed by cytochrome P-450 2E1. *Drug Metab. Dispos.* 21:350–357.

31. Paine MF, Khalighi M, Fisher JM, et al. Characterization of interintestinal and intraintestinal variations in human CYP3A-dependent metabolism. *J. Pharmacol. Exp. Ther.* 1997;283:1552–1562.

32. Patoine D, Petit M, Pilote S, et al. Modulation of CYP3a expression and activity in mice models of type 1 and type 2 diabetes. *Pharmacol. Res. Perspect.* 2014;2.

33. Li CY, Lee S, Cade S, et al. Novel Interactions between Gut Microbiome and Host Drug-Processing Genes Modify the Hepatic Metabolism of the Environmental Chemicals Polybrominated Diphenyl Ethers. *Drug Metab. Dispos.* 2017;45:1197–1214.

34. Lee C, Ding X, Riddick DS. Downregulation of mouse hepatic CYP3A protein by 3-methylcholanthrene does not require cytochrome P450-dependent metabolism. *Drug Metab. Dispos.* 2013;41:1782–1786.

35. Selwyn FP, Cheng SL, Bammler TK, et al. Developmental Regulation of Drug-Processing Genes in Livers of Germ-Free Mice. *Toxicol. Sci.* 2015;147:84–103.

36. Alnouti Y, Csanaky IL, Klaassen CD. Quantitative-profiling of bile acids and their conjugates in mouse liver, bile, plasma, and urine using LC-MS/MS. *J. Chromatogr. B Anal. Technol. Biomed. Life Sci.* 2008;873:209–217.

37. Basit A, Amory JK, Prasad B. Effect of Dose and 5α-Reductase Inhibition on the Circulating Testosterone Metabolite Profile of Men Administered Oral Testosterone. *Clin. Transl. Sci.* 2018;11:513–522.

38. Nelson DR, Zeldin DC, Hoffman SMG, et al. Comparison of cytochrome P450 (CYP) genes from the mouse and human genomes, including nomenclature recommendations for genes, pseudogenes and alternative-splice variants. Pharmacogenetics. 2004. p. 1–18.

39. Chu X, Bleasby K, Evers R. Species differences in drug transporters and implications for translating preclinical findings to humans. Expert Opin. Drug Metab. Toxicol. 2013. p. 237–252.

40. Selwyn FP, Cheng SL, Klaassen CD, et al. Regulation of Hepatic Drug-Metabolizing Enzymes in Germ-Free Mice by Conventionalization and Probiotics. *Drug Metab. Dispos.* 2016;44:262–274.

41. Selwyn FP, Cui JY, Klaassen CD. RNA-Seq Quantification of Hepatic Drug Processing Genes in Germ-Free Mice. *Drug Metab. Dispos.* 2015;43:1572–1580.

42. Morgan ET, Dempsey JL, Mimche SM, et al. Physiological Regulation of Drug Metabolism and Transport: Pregnancy, Microbiome, Inflammation, Infection, and Fasting.

*Drug Metab. Dispos.* 2018;46:503–513.

43. Selwyn FP, Cheng SL, Klaassen CD, et al. Regulation of hepatic drug-metabolizing enzymes in germ-free mice by conventionalization and probiotics. *Drug Metab. Dispos.* 2016;44:262–274.

44. Renaud HJ, Cui JY, Khan M, et al. Tissue distribution and gender-divergent expression of 78 cytochrome p450 mRNAs in mice. *Toxicol. Sci.* 2011;124:261–277.

45. Zhang Y, Klaassen CD. Hormonal regulation of Cyp4a isoforms in mouse liver and kidney. *Xenobiotica*. 2013;43:1055–1063.

46. Ahn I-S, Lang J, Olsen C, et al. Host Genetic Background and Gut Microbiota Contribute to Differential Metabolic Responses to High Fructose Consumption in Mice. *bioRxiv*. 2018;439786.

47. Hoy YE, Bik EM, Lawley TD, et al. Variation in taxonomic composition of the fecal microbiota in an inbred mouse strain across individuals and time. *PLoS One*. 2015;10.

48. Fushuku S, Fukuda K. Inhomogeneity of fecal flora in separately reared laboratory mice, as detected by denaturing gradient gel electrophoresis (DGGE). *Exp. Anim.* 2008;57:95–99.

49. Choo JM, Trim PJ, Leong LEX, et al. Inbred mouse populations exhibit intergenerational changes in intestinal microbiota composition and function following introduction to a facility. *Front. Microbiol.* 2017;8.

50. Hufeldt MR, Nielsen DS, Vogensen FK, et al. Variation in the gut microbiota of laboratory mice is related to both genetic and environmental factors. *Comp. Med.*

2010;60:336–342.

51. Friswell MK, Gika H, Stratford IJ, et al. Site and Strain-Specific Variation in Gut Microbiota Profiles and Metabolism in Experimental Mice. Ahmed N, editor. *PLoS One*. 2010;5:e8584.

52. Zanger UM, Schwab M. Cytochrome P450 enzymes in drug metabolism: Regulation of gene expression, enzyme activities, and impact of genetic variation. Pharmacol. Ther. Pergamon; 2013. p. 103–141.

53. Zhang H, Wu X, Wang H, et al. Effect of pregnancy on cytochrome P450 3a and P-glycoprotein expression and activity in the mouse: mechanisms, tissue specificity, and time course. *Mol. Pharmacol.* 2008;74:714–723.

54. Zhang YKJ, Yeager RL, Klaassen CD. Circadian expression profiles of drug-processing genes and transcription factors in mouse liver. *Drug Metab. Dispos.* 2009;37:106–115.

55. Shuster DL, Risler LJ, Liang CKJ, et al. Maternal-fetal disposition of glyburide in pregnant mice is dependent on gestational age. *J. Pharmacol. Exp. Ther.* 2014;350:425–434.

56. Takagi S, Nakajima M, Mohri T, et al. Post-transcriptional regulation of human pregnane X receptor by micro-RNA affects the expression of cytochrome P450 3A4. *J. Biol. Chem.* 2008;283:9674–9680.

57. Smutny T, Mani S, Pavek P. Post-translational and post-transcriptional modifications of pregnane X receptor (PXR) in regulation of the cytochrome P450 superfamily. *Curr. Drug Metab.* 2013;14:1059–1069.

58. Martínez-Jiménez CP, Jover R, Donato MT, et al. Transcriptional regulation and expression of CYP3A4 in hepatocytes. *Curr. Drug Metab.* 2007;8:185–194.

59. Wang S, Chen L, Wang Q, et al. Strain differences between CD-1 and C57BL/6 mice in expression of metabolic enzymes and DNA methylation modifications of the primary hepatocytes. *Toxicology*. 2019;412:19–28.

60. Miro-Blanch J, Yanes O. Epigenetic regulation at the interplay between gut microbiota and host metabolism. Front. Genet. Frontiers Media S.A.; 2019. p. 638.

61. Zhao BS, Roundtree IA, He C. Post-transcriptional gene regulation by mRNA modifications [Internet]. Nat. Rev. Mol. Cell Biol. Nature Publishing Group; 2016. p. 31–42.

62. Yuan C, Burns MB, Subramanian S, et al. Interaction between Host MicroRNAs and the Gut Microbiota in Colorectal Cancer. *mSystems*. 2018;3.

63. Blasco-Baque V, Coupé B, Fabre A, et al. Associations between hepatic miRNA expression, liver triacylglycerols and gut microbiota during metabolic adaptation to high-fat diet in mice. *Diabetologia*. 2017;60:690–700.

64. Hoban AE, Stilling RM, M Moloney G, et al. Microbial regulation of microRNA expression in the amygdala and prefrontal cortex. *Microbiome*. 2017;5:102.

65. Sachar M, Kelly EJ, Unadkat JD. Mechanisms of CYP3A Induction During Pregnancy: Studies in HepaRG Cells. *AAPS J.* 2019;21:45.

66. Dempsey JL, Wang D, Siginir G, et al. Pharmacological Activation of PXR and CAR Downregulates Distinct Bile Acid-Metabolizing Intestinal Bacteria and Alters Bile Acid

Homeostasis. *Toxicol. Sci.* 2019;168:40–60.

# CHAPTER 5: EFFECT OF THE GUT MICROBIOME ON OVERALL HEPATIC METABOLIC PATHWAYS DURING PREGNANCY

## 5.1 INTRODUCTION

Pregnancy is a time marked by remarkable physiological changes in the maternal body to accommodate the developing fetus. Maternal metabolic processes adapt to growth of the fetus and its expanding needs. Throughout gestation, the maternal body accumulates lipoproteins, cholesterol, triglycerides, and phospholipids to meet the growing fetus's nutritional demands [1]. These metabolic changes and changes in circulating metabolite concentrations in turn trigger the immune system to react to the pregnancy by increasing proinflammatory cytokine levels to further enhance energy storage [1,2]. Another major change that comes with pregnancy is a shift in gut microbiome composition. Studies have shown that a woman's intestinal microbiome composition during pregnancy is characterized by an increase in Proteobacteria and Actinobacteria, relative to other species, from the first trimester through the third trimester [3]. The richness of the microbiome composition is found to be reduced in late pregnancy, with a pronounced increase in bacteria associated with inflammatory processes [2,4,5].

The gut microbiome has become an important area of research the recent years because of increasing evidence of the capability of gut bacteria to modulate host metabolic processes via various gut microbiota – metabolic axes. For example, intestinal bacteria play a critical role in the enterohepatic circulation of endogenous compounds, such as short-chain fatty acids and

primary bile acids, which are crucial for host health [6,7]. The gut microbiome has also been shown to modulate host xenobiotic metabolism both by directly metabolizing the compounds in the intestine or indirectly via the production of metabolites that interact with downstream nuclear receptors to activate host metabolic genes [6,7].

Over the past few decades, gut dysbiosis (imbalance or disruption of the microbiome) has been observed to be on the rise in the westernized populations, possibly due to changes in diet and a more sedentary lifestyle [6,8,9]. This adds another layer of variability to the host and gut supraorganism interactions and its effect on the host wellbeing. Since the gut microbiota composition shifts dynamically as gestation progresses, in addition to its vulnerability to change from lifestyle, diet, and various other factors, the impact of dysbiosis on host drug disposition processes during pregnancy should also be explored [2,10–12].

Previously, we used germ-free mice to investigate how the gut microbiome affects key hepatic drug processing genes during pregnancy and found significant modulation effects (see Chapter 4). For example, mouse hepatic *Cyp3a* gene comes in multiple isoforms (*Cyp3a11, Cyp3a16, Cyp3a41, Cyp3a44)*, and *Cyp3a11* is considered the murine orthologs of human *CYP3A4*, a major cytochrome P450 enzyme known to metabolize numerous endogenous and exogenous substrates. In the absence of the gut microbiome, murine Cyp3a exhibited significantly decreased overall activity. This could lead to altered pharmacokinetics and pharmacodynamics of a medication in pregnant women should the same effect of the gut microbiome occurs in humans. The impact of the gut microbiome and host fitness interaction is not limited to hepatic drug processing genes. In fact, previous studies have demonstrated that the gut microbiome can modulate overall host metabolic pathways as well [6]. Abnormal metabolic changes that are not natural to the progression of pregnancy can pose high risks to both the

mother and the fetus, such as increased risk for gestational hypertension, gestational diabetes, or chronic intestinal illness in the child [2,13,14]. At present, there is no knowledge as to what metabolic pathways important for pregnancy are influenced by the gut microbiome. By gaining insights to these changes, we may better understand sources of interindividual variability of diseases and therapeutic effects of medications during pregnancy. In the previous chapter, we used targeted transcriptomic, proteomic, and metabolomic approaches to describe the effect of the gut microbiome on hepatic gene expressions during pregnancy. However, the effects of pregnancy and the gut microbiome on overall metabolic pathway changes were not analyzed. Thus, the objective of this study was to explore the influence of the gut microbiome on maternal metabolic pathways during pregnancy using the germ-free mouse model. In this chapter, we analyzed gut microbiome composition changes in pregnancy and correlated them with hepatic gene expression analysis via RNA sequencing, and quantitation of plasma metabolites via LC-MS/MS. Then, we combined the transcriptomic and metabolomic data to performing joint pathway analysis to identify metabolic pathways of interest.

## 5.2 METHODS

### ANIMAL STUDY

Four groups of C57BL/6 mice were used in this study, namely conventional non-pregnant (CVNP) mice, conventional pregnant (CVP) mice, germ-free non-pregnant (GFNP) mice, and germ-free pregnant (GFP) mice. Conventional (CV) mice were purchased from The Jackson Laboratory (JAX stock #000664; Bar Harbor, ME). Germ-free (GF) mice are descendants of the original colony from the National Gnotobiotic Rodent Resource Center of the University of North Carolina at Chapel Hill. Animal care and use were all in accordance with the Guide for the

Care and Use of Laboratory Animals published by the National Research Council. This animal protocol was approved by the Institutional Animal Care and Use Committee of the University of Washington (protocol #4035-04).

Details about the care of mice was as previously described (see Chapter 4.2 Method: Animal study). Briefly, all animals were maintained with an autoclaved diet, non-acidified water, and autoclaved bedding. Age matched CV mice were mated overnight at 8 weeks of age. The date on which male and female mice were put together for mating was considered gestation day 0 (gd 0). GF female mice were mated for 72 h and the second day was considered gd 0. All material plasma samples and liver tissues from pregnant mice were collected on gd 15 as described in Chapter 4. We collected fecal pellets from each CV mouse (n = 5 for the pregnant group) prior to mating pregnancy baseline, and on gd 15 post mating (pregnancy day 15). Fecal pellets, tissues, and maternal plasma samples were frozen immediately in liquid $N_2$ and kept at -80°C until further analysis.

### GUT MICROBIOME 16S RRNA SEQUENCING

DNA samples used for bacterial 16S rRNA analysis were extracted from fecal pellets using OMEGA E.Z.N.A. DNA Stool Kit (Omega Bio-tek, Inc., Norcross, GA) following the manufacturer's instruction. DNA concentration, quality, and integrity were determined using Synergy HTX Multi-mode Plate Reader (BioTek, Winooski, VT). Bacterial 16S rRNA data was generated by Illumina (Hiseq) paired-end sequencing, and performed by Novogene Corporation Inc. (Sacramento, CA). 16S rRNA genes of V3/V4 regions were amplified using specific primers. Raw sequence data was then processed using Bioconductor R package DADA2 (Divisive Amplicon Denoising Algorithm), which included filtering, dereplication, sample

interference, chimera identification, and merging of paired-end reads, and produced a sequence variant table [15]. DADA2 implemented the naïve Bayesian classifier method to taxonomically classify the sequenced variants. Differentially abundant features that were changed during pregnancy were then identified. Alpha diversity measurements were calculated by observed richness as well as estimated Shannon's diversity index, which accounts for both richness and abundance. Beta diversity was determined by weighted UniFrac distance. To make group comparisons, a Bioconductor package metagenomeSeq was used to identify differentially abundant taxonomic features in microbiome data. Only features found in more than 8 samples were included in this step. A cumulative sum scaling normalization was performed followed by fitting a zero-inflated Gaussian model [16]. A false discovery rate (FDR) of 10% was used to filter results for subsequent analyses.

### TRANSCRIPTOME DATA

Total RNA was extracted from frozen mice liver tissues and sequenced as previously described (see Chapter 4.2 Method: RNA-seq Analysis). Briefly, we performed paired end RNA sequencing using Illumina NovaSeq 6000 and prepared the transcriptomic library using NEBNext® Ultra™ RNA Library Prep Kit for Illumina®. The reads were aligned to mouse GRCm38.p6 transcriptome and summarized using the Bioconductor tximport package in R (v1.10.1). Then, data was filtered for consistently low basal expression genes using edgeR (v3.24.3). After this filtering step, a total of 18,849 genes remained. A FDR of 10% and minimum fold change of 2 were used to filter results for subsequent analyses.

### METABOLOME DATA

Frozen plasma samples from CV and GF mice (n = 6, 6, 6, and 5 for CVNP, CVP, GFNP, and GFP mice, respectively) were used to perform untargeted metabolomic analysis. Plasma

metabolite extraction was identical to that of plasma steroid hormone extraction, as previously described (see Chapter 4.2 Method: Quantification of Plasma Bile Acids and Steroid Hormones). The $MS^2$ raw data in positive and negative ion modes were acquired to record the high-accuracy MS and MS/MS data of all precursor ions and fragmentation by UPLC-triple TOF (5600 AB Sciex). Then, the data were imported to the Progenesis QI software (Waters Corporation, Milford, USA) for data processing. During the procedure, the software carries out deconvolution, alignment, peak picking, and statistical analysis, identification, and compound measurement with corresponding intensities for all the detected peaks from each data file in the dataset [17]. The peak picking conditions were set as follows: all runs, limits (automatic), sensitivity (3), chromatographic peak width (minimum peak width), and retention time (0.5 to 22.0 min). A total of 4936 compounds from positive mode and 5505 compounds from negative mode were initially selected within this retention time period. Different adduct ion forms were applied to deconvolute the spectral data. The statistical analysis was finished with by one-way analysis of variance (ANOVA) with a threshold of $p < 0.1$ and FDR < 0.1 and following to EZinfo 3.0, which allows preliminarily screening of potential biomarkers and identifying group differences via Orthogonal partial least square-discriminant analysis (OPLS-DA) and principal component analysis (PCA). The parameters, $R^2Y$ and $Q^2$ (>0.85), were used to evaluate the quality of the model. Candidate compounds of significance were filtered under two conditions, that is, VIP values (VIP > 1) and max fold change ≥ 2. The potential biomarkers were reprinted on the Progenesis QI software and created tags. Significant variables were identified and confirmed by comparing MS data, MS/MS fragments and elemental compositions (H (0−50), C (0−50), N (0− 5), and O (0−30), precursor tolerance 10 ppm, and isotope similarity 95%) with the biochemical databases, HMDB (http://www.hmdb.ca/) with both precursor tolerance and fragment tolerance 10 ppm to identify

and confirm potential biomarkers. A threshold of 10% FDR was applied to filter out false-positives, and a minimum fold change of 2 was also applied to identify differentially produced metabolites between groups.

#### JOINT PATHWAY ANALYSIS

MetaboAnalyst 4.0 (http://metaboanalyst.ca) was used to carry out the joint pathway analysis [18,19]. Differentially expressed genes (imported as official gene symbol) and differentially produced metabolites (imported as HMDB ID) between CVNP, CVP, GFNP and GFP mice were used as integrated input for the analysis. Inclusion criteria for genes and metabolites were false discovery rate of 10% and a 2-fold change minimum in at least one group comparisons. The analysis was done in reference to the metabolic pathways in Kyoto Encyclopedia of Genes and Genomes (KEGG) database (Version Oct2019) for Mus musculus. A total of 1182/1231 genes and 1602/2277 metabolites for CVP vs. CVNP group, 797/859 genes and 1580/2223 metabolites for GFP vs GFNP group, 20/20 genes and 1602/2277 metabolites for GFNP vs CVNP group, and 18/18 genes and 2469/3367 metabolites for GFP vs CVP group were successfully mapped to the KEGG database and used for subsequent pathway enrichment analysis. Fisher's exact test and degree centrality were used to determine pathway enrichment and reported with pathway-level weighted FDR-adjusted *p*-value. All pathways with FDR < 0.1 were considered significant.

## 5.3 RESULTS

#### SHIFT OF GUT MICROBIOTA COMPOSITION IN PREGNANCY

We compared changes in gut microbiome composition from non-pregnant to gd 15 pregnant mice. Samples were taken from the same mice (n = 5) at both time points. Taxonomic

composition comparison revealed that amongst the top abundant bacteria belonged to phyla Actinobacteria, Bacteroidetes, and Firmicutes. Of which, we identified 8 most abundant families that were changed during pregnancy (Figure 5-1). The *Muribaculaceae* family of Bacteroidetes phylum was highly abundant at baseline (relative abundance 59%) and decreased to 42% by gd 15 (Figure 5-1). The *Lachnospiraceae* family and *Ruminococcaceae* family of the Firmicutes phylum were second and third highest in abundance at baseline (15% and 10%, respectively) and increased to 22% and 12% at gd 15, respectively (Figure 5-1). Five other familiae that reached FDR < 10% but had much lower relative abundance were *Clostridiaceae_1* (phylum: Firmicutes), *Clostridiales_vadinBB60_group* (phylum: Firmicutes), *Eggerthellaceae* (phylum: Actinobacteria), *Family_XIII* (phylum: Firmicutes), and *Streptococcaceae* (phylum: Firmicutes). All other familiae were clustered into "others" group. Taxonomic classification was ambiguous or unassigned below the family level, thus we did not pursue further classification.

### CHANGES IN HEPATIC GENE EXPRESSION AND PLASMA METABOLITES IN CONVENTIONAL AND GERM-FREE MICE BY PREGNANCY

To determine how many genes were differentially expressed by pregnancy and the gut microbiome in the liver, we performed RNA-seq analysis using liver tissue samples (n = 6, 5, 6, and 5 for CVNP, CVP, GFNP, and GFP mice, respectively). After using the inclusion criteria of FDR < 10% and fold-change > 2 in at least one comparison group, we found a total of 1241 genes that matched these criteria. Figure 5-2A illustrates the number of differentially expressed genes when comparing CVP and CVNP, GFP and GFNP, GFNP and CVNP, and GFP and CVP mice. We identified 516 genes that were upregulated and 244 genes that were downregulated by pregnancy in CV mice; whereas 479 genes were upregulated and 380 genes were downregulated by pregnancy in GF mice. We identified 14 upregulated genes and 6 downregulated genes by the

germ-free state in non-pregnant mice as well as 10 upregulated genes and 8 downregulated genes by the germ-free condition in pregnant mice.

A similar filtering was performed on the levels of metabolites in maternal plasma. As shown in Figure 5-2B, after filtering with the inclusion criteria of FDR < 10% and fold-change > 2, we identified a total of 2277 metabolites for which abundances were altered by pregnancy and/or germ-free status. Of these metabolites, there were 910 and 465 metabolites that were increased and decreased, respectively, by pregnancy in CV mice. There were 438 increased metabolites and 745 decreased metabolites by pregnancy in GF mice. In addition, we identified 679 increased metabolites and 629 decreased metabolites by germ-free in non-pregnant mice; whereas there were 611 metabolites that were increased and 1463 metabolites that were decreased by germ-free in pregnant mice. Taken together, we observed significant effects of pregnancy and/or the gut microbiome on both hepatic gene expression and metabolite levels in maternal plasma. For illustration, we plotted heatmaps to determine global patterns of changes in hepatic gene expression and metabolite abundance by pregnancy and germ-free. As shown in Figure 5-3, hepatic gene expression clusters showed significant differences as a result of pregnancy regardless of germ-free, whereas the effect of gut microbiome is much less. On the contrary, the metabolite heatmap (Figure 5-4) depicted significant differences not only by pregnancy, but due to pronounced effects of the gut microbiome.

### METABOLIC PATHWAY ANALYSIS

To identify what metabolic pathways were altered by pregnancy and/or the gut microbiome, we performed pathway enrichment analysis. A complete set of data about significantly changed pathways and the number of corresponding gene and metabolite hits is summarized in Table 5-1. An overview of pathway enrichment for each comparison group (CVP

vs CVNP, GFP vs GFNP, GFNP vs CVNP or GFP vs CVP) is shown in Figure 5-5 and the most significant pathway hits are summarized in Figure 5-6. We identified 8 pathways significantly associated (FDR < 0.1) with CVP vs. CVNP, 9 pathways significantly associated with GFP vs. GFNP, 1 pathway significantly associated with GFNP vs. CVNP, and 5 pathways significantly associated with GFP vs. CVP. Interestingly, linoleic acid metabolism was significantly enriched for all comparison (FDR < 0.1), suggesting that both pregnancy and the gut microbiome have profound effects on linoleic acid metabolism. Genes and metabolites that were differentially expressed in pregnant vs. non pregnant mice were enriched within the arachidonic acid metabolism pathway (FDR < 0.1), but not with germ-free. Retinol metabolism was highly affected by pregnancy (FDR < 0.1), but not by the gut microbiome in non-pregnant mice (GFNP vs CVNP). Steroid hormone biosynthesis was highly affected by both pregnancy and the gut microbiome status. Other pathways significantly affected by pregnancy included biosynthesis of unsaturated fatty acids, glycerophospholipid metabolism, glycerolipid metabolism, and phenylalanine metabolism, with significant changes observed in both CV and GF mice (FDR < 0.1 for all).

Four of these pregnancy-driven pathway enrichments were further impacted by a germ-free state, namely retinol metabolism, linoleic acid metabolism, arachidonic acid metabolism, and steroid hormone biosynthesis. As this finding highlights the interplay between pregnancy and the gut microbiome, we elected to perform in-depth analysis of these pathways, contrasting GFP vs CVP. The data are shown in Table 5-2. The retinol metabolism pathway was enriched in GFP mice on gd 15 compared to CVP mice on the same gestation day (FDR < 0.001) with 4 genes exhibiting upregulation and 2 metabolites showing increased levels in GFP mice (Table 5-2). Interestingly, the same 4 upregulated genes (*Cyp2b13*, *Cyp2c38*, *Cyp2c50* and *Cyp2c54*) were

included in all four significant pathway enrichments of interest (Table 5-2). *Cyp2b13*, *Cyp2c38*, *Cyp2c50* and *Cyp2c54* were upregulated 528% (FDR < 0.1), 303% (FDR < 0.1), 203% (FDR < 0.1), and 222% (FDR < 0.1), respectively, in GFP mice compared to CVP mice (Table 5-2). For linoleic acid metabolism, four metabolites were significantly decreased in GFP vs CVP mice, namely linoleate by 63% (FDR < 0.1), phosphatidylcholine by 86% (FDR < 0.1), 9(10)-EpOME by 100% (FDR <0.1), and 13-Hpode by 66% (FDR < 0.1). In contrast, only one metabolite, 12(13)-EpOME, was increased by 810% (FDR < 0.1). For arachidonic acid metabolism, the plasma levels of most of the epoxyeicosatrienoic acid (EET) and hydroxyeicosatetraenoic acid (HETE) metabolites were prominently decreased in GFP vs CVP mice, with the exception of arachidonic acid that was increased by 307% (FDR < 0.1). There were 20 differentially abundant metabolites within the Steroid hormone biosynthesis pathway, with certain metabolites upregulated and some metabolites downregulated in GFP vs CVP mice. Notably, corticosterone, cortisol, and their subsequent metabolites were increased by 241 to 423% (FDR <0.1). In contrast, allopregnanolone showed a 100% decrease in GFP vs CVP (FDR < 0.1).

## 5.4 DISCUSSION

Pregnancy imposes substantial adaptive physiological, metabolic, and immunological changes to the mother's body, in a dynamic time-dependent fashion, in order to maintain her fetus's health as well as her own [20–22]. Although many studies have been done to gain better understanding of what these changes are, and how they impact the mother's health, there remains much that is unknown. The gut microbiome has already been shown to shift throughout pregnancy in both humans and animals [2,10–12]. Recent literature has extensively discussed the crosstalk between the gut microbiome and rest of the body (e.g. gut-brain axis, gut-liver axis)

and the potential for gut microbiome to modulate host metabolism of endogenous and exogenous compounds and xenobiotics [6]. This study was designed to fill a knowledge gap concerning the interplay between pregnancy and the gut microbiome on metabolic pathways, using a germ-free mouse model. A previous study (Chapter 4) utilized a targeted transcriptomic and metabolomic approach to assess only differentially expressed hepatic drug processing genes. In this investigation, an untargeted transcriptomic and metabolomic approach was used to explore all possible metabolic differences caused by pregnancy and/or the gut microbiome.

First, we showed that the gut microbiome composition was changed by pregnancy. We found that *Muribaculaceae* (phylum: Bacteroidetes) was significantly enriched prior to pregnancy, and its abundance decreased during pregnancy. In contrast, both *Lachnospiraceae* and *Ruminococcaceae* of phylum Firmicutes were significantly enriched at gd 15 (Figure 5-1). The family *Muribaculaceae* was recently classified and its role in pregnancy still remains to be elucidated [23]. However, its expression in the intestinal tract is found to be low in human compared to mouse, therefore it is not surprising that it was not detected as a predominantly enriched bacteria during human pregnancy [23]. The enrichment of *Lachnospiraceae* and *Ruminococcaceae* is not as surprising, as both familiae have been found associated with energy metabolism and have been observed at high relative abundance in human obesity and is associated with gestational diabetes mellitus during early pregnancy [24,25]. Nevertheless, our findings disconnected with previous knowledge that human pregnancy is associated with increased gut abundance of Proteobacteria and Actinobacteria [3]. The inconsistency between our mouse data and human data is not unexpected, as the human gut microbiome is vastly different from that of mice, with only 4% bacterial gene commonality reported [26]. Part of this differences in microbiome composition may be due to that modern human diet is high in fat and

sugar, whereas mouse chow are plant based and lower in fat, and Turnbaugh et al. showed that feeding mice different foods can shift the gut microbiome composition within a day [27]. Our findings are in part consistent with a study by Gohir et al., where they also described increased abundance of *Lachnospiraceae* in C57BL/6 mice during pregnancy [11]. However, they also found significant increase in abundance of *Bacteroidaceae* and *Bifidobacteriaceae*, and a decrease in abundance of *Ruminococcaceae* in mice during pregnancy, which is the opposite of our findings [11]. Discrepancy in mice gut microbiota studies is not uncommon, and may be attributed to differences in mice age, environment, and facility [28]. In fact, the study by Elderman et al. confirms that C57BL/6 mice, the same strain that was used for this study, exhibited the least microbiota shift during pregnancy compared to other mouse strains [29]. At present, it is not known as to how the shift in gut microbiome composition by pregnancy contributes to the significant changes in hepatic gene expression and maternal plasma metabolite abundance in pregnant mice versus non-pregnant mice. This is an important topic of future studies.

Next, we explored whether metabolic pathways were significantly changed by pregnancy how the gut microbiome impacted these changes using an approach that integrated changes in both hepatic gene expression and maternal plasma metabolites. Overall, we found that the changes in metabolic pathways associated with pregnancy were very similar in CV and GF mice, with 8 metabolic pathways enriched by both groups (Figure 5-6). The 8 metabolic pathways that were significantly enriched include: retinol metabolism, linoleic acid metabolism, arachidonic acid metabolism, biosynthesis of unsaturated fatty acids, steroid hormone biosynthesis, glycerophospholipid metabolism, glycerolipid metabolism, and phenylalanine metabolism. The change in retinol metabolism was most substantial in both CV and GF pregnancies. Retinol, also

known as vitamin A, is believed to be critical for healthy fetal development [30–32]. We also observed enrichments in differentially expressed genes and pathways within the Linoleic acid metabolism, arachidonic acid metabolism, and biosynthesis of unsaturated fatty acids pathways in relation to pregnancy status. All the three metabolic pathways are characterized by their essential roles in providing energy and nutrition to support intrauterine growth [33]. Steroid hormone biosynthesis was also enriched for differentially expressed genes within pregnancy, and it serves a critical role from before the point of conception, during fertilization, and throughout gestation [34]. Glycerophospholipid metabolism, glycerolipid metabolism, and phenylalanine metabolism were also influenced by pregnancy in both CV and GF mice. As all these metabolic pathways are essential for a successful pregnancy, it is not surprising that we observed significant changes in these pathways by pregnancy regardless of the gut microbiome status. Changes in these pathways by pregnancy reflect the maternal body's metabolic response to the rapidly growing fetus and its nutritional demands.

Next, we focused on analysis of the impact of gut microbiome on metabolic pathways in pregnant mice by comparing metabolic pathways in GFP mice versus CVP mice. Among the eight pathways significantly affected by pregnancy regardless of germ-free status, four pathways were most sensitive to the germ-free condition during pregnancy, namely retinol metabolism, linoleic acid metabolism, arachidonic acid metabolism, and steroid hormone biosynthesis (Figure 5-6). Notably, these four metabolic pathways were not affected by the germ-free state at all in non-pregnant mice (Figure 5-6), suggesting that these effects of the gut microbiome are unique for pregnancy. This could be due to the shift of gut microbiome composition during pregnancy as we observed (Figure 5-1). Since our study endpoints did not include health outcomes of the pregnancy, it is unclear what impact these metabolic pathways would have on the overall

maternal and fetal health. It is important to further investigate the pregnancy-specific effects of gut microbiome on metabolism in future studies.

To dissect the results more, we identified all plasma metabolites that were hit in each of the four metabolic pathways. Phosphatidylcholine was mapped to both linoleic acid metabolism and arachidonic acid metabolism pathways, and was markedly decreased by 86% (Table 5-2). Phosphatidylcholine is a major component of the phospholipid membrane of eukaryote cells and has been speculated to be an important mediator for symbiotic relationship between bacteria and host [35]. While phosphatidylcholine is usually obtained via diets such as eggs and soybeans in human, bacteria is also capable of the biosynthesis of phosphatidylcholine via phospholipid *N*-methylation pathway and the CDP-choline pathway [35–37]. Thus, a marked decrease in phosphatidylcholine would be expected in GFP mice. Another significantly decreased (100%) metabolite in GFP mice versus CVP mice was allopregnanolone, a component of the steroid hormone biosynthesis pathway. Previous studies have suggested that allopregnanolone is a ligand that can potentially activate PXR at micromolar concentrations [38]. A significant decrease in this PXR ligand may explain some significant decrease in PXR activated drug processing genes such as *Cyp3a11*(see Chapter 4). Taken together, results from this study suggest that the gut microbiome may have a significant impact on endogenous metabolic processes that are critical for a healthy pregnancy.

Next, we looked at the hepatic genes that were significantly changed in these four metabolic pathways. All the four genes, *Cyp2b13, Cyp2c38, Cyp2c50,* and *Cyp2c54,* were upregulated by 203 to 528% in GFP mice versus in CVP mice. Of the four genes, only *Cyp2c50* is a known to have a clear human homolog, CYP2C19 [39]. Human CYP2C19 activity was shown to decrease during pregnancy [40]. Our previous study on hepatic drug processing genes

also showed downregulation of *Cyp2c50* by pregnancy, regardless of gut microbiome status (Chapter 4). Cyp2c50 plays an important role as arachidonic acid epoxygenase and is considered a major metabolizing enzyme in the production of EETs [41]. We observed a decrease in EETs in GFP mice compared to CVP, whereas we would have expected the opposite since *Cyp2c50* gene was up-regulated in GFP compared to CVP. Similarly, *Cyp2c50* is also known to mediate linoleic acid metabolism, and we observed a significant decrease in its major metabolite, 9(10)-EpOME, in GFP mice compared to CVP mice [42]. These findings suggest less enzymatic activity of Cyp2c50 in GFP mice compared to CVP mice, yet mRNA expression showed up-regulation of the gene in GFP mice. However, as we also showed in Chapter 4, there are clear disconnects between mRNA gene expression and protein expressions and final enzymatic activity. More studies are needed to determine the missing link from gene expression to EETs and EpOME concentrations in plasma.

To the best of our knowledge, this is the first study to provide novel and comprehensive information on an interplay between the gut microbiome and pregnancy that involves multiple metabolic pathways in an animal model. Studies like this provide data that cannot be obtained from human subjects, as it would be unethical to perform tissue biopsies or other invasive procedures, such as gut sterilization, in a pregnant woman. However, caution should be taken when extrapolating these data to humans. First, composition of the human microbiome is vastly different from that of mice, and a germ-free status can never be achieved in a pregnant woman. Secondly, the choice of only one gestation day (gd 15) for tissue sampling in this study may not have captured all dynamic changes that would occur throughout gestation; gene expression can shift significantly from early through late gestation in mice [43]. Nevertheless, results of this

study establish a basis for further investigation of the influence of gut microbiome on metabolic changes that occur during pregnancy and hence maternal health and fetal development.

## 5.5 TABLES AND FIGURES

**Table 5-1.** Top 10 enriched metabolic pathways with the number of corresponding gene and metabolite hits for each comparison group, namely CVP vs CVNP (A), GFP vs GFNP (B), GFNP vs CVNP (C), and GFP vs CVP (D). Inclusion criteria for genes and metabolites are false discovery rate of 10% and a 2-fold change minimum in at least one group comparisons.

**A) CVP vs. CVNP**

| Pathway | # Gene hits | # Metabolite hits | p-value | FDR | Impact |
|---|---|---|---|---|---|
| Retinol metabolism | 22 | 2 | 2.41E-09 | 1.90E-07 | 1.23 |
| Linoleic acid metabolism | 9 | 5 | 6.22E-08 | 2.46E-06 | 2.13 |
| Arachidonic acid metabolism | 16 | 12 | 5.31E-07 | 1.40E-05 | 1.14 |
| Biosynthesis of unsaturated fatty acids | 1 | 9 | 0.002 | 0.032 | 0.46 |
| Steroid hormone biosynthesis | 18 | 20 | 0.003 | 0.042 | 0.76 |
| Glycerophospholipid metabolism | 14 | 8 | 0.005 | 0.057 | 0.86 |
| Glycerolipid metabolism | 10 | 2 | 0.005 | 0.057 | 0.82 |
| Taurine and hypotaurine metabolism | 0 | 3 | 0.010 | 0.091 | 0.40 |
| Phenylalanine metabolism | 2 | 6 | 0.010 | 0.091 | 1.43 |
| Glutathione metabolism | 11 | 0 | 0.022 | 0.175 | 0.24 |

**B) GFP vs. GFNP**

| Pathway | # Gene hits | # Metabolite hits | p-value | FDR | Impact |
|---|---|---|---|---|---|
| Retinol metabolism | 23 | 2 | 2.17E-14 | 1.46E-12 | 1.12 |
| Linoleic acid metabolism | 10 | 5 | 8.80E-12 | 2.95E-10 | 2.13 |
| Arachidonic acid metabolism | 11 | 12 | 1.22E-06 | 2.72E-05 | 0.99 |
| Steroid hormone biosynthesis | 17 | 20 | 6.37E-06 | 1.07E-04 | 0.51 |
| Drug metabolism - other enzymes | 14 | 0 | 2.03E-04 | 0.003 | 0.21 |
| Ascorbate and aldarate metabolism | 5 | 0 | 6.37E-04 | 0.007 | 0.38 |
| Biosynthesis of unsaturated fatty acids | 1 | 9 | 0.001 | 0.008 | 0.67 |
| Glycerolipid metabolism | 8 | 2 | 0.004 | 0.032 | 0.65 |
| Drug metabolism - cytochrome P450 | 11 | 1 | 0.006 | 0.045 | 0.18 |
| Glycerophospholipid metabolism | 9 | 8 | 0.007 | 0.048 | 0.71 |

**C) GFNP vs. CVNP**

| Pathway | # Gene hits | # Metabolite hits | p-value | FDR | Impact |
|---|---|---|---|---|---|
| Steroid hormone biosynthesis | 0 | 20 | 7.62E-09 | 2.82E-07 | 0.30 |
| Arachidonic acid metabolism | 0 | 12 | 5.65E-07 | 1.01E-05 | 0.58 |
| Linoleic acid metabolism | 0 | 5 | 8.17E-07 | 1.01E-05 | 1.50 |
| Phenylalanine metabolism | 0 | 6 | 3.26E-05 | 3.02E-04 | 1.09 |
| Biosynthesis of unsaturated fatty acids | 0 | 9 | 2.11E-04 | 0.002 | 0.20 |
| Phenylalanine, tyrosine and tryptophan biosynthesis | 0 | 3 | 0.001 | 0.005 | 1.70 |
| Glycerophospholipid metabolism | 0 | 8 | 0.001 | 0.006 | 0.49 |
| Taurine and hypotaurine metabolism | 1 | 3 | 0.001 | 0.006 | 0.67 |
| Primary bile acid biosynthesis | 0 | 7 | 0.020 | 0.083 | 0.13 |
| Citrate cycle (TCA cycle) | 0 | 4 | 0.031 | 0.111 | 0.56 |

**D) GFP vs. CVP**

| Pathway | # Gene hits | # Metabolite hits | p-value | FDR | Impact |
|---|---|---|---|---|---|
| Arachidonic acid metabolism | 4 | 12 | 6.75E-10 | 2.43E-08 | 0.76 |
| Steroid hormone biosynthesis | 4 | 20 | 3.30E-09 | 5.94E-08 | 0.32 |
| Linoleic acid metabolism | 3 | 5 | 1.80E-08 | 2.16E-07 | 1.75 |
| Retinol metabolism | 4 | 2 | 2.34E-05 | 2.11E-04 | 0.51 |
| Phenylalanine metabolism | 0 | 6 | 3.26E-05 | 2.35E-04 | 1.09 |
| Biosynthesis of unsaturated fatty acids | 0 | 9 | 2.11E-04 | 0.001 | 0.20 |
| Phenylalanine, tyrosine and tryptophan biosynthesis | 0 | 3 | 0.001 | 0.005 | 1.70 |
| Glycerophospholipid metabolism | 0 | 8 | 0.001 | 0.005 | 0.49 |
| Taurine and hypotaurine metabolism | 1 | 3 | 0.003 | 0.011 | 0.67 |
| Primary bile acid biosynthesis | 0 | 7 | 0.020 | 0.073 | 0.13 |

**Table 5-2. Significantly changed metabolic pathways with gene and metabolite hits in GFP mice versus CVP mice**.
Corresponding gene and metabolite hits that were differentially changed in each pathway are detailed with fold changes. Impact score was calculated based on degree centrality algorithms, and P-values were determined based on pathway-level weighting. Inclusion criteria for genes and metabolites are false discovery rate of 10% and a 2-fold change minimum in at least one group comparisons.

| Pathway | FDR | Impact | Gene Hits | | Metabolite Hits | |
|---|---|---|---|---|---|---|
| | | | Gene | Fold Change | Metabolite | Fold Change |
| Retinol metabolism (mmu00830) | 2.11E-04 | 0.51 | Cyp2b13<br>Cyp2c38<br>Cyp2c50<br>Cyp2c54 | 5.28<br>3.03<br>2.03<br>2.22 | Retinoate<br>9-cis-Retinoic acid | 3.36<br>3.36 |
| Linoleic acid metabolism (mmu00591) | 2.16E-07 | 1.75 | Cyp2c38<br>Cyp2c50<br>Cyp2c54 | 3.03<br>2.03<br>2.22 | Linoleate<br>Phosphatidylcholine<br>9(10)-EpOME<br>12(13)-EpOME<br>13-Hpode | 0.37<br>0.14<br>0.00<br>81.01<br>0.34 |
| Arachidonic acid metabolism (mmu00590) | 2.43E-08 | 0.76 | Cyp2b13<br>Cyp2c38<br>Cyp2c50<br>Cyp2c54 | 5.28<br>3.03<br>2.03<br>2.22 | 5,6-EET<br>8,9-EET<br>11,12-EET<br>14,15-EET<br>Arachidonate<br>Phosphatidylcholine<br>Leukotriene A4<br>16(R)-HETE<br>20-HETE<br>15(S)-HETE<br>19(S)-HETE<br>5(S)-HETE | 0.48<br>0.48<br>0.48<br>0.48<br>3.07<br>0.14<br>0.84<br>0.48<br>0.48<br>0.48<br>0.48<br>0.48 |
| Steroid hormone biosynthesis | 5.94E-08 | 0.32 | Cyp2b13<br>Cyp2c38<br>Cyp2c50 | 5.28<br>3.03<br>2.03 | 11β,17α,21-Trihydroxypregnenolone<br>16α-Hydroxydehydroepiandrosterone<br>Corticosterone | 0.84<br>0.84<br>4.23 |

| | | | | | | |
|---|---|---|---|---|---|---|
| (mmu00140) | | | Cyp2c54 | 2.22 | Aldosterone | 1.73 |
| | | | | | 11β-Hydroxyprogesterone | 1.97 |
| | | | | | Allopregnanolone | 0.00 |
| | | | | | Cortisol | 1.19 |
| | | | | | 11-Deoxycortisol | 4.23 |
| | | | | | Cortisone | 1.73 |
| | | | | | 21-Deoxycortisol | 4.23 |
| | | | | | 2-Methoxyestrone | 1.73 |
| | | | | | 18-Hydroxycorticosterone | 2.41 |
| | | | | | 19-Oxoandrost-4-ene-3,17-dione | 1.73 |
| | | | | | 19-Hydroxytestosterone | 0.84 |
| | | | | | 11β,21-Dihydroxy-3,20-oxo-5β-pregnan-18-al | 0.84 |
| | | | | | 11-Dehydrocorticosterone | 2.41 |
| | | | | | Dihydrocortisol | 0.84 |
| | | | | | 17α,21-Dihydroxy-5β-pregnane-3,11,20-trione | 2.41 |
| | | | | | Adrenosterone | 1.73 |
| | | | | | 7α-Hydroxydehydroepiandrosterone | 0.84 |

**Figure 5-1.**

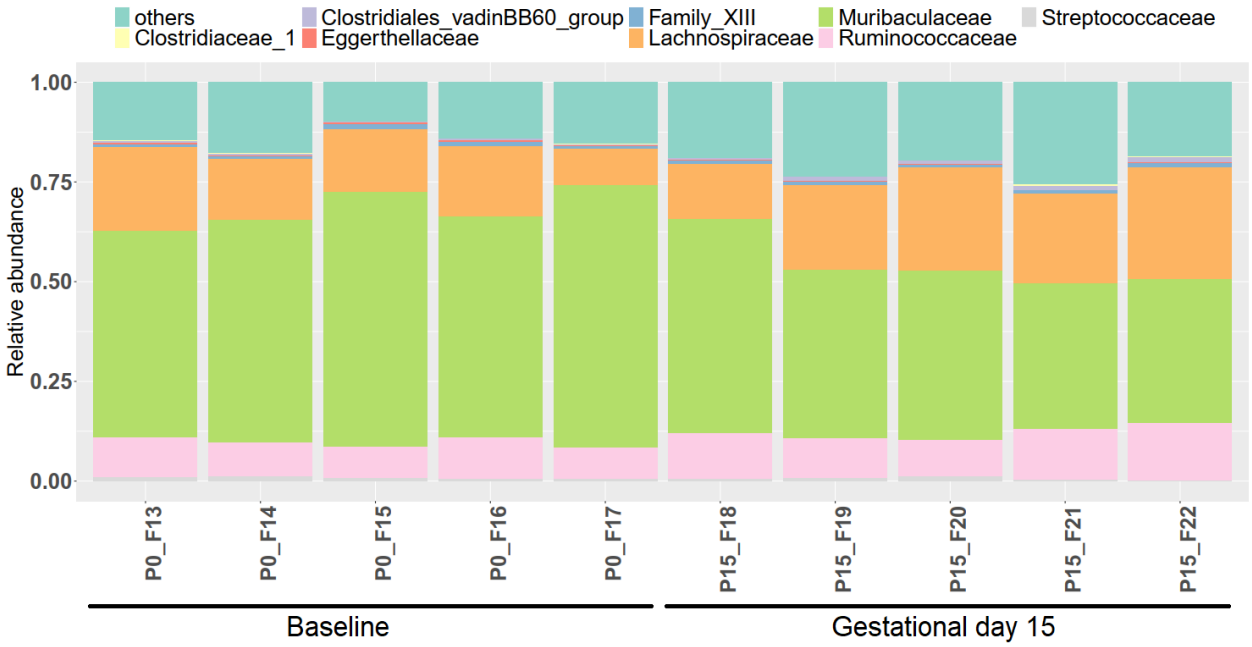


**Figure 5-1. Relative abundance of the gut microbiome taxonomic composition for top eight most abundant families determined using 16S sequencing.** Baseline fecal samples and gestational day 15 fecal samples are collected from 5 conventional C57BL/6 mice prior to mating and 15 days after conception.

**Figure 5-2.**

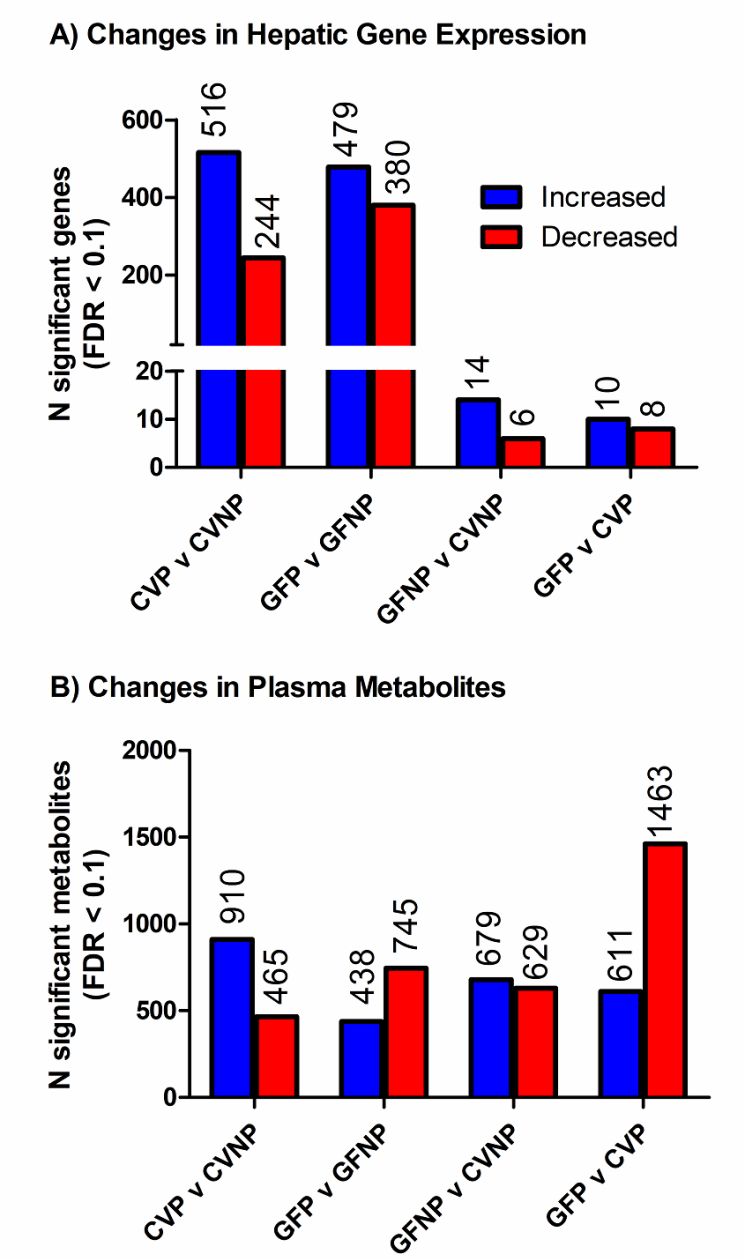


**Figure 5-2. The number of differentially expressed genes and differentially produced metabolites between various comparison mouse groups**. Differentially expressed hepatic genes (**A**) and differentially produced metabolites in maternal plasma (**B**) between CVP and CVNP, GFP and GFP, GFNP and CVNP, and GFP and CVP mice. The number of CVNP, CVP, GFNP and GFP mice used was 6, 5, 6, and 5, respectively. Inclusion criteria for genes and metabolites are false discovery rate of 10% and a 2-fold change minimum in at least one group comparisons.

**Figure 5-3.**

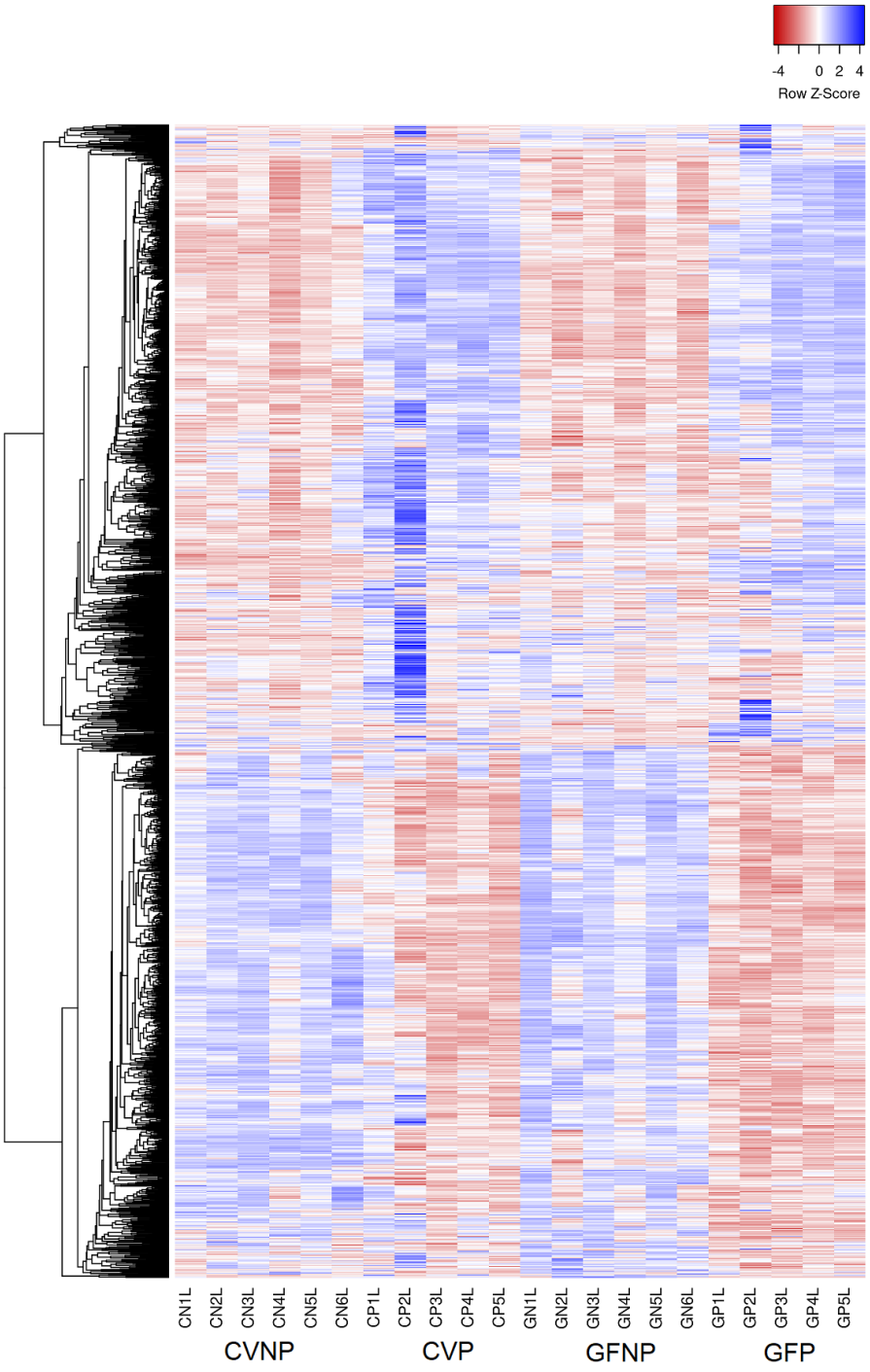


**Figure 5-3. Heatmap of hepatic genes with at least 2-fold change and FDR < 0.1**. Inclusion criteria for genes and metabolites are false discovery rate of 10% and a 2-fold change minimum in at least one group comparisons. CVNP, conventional non-pregnant mice; CVP, conventional pregnant mice; GFNP, germ-free non-pregnant mice; GFP, germ-free pregnant mice.

**Figure 5-4.**

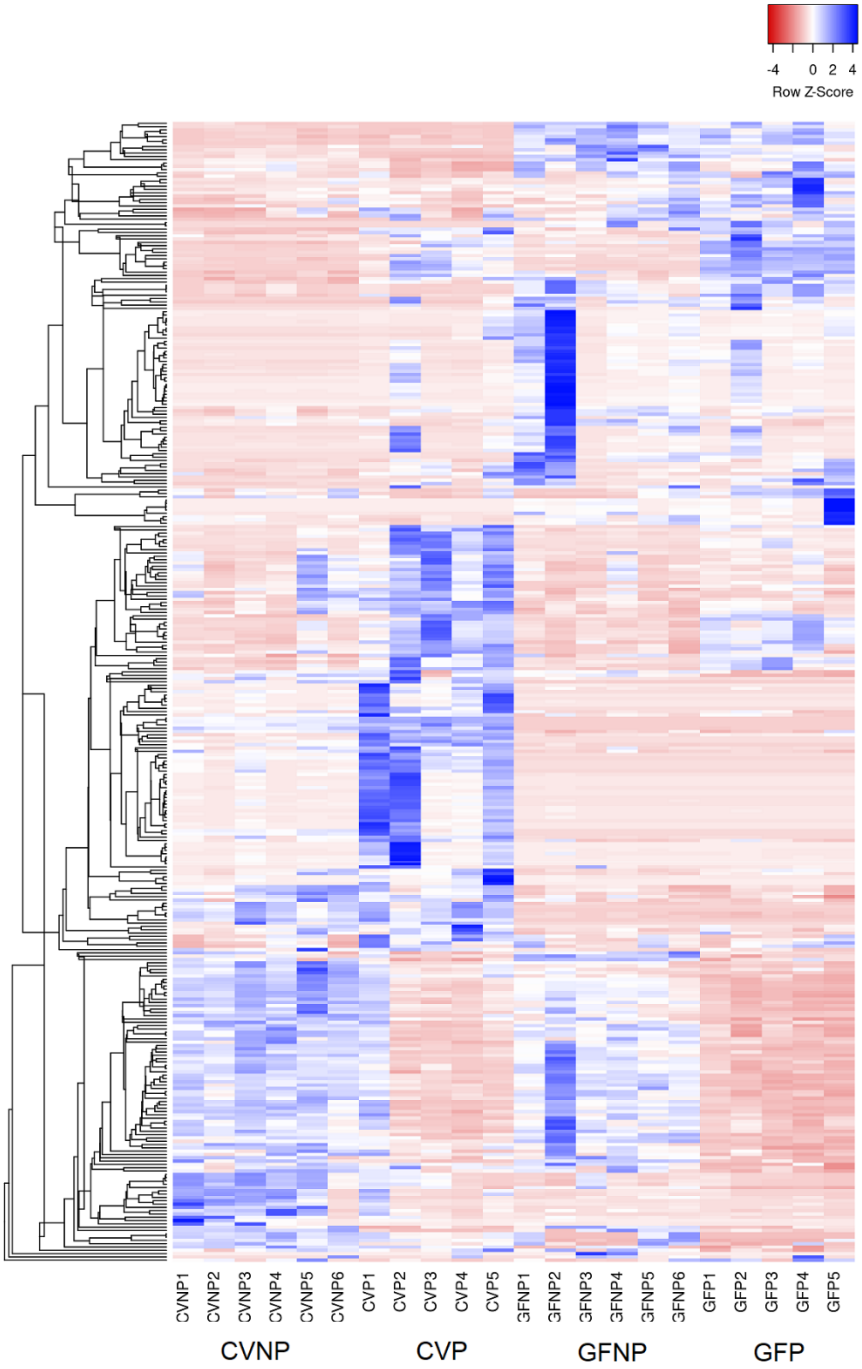


**Figure 5-4. Heatmap of metabolites in maternal plasma with at least 2-fold change and FDR < 0.1**. Inclusion criteria for genes and metabolites are false discovery rate of 10% and a 2-fold change minimum in at least one group comparisons. CVNP, conventional non-pregnant mice; CVP, conventional pregnant mice; GFNP, germ-free non-pregnant mice; GFP, germ-free pregnant mice.

**Figure 5-5.**

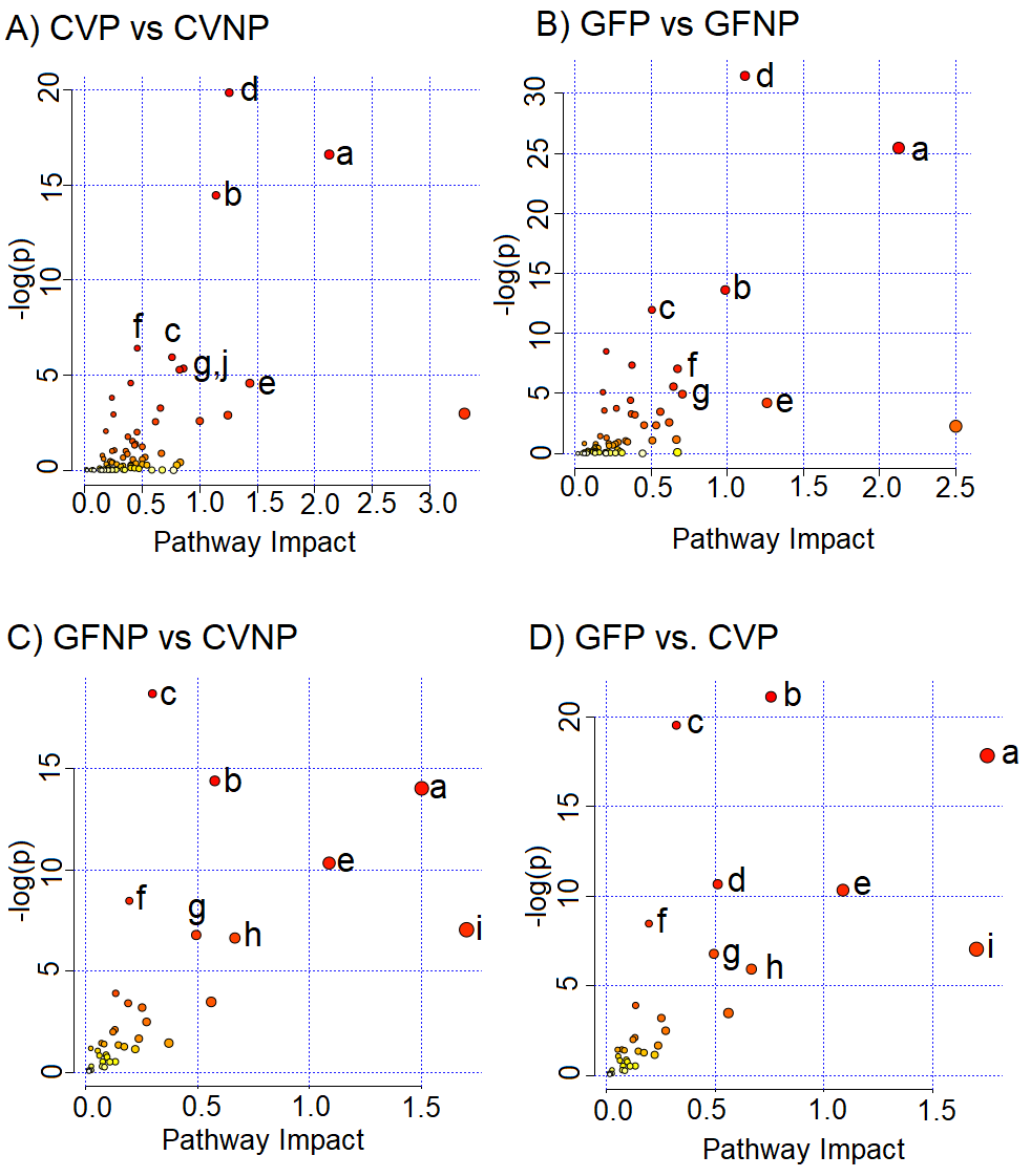


**Figure 5-5. Metabolic pathways affected by pregnancy and/or germ-free after integration of significant changes in hepatic gene expression and maternal plasma metabolites with comparison between CVP and CVNP (A), GFP and GFNP (B), GFNP and CVNP (C), or GFP and CVP (D).** Key pathways affected: a) linoleic acid metabolism; b) arachidonic acid metabolism; c) steroid hormone biosynthesis; d) retinol metabolism; e) phenylalanine metabolism; f) biosynthesis of unsaturated fatty acids; g) glycerophospholipid metabolism; h) taurine and hypotaurine metabolism; i) phenylalanine, tyrosine and tryptophan biosynthesis; Inclusion criteria for genes and metabolites are false discovery rate of 10% and a 2-fold change minimum in at least one group comparisons. CVNP, conventional non-pregnant mice; CVP, conventional pregnant mice; GFNP, germ-free non-pregnant mice; GFP, germ-free pregnant mice.

**Figure 5-6.**

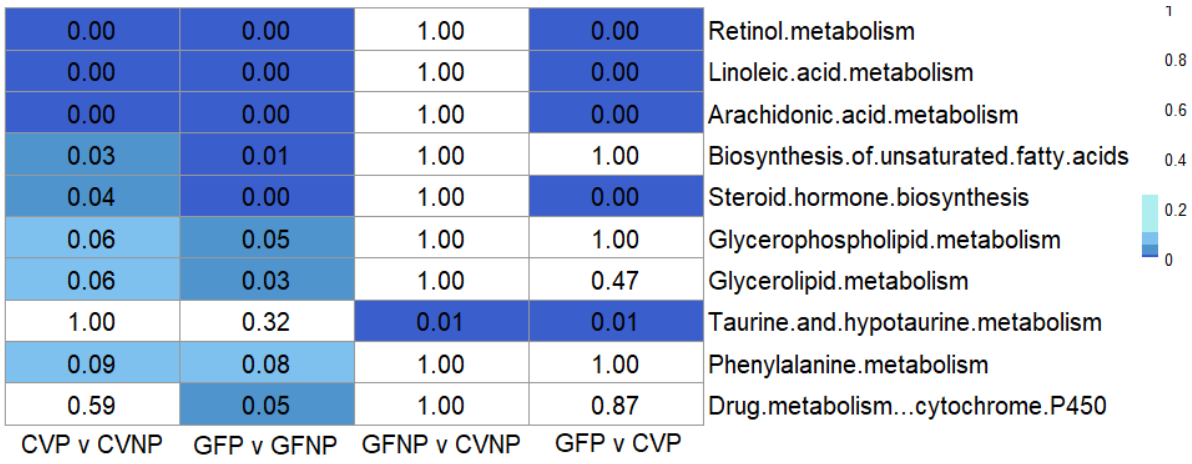


**Figure 5-6. Heatmap of false discovery rates of top metabolic pathway hits among all comparison groups**. Filtering criterion is a minimum of 1 gene and 1 metabolite hit per pathway. Those that failed to meet this criterion is labeled as P = 1. CVNP, conventional non-pregnant mice; CVP, conventional pregnant mice; GFNP, germ-free non-pregnant mice; GFP, germ-free pregnant mice.

## 5.6 REFERENCES


1. Wang Q, Würtz P, Auro K, et al. Metabolic profiling of pregnancy: Cross-sectional and longitudinal evidence. *BMC Med.* 2016;14:205.
2. Edwards SM, Cunningham SA, Dunlop AL, et al. The Maternal Gut Microbiome during Pregnancy. *MCN Am. J. Matern. Nurs.* 2017;42:310–316.
3. Koren O, Goodrich JK, Cullender TC, et al. Host remodeling of the gut microbiome and metabolic changes during pregnancy. *Cell*. 2012;150:470–480.
4. Koren O, Goodrich JK, Cullender TC, et al. Host remodeling of the gut microbiome and metabolic changes during pregnancy. *Cell*. 2012;150:470–480.
5. Santacruz A, Collado MC, García-Valdés L, et al. Gut microbiota composition is associated with body weight, weight gain and biochemical parameters in pregnant women. *Br. J. Nutr.* 2010;104:83–92.
6. Nicholson JK, Holmes E, Kinross J, et al. Host-gut microbiota metabolic interactions. Science (80-. ). American Association for the Advancement of Science; 2012. p. 1262–1267.
7. Spanogiannopoulos P, Bess EN, Carmody RN, et al. The microbial pharmacists within us: a metagenomic view of xenobiotic metabolism. *Nat. Rev. Microbiol.* 2016;14:273–287.
8. Martinez KB, Leone V, Chang EB. Western diets, gut dysbiosis, and metabolic diseases: Are they linked? [Internet]. Gut Microbes. Taylor and Francis Inc.; 2017. p. 130–142.
9. He Y, Wu W, Wu S, et al. Linking gut microbiota, metabolic syndrome and economic status based on a population-level analysis. *Microbiome*. 2018;6:172.
10. Nuriel-Ohayon M, Neuman H, Koren O. Microbial changes during pregnancy, birth, and infancy. *Front. Microbiol.* 2016;7:1031.
11. Gohir W, Whelan FJ, Surette MG, et al. Pregnancy-related changes in the maternal gut microbiota are dependent upon the mother's periconceptional diet. *Gut Microbes*. 2015;6:310–320.
12. Neuman H, Koren O. The Pregnancy Microbiome. *Nestle Nutr. Inst. Workshop Ser.* S. Karger AG; 2017. p. 1–9.
13. Mayer EA, Knight R, Mazmanian SK, et al. Gut microbes and the brain: Paradigm shift in neuroscience. *J. Neurosci.* 2014;34:15490–15496.
14. Josefson JL, Hoffmann JA, Metzger BE. Excessive weight gain in women with a normal pre-pregnancy BMI is associated with increased neonatal adiposity. *Pediatr. Obes.* 2013;8:e33-6.
15. Callahan BJ, McMurdie PJ, Rosen MJ, et al. DADA2: High-resolution sample inference from Illumina amplicon data. *Nat. Methods*. 2016;13:581–583.
16. Paulson JN, Colin Stine O, Bravo HC, et al. Differential abundance analysis for microbial marker-gene surveys. *Nat. Methods*. 2013;10:1200–1202.

17. Gu R, Rybalov L, Negrin A, et al. Metabolic Profiling of Different Parts of *Acer truncatum* from the Mongolian Plateau Using UPLC-QTOF-MS with Comparative Bioactivity Assays. *J. Agric. Food Chem.* 2019;67:1585–1597.

18. Chong J, Soufan O, Li C, et al. MetaboAnalyst 4.0: towards more transparent and integrative metabolomics analysis. *Nucleic Acids Res.* 2018;46:W486–W494.

19. Xia J, Wishart DS. Metabolomic Data Processing, Analysis, and Interpretation Using MetaboAnalyst. *Curr. Protoc. Bioinforma.* 2011;34:14.10.1-14.10.48.

20. Konstantinov SR, van der Woude CJ, Peppelenbosch MP. Do pregnancy-related changes in the microbiome stimulate innate immunity? *Trends Mol. Med.* 2013;19:454–459.

21. Soma-Pillay P, Nelson-Piercy C, Tolppanen H, et al. Physiological changes in pregnancy. *Cardiovasc. J. Afr.* 2016;27:89–94.

22. Zeng Z, Liu F, Li S. Metabolic Adaptations in Pregnancy: A Review [Internet]. Ann. Nutr. Metab. S. Karger AG; 2017. p. 59–65.

23. Lagkouvardos I, Lesker TR, Hitch TCA, et al. Sequence and cultivation study of Muribaculaceae reveals novel species, host preference, and functional potential of this yet undescribed family. *Microbiome*. 2019;7:28.

24. Ferrocino I, Ponzo V, Gambino R, et al. Changes in the gut microbiota composition during pregnancy in patients with gestational diabetes mellitus (GDM). *Sci. Rep.* 2018;8:1–13.

25. Gomez-Arango LF, Barrett HL, McIntyre HD, et al. Connections between the gut microbiome and metabolic hormones in early pregnancy in overweight and obese women. *Diabetes*. 2016;65:2214–2223.

26. Hugenholtz F, de Vos WM. Mouse models for human intestinal microbiota research: a critical evaluation [Internet]. Cell. Mol. Life Sci. Birkhauser Verlag AG; Jan, 2018 p. 149–160.

27. Turnbaugh PJ, Ridaura VK, Faith JJ, et al. The effect of diet on the human gut microbiome: A metagenomic analysis in humanized gnotobiotic mice. *Sci. Transl. Med.* 2009;1:6ra14.

28. Choo JM, Trim PJ, Leong LEX, et al. Inbred mouse populations exhibit intergenerational changes in intestinal microbiota composition and function following introduction to a facility. *Front. Microbiol.* 2017;8.

29. Elderman M, Hugenholtz F, Belzer C, et al. Changes in intestinal gene expression and microbiota composition during late pregnancy are mouse strain dependent. *Sci. Rep.* 2018;8:1–12.

30. Sapin V, Alexandre MC, Chaïb S, et al. Effect of vitamin A status at the end of term pregnancy on the saturation of retinol binding protein with retinol. *Am. J. Clin. Nutr.* 2000;71:537–543.

31. Chambon P. The retinoid signaling pathway: Molecular and genetic analyses. *Semin. Cell*

*Dev. Biol.* 1994;5:115–125.

32. Morriss-Kay GM, Sokolova N. Embryonic development and pattern formation [Internet]. FASEB J. 1996. p. 961–968.

33. Bobiński R, Mikulska M. The ins and outs of maternal-fetal fatty acid metabolism [Internet]. Acta Biochim. Pol. Polskie Towarzystwo Biochemiczne; 2015. p. 499–507.

34. Kallen CB. Steroid hormone synthesis in pregnancy [Internet]. Obstet. Gynecol. Clin. North Am. 2004. p. 795–816.

35. Geiger O, López-Lara IM, Sohlenkamp C. Phosphatidylcholine biosynthesis and function in bacteria. Biochim. Biophys. Acta - Mol. Cell Biol. Lipids. 2013. p. 503–513.

36. Sohlenkamp C, López-Lara IM, Geiger O. Biosynthesis of phosphatidylcholine in bacteria. *Prog. Lipid Res.* 2003;42:115–162.

37. Martínez-Morales F, Schobert M, López-Lara IM, et al. Pathways for phosphatidylcholine biosynthesis in bacteria. *Microbiology.* 2003;149:3461–3471.

38. Mellon SH. Neurosteroid regulation of central nervous system development. *Pharmacol. Ther.* 2007;116:107–124.

39. Renaud HJ, Cui JY, Khan M, et al. Tissue distribution and gender-divergent expression of 78 cytochrome p450 mRNAs in mice. *Toxicol. Sci.* 2011;124:261–277.

40. Anderson GD. Pregnancy-induced changes in pharmacokinetics: A mechanistic-based approach [Internet]. Clin. Pharmacokinet. 2005. p. 989–1008.

41. Isobe Y, Itagaki M, Ito Y, et al. Comprehensive analysis of the mouse cytochrome P450 family responsible for omega-3 epoxidation of eicosapentaenoic acid. *Sci. Rep.* 2018;8.

42. Wang H, Zhao Y, Bradbury JA, et al. Cloning, expression, and characterization of three new mouse cytochrome P450 enzymes and partial characterization of their fatty acid oxidation activities. *Mol. Pharmacol.* 2004;65:1148–1158.

43. Paquette A, Baloni P, Holloman AB, et al. Temporal transcriptomic analysis of metabolic genes in maternal organs and placenta during murine pregnancy. *Biol. Reprod.* 2018;99:1255–1265.

# CHAPTER 6: CONCLUSIONS

Medication use is increasingly prevalent during pregnancy, but there still exist large knowledge gaps on how drug kinetics are changed in pregnant women. Traditional drug clinical testing excludes pregnant women for safety and ethical reasons. Thus, there is a need for more research to focus on better understanding the various aspects that can alter drug disposition in pregnancy. Of the four key pharmacokinetic processes (absorption, distribution, metabolism, and excretion), hepatic enzymatic metabolism and transporters are especially important as their expressions and activities have been shown to change during pregnancy. More recently, the gut microbiome has also been considered a potential important factor that may contribute to drug pharmacokinetics. The overall goal of the dissertation research was to better understand various aspects of drug disposition during pregnancy. For transport, we used overexpressed cell lines and membrane vesicles to characterize the role of hepatic and placental transporters in the uptake and efflux of bupropion, an antidepressant and smoking cessation aid. For metabolism, we assessed the role of *NAT2* genotype on oral hydralazine, an antihypertensive agent, in pregnant women. Finally, we analyzed the role of the gut microbiome on host hepatic drug metabolizing enzymes and transporter gene expressions and metabolic pathways. Overall, these specific aims provided novel information on transport of bupropion and its active metabolites, metabolism of oral hydralazine, and modulation of hepatic drug metabolizing enzymes and transporters in absence of the gut microbiome during pregnancy.

## 6.1 TRANSPORT OF BUPROPION AND ITS METABOLITES BY THE MODEL CHO AND HEK293 CELL LINES

Several significant DDIs involving BUP have been reported with mechanisms not fully understood. It was postulated that modulation of BUP transport might explain such reports. However, this study showed that BUP and its active metabolites (OHB, TB and EB) are not substrates of the major hepatic transporters (OATP1B1, OATP1B3, OATP2B1, OCT1, MRP2, P-gp and BCRP) and the placental transporter OATP4A1. A flow chart of the experimental process that led to this conclusion is illustrated in Figure S6. These findings suggest that the major hepatic drug transporters likely play a minor role in the overall disposition, systemic clearance, and local tissue exposure of BUP and its metabolites. They narrow the possible mechanisms that mediate the DDIs involving BUP. Thus, such DDIs are likely mediated by drug-metabolizing enzymes, not the major hepatic drug transporters.

Not all of the study findings were readily interpretable. We observed active net uptake of BUP and its metabolites in overexpressed cell lines (CHO and HEK293) for OATP1B1, OATP1B3, and OATP2B1, but the inhibition could not be inhibited by prototypical inhibitors rifampin and cyclosporin A. It would be interesting, if future studies could be done to explain the net uptake of BUP and its metabolites into the overexpressing cell lines that was observed in our cell-based study. This is important as it could highlight potential limitations with using HEK or CHO cell lines to screen OATP substrates if the discrepancy could be resolved.

## 6.2 EFFECT OF *N*-ACETYLTRANSFERASE 2 (NAT2) GENOTYPE ON THE PHARMACOKINETICS OF HYDRALAZINE DURING PREGNANCY

With this investigation, we describe, for the first time, the impact of *NAT2* genotype on oral hydralazine PK during mid- and late pregnancy. We report significantly higher hydralazine exposure, lower apparent oral clearance, and lower MTP-to-hydralazine ratio in subjects identified as slow acetylators compared to rapid acetylators. Our results did not show evidence of a significant effect of dose or gestational age on the PK and hemodynamic outcomes of hydralazine, possibly due to the small sample size. Clinicians should be mindful of the substantial variations in oral hydralazine exposure in pregnant women. Larger studies are needed to assess whether the PK differences lead to differences in safety or efficacy of hydralazine during pregnancy.

In the future, a prospective study to recruit women with chronic hypertension prior to pregnancy can be done to obtain non-pregnant baseline data. Furthermore, if a method could be developed to stabilize urine samples as soon as they are collected, it would also be possible to perform a mass balance study to assess whether there is a difference in metabolite formation clearance between the rapid and slow *NAT2* acetylators.

## 6.3 IMPACT OF MICROBIOME ON HEPATIC DRUG PROCESSING GENES IN MICE DURING PREGNANCY

Results from this study show that the microbiome can differentially affect the expression and/or activity of hepatic DMETs in pregnant and non-pregnant mice. The gut microbiome helps regulate hepatic DMET processes, most likely via formation of secondary bile acids, some of which are ligands of nuclear receptors such as PXR and FXR that regulate downstream

transcription of drug metabolizing enzymes and transporters. However, the impact of the gut microbiome on DMET expression depends on the physiological state of the woman (e.g. pregnancy) and circulating sex hormone concentrations. The microbiome could potentially alter hepatic DMETs in pregnant mice in three different ways: 1) to alter pregnancy-induced fold-change in gene expression by changing baseline gene expression levels such as *Cyp3a16; 2)* to alter pregnancy-induced fold-change in activity by changing protein expression of metabolic enzymes such as the Cyp3a isoforms; 3) to possibly alter posttranscriptional or epigenomic regulation, leading to a disconnection between gene (mRNA) and protein expression of certain DMETs such as *Cyp3a11* and *Cyp3a41*. Such microbiome-mediated alterations appear to be gene-dependent. Details of these mechanisms remain to be investigated in future studies. However, due to the fact that the human microbiome differs markedly from that of mice, one should be cautious in translating these findings to humans. Nevertheless, this study provides the basis for further investigation of the impact of the microbiome on drug disposition during pregnancy.

Potential future studies include introducing humanized microbiome (composition that represents early, mid, and late human pregnancy) to germ-free mice, and using germ-free mice that have humanized CYP enzymes (particularly *CYP3A4*) for more extrapolation value. Another possibility is to conduct a human clinical study and collect fecal sample from pregnant women throughout gestation, while giving safe CYP3A probes to assess any correlation between activity change and the gut microbiome composition. This could potentially lead to the identification of key bacteria responsible for CYP3A interindividual variability during pregnancy.

## 6.4 EFFECT OF THE GUT MICROBIOME ON OVERALL HEPATIC METABOLIC PATHWAYS DURING PREGNANCY

To extend the preliminary findings found in Chapter 4, we conducted a global assessment of metabolic processes in the mouse, using the hepatic transcriptome data from previous Chapter and adding in untargeted plasma metabolome data to perform joint pathway analyses. In Chapter 5, we report eight hepatic metabolic pathways that were changed during pregnancy, regardless of the gut microbiome status. However, in germ-free pregnant mice, we observed significant changes in four key hepatic metabolic pathways compared to conventional pregnant mice: retinol metabolism, linoleic acid metabolism, arachidonic acid metabolism, and steroid hormone biosynthesis. This suggests that the gut microbiome can potentially modulate host metabolic processes that are critical for maternal health and fetal development. Moreover, perturbation of these metabolic pathways by germ-free conditions only occurs in pregnant mice, not in non-pregnant mice, suggesting that such changes are possibly associated with a shift of gut microbiome composition during pregnancy. Multiple plasma metabolites were also identified to be significantly altered by germ-free in pregnant mice, with the highest fold changes observed for phosphatidylcholine, linoleic acid epoxides, and allopregnanolone. In addition, we identified four Cyp enzymes (*Cyp2b13, Cyp2c38, Cyp2c50,* and *Cyp2c54*) that were differentially expressed during pregnancy in germ-free mice compared to conventional mice, and they could be functionally tied to all of these altered metabolic pathways. Of these enzymes, only *Cyp2c50* has a human homolog, *CYP2C19*, whereas others are murine specific. *CYP2C19* has epoxygenase activity and is a major enzyme in the metabolism of endogenous polyunsaturated fatty acids such as arachidonic acid and linoleic acid. We observed significant decrease in epoxyeicosatrienoic acids and epoxyoctadecenoic acids (metabolites of arachidonic acid and

linoleic acid) in germ-free pregnant mice compared to conventional pregnant mice. This study is a first step to filling the knowledge gap in our understanding of what metabolic processes may be affected by dysbiosis during pregnancy and physiological and therapeutic implications of our findings.

Although the studies reported in this Chapter enhance our understanding of drug disposition and response in pregnancy, further work is necessary to better extrapolate these data to human pregnancy. As previously mentioned, translational value of the study could be improved by transplanting human gut bacteria from pregnant women into germ-free mice. Multiple gestational age studies can be useful to illustrate a more dynamic metabolic change throughout gestation, rather than a single time point comparison. Validation of the metabolites and genes we identified via for instance genetic knockouts or the use of inhibitors in mice will further enhance mechanistic understanding of our findings reported in this study.